

PHYSIOLOGICAL REGULATION OF  
NITROGEN FIXATION IN SOYBEAN ROOT NODULES

*A THESIS SUBMITTED FOR THE DEGREE OF  
DOCTOR OF PHILOSOPHY*



*AT*

*THE AUSTRALIAN NATIONAL UNIVERSITY*

RICHARD PARSONS

SEPTEMBER 1989

### Declaration

The research in this thesis is my own work, except where acknowledgement is made.  
No material in this thesis has been submitted for any other degree.

*R Parsons*

(Richard Parsons)

## Acknowledgements

Professionally, I wish to sincerely thank David Day, my supervisor, for his support and guidance. Alan Gibson and Graham Farquhar are thanked for their role as advisors.

Technical assistance provided by ANU staff is gratefully acknowledged. In particular, Neda Plovanic is thanked for preparing the microscope sections, Keith Herbert for assistance with photography and staff of the ANU Electron Microscope Unit for assistance with the electron microscopy.

On a professional and personal level, the support of Bernie Carroll, Terry Murphy, Peter Thygesen, Michael Udvardi and Kerry Walsh has been appreciated. The many and varied discussions in the dungeons of the Botany building will be remembered.

My special friends Meredith Bradbury, Katherine Bryant and Paul Geissler are thanked professionally and especially personally. My parents, William and Dorothy Parsons and my sisters Sarah and Kathryn Parsons are thanked for their support from New Zealand.

I have appreciated the financial assistance received both from the people of Australia through an ANU Scholarship and from a William Georgetti Scholarship from New Zealand.

## Abstract

Soybean (*Glycine max*) nodules were able to adapt to fix nitrogen at oxygen pressures of 4.7, 19, 47 and 75 kPa. This adaptation involved changes in the distribution and volume of intercellular spaces in the nodule cortex. In all oxygen treatments, there was a similar distribution of interconnecting intercellular spaces in the central infected zone and in an aerated layer of cells surrounding the infected zone. Outside this layer, within the inner and outer cortex, the number and size of intercellular spaces decreased with increasing  $pO_2$ , in a manner that probably acted to increase the resistance of the cortex to oxygen diffusion. Plants grown with nodulated roots in oxygen concentrations from 4.7 to 47 kPa had a similar rate of growth and showed a similar decline of nitrogenase activity when exposed to saturating acetylene.

Exposure of air-grown soybean nodules to saturating pressures of acetylene or to nitrogen free atmospheres caused a decline in nodulated root respiration and nitrogenase activity. In an atmosphere of argon/oxygen, nodules formed on soybean roots and expressed nitrogenase activity. These nodules did not show an acetylene-induced decline. When nodules formed in argon/oxygen were placed in air they developed a decline response to acetylene over a period of several days.

Subsaturating pressures of acetylene detected proportionally less activity and caused less of a decline in nitrogenase activity and nodulated root respiration. Very low pressures of acetylene (<0.5 kPa) did not cause a decline and could be used to estimate nitrogenase activity. These low pressures of acetylene were used to continuously monitor nitrogenase activity, a method useful for studies of nodule physiology.

In addition to acetylene, nodules showed a decline in nitrogenase activity when exposed to the inhibitors of ammonia assimilation and ureide synthesis, methionine sulfoximine (MSO) and allopurinol. Plants treated with MSO did not show an acetylene-induced decline. These inhibitor-induced declines could be recovered by exposure of nodulated roots to hyperbaric oxygen, indicating that the cause of these declines may have been an increase in the diffusion resistance of the nodule.

In anatomical studies of the nodule cortex, a layer of cells with thin radially orientated walls was observed. Intercellular spaces occur on either side of this layer, but did not appear to extend across it. This layer of cells was present on the inside of the inner cortex and formed a tier of cells around the infected zone. In resin-mounted and free-hand cut sections of nodules, cells within this layer were sometimes collapsed. A role for these putative extensible cells in the regulation of nitrogenase activity via changes in cortical resistance to oxygen diffusion is discussed.

## Key to Abbreviations

Abbreviation	Chemical or process
3PG	3-phospho-D-glycerate
5,10 MTHF	5,10-methenyl-tetrahydrofolate
5,10M THF	5,10-methylene-tetrahydrofolate
10,F,THF	10-formyl-tetrahydrofolate
ADP	adenosine diphosphate
AICAR	5-phospho-ribosyl-5-amino-4-imidazole carboxamide
Asp	aspartate
ATP	adenosine triphosphate
<i>D</i>	diffusion coefficient
DW	dry weight
ETS	electron transport system
FAD	flavin-adenine dinucleotide
FADH <sub>2</sub>	flavin-adenine dinucleotide, reduced
FGAM	5-phospho-ribosyl-N-formylglycineamidine
FGAR	5-phospho-ribosyl-N-formylglycineamide
FW	fresh weight
G3P	D-glyceraldehyde-3-phosphate
GAR	5-phospho-ribosyl-glycineamide
Gln	glutamine
Glu	glutamate
Gly	glycine
IMP	inosine-5-phosphate
IRGA	infra-red gas analyser
MES	2[N-morpholino]ethanesulfonic acid
MSO	methionine sulfoximine
NAD(P)	nicotinamide-adenine dinucleotide (phosphate)
NAD(P)H <sub>2</sub>	nicotinamide-adenine dinucleotide (phosphate), reduced
OAA	oxaloacetate
PEP	phosphoenol pyruvate
PIPES	1,4-piperazinediethanesulfonic acid
PRPP	α-D-5-phospho-ribosyl-pyrophosphate
<i>Q</i>	flux
RQ	respiratory quotient (CO <sub>2</sub> /O <sub>2</sub> )
TCA cycle	tricarboxylic acid cycle
THF	5,6,7,8, tetrahydrofolate
αketoglutarate	α-ketoglutarate (oxoglutarate)
XMP	xanthosine-5-phosphate

## Table of Contents

<b>1. Introduction</b>	<b>1</b>
1.1. General	1
1.2. Functioning of Nodules and the Importance of Scale	3
1.3. Initiation of Nodulation and the Structure of Nodules	4
1.4. Carbon and Nitrogen Metabolism	7
1.4.1. Carbon metabolism	7
1.4.2. Nitrogen metabolism	9
1.4.3. Linkage of carbon and nitrogen metabolism	11
1.5. Acetylene Reduction and the Measurement of Nitrogen Fixation	11
1.6. Plant Regulation of Nitrogen Fixation	13
1.7. Gas Environment of Root Nodules	15
1.7.1. Soil environment	15
1.7.2. Composition of soil air	15
1.8. Diffusion and Solubility of Gases	16
1.9. Modelling of Gas Exchange in Root Nodules	18
1.10. Modelling Plant Growth and Function	18
1.11. The Present Study	19
<b>2. Materials and Methods</b>	<b>20</b>
2.1. Introduction	20
2.2. Plant Culture	21
2.3. Inoculum	21
2.4. Recirculating Gas System	23
2.5. Gas Analysis	24
2.6. Open-Flow Assay System	25
2.7. Analysis of Plant Material	25
2.8. Chlorophyll Determination	26
2.9. Measurement of Photosynthesis	26
2.10. Haem Content	26
2.11. Microscopy	27
<b>3. Nitrogen and Carbon Partitioning in Soybean Seedlings</b>	<b>28</b>
3.1. Introduction	28
3.2. Method of Calculation	28
3.3. Results	31
3.4. Discussion	39
<b>4. Effects of Ethylene, Acetylene and the Absence of N<sub>2</sub> on     Nodulation and Nitrogen Fixation in Soybean</b>	<b>41</b>
4.1. Introduction	41
4.2. Results	43
4.2.1. Experimental	43
4.2.2. Effect of ethylene on growth and nodulation of soybean	43
4.2.3. Acetylene-induced decline	45
4.2.4. Growth of plants in the absence of N <sub>2</sub>	49
4.3. Discussion	56

<b>5. Measurement of Nitrogenase Activity with Subsaturating Acetylene Pressures</b>	<b>59</b>
5.1. Introduction	59
5.2. Results	62
5.2.1. Nitrogenase activity at low acetylene pressures	62
5.2.2. Estimating total nitrogenase activity with low acetylene	64
5.2.3. Estimation of apparent $K_M$ of nodules for acetylene	67
5.2.4. Use of low pressures of acetylene in physiological studies	68
5.3. Discussion	73
5.3.1. Nitrogenase activity and the acetylene-induced decline	73
5.3.2. Quantitative determination of nitrogenase activity	74
5.3.3. Model of ethylene production at low pressures of acetylene	75
5.3.4. Conclusion	82
<b>6. Effects of Inhibitors of Nitrogen Assimilation on Nodulated Root Respiration and Nitrogenase Activity</b>	<b>83</b>
6.1. Introduction	83
6.2. Results	86
6.2.1. Spray and water controls	86
6.2.2. Osmotic and ionic controls	86
6.2.3. Effect of hyperbaric oxygen on control plants	89
6.2.4. Effect of acetylene on root respiration and $N_2$ ase activity	89
6.2.5. Effect of MSO spray	89
6.2.6. Effect of cycloserine spray	90
6.2.7. Effect of allopurinol spray	91
6.3. Discussion	96
<b>7. Nodule Adaptation to Altered Oxygen Pressure</b>	<b>98</b>
7.1. Introduction	98
7.2. Results	99
7.2.1. Plant growth	99
7.2.2. Nodule structure	100
7.2.3. Nodule physiology	111
7.3. Discussion	113
<b>8. General Discussion</b>	<b>116</b>
8.1. The Acetylene-Induced Decline and Nodule Adaptation to Oxygen	116
8.2. Oxygen Diffusion Within the Nodule	117
8.3. Rates of Metabolism in Nodules	120
8.4. Possible Metabolic Control of Nodule Activity	122
8.5. Alteration of the Diffusion Resistance of Nodules	124
8.6. How Could the Cortex Cells Respond to Oxygen ?	132
8.7. Future Work	133
8.8. Conclusion	134
<b>References</b>	<b>135</b>
<b>Appendix I</b>	<b>149</b>
<b>Appendix II</b>	<b>154</b>
<b>Appendix III</b>	<b>156</b>

## Chapter 1

### Introduction

#### 1.1. General

Legumes are an agriculturally important group of plants capable of forming a root nodule symbiosis with the soil bacteria, rhizobia. Soybean (*Glycine max*), a tropical legume endemic in Eastern Asia, is the most economically important legume crop (ninth in world crop production : FAO Production Yearbook 1986) and has become a model for the study of legume physiology. When available nitrogen limits growth, soybean enters a symbiosis with *Bradyrhizobium japonicum* to form nitrogen fixing root nodules.

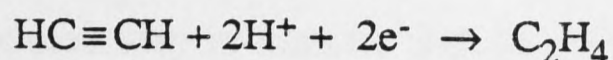
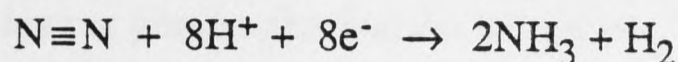
The physiology of soybean root nodules involves many aspects of the growth of soybean and rhizobia. Formation and subsequent development of root nodules is regulated by the plant and occurs when infective rhizobia are present and environmental conditions favour nodule formation. Of particular interest is the exchange of fixed carbon and nitrogen between the symbiotic partners and the supply of oxygen for respiration, to support the oxygen labile, but energy requiring nitrogenase enzyme system. In functioning nodules, carbohydrate from photosynthesis of the shoot is available to bacteroids in the infected zone of the nodule. Within the bacteroids, the enzyme nitrogenase is located and dinitrogen gas is fixed to ammonia which is available to the plant.

Plant growth is frequently limited by either reduced carbon or reduced nitrogen. Together with oxygen and hydrogen, they form the major constituents of plants (approximately 96 % of the total dry weight), largely as carbohydrates, lipids and proteins. In nitrogen fixing plants, such as soybeans, carbon and nitrogen nutrition is linked through the action of nodules, with important consequences for the patterns of growth of these plants. Nitrogen is available to the plant through fixation, but its reduction is energetically more expensive than uptake of nitrate or ammonia through the roots (Silsbury 1977, Ryle *et al.* 1978). Nitrogen fixing plants are, in a sense, not limited for nitrogen, but become more limited for carbon or reducing power. In addition, the establishment of nitrogen fixation requires an investment of other plant resources and there is a time delay before nitrogen becomes available. The metabolic relationships of carbon and nitrogen within nodules have been the focus of considerable



research and most, although not all, of the metabolic processes involved have been detailed. An area of current research is the interaction between the metabolism and the gas exchange of root nodules, in particular the possible role of oxygen diffusion in the regulation of nitrogen fixation.

Measuring nitrogen fixation involves either the use of direct methods, which determine the actual amount of nitrogen fixed by plants, or indirect methods such as acetylene reduction which determine the activity of the nitrogenase enzyme. Acetylene substitutes for dinitrogen in the nitrogenase catalysed reaction ;



and results in the production of ethylene rather than ammonia and hydrogen. However, the exposure of many types of root nodules to saturating levels of acetylene leads to a rapid decline in nitrogenase activity (Minchin *et al.* 1983) producing inaccuracies in the conventional, closed system, acetylene reduction assay. Lack of ammonia production appears to be the predominant reason for the acetylene-induced decline, as a similar decline occurs if nodules are exposed to an atmosphere in which nitrogen is replaced with an inert gas. This decline in activity of root nodules has led to proposals that nodules are able to regulate nitrogen fixation via their gas diffusion pathways. Intuitively it would seem advantageous for plants to be able to regulate nitrogen fixation if fixed nitrogen is not required, or fixed carbon is not available. For example, when nitrate is present, nodulation in soybeans is reduced and a decline in the specific nitrogenase activity of nodules occurs. Current hypotheses are that regulation of activity is achieved by control of oxygen diffusion within the nodules.

To understand the physiology of root nodules and the regulation of gas exchange, some knowledge of the environment of root nodules and the physical behaviour of gases is required. This information can be combined with current knowledge of the physiology of root nodules and used to model their gas exchange. If the underlying assumptions are correct, these models further our understanding of the physiology of root nodules.

Another form of modelling involves examining and predicting plant growth. This modelling is valuable in determining the importance of various parameters to plant growth and allows the prediction of the response of plant growth to changes in these parameters.

## 1.2. Functioning of Nodules and the Importance of Scale

To gain a clearer understanding of nitrogen fixation it is informative to consider the scale of the processes involved in terms of size and time. Ninety five million tonnes of soybean were produced by primary producers throughout the world in 1986 (FAO Production Yearbook 1986). Yields in developed countries are generally much higher than in developing countries, but at a mean yield of  $1.8 \text{ t ha}^{-1}$ , there are some 52 million hectares of soybeans planted per year, which represents approximately  $1.5 \times 10^{13}$  soybean plants. If each plant has 30 nodules then there are some 90,000 cultivated soybean nodules per person per year on the earth.

Soybean nodules vary in number and size depending on environmental, biological and time factors. In the vegetative stages of plant growth, nodule growth follows total plant growth (Lawn and Brun 1974), and large nodules may have a fresh weight of up to 60 mg. Nodules have a bulk density of approximately  $1 \text{ g mL}^{-1}$  (Bergersen and Goodchild 1973b) and contain 80 % water by weight. One function of the nodule is to provide an environment where respiration of cells in the internal region and resistance to gas movement of the external region combine to produce a micro-aerobic environment in which nitrogenase can function. This implies a minimum functional size of nodules, below which respiration rates and resistance to gas diffusion are insufficient to lower the oxygen concentration so that nitrogen fixation can occur. A recent modelling study (Sheehy and Thornley 1988) predicts a minimum nodule size of 0.55 mm radius and the same study estimates from experimental data (Bergersen and Goodchild 1973b) a minimum nitrogen fixing nodule size of 0.4 mm radius (3 days after first appearance of nodules). However, from Figure 5 of Bergersen and Goodchild (1973b), the mean nodule size at four days is 1 mg and using a nodule density of  $0.815 \text{ g cc}^{-1}$  (their Table 3, day 8), this represents a nodule volume of  $1.2 \times 10^{-9} \text{ m}^3$ , which if spherical, would have a radius of 0.66 mm. Regardless of which experimental estimation is correct, there appears to be a minimum functional size for nodules.

A typical mature nodule may be considered as having a volume of  $30 \text{ }\mu\text{L}$ , a radius of 1.9 mm, a fresh weight of 30 mg and a dry weight of 6 mg. The central infected region of this nodule has an approximate volume of  $18 \text{ }\mu\text{L}$ , with approximately 150,000 bacteroid containing cells (ca.  $90 \text{ pL}$  each), making up 75 % of this volume (Bergersen 1982). Each infected cell contains about 8,000 peribacteroid units enclosing an average of five bacteroids (Bergersen 1982) indicating that  $6 \times 10^9$  bacteroids may be present in a typical nodule.

An estimate of nitrogen fixation rates can be made using these calculations. Soybean nodules fix nitrogen at approximately  $50 \text{ }\mu\text{mol N}_2 \text{ g}^{-1} \text{ nodule DW h}^{-1}$  ( $200\text{-}250 \text{ }\mu\text{mol C}_2\text{H}_4 \text{ g}^{-1} \text{ nodule DW h}^{-1}$ ), and a 6 mg nodule will therefore fix  $1.81 \times 10^{17}$  molecules  $\text{N}_2$  per hour ( $50 \times 10^{-6} \times 6.023 \times 10^{23} \times 0.006$ ). Each bacteroid will fix approximately

8000 molecules of  $N_2$  per second and the nodule will fix  $8.6 \mu\text{g N}$  per hour, or  $1 \text{ mg N}$  every five days. The size relation of some aspects of soybean production is summarized in Figure 1.1, utilizing a logarithmic axis.

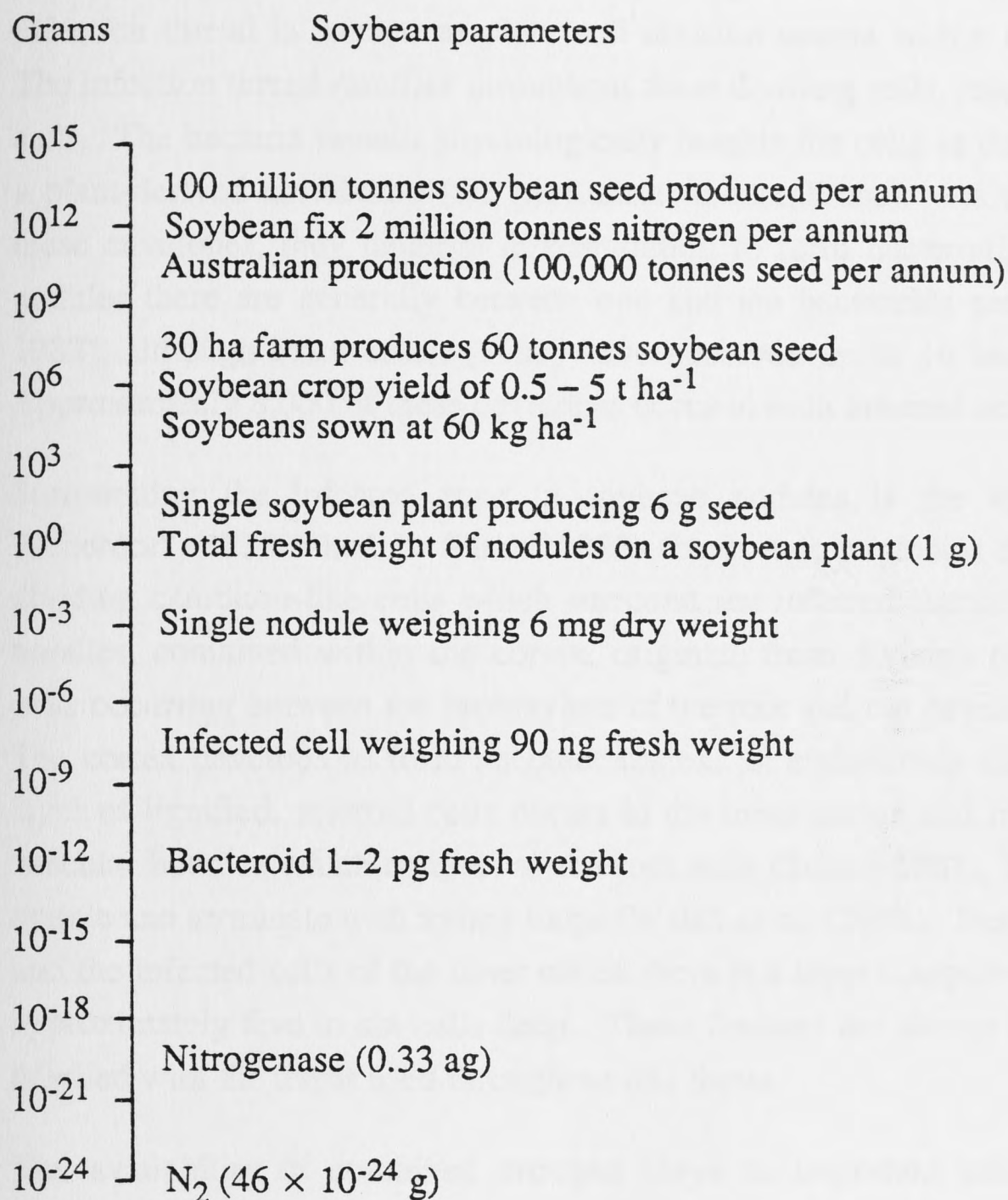


Figure 1.1 : Comparative weights in grams of various soybean parameters.

### 1.3. Initiation of Nodulation and the Structure of Nodules

Soybeans produce nodules that are typical of tropical legumes. They are classified as determinate or spherical (Sprent 1979) and are further characterised by the export of fixed nitrogen in the form of ureides (McClure and Israel 1979). Formation of active nodules involves a complex series of events, requiring the coordinated expression of both bacterial and plant genes (see reviews by Vance *et al.* 1988, Downie and Johnston 1988, Sprent 1989). Plant and bacterial compatibility is required and the environmental conditions present must also favour nodule formation.

Nodulation begins with the exchange of chemical signals between the plant and the soil rhizobia, which involves the release of flavones and flavanones from roots, which induce the expression of bacterial *nod* genes. The products of *nod* genes appear to cause root hair curling which is followed by the infection of root hair cells. An infection thread is formed as plant cell division occurs within the cortex of the root. The infection thread ramifies throughout these dividing cells, releasing rhizobia into the cells. The bacteria remain physiologically outside the cells as they are enclosed within a plant-derived membrane (the peribacteroid membrane). As rhizobia divide within these envelopes, they undergo differentiation to form bacteroids. In mature soybean nodules there are generally between one and ten bacteroids per envelope (Bergersen 1982), although Price *et al.* (1987) have observed up to 16 bacteroids per envelope. Approximately 8,000 of these envelopes occur in each infected cell (Bergersen 1982).

Surrounding the infected zone in soybean nodules is the cortex. According to Bieberdorf (1938, cited in Sutton 1983) the cortex originates from several layers of dividing cambium-like cells which surround the infected tissue. The nodule vascular bundles, contained within the cortex, originate from division of cortical parenchyma cells occurring between the protoxylem of the root and the developing infection thread. The cortex develops to form an outer cortex, an endodermis and an inner cortex. A layer of lignified, scleroid cells occurs in the inner cortex and inside this layer are the vascular bundles which connect to the root stele (Sutton 1983), branch to surround the nodule and terminate with xylary loops (Walsh *et al.* 1989b). Between the scleroid cells and the infected cells of the inner cortex there is a layer composed of parenchyma cells approximately five to six cells deep. These features are shown in Figure 1.2 which is labelled with the terms used throughout this thesis.

The availability of combined nitrogen plays an important role in the regulation of nodulation and nitrogen fixation. Low levels of combined nitrogen stimulate nodule formation and nitrogen fixation (Fred and Wilson 1934; cited in Nutman 1956, Orcutt and Wilson 1935; cited in Nutman 1956) and allow plants to avoid a brief nitrogen starvation period (Pate and Dart 1961, Mahon and Child 1979), which occurs because of the inherent delay in nodule formation and nitrogen fixation (Nutman 1956). Larger amounts of available nitrogen inhibit nodule formation at various stages of nodule development and also cause a decrease in nitrogen fixation. (For recent reviews see Streeter 1988 and Drevon *et al.* 1988a.)

1.2

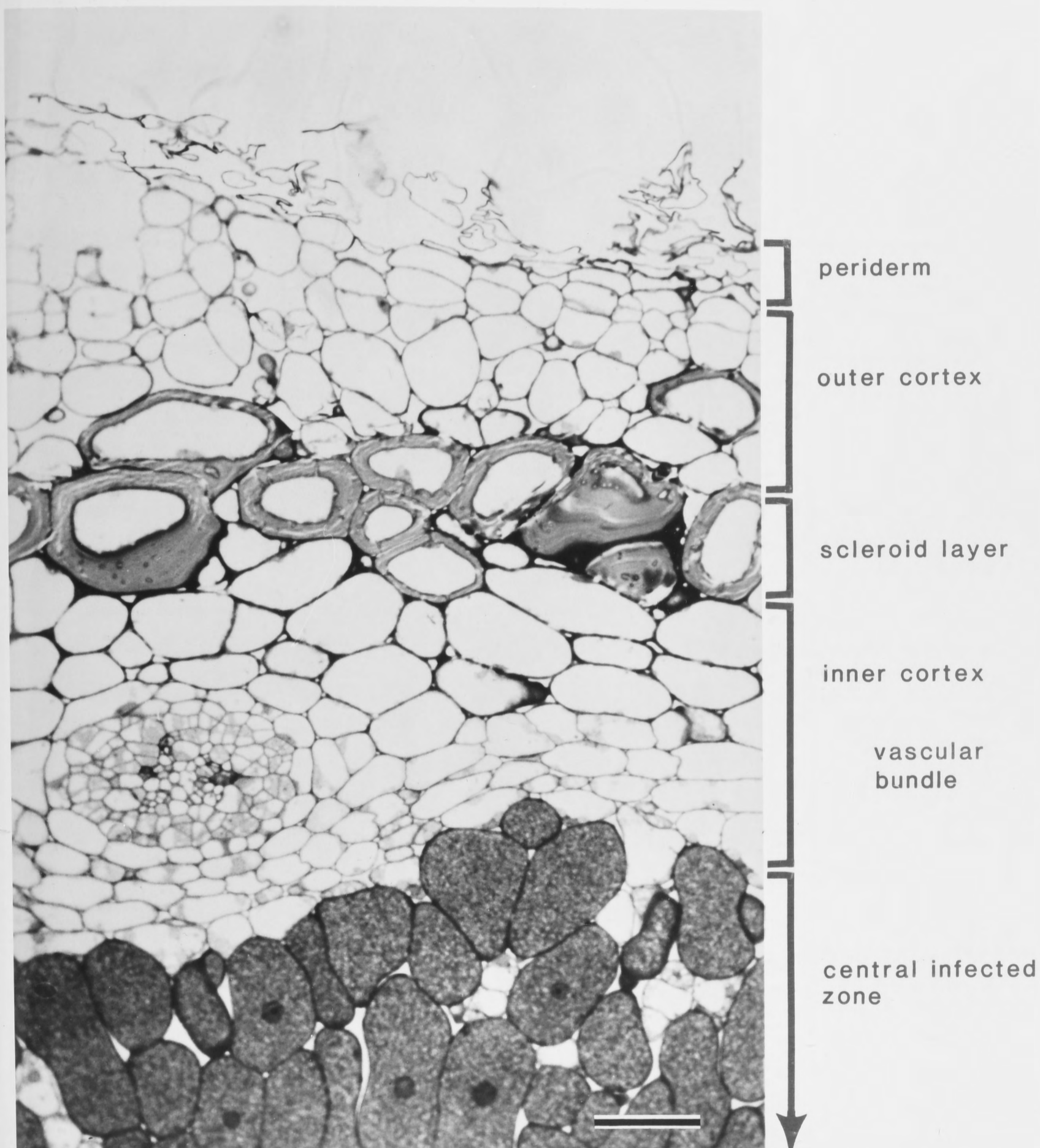


Figure 1.2 : Anatomy of the cortex of a soybean root nodule. Transverse section, light micrograph. Scale bar represents 50  $\mu\text{m}$ .

## 1.4. Carbon and Nitrogen Metabolism

Functioning nodules are organs adapted for the production of reduced nitrogen for the host plant.

Major inputs to the system are :

1. Sucrose, as the reduced carbon compound, transported to the nodules for energy, reducing power and carbon skeletons.
2. Oxygen, utilized as a terminal electron acceptor.
3. Nitrogen, as a substrate for nitrogenase.

Major outputs from the nodule are :

1. Ureides, the major compound rich in reduced nitrogen (and a smaller concentration of amides and amines) (McClure and Israel 1979), which are rapidly transported to plant parts requiring nitrogen.
2. CO<sub>2</sub>, released in respiration.
3. H<sub>2</sub>O, released in respiration.
4. H<sub>2</sub>, released as a byproduct of nitrogen fixation, although some strains of rhizobia are capable of reassimilating this H<sub>2</sub> (Robson and Postgate 1980).

This transformation involves the complex metabolism of the compartments contained within nodules. A summary of the major pathways of soybean carbon and nitrogen metabolism is presented in Figure 1.3.

### 1.4.1. Carbon metabolism

Carbon, supplied from the host in the form of sucrose, enters the nodule continuously. Kouchi and Nakaji (1985) used <sup>13</sup>C leaf feeding experiments to demonstrate the dependence of nodule respiration on recently assimilated carbon during the day. Sucrose is the major form of carbon translocated from the leaves to the nodulated roots of soybean (Clauss *et al.* 1964, Pate 1975). In <sup>13</sup>CO<sub>2</sub> photoassimilation labelling experiments, nodules began to respire <sup>13</sup>CO<sub>2</sub> within one hour of leaf feeding and labelled carbon reached 85 % of nodule respired carbon within four hours (Kouchi *et al.* 1985). Chase experiments with <sup>12</sup>CO<sub>2</sub> showed a rapid reduction in labelled <sup>13</sup>CO<sub>2</sub> from nodule respiration after approximately 12 hours, and less than 10 % of total respired carbon was labelled after 24 hours (Kouchi *et al.* 1985). In these experiments, the kinetics and level of labelling of nodule sucrose was similar to the labelling of respired CO<sub>2</sub> (Kouchi *et al.* 1985). Nodule respiration during the night is also dependent on sucrose from the shoot, which arises from starch, stored during the day in leaves and exported at night (Walsh *et al.* 1987). Leaf starch levels vary from approximately 15 mg dm<sup>-2</sup> at the beginning of the light cycle to three times that level at

the end (Upmeyer and Koller 1973). Similar variations were recorded by Kouchi *et al.* (1985) and Kerr *et al.* (1985) who reported additional changes in the starch content of petioles, stems and roots.

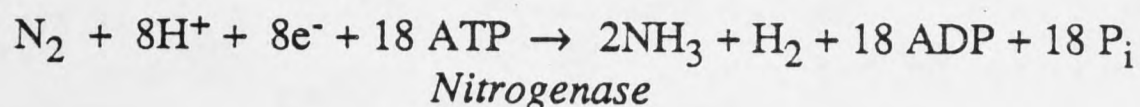
Diurnal variations in nodule respiration and nitrogen fixation rates may be considerable or non-existent, depending on the circumstances (reviewed by Minchin *et al.* 1981). Diurnal changes in temperature appear to be the major factor causing variation in day and night rates, with Schweitzer and Harper (1980) showing that shoot temperature has an effect on nodule activity probably by altering the release of stored photosynthate. Continuous nitrogen fixation during the day and night ensures efficient utilization of the plant resources invested within the nodule.

Metabolism of carbon compounds, within the nodule, begins with the cleavage of sucrose by the cytosolic enzymes alkaline invertase or sucrose synthase (Morell and Copeland 1984). Glucose and fructose produced by sucrose cleavage enter glycolysis through either the ATP-dependent phosphofructokinase/aldolase pathway or the pyrophosphate-dependent phosphofructokinase/sucrose synthase pathway (Emerich *et al.* 1988). Evidence is accumulating that the major forms of carbon taken up by bacteroids from the host are organic acids, probably malate and/or succinate. Phosphoenol-pyruvate carboxylase and cytosolic malate dehydrogenase, both key enzymes of malate synthesis are very active in nodules (Day and Mannix 1988) and using  $^{13}\text{CO}_2$  labelling, Kouchi and Yoneyama (1984) have shown that labelled succinate and malate are produced rapidly from labelled sucrose within the nodules. Furthermore, isolated bacteroids respire and fix nitrogen fastest when malate or succinate is supplied (Bergersen and Turner 1967) and recently Day *et al.* (1989) have shown malate and succinate can be taken up rapidly through the peribacteroid membrane, while disaccharides, monosaccharides and the amino acid glutamate cross the peribacteroid membrane slowly, if at all.

Bacteroid carbon metabolism acts primarily to supply reducing power and ATP for nitrogenase. Malate can be converted to pyruvate by malic enzyme which is present in bacteroids (Copeland *et al.* 1989a), and pyruvate fed into the tricarboxylic acid cycle where reduced NAD(P)H is formed. A recent study (Bergersen and Turner 1989), examining bacteroid metabolism with a low free oxygen, continuous flow technique, has suggested that bacteroids use succinate and malate to build up endogenous reserves, which subsequently become the source of reducing power for nitrogenase. Reducing equivalents, produced by either mechanism, may be utilized either as a source of reducing power for nitrogenase or by an electron transport chain to produce ATP, also required by nitrogenase.

### 1.4.2. Nitrogen metabolism

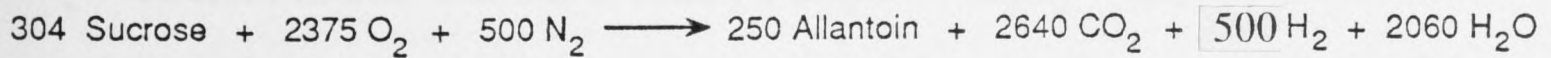
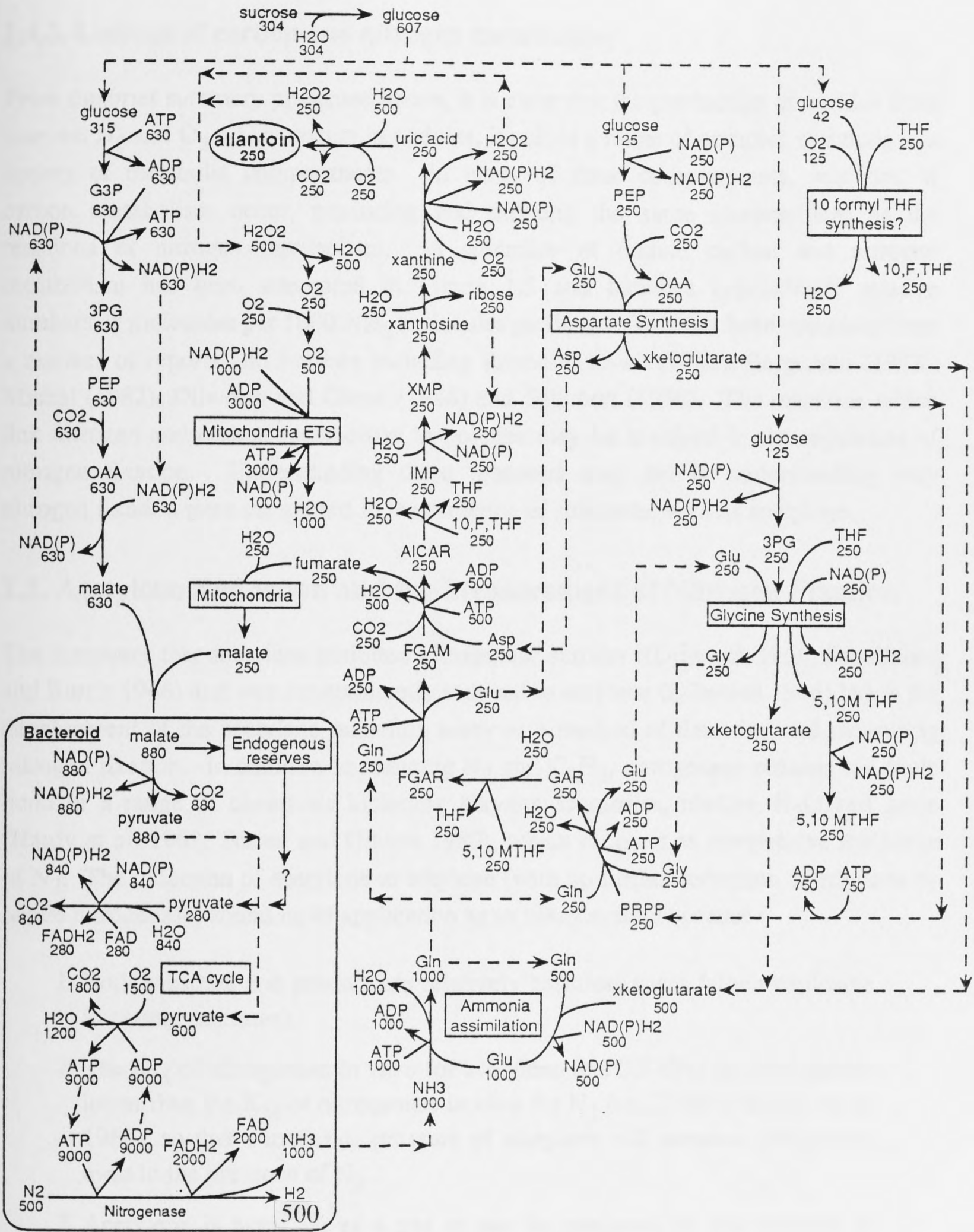
The metabolism of nitrogen within soybean nodules begins with nitrogenase, a two component enzyme complex, which is located within the bacteroids and reduces  $N_2$  to  $2NH_3$  while consuming reducing equivalents and ATP.



Ammonia, as an uncharged species, is able to diffuse relatively freely through membranes, although at neutral cellular pH levels most ammonia will be in the form of ammonium ( $NH_4^+$ ), which is observed as the first stable product of nitrogen fixation (Bergersen 1965, Kennedy 1966). Assimilation of ammonium occurs in the plant cytosol by the activity of glutamine synthetase (GS), aminating glutamate to form glutamine which undergoes transamination in the plastid by the enzyme glutamine oxoglutarate amino transferase (GOGAT), which produces two glutamate molecules from glutamine and oxoglutarate (Meeks *et al.* 1978, Schubert 1986).

Subsequent conversion of glutamate into ureides, which are the major nitrogen-export compounds of soybean nodules, involves a complex series of reactions occurring within a number of different compartments in nodule cells (Schubert 1986). The ureides, allantoin and allantoic acid, make up 60 to 80 % of the xylem transported nitrogen in nitrogen fixing cowpea (Herridge *et al.* 1978) and 78 % of the seasonally averaged xylem sap nitrogen in soybean plants depending solely on  $N_2$  fixation (McClure and Israel 1979). Ureides are formed in nodules by *de novo* purine synthesis and subsequent partial purine oxidation to allantoin and allantoic acid. Ureide synthesis in nodules is an excellent example of the role of compartmentalization in metabolism. The glycolytic enzymes of the cytosol which cleave sucrose to supply organic acids for oxidation within the bacteroids, also produce the carbon skeletons necessary for purine biosynthesis. In the plastid of infected cells purine biosynthesis occurs, producing inosine monophosphate and subsequently xanthosine monophosphate, xanthosine, then xanthine. Purine oxidation begins with the enzyme xanthine dehydrogenase which converts hypoxanthine to xanthine and xanthine to uric acid (Schubert 1986). Two recent reports put the location of this enzyme in either the cytosol of the infected cells (Triplett 1985) or the uninfected cells (Nguyen *et al.* 1986). Xanthine dehydrogenase is inhibited by the compound allopurinol. Uric acid is converted to allantoin in the peroxisome of uninfected cells by the enzyme uricase, which requires  $O_2$  (Reynolds *et al.* 1982). This requirement for oxygen in the low oxygen environment of the nodule suggests possible oxygen limitation of ureide synthesis. Conversion of allantoin to allantoic acid occurs in the endoplasmic reticulum of uninfected cells and these two types of ureides are subsequently transported in the xylem sap.





**Figure 1.3 :** An attempt to quantitatively summarize nitrogenase linked metabolism in soybean nodules. Relative numbers of molecules are expressed per 1000 ammonia molecules fixed by nitrogenase, assuming 100 % export of N in ureides. Many reactions are simplified, but most transformations of energy, reducing power, carbon, nitrogen and oxygen are included. A key to abbreviations is presented at the beginning of this thesis. (Reynolds *et al.* 1982, Bergersen 1982, Michal 1982, Dilworth and Glenn 1984 and Schubert 1986).

### 1.4.3. Linkage of carbon and nitrogen metabolism

From the brief summary presented above, it is clear that the production of ureides from sucrose,  $N_2$  and  $O_2$  which occurs in nodules, involves a range of complex reactions in a variety of metabolic compartments. In many of these compartments, reactions of carbon metabolism occur, producing and utilizing the same intermediates as the reactions of nitrogen metabolism. A summary of nodule carbon and nitrogen metabolism has been attempted in Figure 1.3 and includes approximate relative numbers of molecules per 1000  $NH_3$  molecules produced. This has been compiled from a number of reports and reviews including Reynolds *et al.* (1982), Bergersen (1982), Michal (1982), Dilworth and Glenn (1984) and Schubert (1986). The reactions which link nitrogen and carbon metabolism in nodules may be involved in the regulation of nitrogen fixation. Understanding these reactions may aid in understanding why nitrogen fixation rates are altered in the presence of substrates such as acetylene.

### 1.5. Acetylene Reduction and the Measurement of Nitrogen Fixation

The discovery that acetylene inhibited nitrogenase activity ((Dilworth 1966, Schollhorn and Burris 1966) and was concomitantly reduced to ethylene (Dilworth 1966) led to the development of the acetylene reduction assay as a method of detecting and measuring nitrogen fixation. In addition to reducing  $N_2$  and  $C_2H_2$ , nitrogenase reduces the triple bond of a range of chemicals including alkynes, isonitriles, nitriles,  $N_2O$  and azide (Hardy *et al.* 1968, Turner and Gibson 1980), which each act as competitive inhibitors of  $N_2$ . The reduction of acetylene to ethylene (with no further reduction of ethylene by MoFe nitrogenase) found rapid application as an assay system because :

1. Both substrate and product are relatively harmless gases (albeit explosive in certain mixtures).
2. The  $K_M$  of nitrogenase *in vitro* for acetylene (ca. 0.5 kPa) is considerably lower than the  $K_M$  of nitrogenase *in vitro* for  $N_2$  (ca. 10 kPa) (Hardy *et al.* 1968), so that a moderate pressure of acetylene will saturate nitrogenase even in the presence of  $N_2$ .
3. Acetylene is available as a gas or can be produced by the reaction of calcium carbide and water; ( $CaC_2 + 2H_2O \rightarrow C_2H_2 + Ca(OH)_2$ ).
4. Acetylene and ethylene can be separated by gas chromatography and a sensitive flame ionization detector enables measurement of concentrations in the order of  $4 \times 10^{-13}$  moles in 0.1 mL or 0.1 parts per million.

The conventional acetylene reduction assay was developed in the late 1960s in a number of laboratories and generally involved removing the nodules or nodulated root system from the plants, sealing them in an air-tight jar, adding saturating levels of

acetylene (10 %), then sampling the gas phase some time later (often 30 to 60 minutes) and determining the amount of ethylene produced (Hardy *et al.* 1968). Careful investigators included  $^{15}\text{N}$  analysis, using the same procedure, but introducing a known concentration of  $^{15}\text{N}_2$  rather than acetylene and this allowed calibration of the acetylene reduction to actual nitrogen fixation. Considerable variations in the ratio of acetylene reduction to  $^{15}\text{N}_2$  fixation were reported, ranging from 2:1 to 6:1 and greater (Hardy *et al.* 1973), and explanations for this range of ratios were equally diverse.

In hind-sight, the waters become clearer. Using the conventional acetylene assay, Bergersen (1970) found the specific activity of nodulated soybean roots was higher than detached nodules. In 1973 Fishbeck *et al.* (1973), also using the conventional assay, showed that acetylene reduction rates in soybean were considerably reduced if nodules were detached from the plant ( $7 \mu\text{mol g}^{-1}$  nodule FW  $\text{h}^{-1}$ ), slightly reduced if the shoots were removed from the root system ( $12.8 \mu\text{mol g}^{-1}$  nodule FW  $\text{h}^{-1}$ ) and highest in intact plants ( $13.5 \mu\text{mol g}^{-1}$  nodule FW  $\text{h}^{-1}$ ). With intact plants, Huang *et al.* (1975), observed that acetylene reduction rates decreased in the first 30 minutes of the assay, and in their subsequent analysis they measured acetylene reduction between 60 and 120 minutes as it was linear in this period ! In 1983, Minchin, Witty, Sheehy and Müller published a paper entitled : *A major error in the acetylene reduction assay: Decreases in nodular nitrogenase activity under assay conditions*. Using a continuous-flow assay system and adding saturating levels of acetylene, they detected rapid declines in nitrogenase activity (of the order of 70 %) and simultaneous declines in nodulated root respiration, for a range of symbiotic legumes. Subsequent adoption of continuous or open-flow techniques by other workers have confirmed the occurrence of the acetylene-induced decline in many legume symbioses examined (Davey and Simpson 1988), including soybean (Minchin *et al.* 1986). Interestingly, a number of workers have reported the absence of any acetylene effects for intact plants of soybean assayed by continuous-flow (Mederski and Streeter 1977, Minchin *et al.* 1983, Weisz and Sinclair 1987a,b, Drevon *et al.* 1988b, Heckmann *et al.* 1989), although the frequency of these reports is decreasing as researchers become more experienced with continuous-flow techniques. In actinorhizal plants, significant changes in nitrogenase activity rates in response to acetylene are also observed (Tjepkema *et al.* 1988, Silvester *et al.* 1988a,b).

Many other factors have also been observed to cause significant declines in nitrogenase activity. Carbohydrate deprivation caused by extended darkness (Minchin *et al.* 1985), phloem girdling (Walsh *et al.* 1987), nodule detachment (Ralston and Imsande 1982) or shoot removal (Ryle *et al.* 1985a,b, Minchin *et al.* 1986, Hartwig *et al.* 1987), causes declines in nitrogenase activity and nodulated root respiration. The presence of nitrate causes a decline in soybean (Vessey *et al.* 1988a, Carroll *et al.* 1987, Schuller *et al.* 1988) and low temperatures also lead to a reduction in nitrogenase activity and root respiration (Duke *et al.* 1979, Layzell *et al.* 1984). Even shaking the root systems to remove rooting media causes a decline in activity (Minchin *et al.* 1986).

The decline of nitrogenase activity and nodulated root respiration in response to acetylene also occurs when  $N_2$  is replaced with argon in the gas phase surrounding root nodules (Minchin *et al.* 1983). Both these results suggest that it is the lack of  $NH_3$  production which causes the decline in nitrogenase activity and nodulated root respiration (Minchin *et al.* 1983). The mechanics of this decline appear to involve an alteration to the resistance to gas diffusion within the nodules. Witty *et al.* (1984) showed that the activity of nodules exposed to acetylene could be recovered with the addition of extra oxygen, and suggested that nodule activity rates may be regulated by control of diffusion of oxygen through the inner cortex.

The conventional acetylene reduction assay continues to be used, although its inaccuracy is recognised and its use should be limited to giving a qualitative indication of nitrogenase activity only. For quantitative studies, open-flow acetylene reduction systems should be employed or alternatives such as  $^{15}N$  methods, utilized.

## 1.6. Plant Regulation of Nitrogen Fixation

The recovery of declines in nodule activity (induced by stresses such as acetylene or carbohydrate deprivation) by the addition of extra oxygen, has led to the conclusion that the resistance to gas diffusion of the nodules is altered. This has further led to suggestions that plants alter the diffusion resistance of nodules, controlling oxygen flux to the bacteroids and thus regulating nitrogen fixation rates. The facts, logic and development of this argument deserve careful examination. Set out below are a series of premises and the conclusions drawn are discussed.

### Premises

1. Nitrogenase is inhibited and irreversibly damaged by excess oxygen (Bergersen 1962, Robson and Postgate 1980).
2. Plant and bacterial respiration consumes oxygen, especially in the infected central regions of nodules.
3. Interconnecting air-spaces and leghaemoglobin facilitate rapid diffusion of oxygen within the infected zone (Bergersen 1982, Appleby 1984).
4. A gradient of oxygen exists across the inner cortex. Oxygen concentrations are close to atmospheric in the outer cortex and extremely low in bacteroid zones (Tjepkema and Yocum 1974, Witty *et al.* 1987).
5. There is a resistance to the diffusion of oxygen across the inner cortex. A layer of tightly packed cells occurs in this region, while in comparison the rest of the nodule contains many air-spaces (Bergersen and Goodchild 1973a, Tjepkema and Yocum 1973, 1974, Witty *et al.* 1987).
6. Diffusion flux is proportional to the concentration gradient divided by the resistance to gas diffusion (Fick's law) (Jacobs 1967).

7. Exposure of nodules to stress (for example, acetylene (Minchin *et al.* 1983), phloem girdling (Vessey *et al.* 1988a)) causes declines in respiration and nitrogenase activity.
8. Increasing oxygen concentration around root nodules after exposure to stress temporarily recovers the activity lost following exposure to stress (Ralston and Imsande 1982, Witty *et al.* 1984, Hunt *et al.* 1987, Vessey *et al.* 1988a,b).
9. Increasing oxygen concentration around root nodules which have not been exposed to stress does not cause a large increase in activity (Sheehy *et al.* 1983, Vessey *et al.* 1988a, Davey and Simpson 1989).

### Conclusions

From the first five premises it is concluded that a balance between oxygen diffusion and oxygen consumption is essential and is achieved in nodules. This implies that the oxygen concentration within the nodule is neither insufficient, so as to severely limit respiration, nor excessive, so as to damage nitrogenase. Evidence that this occurs can be drawn from a number of experiments. Nodules of different sizes have similar specific nitrogenase activities (Sen and Weaver 1985), indicating that larger nodules are not any more limited for oxygen than smaller ones. Indeed, if large nodules were limited for oxygen, then a different, more diffusion-efficient nodule shape would probably have evolved. Nitrogenase, within pea nodules, has a half life of approximately two days, identical to the average rate of bacteroid and plant nodule protein turnover (Bisseling *et al.* 1980), which shows that oxygen damage to nitrogenase *in vivo* is not excessive. Finally, Criswell *et al.* (1976) have shown that nodules are able to adapt to long-term changes in oxygen concentration and maintain similar rates of activity. Short-term increases in nitrogenase activity when extra oxygen is added can be explained either by the fact that a stress has been imposed on the nodule (for example, Tjepkema and Yocum 1973; the stress of detachment and acetylene exposure), or that the increase represents only a short-term gain, and in the longer term, slight limitation of the nodule for oxygen may be required for efficient utilization of carbohydrates and protection for nitrogenase.

Many stresses imposed on nodules or nodulated plants cause a decline in activity (premise 7), which in many cases can be recovered temporarily, by the exposure of stressed nodules to higher levels of oxygen (premise 8). This has led to the conclusion that in stressed nodules the resistance to diffusion of oxygen through the inner cortex is increased, resulting in a strong limitation of oxygen within the nodule. Evidence supporting this conclusion has been obtained with the use of micro-electrodes (Witty *et al.* 1987). However, alternative explanations for the increase in apparent diffusion resistance, such as mechanisms of nitrogenase protection or possible changes in the

regions of oxygen consumption, changes in the amount of oxygen consumption and alteration of the respiratory quotient, need to be considered. Bergersen and Turner (1989) have shown that bacteroids isolated from soybean exhibit a plasticity of oxygen use, with an increased demand for oxygen when free oxygen concentrations reached 40 to 90 nM. Furthermore, when malate or succinate supply to the bacteroids is altered, considerable changes in RQ and nitrogen fixation rates occur (Bergersen and Turner 1989). The implications of these results for the understanding of whole plant responses to various treatments have not been determined.

Inferences have been drawn that the increase in apparent diffusion resistance of nodules after exposure to stress, represents a controlled response by the plant to regulate nitrogenase activity (Sheehy *et al.* 1983, Witty *et al.* 1984, Hunt *et al.* 1987). Current research is focusing on possible mechanisms of changes in the diffusion resistance of nodules, how these changes may be linked to metabolism of the nodules and whether these responses are a plant-controlled response.

## 1.7. Gas Environment of Root Nodules

### 1.7.1. Soil environment

Soybean root nodules are adapted to the soil environment and while this varies across different types of soils, productive agricultural soils have generally similar characteristics. A soil structure that allows retention of moisture and free air movement is essential. The amount of air-spaces in soils of different types may vary and will change as the total porosity and moisture content of a soil changes. Generally air-spaces do not exceed  $0.4 \text{ m}^3 \text{ m}^{-3}$  (Glinski and Stepniewski 1985). The porosity of a soil primarily determines the diffusion coefficient of gases within the soil and, in conjunction with chemical and biological activities within the soil, determines the composition of soil air.

### 1.7.2. Composition of soil air

Dry atmospheric air at sea level contains (on a volume or atom basis) 78.09 %  $\text{N}_2$ , 20.95 %  $\text{O}_2$ , 0.92 % Ar and 0.035 %  $\text{CO}_2$ . The amount of  $\text{H}_2\text{O}$  present in air varies (measured as the humidity) and displaces other gases in proportion to their concentration in dry air. At 100 % relative humidity this water vapour displaces 0.6 % of each other gas at 0 °C and 4.2 % at 30 °C (Glinski and Stepniewski 1985). The relative humidity of soil air generally approaches 100 % and thus other gaseous components are diluted slightly in soil air. Nitrogen in soil air is not significantly reduced or enriched by any of the processes of the nitrogen cycle occurring in soils, although  $\text{N}_2$  concentration may vary as it compensates for the differences in the sum of

O<sub>2</sub> and CO<sub>2</sub> partial pressures. Argon, an inert gas, also does not vary in concentration, except in a similar compensatory manner (Glinski and Stepniewski 1985). Oxygen and CO<sub>2</sub> concentrations in soils vary considerably, largely due to the metabolic activities of plants, animals and micro-organisms present in soil. Oxygen in well aerated, cultivated soils does not usually fall below 15 %, although in water logging conditions, the concentration will become almost zero. The respiratory quotient of most aerobic soils is generally close to one, and so carbon dioxide concentration generally varies between 5 and 0.1 % (Glinski and Stepniewski 1985).

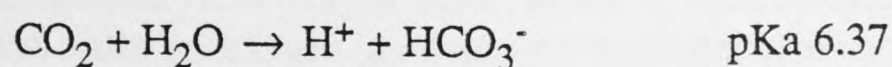
The exposure of nodules to gas molecules is a function of the composition of the soil air and its total pressure. Pressure of soil air is determined by the weight of the atmosphere above and thus varies with weather and altitude. At moderate altitudes (<1,500 m) and within extremes of weather, total pressure may vary between 83 and 104 kPa and has a mean pressure in Canberra (600 m altitude) of 95 kPa. The composition of soil air and the total pressure of this air, determine the amount of gas available for exchange at the nodule surface. Within the nodule, gas solubility and rates of diffusion become important.

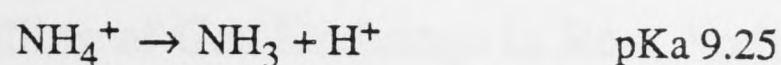
### 1.8. Diffusion and Solubility of Gases

Gas movement in nodules occurs through both the gas phase and the liquid phase. Rates of flux through the gas phase depend upon the length and shape of the pathway, the pressure gradient and the diffusion coefficient of the gas. The diffusion coefficients of gases vary approximately inversely with the square root of the molar mass (Jacobs 1967) and so most of the gases related to nitrogen fixation and the measurement of nitrogenase activity (N<sub>2</sub>, O<sub>2</sub>, CO<sub>2</sub>, NH<sub>3</sub>, Ar, C<sub>2</sub>H<sub>2</sub> and C<sub>2</sub>H<sub>4</sub>) have similar values of diffusion coefficients (see Table 1.1), except for H<sub>2</sub> which diffuses over three times faster.

Rates of gas movement through the liquid phase of nodules depend again on the length and shape of the pathway, the diffusion coefficient values in nodule solution (which for water follow a similar pattern to gas diffusion coefficients, but are some 10,000 times lower), and the concentration difference, a function of the air pressure of the gas and the relative rates of consumption or production within the nodule (Table 1.1).

The solubility of a gas in water depends upon its physical and chemical properties. The diatomic molecules O<sub>2</sub>, N<sub>2</sub> and H<sub>2</sub> are considerably less soluble than CO<sub>2</sub>, NH<sub>3</sub>, and C<sub>2</sub>H<sub>2</sub> as shown in Table 1.1. Some gases undergo a chemical reaction with water and this converts a proportion of the gas into ions in solution and thus increases the solubility. The two important gases, CO<sub>2</sub> and NH<sub>3</sub>, react with water to form carbonic acid and ammonium hydroxide respectively;





From the pKa values of the above equilibria, and assuming a cytoplasmic pH of approximately 7, it can be calculated that  $\text{CO}_2 : \text{HCO}_3^-$  will exist in a ratio of approximately 1 : 4 and  $\text{NH}_3 : \text{NH}_4^+$  in a ratio of approximately 1 : 180. Physiological or experimental values for pKs (pK in the presence of salt) may be considerably different from the values presented here and are dependent on (amongst other things) salt concentration and temperature (Yokota and Kitaoka 1985). Diffusion rates in water for  $\text{CO}_2$  and  $\text{NH}_3$  are therefore effectively increased and prediction of these rates is considerably more complicated. Rates of diffusion across different cell structures (such as polar cell membranes) will be different for charged species compared to the uncharged gases. Gas diffusion is influenced by the content of solids in water in an exponential manner, so that at 80 % water content, the diffusion rate of  $\text{O}_2$  is half that in pure water (Davis *et al.* 1987). Knowledge of gas diffusion rates within nodules (albeit only approximate) can be combined with information on nodule structure and physiology to allow the gas exchange of root nodules to be modelled.

**Table 1.1** : Some physical parameters of gases related to nitrogen fixation and the measurement of nitrogen fixation.

Gas	Formula	Molecular weight	$D_{\text{Air}}^a$ $\times 10^{-5} \text{m}^2 \text{s}^{-1}$	$D_{\text{Water}}^b$ $\times 10^{-9} \text{m}^2 \text{s}^{-1}$	Solubility <sup>c</sup> ( $\alpha$ )
Hydrogen	$\text{H}_2$	2.0	6.34 <sup>d</sup>	5.85 <sup>d</sup>	0.0182
Ammonia	$\text{NH}_3$	17.0	1.98 <sup>e</sup>	2.00 <sup>e</sup>	702
Acetylene	$\text{C}_2\text{H}_2$	26.0	1.42 <sup>g</sup>	1.76 <sup>f</sup>	1.03
Ethylene	$\text{C}_2\text{H}_4$	28.0	1.37 <sup>f</sup>	1.70 <sup>h</sup>	0.122
Nitrogen	$\text{N}_2$	28.0	1.90 <sup>d</sup>	1.62 <sup>d</sup>	0.0154
Oxygen	$\text{O}_2$	32.0	1.78 <sup>d</sup>	1.72 <sup>d</sup>	0.0310
Argon	Ar	39.9	1.59 <sup>i</sup>	1.54 <sup>i</sup>	0.034 <sup>j</sup>
Carbon dioxide	$\text{CO}_2$	44.0	1.39 <sup>d</sup>	1.96 <sup>e</sup>	0.878

<sup>a</sup> Diffusion coefficient in air. <sup>b</sup> Diffusion coefficient in water. <sup>c</sup> Dean 1973 (20°C),  $\alpha$  represents the volume of gas reduced to standard conditions dissolved in one volume of water when the pressure of the gas is 101.3 kPa. <sup>d</sup> Hunt *et al.* 1988 (20°C). <sup>e</sup> Glinski and Stepniewski 1985 (25°C). <sup>f</sup> Jost 1960 (18°C). <sup>g</sup> Calculated from ethylene value assuming diffusion rate is proportional to the inverse square root of molecular weight (Jacobs 1967). <sup>h</sup> Calculated from acetylene value, as for <sup>g</sup>. <sup>i</sup> Calculated from oxygen value, as for <sup>g</sup>. <sup>j</sup> Clever and Battino 1975, and calculated from value for oxygen (d) to convert to comparative units and 20°C.



## 1.9. Modelling of Gas Exchange in Root Nodules

The legume root nodule has adapted to allow the efficient operation of the oxygen-sensitive enzyme nitrogenase in an aerobic environment. This is achieved by the presence of a barrier to the diffusion of oxygen, probably located in the inner cortex of soybean nodules, and the presence of leghaemoglobin in the bacteroid zone, facilitating rapid oxygen diffusion at very low free oxygen concentrations. Modelling of root nodules involves combining information on nodule structure, nodule reaction rates and gas diffusion rates so that an understanding of the operation of root nodules is gained.

Different approaches have been used by different authors and their models vary in their degree of complexity. All require some assumptions to be made, allowing calculations to be simplified, and rely on experimentally obtained values. For instance, Sheehy *et al.* (1987) assume the stoichiometry of one mole H<sub>2</sub> released per mole N<sub>2</sub> reduced, which requires eight moles O<sub>2</sub> and releases eight moles CO<sub>2</sub>. Fick's law, which states that rates of diffusion are directly proportional to the concentration gradient multiplied by the diffusion coefficient of the gas, is generally assumed to be adequate to describe diffusion rates between regions of different gas concentration across the nodule cortex and is expressed as :

$$dQ = -DA \frac{\partial u}{\partial x} dt$$

Where  $dQ$  = Amount of gas with a diffusion coefficient  $D$  diffusing in time  $dt$  across area  $A$ , with the concentration gradient at the plane =  $\frac{\partial u}{\partial x}$  (Jacobs 1967).

Sinclair and Goudriaan (1981), Sheehy *et al.* (1985, 1987), Layzell *et al.* (1988) and Hunt *et al.* (1988) demonstrate the use of such models to investigate aspects of the cortical diffusion barrier, and gas concentrations within nodules.

## 1.10. Modelling Plant Growth and Function

Models are produced to simplify parts of the real world and thus help our understanding of some of the processes involved. Many plant growth models have been developed and most can be classified as either empirical or mechanistic. An empirical model fits an equation to the data, but says nothing about the underlying mechanisms, while the alternative, a mechanistic model, describes plant growth in terms of a least some of the mechanisms determining growth (Bell 1981).

## 1.11. The Present Study

The experimental chapters of this thesis are written in the format of scientific papers, each containing an introduction, results and discussion section. The work investigates growth, development and physiology of soybean during nodulation and initial nitrogen fixation, with an emphasis placed on the role of possible regulation of nitrogen fixation by the plant.

General materials and methods which were used throughout the experimental chapters are described in Chapter 2.

A mechanistic model of nodulated soybean growth is presented in Chapter 3. This model is written in BASIC and was developed to simulate the growth of nodulated soybean and the relative importance of carbon and nitrogen. The results of model simulations are presented and compared with experimental results.

The response of nodules to atmospheres containing acetylene and argon/oxygen is examined in Chapter 4, including experiments showing the apparent recovery of acetylene-inhibited nitrogenase activity with high oxygen pressures and the development of nodulated plants in the absence of  $N_2$ .

In Chapter 5 the method of using subsaturating levels of acetylene to detect nitrogenase activity is examined. An attempt is made to quantify this method and some experiments using subsaturating acetylene are described. A model simulating rates of acetylene reduction at subsaturating pressures of acetylene is presented.

The effect of a number of metabolic inhibitors on nodulated root respiration and nitrogenase activity is described in Chapter 6. In these experiments an inhibitor was sprayed on the surface of nodules and the response of nitrogenase activity followed by the use of subsaturating levels of acetylene.

Chapter 7 describes experiments which investigate adaptation of soybean nodules to various oxygen pressures and details some metabolic and structural differences. In particular, the growth of plants and the effect of acetylene on plants grown at different oxygen pressures is examined. Sections were prepared and the structure of these nodules examined by light and electron microscopy. A detailed examination of the distribution of cells and intercellular spaces within the cortex is presented.






The general discussion (Chapter 8) examines adaptation and regulation of root nodules. Oxygen diffusion within nodules is modelled and approximate rates of nodule metabolism are calculated. The anatomy and possible physiology of a previously undescribed mechanism of nodule regulation is presented and discussed.

## Chapter 2

### Materials and Methods

#### 2.1. Introduction

Throughout this study the variations in biological, environmental and experimental conditions were kept to a minimum. The plant cultivar and bacterial strain were obtained from the same stocks for all experiments and are detailed below. Plant growth conditions were standardized by using a controlled environment growth cabinet, which also allowed growth of plants throughout the year. Methods for measuring growth, gas concentrations and other experimental parameters were standardized and regularly checked during experimental work. All the research work was carried out at the Botany Department of the Australian National University. Data storage, calculations, statistics and graphics utilized the university's VAX 8700 computer system and the package SAS (Statistical Analysis System).

Symbols used on the figures throughout this thesis are standardized. Carbon dioxide efflux is represented by a solid line with no symbols (representing the trace of the infra-red gas analyser), ethylene is represented by ( ▲ ) at saturating pressures of acetylene and ( ■ ) at subsaturating pressures, with a solid line connecting the points. Acetylene is represented by ( ★ ) at low pressures and ( ● ) at saturating pressures with a large dashed line. Oxygen pressure is represented by a small dashed line without symbols. Nitrogenase activity is expressed as  $\mu\text{mol C}_2\text{H}_4$  produced  $\text{g}^{-1}$  nodule dry weight  $\text{hour}^{-1}$  or  $\mu\text{mol C}_2\text{H}_4$  produced  $\text{plant}^{-1}$   $\text{hour}^{-1}$ . Root respiration (nodule + root) was measured as carbon dioxide efflux and is expressed as  $\mu\text{mol CO}_2$  produced  $\text{g}^{-1}$  root and nodule dry weight  $\text{hour}^{-1}$  or  $\mu\text{mol CO}_2$  produced  $\text{plant}^{-1}$  (root and nodule)  $\text{hour}^{-1}$ . In the histograms of plant dry weight  represents cotyledons,  leaf,  stem,  root and  nodules.

## 2.2. Plant Culture

Seed of the cultivar Bragg of soybean (*Glycine max* (L.) Merr.) was obtained from Pacific Seed Company, Toowoomba, in September 1986 and stored in containers open to the air at 4°C. A large quantity of seed was stored and this was used for all experiments and maintained high germination rates (> 90 %) at the end of experiments in 1989. After an initial growth trial, in which wide variation in growth of seeds was observed (see section 3.3, page 32), seeds were sorted before planting and only healthy oval seeds weighing between 195 and 225 mg fresh weight were used for experiments.

For germination, approximately 60 seeds per tray (270 × 330 mm) were spread on 30 mm of rinsed vermiculite and covered with another 10 mm layer of vermiculite, and watered daily. Plants were inoculated at day five and transferred on day seven or eight into pots for solution culture. Seedlings were carefully uprooted, washed to remove vermiculite and sealed into the lid of the solution container. This was achieved by wrapping approximately 10 mL of a plastic sealing compound, Terostat VII (Teroson, GmbH, Heidelberg, West Germany), around the stem and placing the roots through a 25 mm hole in the lid of the container and sealing the Terostat VII to the lid. Generally four plants were grown in each 2.5 L plastic pot which was wrapped in aluminium foil.

Initially each pot was filled with 2.5 L of nutrient solution (Table 2.1), and the solution level was gradually reduced by transpiration, evaporation and gas bubbling. The level was maintained at approximately 800 mL in each pot by the addition of tap water every two to three days after day 15. The pH of the nutrient solution was checked every two days and adjusted to 6.3-6.7 when necessary by the addition of KOH (20 % w/v). Pots were continuously purged with air at approximately 500 mL minute<sup>-1</sup>. Almost all nodules developed on the upper part of the root in the gas phase of the pot.

The growth cabinet was set to a 16/8 hour, 26/20°C day-night cycle and irradiated with a combination of white fluorescent and incandescent lights producing 650 μE m<sup>-2</sup> s<sup>-1</sup> at the pot level. Gas purging through the pots produced a temperature around the roots of approximately 26°C during the day and 19°C at night. Plants for growth experiments were harvested between 28 and 30 days and plants for physiological studies were aged between 26 and 36 days.

## 2.3. Inoculum

*Bradyrhizobium japonicum*, strain S32a, was obtained from Dr Alan Gibson of the Division of Plant Industry, CSIRO, Canberra, and regularly sub-cultured on solid FGM medium containing 10 mM (NH<sub>4</sub>)<sub>2</sub>SO<sub>4</sub> (Howitt and Gresshoff 1985). This strain was used for all inoculations; it effectively nodulates soybean and does not express an uptake hydrogenase. For inoculation, bacteria were grown for six to seven days in

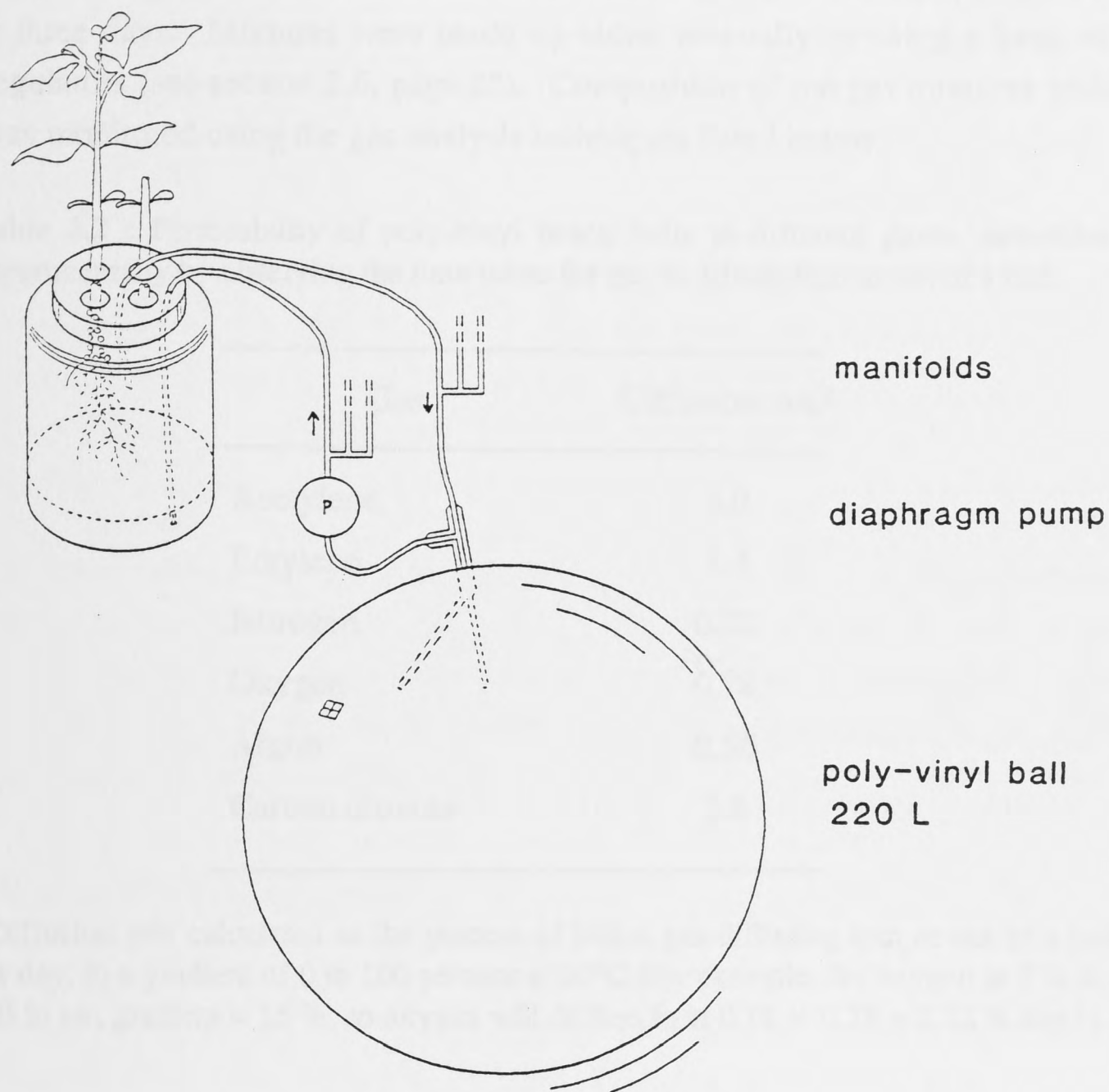
100 mL FGM media at 25°C, at which time an absorbance reading at 650 nm of approximately 0.4 was obtained. Plants were inoculated in vermiculite trays with 10 mL of culture sprinkled onto the surface, followed by a light watering. Nodules appeared six to seven days after inoculation and were functional at 10 to 11 days after inoculation.

**Table 2.1** : Composition of nitrogen free nutrient solution (Dr Alan Gibson, personal communication)

Compound	Stock g L <sup>-1</sup>	Stock added <sup>a</sup> to 50 L (mL or g)	Final conc. in µM
CaCl <sub>2</sub>	69.4	100	940
K <sub>2</sub> SO <sub>4</sub>	108.9	40	500
MgSO <sub>4</sub> ·7H <sub>2</sub> O	308.1	40	1000
KH <sub>2</sub> PO <sub>4</sub>	14.02	40	82
K <sub>2</sub> HPO <sub>4</sub>	35.88		160
Fe-seq. <sup>b</sup>	13.75	80	24
CaSO <sub>4</sub> ·2H <sub>2</sub> O		17.2 g	2000
MES <sup>c</sup>		10.5 g	1080
KOH		2.4 g	800
CuSO <sub>4</sub> ·5H <sub>2</sub> O	3.1	40	9.9
MnSO <sub>4</sub> ·4H <sub>2</sub> O	0.558		2.0
ZnSO <sub>4</sub> ·7H <sub>2</sub> O	0.288		0.80
(NH <sub>4</sub> ) <sub>2</sub> Mo <sub>7</sub> O <sub>24</sub>	0.001		0.00065
H <sub>3</sub> BO <sub>3</sub>	0.386		5.0
CoCl <sub>2</sub> ·6H <sub>2</sub> O	0.01		0.033

<sup>a</sup> mL of stock solution or grams of compound added to 50 L water, <sup>b</sup> Iron sequestrene chelate, <sup>c</sup> 2[N-Morpholino]ethanesulfonic acid. The pH of the final solution was adjusted to 6.5 with KOH.

## 2.4. Recirculating Gas System



**Figure 2.1** : Diagram of the recirculating gas system designed to allow growth of plants with roots exposed continuously to various gas mixtures.

A simple recirculating gas system with large poly-vinyl beach balls, air pumps and sealed pots was used to allow alteration of the gas composition around the roots of plants (Figure 2.1). Five complete systems were set up in parallel. In each system, gas was pumped from a 220 L poly-vinyl beach ball (750 mm diameter) to a manifold from which 3 or 4 pots were supplied. Tubes from the manifold to the bottom of each pot contained a resistance at the outlet (20 gauge syringe needle), to ensure an even flow of gas into each pot. Plants were sealed into the lids as described previously (see section 2.2, page 21) and the lids of the pots were sealed with a gasket made from slightly compressible, 3 mm, closed cell foam. An outlet tube from the top of each pot passed into another manifold and then returned into the beach ball.

The poly-vinyl material of the beach balls had a very low permeability to nitrogen, oxygen and argon and slightly higher permeability to ethylene, acetylene and carbon dioxide, as is shown in Table 2.2. Thus carbon dioxide produced by respiration did not build up in the recirculating system, while concentrations of nitrogen and oxygen did

not change significantly. Biological consumption of nitrogen and oxygen did not noticeably alter gas concentrations, and balls were replaced with fresh mixtures every two or three days. Mixtures were made up either manually or using a bank of mass flow regulators (see section 2.6, page 25). Composition of the gas mixtures within the balls was monitored using the gas analysis techniques listed below.

**Table 2.2** : Permeability of poly-vinyl beach balls to different gases, determined experimentally by observing the time taken for gas to diffuse into or out of a ball.

Gas	Diffusion rate <sup>a</sup>
Acetylene	3.0
Ethylene	1.4
Nitrogen	0.22
Oxygen	0.78
Argon	0.56
Carbon dioxide	3.6

<sup>a</sup> Diffusion rate calculated as the percent of initial gas diffusing into or out of a ball, per day, in a gradient of 0 to 100 percent at 20°C (for example, for oxygen at 5 % in a ball in air, gradient = 16 %, so oxygen will diffuse in at  $0.16 \times 0.78 = 0.12$  % day<sup>-1</sup>).

## 2.5. Gas Analysis

Nitrogen, oxygen and argon were analysed by thermal conductivity gas chromatography. Samples of gas (0.5 mL), were injected into a Varian Aerograph Series 1750 gas chromatograph, equipped with a thermal conductivity detector and a 1.5 m × 6 mm molecular sieve 5A (60/80 mesh) column run at 80°C with helium as the carrier gas. Concentrations were determined by comparison to known standards or air (21 % O<sub>2</sub> + 1 % Ar, 78 % N<sub>2</sub>). Argon and oxygen co-elute on this column and in experiments where argon and oxygen mixtures were used, oxygen concentration was determined by using an in-line oxygen electrode, calibrated in air (21 %).

Ethylene and acetylene concentrations were determined by flame ionization detection gas chromatography using a Perkin Elmer F11 model, equipped with a flame ionization detector, and a 1.75 m × 3 mm Porapak Q (60/80 mesh) column run at 60°C with nitrogen as the carrier gas. Samples could be analysed every 90 seconds. The sensitivity of the chromatograph to ethylene and acetylene was determined using prepared standards. The response of the detector to concentrations of ethylene or

acetylene between 0 and 5 kPa was linear, producing an absolute detection of  $3.71 \times 10^{-13}$  mol  $C_2H_4$  per chart unit (100  $\mu V$ ) and  $4.15 \times 10^{-13}$  mol  $C_2H_2$  per chart unit. A 1 mL plastic syringe, with very little dead space, (B-D Plastipak, Microfine III needle, no. 678410A) was set to accurately deliver  $100 \mu L \pm 2\%$ . In all open-flow studies the  $100 \mu L$  samples were injected into the gas chromatograph immediately after collection.

Carbon dioxide concentration in the flow gas was determined using an infra-red gas analyser (IRGA), ADC model 225. Gas from the assay system was passed through a condensation chamber at  $0^\circ C$  and then through the 5% analysis cell of the IRGA. The response of the IRGA was standardized with the use of gas mixing pumps and regularly checked with a calibrated gas containing 365 ppm  $CO_2$ .

Calculations to determine the molecular concentrations of gases were corrected for temperature and pressure. As outlined in section 1.7.2, page 16, the pressure in Canberra is significantly lower than standard atmospheric pressure (101.3 kPa) and varies generally between 94.5 and 96.5 kPa in the Botany Department at the Australian National University (altitude = 590 m).

## 2.6. Open-Flow Assay System

Nodulated root respiration and acetylene reduction was examined by exposing plants in their growth pots to a regulated flow of gas, normally  $600 \text{ mL minute}^{-1}$ , and monitoring gas concentrations in the outflow gas. Gas mixtures were made up manually or, when available, with a bank of six mass flow regulators (Tylan FC261 20 SLPM air, Tylan FC260 5 SLPM air, Tylan FC260 2 SLPM air, Tylan FC260 500 SCCM air, Tylan FC260 200 SCCM air, Tylan FC260 10 SCCM air, controlled by a Tylan RO28 controller).

Instrument-grade acetylene was bubbled through concentrated sulphuric acid and two water scrubbers to remove impurities and acetone. All other gases were instrument-grade (Commonwealth Industrial Gases, Canberra) and used as supplied.

## 2.7. Analysis of Plant Material

Plants for growth analysis were individually harvested, dried to a constant weight at  $80^\circ C$  and divided into cotyledons, leaves, stems (+ petioles), roots and nodules for dry weight determination.

Nitrogen and carbon content of plant material was determined using a Carlo Erba NA 1500 nitrogen carbon analyser, by combustion of dried samples and quantitative analysis of gases produced ( $N_2$  and  $CO_2$ ). Plant material was separated into leaves,



stems (+ petioles), roots, nodules and cotyledons, oven dried (80°C) and ground in a high speed mill. Homogeneous samples weighing between 5 and 20 mg were analysed in duplicate against acetanilide standards. Duplicate samples did not vary more than 0.05 % absolute nitrogen or 0.5 % absolute carbon.

## 2.8. Chlorophyll Determination

Total chlorophyll content of leaf discs was determined using a technique developed from Arnon (1949) (C.A. Critchley unpublished). Fresh discs were ground in a measured volume of 80 % acetone and centrifuged at 5000 rpm in a MSG benchtop centrifuge. Absorbances at 645, 663 and 710 nm were determined and chlorophyll concentration calculated using the formula,

$$\text{chlorophyll concentration (mg mL}^{-1}\text{)} = 8.02(A_{663} - A_{710}) + 20.2(A_{645} - A_{710}).$$

## 2.9. Measurement of Photosynthesis

Photosynthesis of primary leaves was determined with a Li-Cor LI-6200 portable photosynthesis system, while the plant was in the growth cabinet. Individual leaves were clamped into the 4 L chamber and analysis was completed within approximately one minute.

## 2.10. Haem Content

Haem content of nodules was estimated using the procedure of Appleby and Bergersen (1980). A weighed amount of whole nodules were ground in 10 mL buffer (50 mM  $\text{KH}_2\text{PO}_4$ , 1 mM EDTA, pH 7.4) and a 5 mL sample centrifuged at 20,000 g for 15 minutes in a Sorvall SS-34 rotor. A 1.5 mL aliquot of the supernatant was added to 1.5 mL alkaline pyridine reagent (4.2 M pyridine, 0.2 M NaOH) and mixed. One mL was poured into each of two cuvettes and the baseline determined (500-600 nm); the sample cuvette was reduced with a few crystals of sodium dithionite and the reference oxidised with a few crystals of potassium ferricyanide and the spectrum recorded. Haem content (mM) was calculated as  $(A_{556} - A_{539})$ , using a difference extinction coefficient of 23.4 (Appleby and Bergersen 1980).

$$\text{Haem concentration (mM)} = \frac{(A_{556} - A_{539}) \times 2D}{23.4}.$$

## 2.11. Microscopy

Transverse sections (0.6 to 1 mm) were cut through the centre of fresh nodules of uniform size (ca. 3 mm) and immediately fixed in 2.5 % glutaraldehyde in 30 mM 1,4-piperazinediethanesulfonic acid (PIPES)-NaOH (pH 7.0), plus 5 mM  $MgCl_2$  and stored overnight at 4°C. Fixed nodule slices were washed in 50 mM PIPES-NaOH (pH 6.8) for 30 minutes for three cycles, post-fixed in the wash buffer with 1 %  $OsO_4$  for two hours at 0°C, washed again as above and placed overnight in 1 % uranyl acetate in 50 mM Na-acetate buffer (pH 5.5) at 4°C. The samples were then dehydrated through an ethanol series (5, 10, 20, 40, 50, 70, 95, 100 %) in 20 minute steps, stored overnight in 100 % ethanol, transferred to propylene oxide and embedded in Spurr's resin.

For light microscopy, thin sections (1  $\mu m$ ) were cut on an ultramicrotome and stained with 0.5 % toluidine blue in 25 mM phosphate buffer (pH 7). An Ortholux II (Leitz, Wetzlar) photo-microscope was used to examine the sections. For transmission electron microscopy ultrathin sections were mounted on a copper grid, stained with 2 % barium permanganate and examined on a Zeiss EM 109 transmission electron microscope.

## Chapter 3

### Nitrogen and Carbon Partitioning in Soybean Seedlings

#### 3.1. Introduction

Theoretically plant growth is limited only by genetic potential, but environmental factors almost always modify this potential. Water is the most common factor limiting plant growth, and other major factors include light, temperature, CO<sub>2</sub> concentration, nutrient availability, competition, predation and toxicity. There are a vast number of reports examining the growth of plants and many models describing plant growth have been constructed.

Of particular interest to this study is the effect of carbon and nitrogen availability on the growth of symbiotic soybean. Nodules are an important sink for carbon and source of nitrogen within plants. This brief study of the early growth of soybean helped to clarify the role of nitrogen fixation in early plant development. Two experiments investigating plant growth using the functional analysis technique (Hunt 1982) were carried out, providing information on the pattern of soybean growth over the first 30 days after sowing. A simple mechanistic model in the form of a computer program was developed to simulate this early growth period.

#### 3.2. Method of Calculation

A copy of the program, named Soyfix, is contained in Appendix I (page 149). This program is written in the computer language BASIC (VAX BASIC, 3.2) and is divided into separate, ordered segments. The model uses published values, and those obtained experimentally in this thesis (see section 3.3, page 32), of photosynthesis, respiration and nitrogen fixation rates, combined with relative partitioning coefficients for carbon and nitrogen derived empirically from growth experiments, to produce daily increments in dry weight and nitrogen content of model plants. Written below is a guide to the program (referenced to line numbers), which outlines the purpose of each section, the assumptions made and the origin of the parameters used.

##### *Output (25-27, 400-500)*

Two files are opened to receive output which is formatted in the lines 400 to 500. These output files are written so they can be read into a program for graphic display.

Lines 440 and 445 print output to the terminal to give an instant check on the program. These output lines can be varied depending on which variables are of interest.

#### *Defining initial values (28-122)*

Most variables are initially set to 0. Other variables such as nodule number, cotyledon dry weight and daylength are assigned a value which can be altered by changing the value or including input statements. Cotyledon and leaf photosynthesis are assigned the values of 0.2 and 0.7 mg CO<sub>2</sub> m<sup>-2</sup> s<sup>-1</sup> respectively (Upmeyer and Koller 1973, Boon-Long *et al.* 1983, Harris *et al.* 1986). Nitrogen content of the seed was set at 6 % (this study).

#### *Growth stage control (510-560)*

When plants are less than three days old, there is no photosynthesis and all carbon comes from export from the cotyledon. When they are older than three days, cotyledon and leaf photosynthesis are calculated and added to the carbon exported from the cotyledon. The program finishes when plants are 30 days old.

#### *Growth at less than three days (600-692)*

Carbon available from the cotyledon is calculated as 1/30 of the original cotyledon dry weight multiplied by the carbon content of the cotyledon (0.52, this study), and partitioned to the roots, stems and leaves; half of this is lost in respiration. This rate of carbon export approximates that observed in experiments and a portion of the carbon remains with the cotyledons when they fall.

#### *Cotyledon export, days 3 to 17 (700-750)*

Carbon available from the cotyledon is calculated as above, partitioned and exported to the root, stem or leaf. If the day is greater than 17, then cotyledon export ceases as the cotyledons have abscised.

#### *Cotyledon and leaf photosynthesis (770-855, 1280-1290)*

Cotyledon or leaf area is calculated. Cotyledon area depends on the age of the cotyledon (4 or 6 cm<sup>2</sup>), leaf area is dependent on the leaf dry weight and the age of the plant, as leaves get heavier with age (experimental data, this study). Leaf photosynthesis is multiplied by a leaf nitrogen factor (1280-1290), as photosynthesis rate is dependent on the nitrogen content of the leaves (experimental data, page 33, Tolley-Henry and Raper 1986). Total photosynthetic carbon from the cotyledons and leaves is combined into one variable for allocation.

*Allocation of photosynthate (860-888)*

Carbon available from cotyledon export and from cotyledon and leaf photosynthesis is partitioned for import into stems, leaves, roots or nodules and converted into carbohydrate. Partitioning depends on the age of the plant, as import by the nodule only begins at day 13 and the leaf to stem partitioning ratio changes as the plant gets older (experimental data, this study).

*Maintenance and growth respiration (900-986)*

Maintenance respiration is calculated as a fraction of dry weight with different rates for each plant part, obtained from published values (Ryle *et al.* 1983) and my own experiments. Leaf and stem respiration is assumed to occur only at night. Respiration associated with growth is taken as half of the carbohydrate imported into each part. Total respiration is the sum of maintenance and growth respiration for each part.

*Daily dry weight calculation (988-1025)*

Daily dry weight is calculated for each plant part by adding the carbohydrate import to the previous day's dry weight and subtracting the total daily respiration.

*Calculation of available nitrogen (1035-1056)*

Nitrogen is available from cotyledon, nodule and applied nitrogen sources. Cotyledon nitrogen is available at a rate of 1/19 of the initial cotyledon nitrogen per day, for the first 17 days (experimental data, this study). Nitrogen available from nodule fixation is calculated as 1/8 of the nodule maintenance respiration (Rainbird *et al.* 1984), if the individual nodule respiration is greater than 0.5 mg CH<sub>2</sub>O day<sup>-1</sup> (this sets a minimum limit on functional nodule size). The amount of applied nitrogen available depends upon the relative amount supplied and the root respiration rate. Total nitrogen available is calculated as the sum of all nitrogen sources.

*Partitioning of nitrogen (1062-1150)*

The total available nitrogen is divided between the plant parts by first allocating nitrogen to the nodules at a set percentage of the nodule dry weight (6 %, this study). The remaining nitrogen is partitioned between the leaves, stems, and roots by calculating a factor for the maximum possible nitrogen content and then partitioning available nitrogen as a fraction of this factor to each plant part.

*Daily increment and program cycling (1500-10000)*

Having completed the calculations, the program cycles to print the daily results and calculate the next days growth. Further modifications can be easily made to the

program to enable repeated loops as one factor is altered slightly for each successive loop. For example, to determine the effect of cotyledon dry weight on final dry weight at 30 days, a loop can be added to increase cotyledon dry weight in steps of 27 mg. This is done by inserting the following lines :

```

32      Let cotyori = 103.5
34      For I = 1 to 6 step 1
36          Let cotyori = cotyori + 27

10000   Next I
11000   End

```

Loops can be created inside other loops so the effect of changing two factors can be determined. The output is sent to files which can be visualised as graphs.

### 3.3. Results

An initial growth experiment was carried out to gain an understanding of the balance of carbon and nitrogen supply in developing soybeans. The sequential harvest method was used, with four plants, each from a different pot, harvested each day and the means of each daily harvest are presented in Figure 3.1. The results show that cotyledon dry weight is steadily reduced as the growth of other plant parts occurs. Significant nodule dry weight is present after day 15.

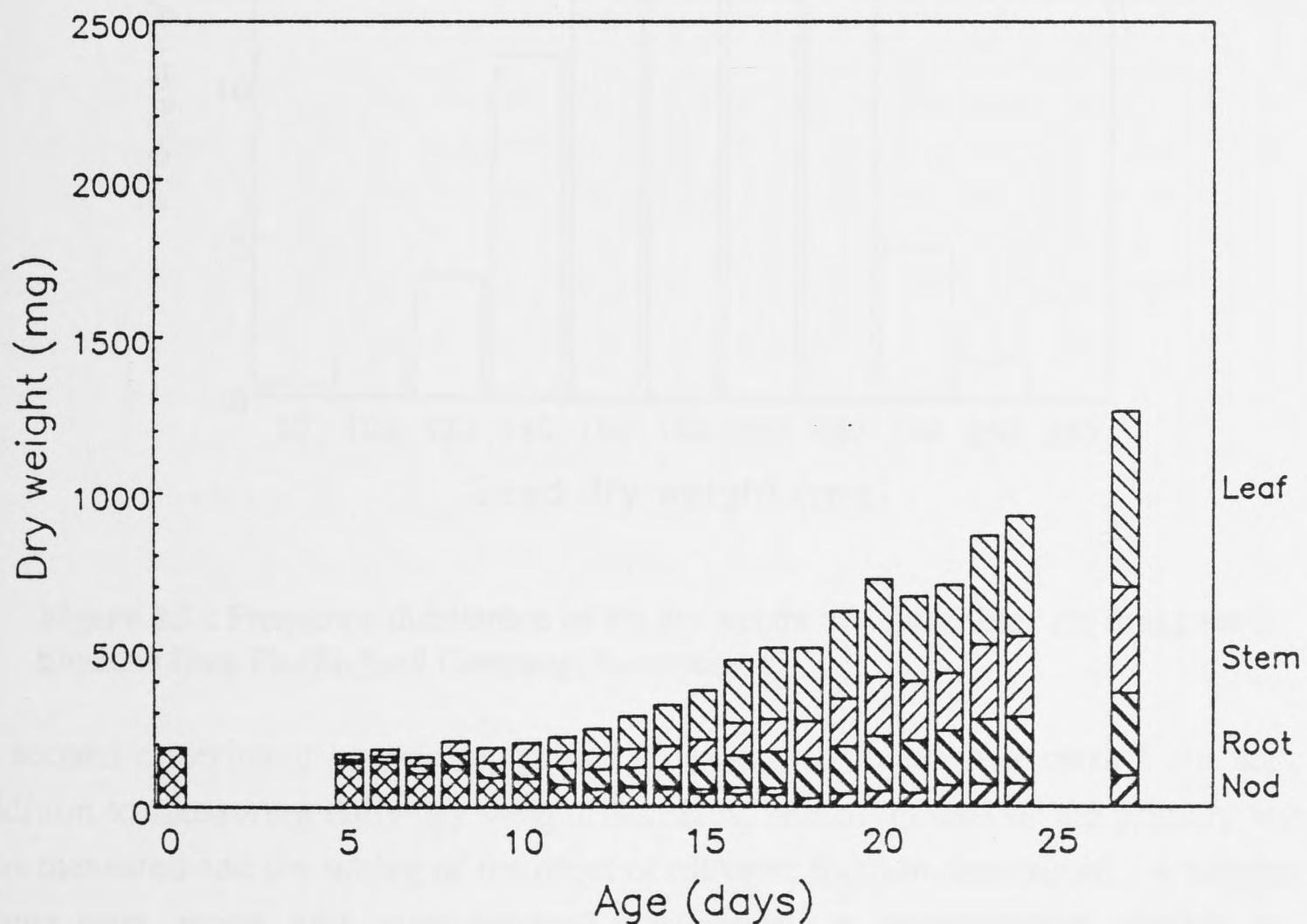

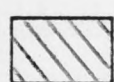
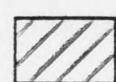

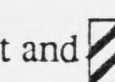
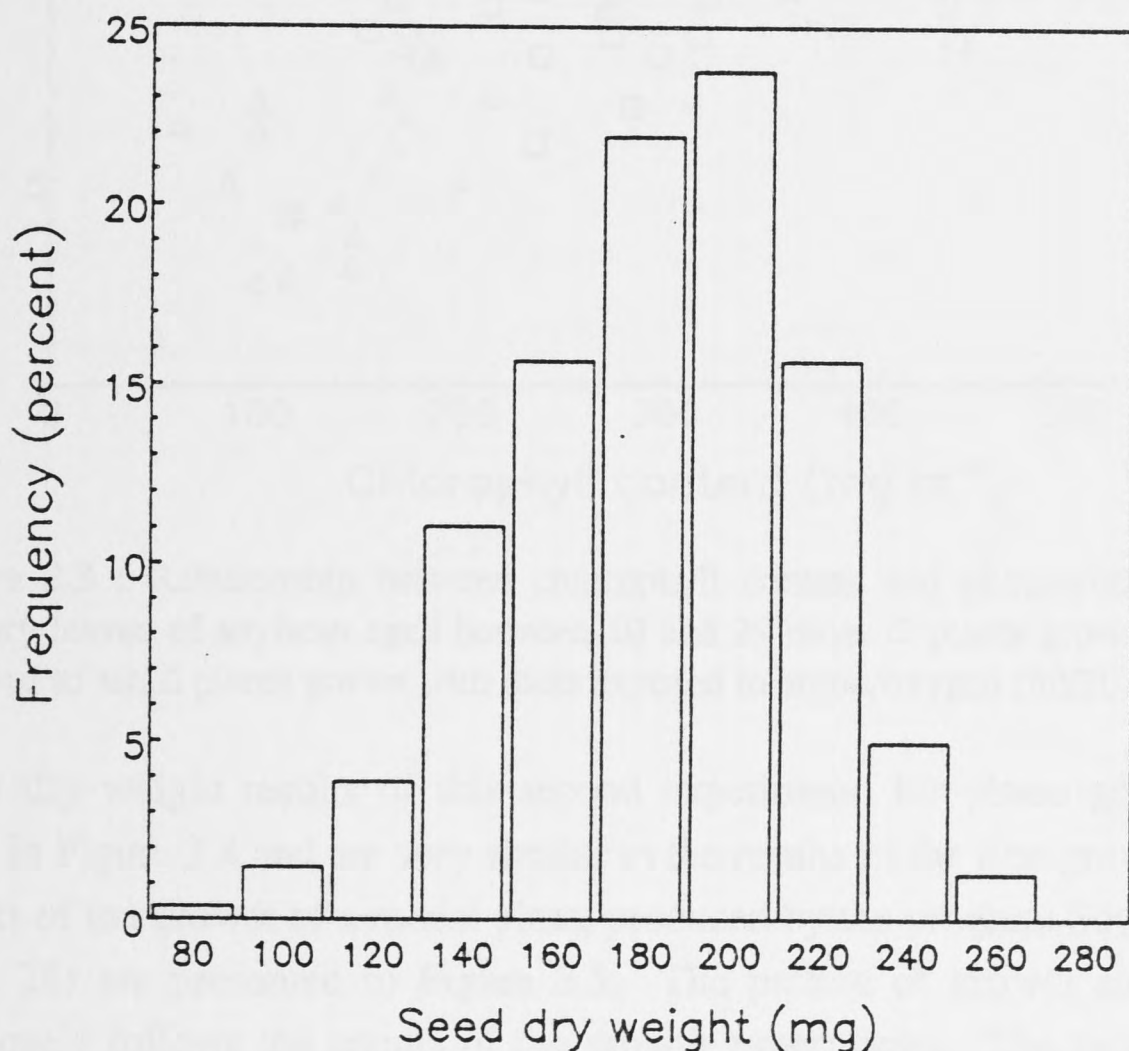


Figure 3.1 : Growth of soybean from seed. Bars represent the mean of three plants harvested on each day.

 represents cotyledon, 
  leaf, 
  stem, 
  root and 
  nodule.

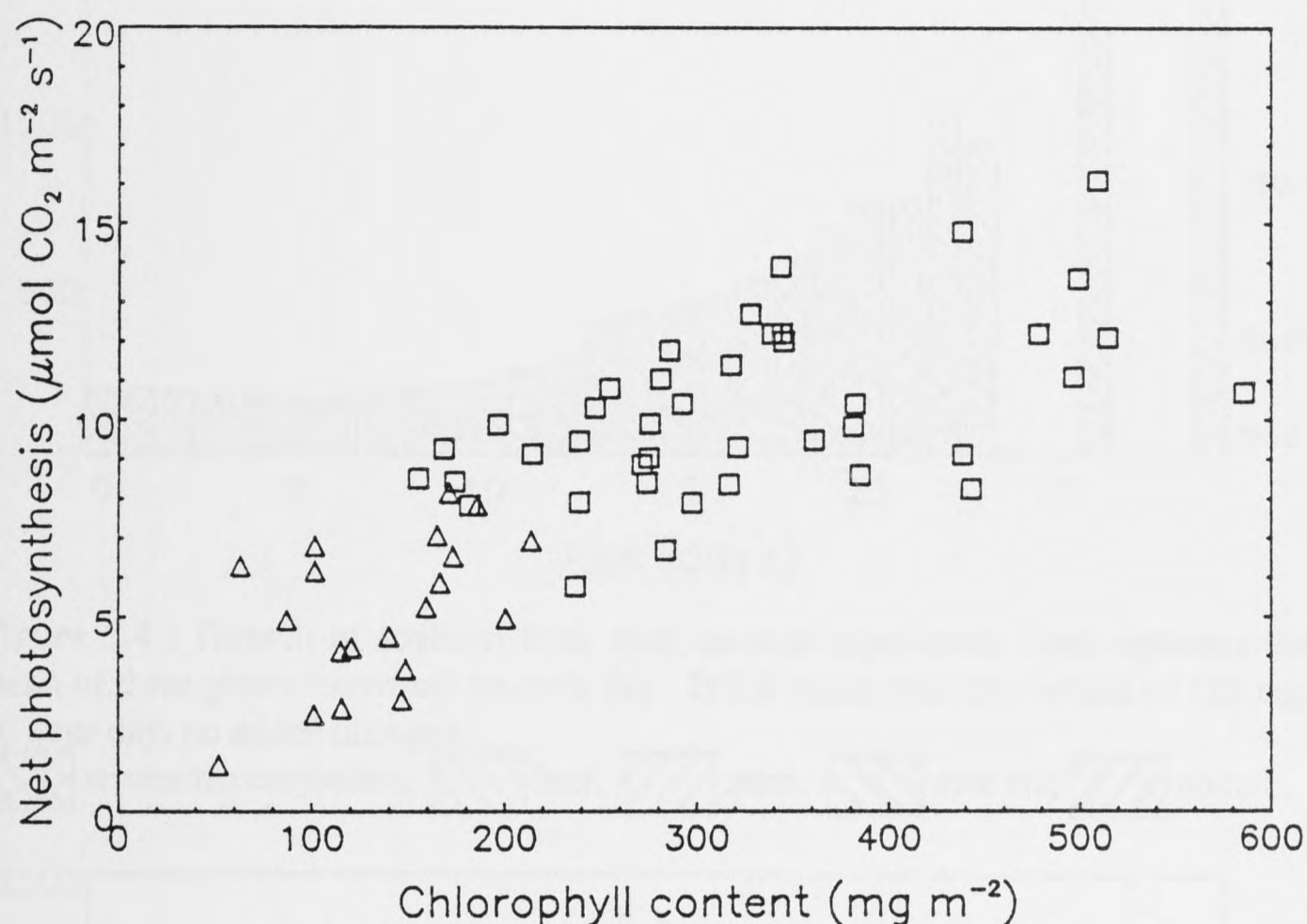
There was a considerable variation present in the results of this first growth experiment and the range of initial seed weights present in the seed source was investigated as a possible cause of this variation. Over 500 seeds were oven dried and weighed (Figure 3.2). The seeds ranged in size from 80 mg to 260 mg, although most seeds weighed between 150 and 230 mg. In large seeded plants, such as soybean, early growth is very dependent on stored seed reserves and, clearly, seeds of different size will produce a range of different sized plants, even if the subsequent relative growth rate is the same. For all subsequent experiments, only seeds with fresh weights of between 195 and 225 mg were used to avoid excessive variation in growth caused by the variation in seed weight. Fresh weight of seeds was approximately 10 % higher than the oven dried weight.



**Figure 3.2** : Frequency distribution of the dry weight of *Glycine max* cv. Bragg seeds obtained from Pacific Seed Company, Toowoomba.

A second experiment examining growth in young soybeans was carried out and, in addition to measuring daily dry weight increases, photosynthesis of the primary leaves was measured and the timing of the onset of nitrogen fixation determined. A number of plants were grown with roots exposed continuously to argon/oxygen (80/20) gas to prevent nitrogen fixation and cause severe nitrogen starvation. Leaf photosynthesis rate showed a correlation with chlorophyll content in plants grown in both air and

argon/oxygen at a variety of ages (Figure 3.3). The chlorophyll content of the leaf is largely determined by the available nitrogen, with a chlorophyll content of  $500 \text{ mg m}^{-2}$  occurring in leaves containing approximately 4 % nitrogen (data obtained in this study). Using the conventional acetylene reduction assay, nitrogenase activity was first detected at 14 days and increased to significant levels after day 16.




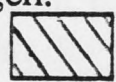



**Figure 3.3** : Relationship between chlorophyll content and photosynthesis in the primary leaves of soybean aged between 10 and 29 days.  $\square$  plants grown with roots exposed to air,  $\Delta$  plants grown with roots exposed to argon/oxygen (80/20).

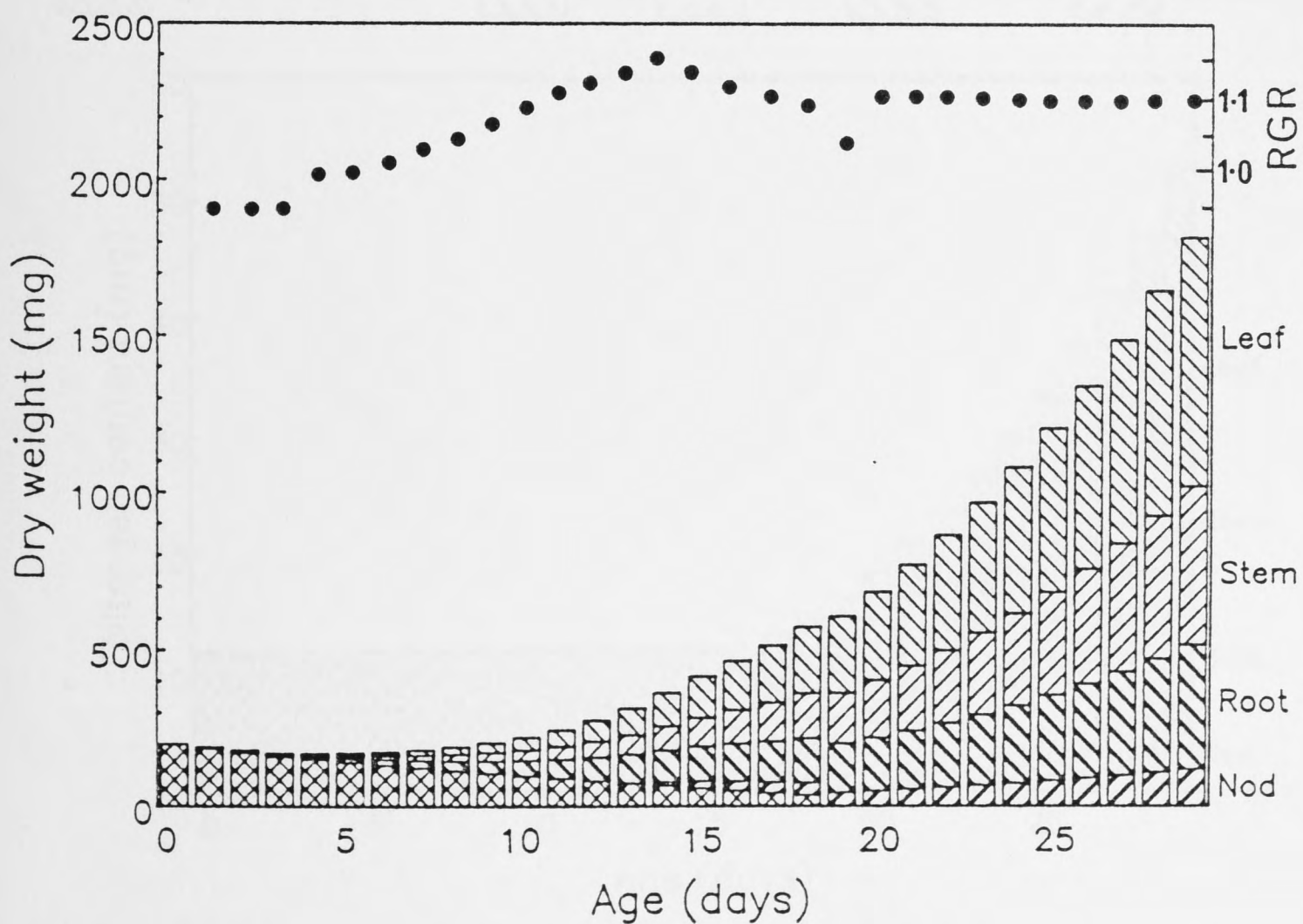
The daily dry weight results of this second experiment, for plants grown in air, are presented in Figure 3.4 and are very similar to the results of the first growth experiment. The results of the growth of a model plant, produced by the program Soyfix (see section 3.2, page 28) are presented in Figure 3.5. The pattern of growth simulated by the model, closely follows the results of the growth experiments. The model is based on data from these experiments and other published accounts, referenced in the preceding section. Both the experimental and model results show that the dry weight of cotyledons is reduced as leaf, stem, root, and nodule dry weight increases. There is an initial decrease in total plant dry weight as respiration of the plant exceeds photosynthesis. At day 5 plant dry weight begins to increase. In the model, relative growth rate continues to increase to day 14, then decreases from day 14 to 20, before increasing again to stabilize at about 10 % per day. This inflexion of growth rate also seems to occur in the growth experiments, but is not as obvious because of variation in the data. It probably represents a stage when nitrogen is limiting growth.




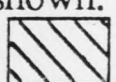





**Figure 3.4 :** Growth of soybean from seed, second experiment. Bars represent the mean of three plants harvested on each day. Initial mean seed dry weight of 195 mg, 16 hour day, no added nitrogen.

 represents cotyledon, 
  leaf, 
  stem, 
  root and 
  nodule.



**Figure 3.5 :** Simulated growth of soybean by the model Soyfix. Initial seed dry weight of 195 mg, 16 hour day, 23 nodules per plant, no added nitrogen. Calculated daily relative growth rate is shown.

 represents cotyledon, 
  leaf, 
  stem, 
  root and 
  nodule.

The nitrogen content of plants of the first experiment (Figure 3.6), shows that nitrogen does not increase significantly in the plant until after day 19. This also occurs in the model (Figure 3.7), making plant growth limited for nitrogen between days 14 and 19.

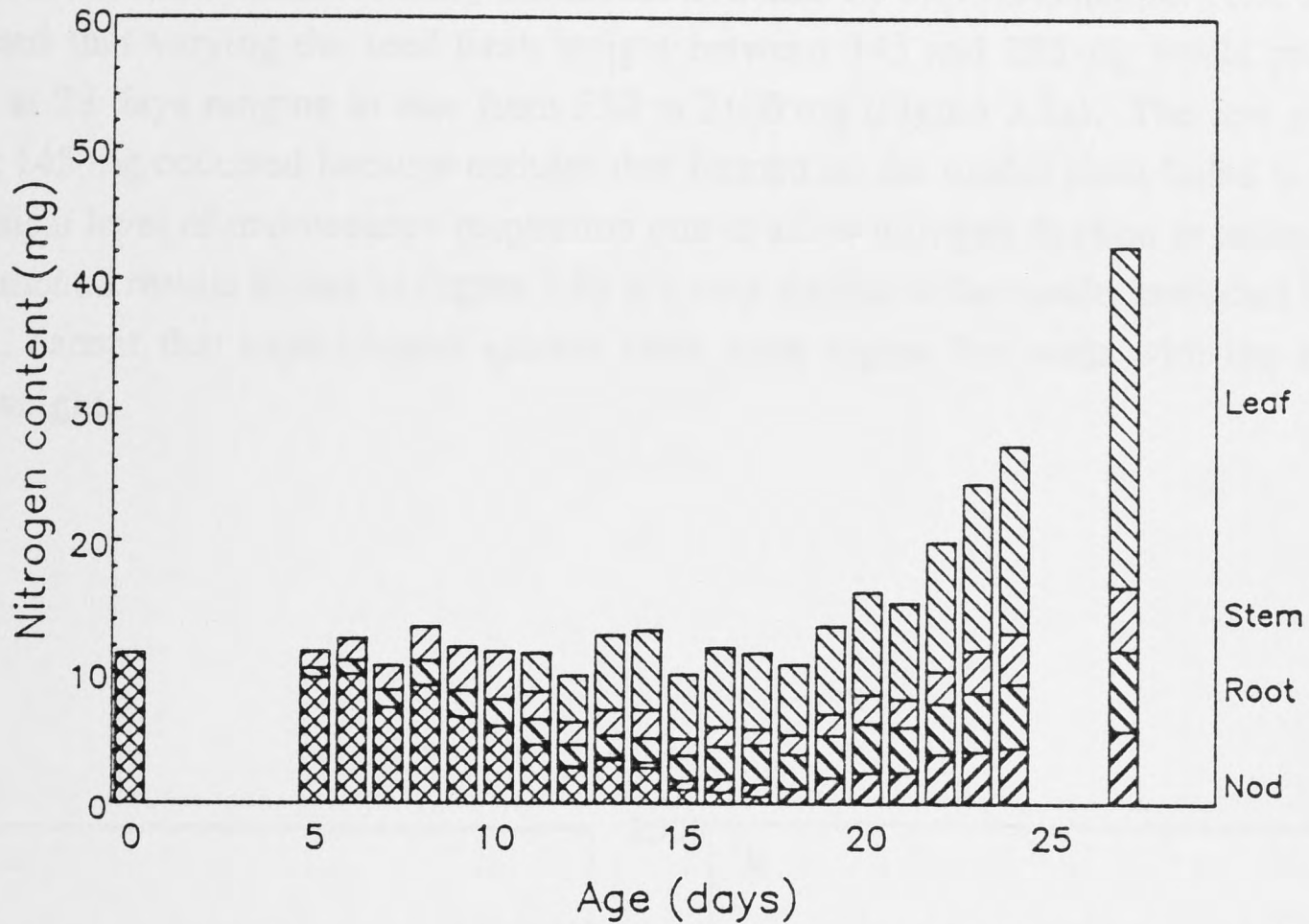


Figure 3.6 : Nitrogen content of plant parts of developing soybean. Initial mean seed dry weight of 195 mg, 16 hour day, no added nitrogen.

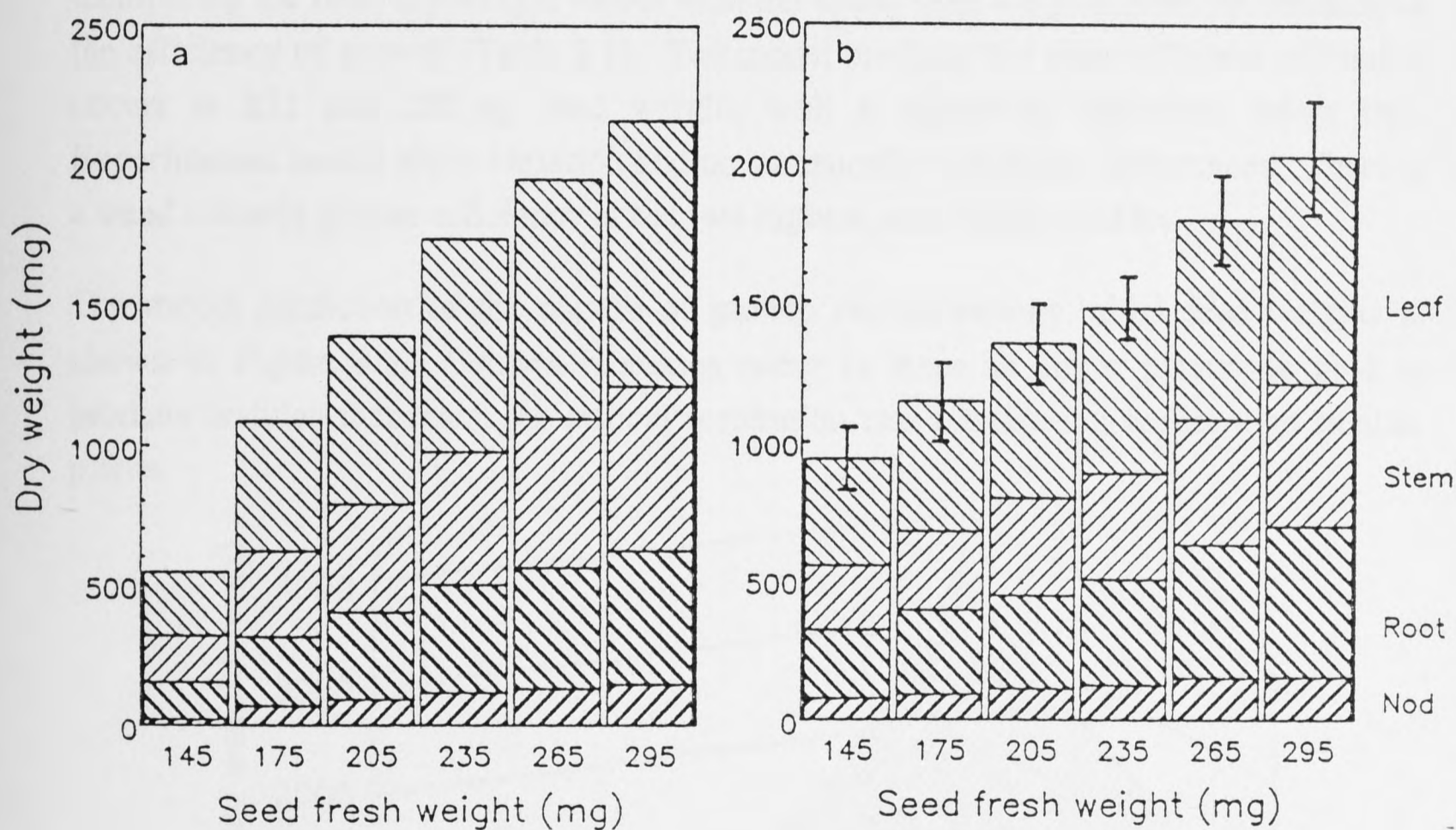
represents cotyledon, leaf, stem, root and nodule.



Figure 3.7 : Simulated nitrogen content of soybean using the model Soyfix. Initial seed dry weight of 195 mg, 23 nodules per plant, 16 hour day, no added nitrogen.

represents cotyledon, leaf, stem, root and nodule.

The model was used to test how changes in various parameters may affect plant growth. The effect of variation in initial seed dry weight, which had been standardized for other experiments, was examined using the model and also by experimentation. The model predicted that varying the seed fresh weight between 145 and 295 mg would produce plants at 28 days ranging in size from 550 to 2100 mg (Figure 3.8a). The low growth rate at 145 mg occurred because nodules that formed on the model plant failed to reach the critical level of maintenance respiration rate to allow nitrogen fixation to occur. The experimental results shown in Figure 3.8b are very similar to the results predicted by the model, except that experimental growth rates were higher for seeds with the lowest fresh weight.



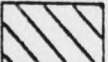



**Figure 3.8** : Dry weight of plant parts at 28 days after planting seeds of varying initial fresh weight. (a) Results predicted by the model Soyfix, at 16 hour daylength, 23 nodules per plant and no added nitrogen. (b) Experimental results, 8 plants per treatment, at 16 hour daylength and no added nitrogen. 95% confidence limits shown.  represents leaf,  stem,  root and  nodule.

Table 3.1 : Efficiency of growth of soybean with different initial seed fresh weight.

Seed fresh weight	Model relative <sup>a</sup> growth rate	Expt. relative <sup>a</sup> growth rate
145	1.0523	1.0727 ± 0.0039
175	1.0715	1.0733 ± 0.0038
205	1.0749	1.0735 ± 0.0037
235	1.0780	1.0718 ± 0.0026
265	1.0779	1.0747 ± 0.0033
295	1.0777	1.0750 ± 0.0041

<sup>a</sup> Mean relative growth rate, day 0 to day 28. Experimental values ± 95 % confidence limits.

Comparing the final dry weight values with the initial seed weights gives an estimate of the efficiency of growth (Table 3.1). The model predicts that most efficient utilization occurs at 235 and 265 mg seed weight, with a significant reduction below this. Experimental results show variation and no statistically significant differences. There is a trend towards greater efficiency at the two highest seed weight classes.

The model prediction of the pattern of growth rate at various initial seed weights is shown in Figure 3.9. Growth increases occur in steps as larger plants are able to produce nodules that reach the critical respiration rate for fixation earlier than smaller plants.

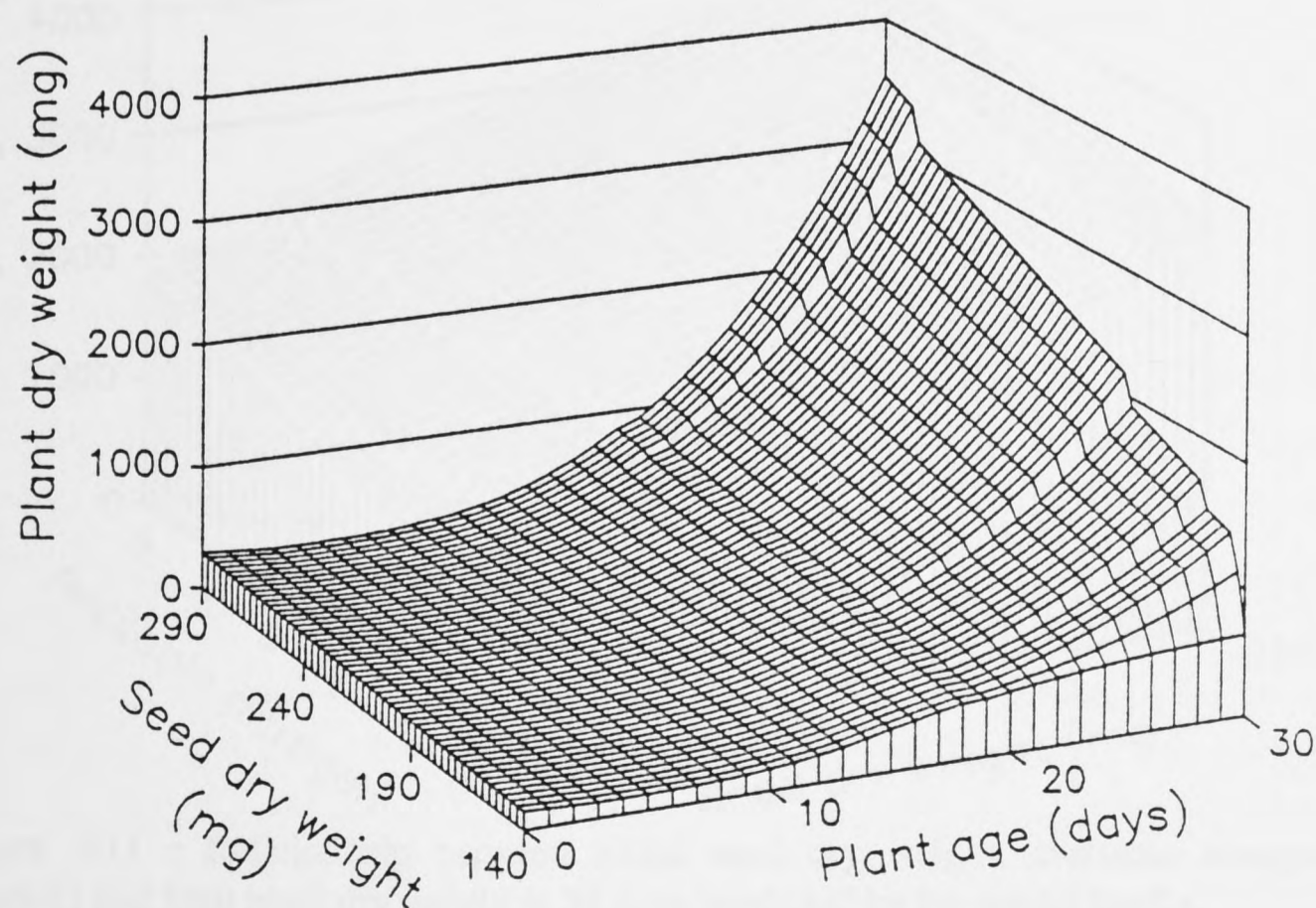
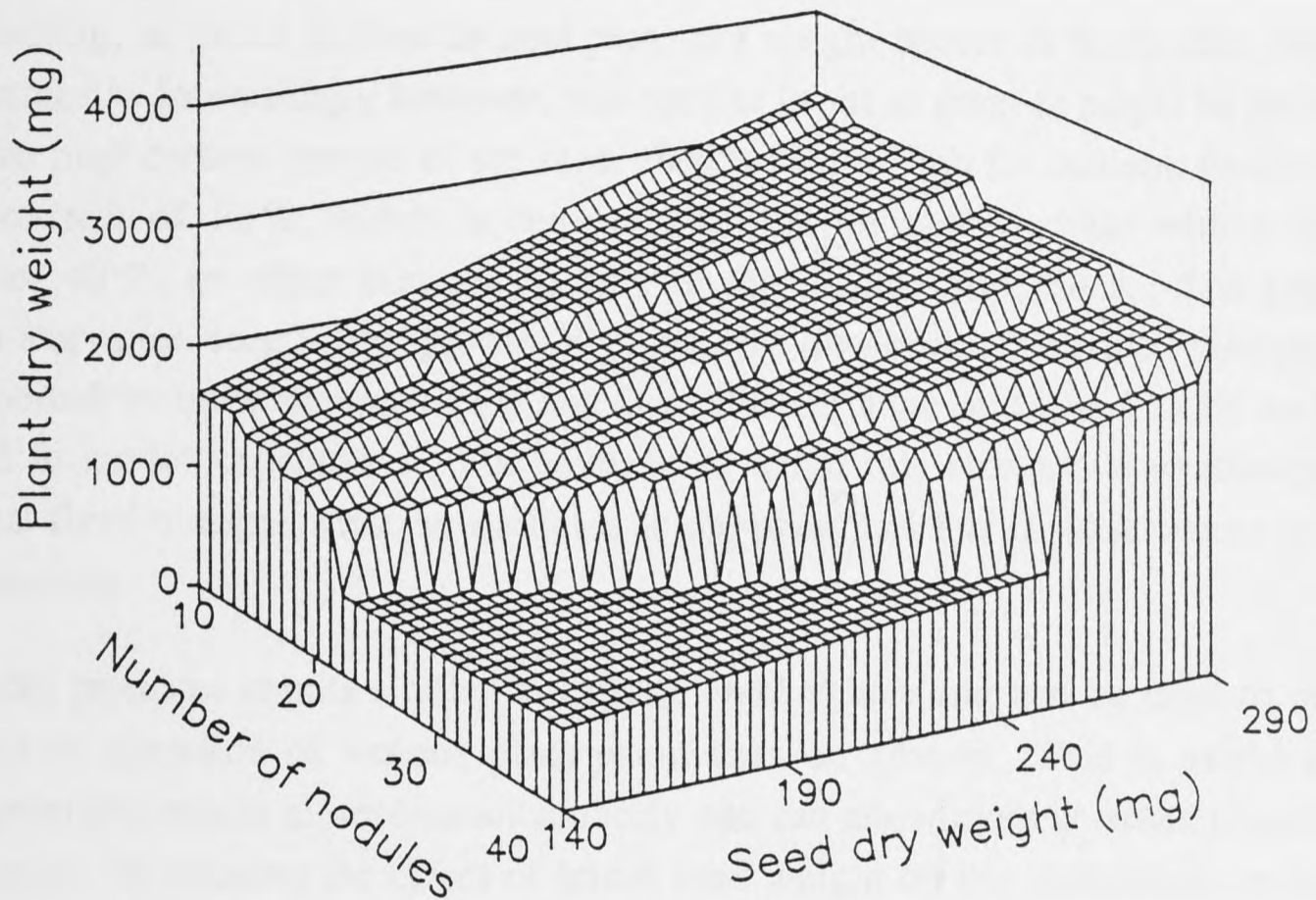
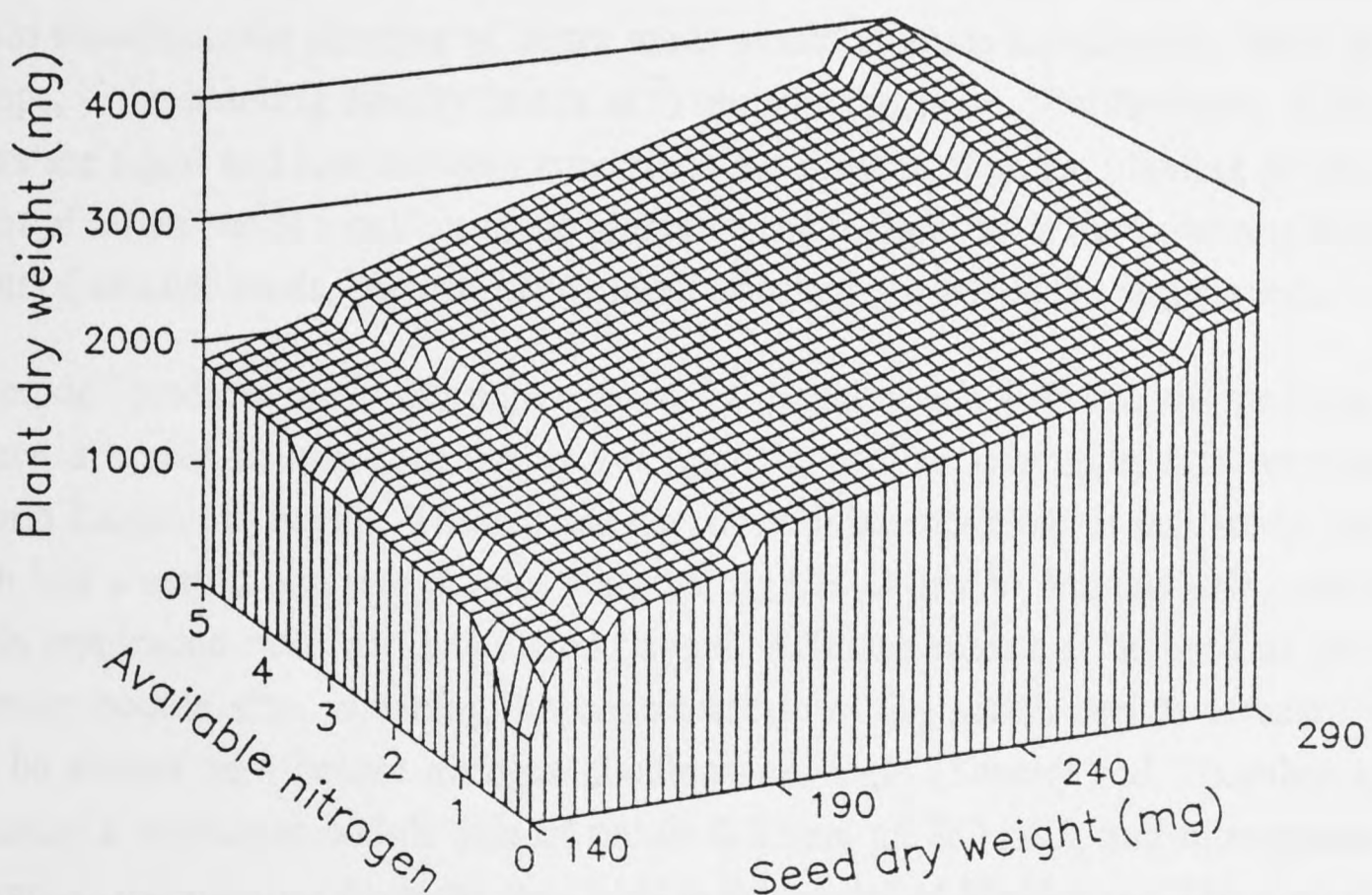


Figure 3.9 : Relationship between initial seed dry weight, plant age and plant dry weight, predicted by the model Soyfix.

The effect of this restriction of nitrogen fixation on growth rate is shown clearly if the relationship between initial seed dry weight and number of nodules forming on a plant is examined (Figure 3.10). With fewer nodules the model plants are able to grow larger as the nodules reach the critical respiration rate for fixation at an earlier stage. Making nitrogen available to the model plant decreases the limiting effect of establishment of nodules and allows larger plants to develop (Figure 3.11).



**Figure 3.10 :** Relationship between initial seed dry weight, nodule number and final plant dry weight at 30 days, predicted by the model Soyfix.



**Figure 3.11 :** Relationship between initial seed dry weight, available nitrogen (relative) and final plant dry weight at 30 days, predicted by the model Soyfix.

### 3.4. Discussion

The pattern of growth of developing soybeans and the use of a simple model to simulate this growth has been outlined. The first 30 days of the growth of soybean involves the important stages of germination, nodulation, cotyledon export and photosynthesis, leaf photosynthesis and nitrogen fixation.

After planting, an initial decline in total plant dry weight occurs as respiration exceeds photosynthesis. Interestingly however, this decline is not as great as might be predicted due to the high carbon content of the seed. Seeds have a high fat content, producing a carbon content of 52 %, which is converted to heavier carbohydrate with a carbon content of 40 %, an effect that also occurs in the model simulations. The stage of nitrogen starvation seen in the growth of plants that do not receive added nitrogen has been reported by other workers (Pate and Dart 1961, Mahon and Child 1979) and also occurred in model simulations. For soybean to avoid this nitrogen starvation phase, additional fixed nitrogen must be available to the plant and this is what occurs in most field situations.

The model produces results similar to experimental values and can be used to predict the effect of alteration of various plant parameters on growth. This is useful as the model generates results almost instantaneously and can allow more accurate planning of experiments. Examining the effect of initial seed weight on the subsequent growth of experimental plants demonstrates the value of the model. Both model and experimental results show that plants from larger seeds grow faster (Figure 3.8) and growth of plants from larger seeds may also show more efficient utilization of seed reserves (Table 3.1). In field situations, the planting of larger seeds would produce significantly faster growth in crops, if the planting density (seeds  $m^{-2}$ ) remains the same. Furthermore, if all other factors are equal and low nitrogen conditions are present, then the planting of the same weight of larger seeds would produce plants giving higher yields than planting the same weight of smaller seeds, because of the more efficient growth of the larger seeds.

The model predicts more efficient growth of larger seeds because the nodules they produce are able to reach, at a younger age, the critical minimum size required for nitrogen fixation to begin. The critical size of nodules modelled in this study was one which had a respiration rate greater than  $0.5 \text{ mg CH}_2\text{O day}^{-1}$ . Models using measured nodule respiration rates and calculated oxygen diffusion rates can be used to predict a minimum nodule size, assuming the concentration of  $O_2$  within nodule infected zones must be almost zero before nitrogen fixation can begin (Sheehy and Thornley 1988). Assuming a minimum nodule size of radius 0.6 mm, an RQ of 1, and nitrogenase-like respiration, calculations from the data used in the model of Sheehy and Thornley (1988) give a respiration rate for a nodule of this size of  $0.18 \text{ mg CH}_2\text{O day}^{-1}$ . The value used in the growth model described in this chapter, of  $0.5 \text{ mg CH}_2\text{O day}^{-1}$  represents a

nodule with a radius of approximately 0.8 mm. This effect of restricting nitrogen fixation to nodules larger than a certain size, means that the number of nodules forming on a plant can have a significant effect on plant growth (Figure 3.10). The less the available nitrogen and the greater the number of nodules, the lower the growth rate. This probably contributes in part to the observed slower growth of a super-nodulating cultivar of soybean (Day *et al.* 1986), which form many more, but smaller, nodules than does the wild-type.

### Conclusion

By determining the contribution of individual factors to plant growth, the model simplifies growth processes, and helps in understanding. The model can be used to investigate the effects of changing various parameters; in this way it is useful for planning experiments. For example, a model simulating plant development when nodules are unable to fix nitrogen, produces a growth pattern very similar to that observed in the next chapter, where some plants were grown in atmospheres of argon/oxygen and were unable to fix nitrogen. The importance of the regulation of various aspects of plant growth is demonstrated within the model, but physiological mechanisms of regulation can only be determined by further experimentation.

## Chapter 4

### Effects of Ethylene, Acetylene and the Absence of N<sub>2</sub> on Nodulation and Nitrogen Fixation in Soybean

#### 4.1. Introduction

Exposing nodulated plants to ethylene, acetylene and the absence of N<sub>2</sub> is a valuable method for investigating aspects of nitrogen fixation, since nodule formation and nitrogen fixation may be affected by these gases. In particular, exposure of nodulated roots to acetylene or the absence of N<sub>2</sub> has an immediate and dramatic effect on nitrogenase activity. Longer term exposure to the absence of N<sub>2</sub> prevents nitrogen fixation and changes carbon and nitrogen partitioning within the plant.

##### *Ethylene*

Ethylene is an endogenous plant growth regulator and is also produced during acetylene reduction assays. Nodulation is reported to be totally inhibited by exposure to ethylene in bean (Grobbelaar *et al.* 1971), and is reduced by 90 % (Drennan and Norton 1972) and 75 % (Goodlass and Smith 1979) in pea and 40 % in clover (Goodlass and Smith 1979). Nitrogen fixation is severely inhibited by ethylene in bean (Grobbelaar *et al.* 1971), and ethylene inhibits nitrogenase activity in clover and pea (Goodlass and Smith 1979). Dilworth (1966), on the other hand, found that ethylene did not inhibit the nitrogenase activity of nitrogen fixing cell free extracts prepared from *Clostridium*.

##### *Acetylene*

Acetylene acts as an analogue of ethylene in the control of many plant processes (Abeles 1973), and as such, may have effects on the long-term growth of plants. In nodulated plants it has the additional important effect of inhibiting nitrogen fixation as a competitive substrate for nitrogenase (Hardy *et al.* 1968). When saturating levels of acetylene (> 4 kPa in the gas phase) are present, very little N<sub>2</sub> reduction by nitrogenase occurs (Meeks *et al.* 1978) and in many nodulated plants examined there is a rapid decline of nitrogenase activity following exposure to acetylene (Minchin *et al.* 1983, 1986, Davey and Simpson 1988, see section 1.5, page 12).



### *Absence of N<sub>2</sub>*

Exposure of root nodules to atmospheres containing O<sub>2</sub> in similar concentrations to air, but no N<sub>2</sub>, causes a similar decline in nodule respiration as does exposure to acetylene (Minchin *et al.* 1983). These gas mixtures normally contain an inert gas (usually argon, the cheapest) and oxygen (80:20 v/v). Other effects of argon/oxygen atmospheres in the intermediate and longer term have been investigated. In older plant material exposed to 10 days argon/oxygen treatment (lupin, day 39-49), Pate *et al.* (1984) found little difference in carbon fixation rates although nodule respiration decreased under argon/oxygen, as did levels of nitrogen in plant parts. Atkins *et al.* (1984) examined short-term (up to three days) effects of argon/oxygen on nodulated root systems of cowpea and lupin and noted reductions in activities of the glutamine utilizing enzymes, glutamate synthase and asparagine synthetase in lupin, and *de novo* purine synthesis in cowpea.

Kossak and Bohlool (1984) have shown that ammonia production is not required for autoregulation (the rapid regulatory plant response inhibiting further nodulation) and so presumably argon/oxygen treatments would have no effect on the initial formation of nodules. However, subsequent to nodule formation, differences in the growth of active or inactive nodules on plants can occur. Singleton and Stockinger (1983), for example, have shown that there is compensation against ineffective nodulation in soybean. In plants inoculated with both effective and ineffective rhizobia in different concentrations, the average weight of effective nodules increased as the number of effective nodules decreased. Using argon/oxygen and a split root system, Singleton and van Kessel (1987), have shown that nodule growth, root growth and total root respiration are markedly increased on the portion of nodulated split roots developing in air rather than argon/oxygen. Both these studies suggest that growth of nitrogen fixing nodules is enhanced over nodules not fixing nitrogen.

### *Foliar application of nitrogen*

Foliar application of nitrogen is another experimental technique useful in the study of nitrogen fixation. Nitrogen can be added to the leaves and stems without exposure of the roots and nodules to combined nitrogen. Dart and Wildon (1970) found that immersion of cowpea shoots in urea, potassium nitrate, ammonium sulphate and ammonium nitrate solutions led to a decrease in nodule formation with increasing nitrogen concentration, but growth of shoots in all their treatments, except urea, was also markedly reduced. In soybeans, Afza *et al.* (1987) have shown foliar nitrogen application leads to an increase in yields without a decrease in nitrogen fixation, while Parker and Boswell (1980) report foliage damage and suppression of yields with foliar fertilization.

## 4.2. Results

### 4.2.1. Experimental

In this chapter experiments investigated firstly, aspects of the control of nodulation in soybeans, secondly, the inhibition of nitrogenase activity and thirdly, the growth and development of plants in the absence of N<sub>2</sub>. The recirculating gas system used for growing plants in the presence of ethylene and the absence of N<sub>2</sub> is described on page 23, and the open-flow assay system used in investigations with acetylene and argon/oxygen on page 25.

### 4.2.2. Effect of ethylene on growth and nodulation of soybean

The endogenous production of ethylene by root systems and the effects of exposure of root systems to exogenous ethylene were investigated. Endogenous plant ethylene production was measured in seedlings aged between 5 and 13 days old. These plants showed only trace levels of ethylene production of between 200 and 300 pmol g<sup>-1</sup>root DW h<sup>-1</sup>. This level of ethylene production is not detectable during conventional or open-flow acetylene reduction assays, and did not cause a detectable accumulation of ethylene in the recirculating gas system.

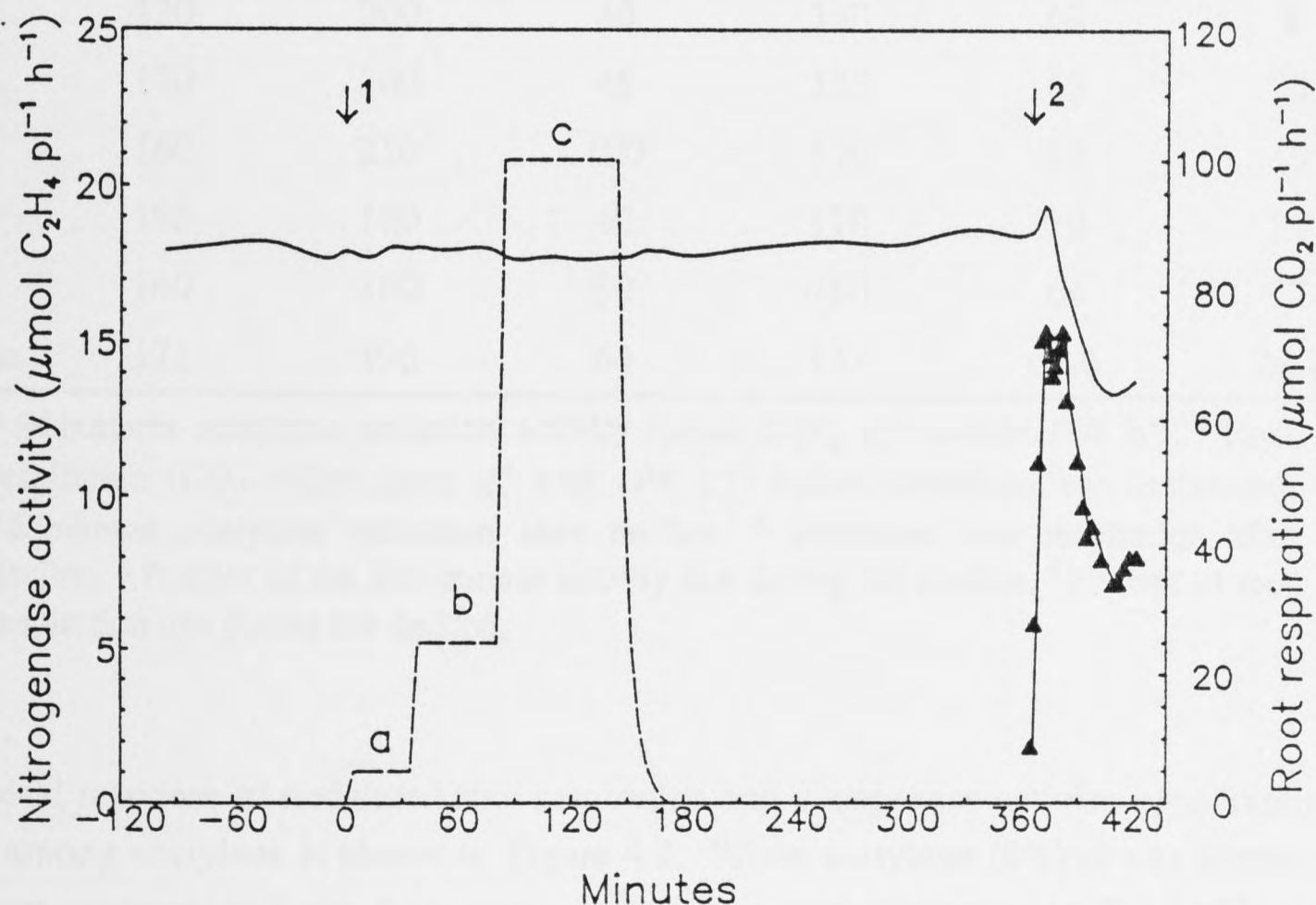
The effects of ethylene on growth and nodulation were investigated in a small experiment by growing plants with their root systems continuously exposed to various concentrations of ethylene using the recirculating gas system. Four plants per treatment were exposed to ethylene between day 5, when they were inoculated, and day 20, when they were harvested. The results (Table 4.1) show no significant difference in plant dry weights, although there is a trend towards smaller plants at higher ethylene concentrations. Mean nodule number per plant showed a similar decrease with increasing ethylene concentration, and the most dramatic effect was a significant reduction in maximum root length observed with increasing ethylene concentration, although overall shoot to root dry weight ratios did not vary. Clearly, levels of ethylene of 1 ppm and greater had a significant effect on the growth of soybean.

**Table 4.1** : Development of soybeans with roots exposed to traces of ethylene. Plants were harvested at 20 days after sowing.  $\pm$  95 % confidence limits.

Treatment	Plant dry weight (mg)	Shoot:Root ratio <sup>a</sup>	Mean root length (cm)	Mean shoot height (cm)	Nodule number <sup>b</sup>
Control	638 $\pm$ 125	1.96 $\pm$ 0.41	52 $\pm$ 16	14.5 $\pm$ 2.9	62.3 $\pm$ 13.2
1ppm C <sub>2</sub> H <sub>4</sub>	767 $\pm$ 42	1.79 $\pm$ 0.12	33 $\pm$ 11	13.4 $\pm$ 2.0	54.7 $\pm$ 6.0
10ppm C <sub>2</sub> H <sub>4</sub>	693 $\pm$ 178	1.87 $\pm$ 0.30	16 $\pm$ 4.1	14.9 $\pm$ 1.8	34.0 $\pm$ 13.7
100ppm C <sub>2</sub> H <sub>4</sub>	553 $\pm$ 144	2.00 $\pm$ 0.10	13 $\pm$ 3.0	12.9 $\pm$ 3.9	37.5 $\pm$ 5.9

<sup>a</sup> Shoot dry weight to root dry weight ratio, <sup>b</sup> Mean nodule number per plant.

Short-term exposure of plants to ethylene had no effect on nodulated root respiration (Figure 4.1). In this experiment ethylene concentration was increased in three steps, up to a maximum of 1 kPa, while oxygen and nitrogen pressures remained constant. The carbon dioxide efflux from the nodulated roots remained constant as ethylene was introduced at 0.05, 0.25 and 1 kPa and then removed. Three hours after ethylene concentrations were removed, saturating acetylene (8 kPa) was added and a large decline in nodulated root respiration and nitrogenase activity was observed.



**Figure 4.1** : Effect of exposure to various concentrations of ethylene on the root respiration of a nodulated root system in an open-flow assay system. Ethylene was added into the flow gas beginning at time zero (arrow 1), at pressures of 0.05 kPa (a), 0.25 kPa (b) and 1.0 kPa (c). Root respiration was monitored as CO<sub>2</sub> efflux (—  $\mu\text{mol pl}^{-1} \text{h}^{-1}$ ). Saturating acetylene was introduced at 360 minutes (arrow 2) and ethylene production ( $\blacktriangle$   $\mu\text{mol C}_2\text{H}_4 \text{pl}^{-1} \text{h}^{-1}$ ) monitored.

### 4.2.3. Acetylene-induced decline

An acetylene-induced decline in nodule nitrogenase activity and nodulated root respiration was observed in soybean plants of a variety of ages, during short-term exposure to saturating levels of acetylene. The response of plants to acetylene was generally similar, although some variation was seen in the relative amount of the decline (Table 4.2).

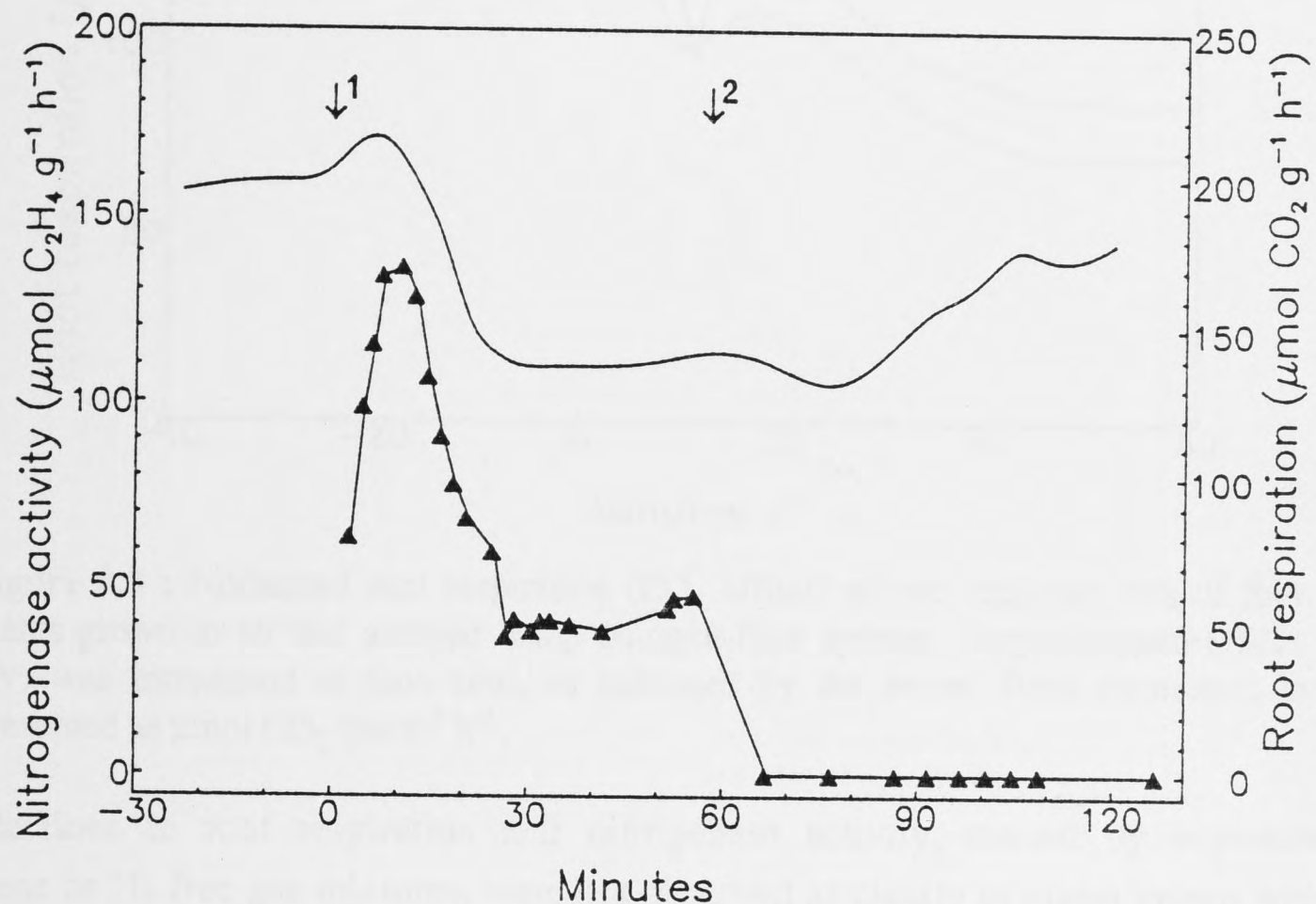
**Table 4.2** : Acetylene-induced decline in nitrogenase activity and root respiration in 10 pots, each containing four plants. Plants were grown and inoculated as described in the materials and methods and assayed using the open-flow system.

Age (days)	Peak <sup>a</sup> ethylene	Initial <sup>b</sup> root resp	Declined <sup>c</sup> acetylene	Declined <sup>d</sup> root resp	% decline <sup>e</sup> ethylene	% decline <sup>f</sup> root resp
26	220	190	90	120	59	37
26	180	180	90	130	50	28
28	180	210	50	170	72	19
28	200	230	45	160	77	30
29	180	200	90	150	50	25
29	130	200	40	180	69	9
29	130	200	45	135	65	32
30	160	210	100	170	38	19
31	195	160	40	110	79	31
34	140	180	50	150	64	17
Mean	171	196	64	147	62.6	24.7

<sup>a</sup> Maximum acetylene reduction activity ( $\mu\text{mol C}_2\text{H}_4 \text{ g}^{-1} \text{ nodule DW h}^{-1}$ ), <sup>b</sup> Root respiration ( $\text{CO}_2$  efflux  $\mu\text{mol g}^{-1} \text{ root DW h}^{-1}$ ) before acetylene was introduced, <sup>c</sup> Minimum acetylene reduction after decline, <sup>d</sup> minimum root respiration after decline, <sup>e</sup> Percent of the nitrogenase activity lost during the decline, <sup>f</sup> Percent of root respiration lost during the decline.

A typical response of nodulated root respiration and nitrogenase activity upon exposure to saturating acetylene is shown in Figure 4.2. When acetylene (8 kPa) was introduced (oxygen pressure and gas flow rates constant), a slight increase in  $\text{CO}_2$  efflux was observed, reaching a peak after approximately 10 to 12 minutes, at which time ethylene production also peaked. Carbon dioxide efflux and ethylene production then declined steadily for the next 30 to 40 minutes. The decline in ethylene production was between 40 and 75 % of the peak value and for  $\text{CO}_2$  was between 20 and 40 % of the initial

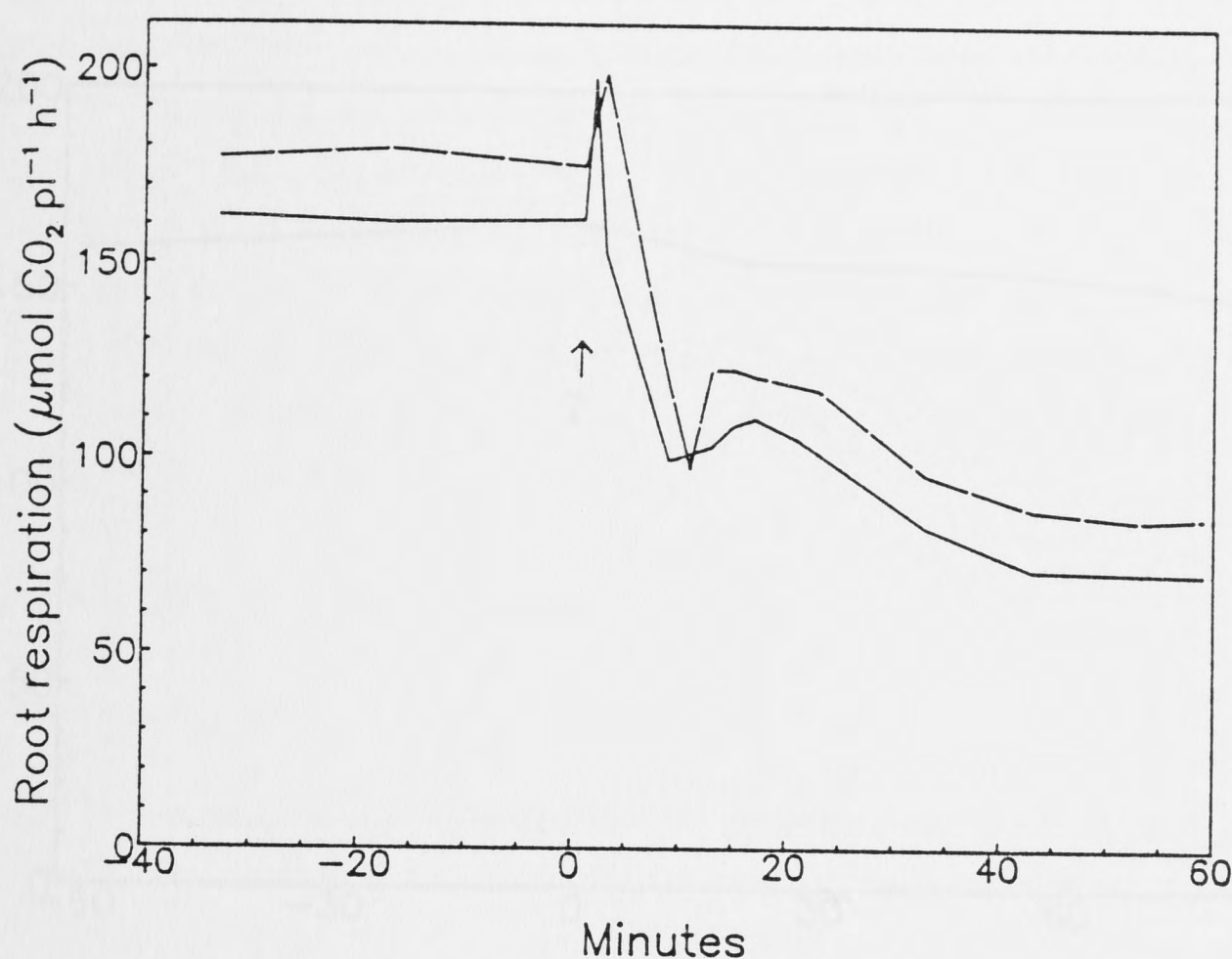
efflux rate (Table 4.2). Activity generally recovered slightly after 60 minutes and then remained constant for the next 120 minutes. In the experiment presented in Figure 4.2, acetylene was introduced at time zero and removed from the gas stream at 60 minutes. The figure shows the decline of root respiration (CO<sub>2</sub> efflux) and ethylene production following the introduction of acetylene and the gradual recovery of respiration after the acetylene was removed.



**Figure 4.2 :** Nitrogenase activity and nodulated root respiration (CO<sub>2</sub> efflux) of plants grown in air assayed using an open-flow system. Acetylene (8 kPa) was introduced at time zero (arrow 1) and removed at 60 minutes (arrow 2). Nitrogenase activity (—▲—) is μmol C<sub>2</sub>H<sub>4</sub> g<sup>-1</sup> nodule DW h<sup>-1</sup>. Respiration (—) is μmol CO<sub>2</sub> g<sup>-1</sup> root DW h<sup>-1</sup>.

In this figure and in the following examples only one representative experiment is presented which is typical of repeated experiments. An acetylene-induced decline in respiration and nitrogenase activity was observed in at least 30 separate experimental runs on different plants.

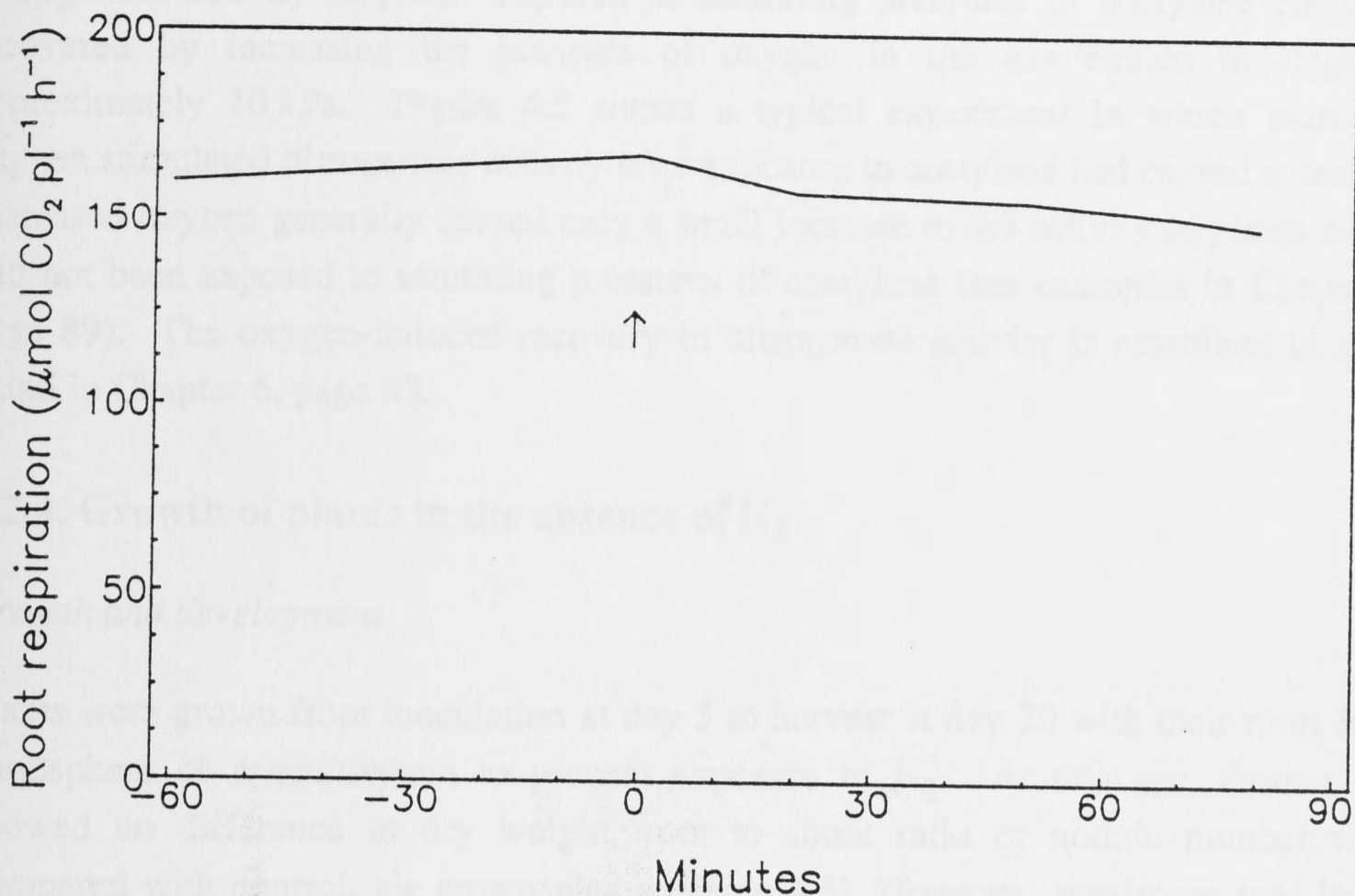
Removing N<sub>2</sub> from the gas surrounding the roots and nodules by adding an inert gas, such as argon, while the oxygen pressure was held constant, caused a similar decline in the CO<sub>2</sub> efflux of nodulated root systems (Figure 4.3). An initial slight increase in CO<sub>2</sub> efflux was observed before a decline, followed by a slight recovery and another decline to stabilize at 50 to 70 % of the initial rate.



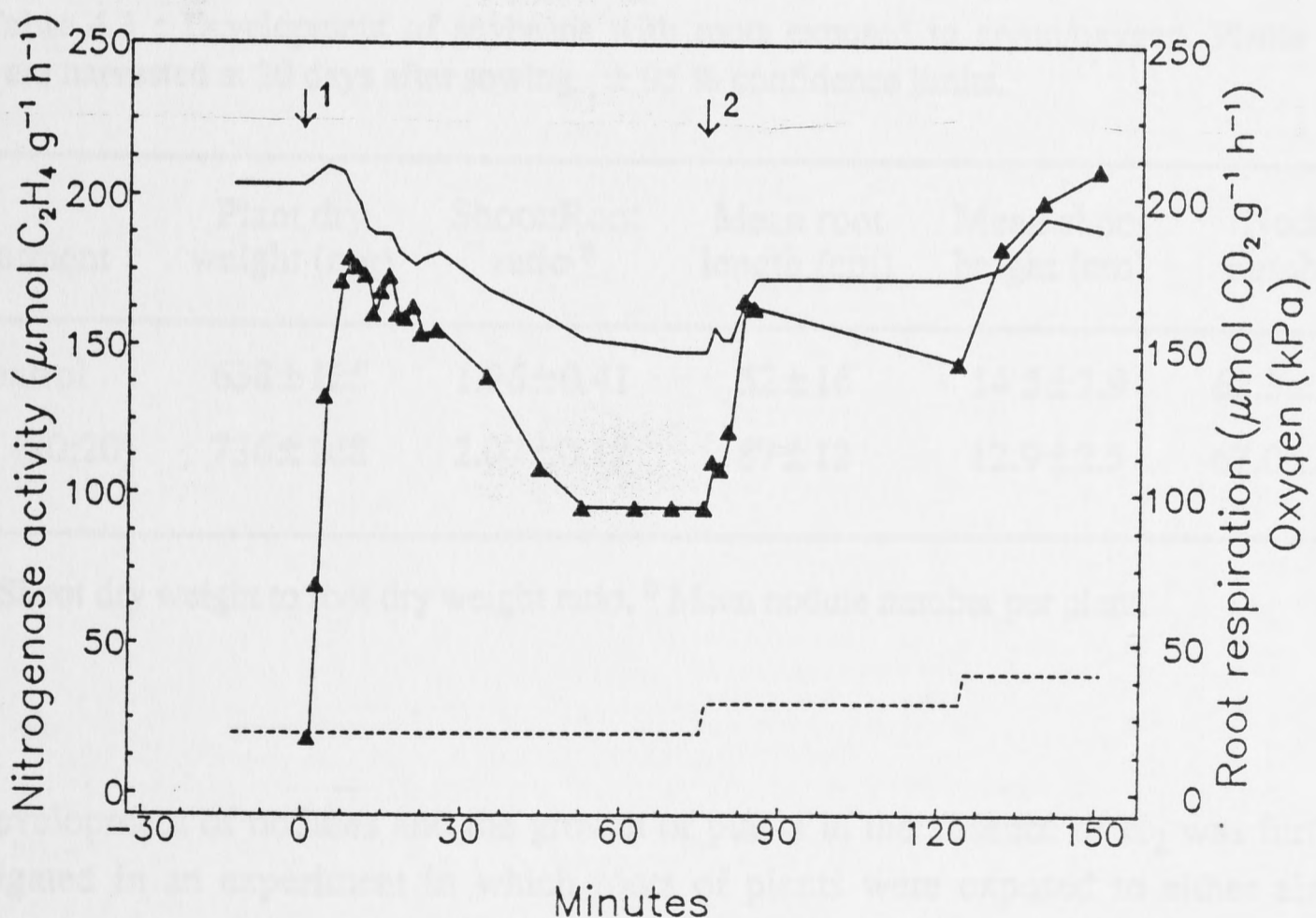
**Figure 4.3 :** Nodulated root respiration (CO<sub>2</sub> efflux) of two replicate pots of four plants grown in air and assayed using an open-flow system. Argon/oxygen (79/21 v/v) was introduced at time zero, as indicated by the arrow. Root respiration is presented as  $\mu\text{mol CO}_2 \text{ plant}^{-1} \text{ h}^{-1}$ .

The declines in root respiration and nitrogenase activity, caused by exposure to acetylene or N<sub>2</sub> free gas mixtures, were not observed as clearly in plants grown with all nodules submerged in nutrient solution (Figure 4.4). In this experiment argon/oxygen replaced air at time zero and the nodules which were grown submerged and assayed while submerged showed only a slight decline in activity.

Acetylene and argon/oxygen gas mixtures had no effect on the root respiration of denodulated root systems. Increases in oxygen concentration around denodulated roots in steps of approximately 9 kPa did not cause a significant increase or decrease in denodulated root respiration (data not presented).



**Figure 4.4 :** Effect of argon/oxygen on the nodulated root respiration of plants grown and assayed with roots and nodules submerged in nutrient solution. Argon/oxygen gas was introduced at time zero (arrow). Root respiration (—) is  $\mu\text{mol CO}_2 \text{ g}^{-1} \text{ root DW h}^{-1}$ .



**Figure 4.5 :** Response of nitrogenase activity and nodulated root respiration (CO<sub>2</sub> efflux) to saturating acetylene (8 kPa) introduced at time zero (arrow 1) and subsequent 10 kPa step increases in oxygen concentration (arrow 2). Nitrogenase activity (—▲) is  $\mu\text{mol C}_2\text{H}_4 \text{ g}^{-1} \text{ nodule DW h}^{-1}$ . Root respiration (—) is  $\mu\text{mol CO}_2 \text{ g}^{-1} \text{ root DW h}^{-1}$ . Oxygen pressure in kPa (-----).

Nitrogenase activity in plants exposed to saturating pressures of acetylene could be recovered by increasing the pressure of oxygen in the gas stream in steps of approximately 10 kPa. Figure 4.5 shows a typical experiment in which increased oxygen stimulated nitrogenase activity after exposure to acetylene had caused a decline. Increased oxygen generally caused only a small increase in the activity of plants which had not been exposed to saturating pressures of acetylene (see examples in Chapter 6, page 89). The oxygen-induced recovery in nitrogenase activity is examined in more detail in Chapter 6, page 83.

#### 4.2.4. Growth of plants in the absence of N<sub>2</sub>

##### *Growth and development*

Plants were grown from inoculation at day 5 to harvest at day 20 with their roots in an atmosphere of argon/oxygen to prevent exposure to N<sub>2</sub>. At this age, these plants showed no difference in dry weight, root to shoot ratio or nodule number when compared with control, air grown plants (Table 4.3). However, maximum root length was significantly longer in plants grown in the absence of N<sub>2</sub> and the leaves appeared pale green presumably indicating a nitrogen deficiency.

**Table 4.3** : Development of soybeans with roots exposed to argon/oxygen. Plants were harvested at 20 days after sowing.  $\pm$  95 % confidence limits.

Treatment	Plant dry weight (mg)	Shoot:Root ratio <sup>a</sup>	Mean root length (cm)	Mean shoot height (cm)	Nodule number <sup>b</sup>
Control	638 $\pm$ 125	1.96 $\pm$ 0.41	52 $\pm$ 16	14.5 $\pm$ 2.9	62.3 $\pm$ 13.2
ArO <sub>2</sub> (80:20)	736 $\pm$ 168	2.07 $\pm$ 0.12	87 $\pm$ 12	12.9 $\pm$ 2.5	67.0 $\pm$ 23.4

<sup>a</sup> Shoot dry weight to root dry weight ratio, <sup>b</sup> Mean nodule number per plant.

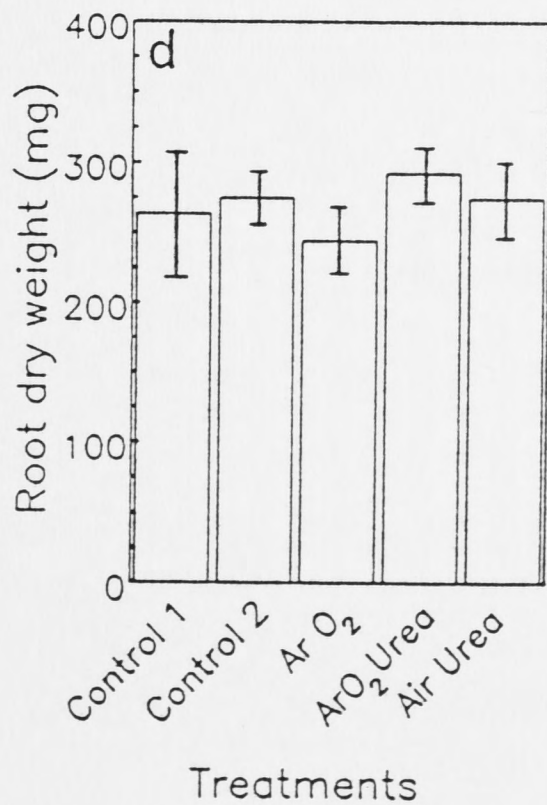
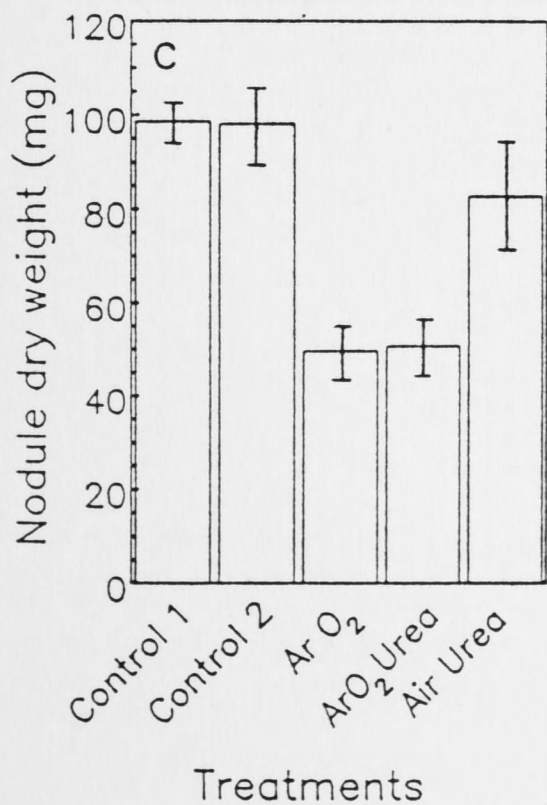
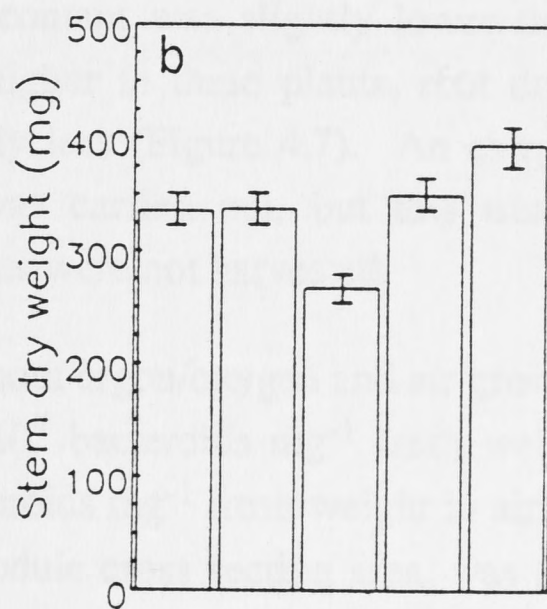
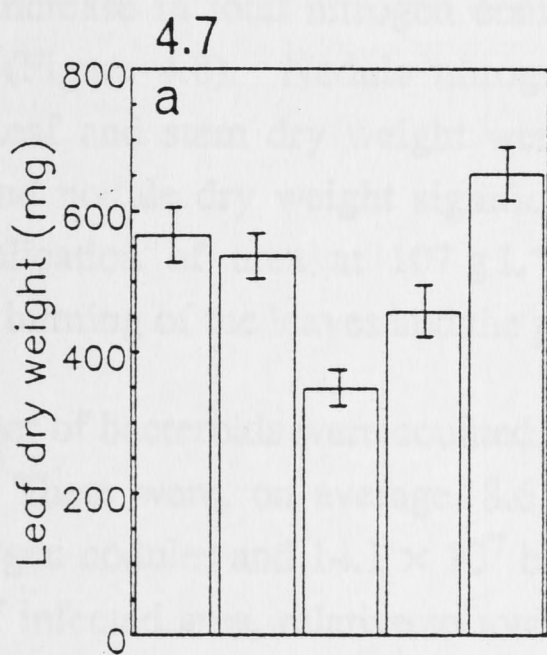
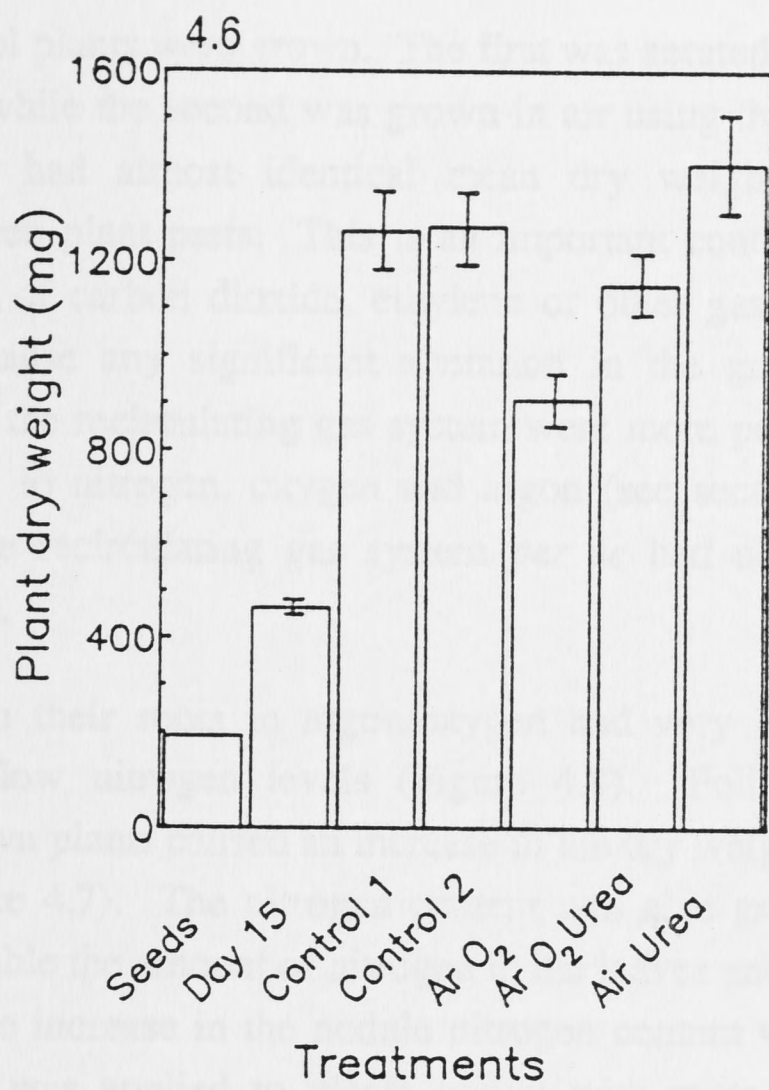
The development of nodules and the growth of plants in the absence of N<sub>2</sub> was further investigated in an experiment in which roots of plants were exposed to either air or argon/oxygen treatments and foliar applications of nitrogen (as urea) were made. The results of the dry weight of plants at harvest (27 days) are presented in Figures 4.6 and 4.7 and the nitrogen content in Figure 4.8.



Figure 4.6 : Dry weight at 27 days of plants grown with roots exposed to air or argon/oxygen, with and without foliar fertilization with urea. 95 % confidence limits shown. Detailed treatments were as follows :

Seeds	represents the mean dry weight or nitrogen content of the seeds at planting
Day 15	represents the mean dry weight or nitrogen content immediately prior to the commencement of treatments
Control 1	plants grown with roots in air, with an open gas supply, receiving no added nitrogen
Control 2	plants grown with roots in air, in a recirculating gas system, receiving no added nitrogen
ArO <sub>2</sub>	plants grown with roots in argon/oxygen (80:20), in a recirculating gas system, receiving no added nitrogen
ArO <sub>2</sub> urea	plants grown with roots in argon/oxygen (80:20), in a recirculating gas system, and the leaves sprayed four times (day 16, 20, 22, 25) with a solution of 10.7 g L <sup>-1</sup> of urea and one drop of Tween 80 L <sup>-1</sup> as surfactant
Air urea	plants grown with roots in air in an open gas system, and the leaves sprayed four times (day 16, 20, 22, 25) with a solution of 10.7 g L <sup>-1</sup> of urea.

Figure 4.7 : Dry weight at 27 days of a/ leaves, b/ stems, c/ nodules, d/ roots from plants grown with roots exposed to air or argon/oxygen, with and without foliar fertilization by urea. 95 % confidence limits shown. Details are given in Figure 4.6.



Two sets of control plants were grown. The first was aerated from an external source in an open system, while the second was grown in air using the recirculating gas system. These treatments had almost identical mean dry weights and equal dry weight partitioning between plant parts. This is an important control experiment. It showed that any build up of carbon dioxide, ethylene or other gases in the recirculating gas system did not cause any significant alteration in the growth of plants. The gas reservoirs used in the recirculating gas system were more permeable to carbon dioxide and ethylene than to nitrogen, oxygen and argon (see section 2.4, page 24). It was concluded that the recirculating gas system *per se* had no effect on the growth of nodulated soybean.

Plants grown with their roots in argon/oxygen had very low dry weight at harvest (Figure 4.7) and low nitrogen levels (Figure 4.8). Foliar application of urea to argon/oxygen grown plants caused an increase in the dry weight of all plant parts except the nodules (Figure 4.7). The nitrogen content was also greater in these plants, with approximately double the amount of nitrogen in the leaves and stems, and a third greater in the roots, but no increase in the nodule nitrogen content was observed (Figure 4.8). When foliar urea was applied to plants grown with roots exposed to air, a similar absolute increase in total nitrogen content, which occurred largely in the leaves was observed (Figure 4.8). Nodule nitrogen content was slightly lower than in control plants. Leaf and stem dry weight were higher in these plants, root dry weight was similar, and nodule dry weight significantly less (Figure 4.7). An extra treatment of foliar application of urea at 107 g L<sup>-1</sup> was carried out, but this treatment caused excessive burning of the leaves and the plants were not harvested.

The number of bacteroids were counted in both argon/oxygen and air grown plants aged 30 days. There were, on average,  $8.6 \times 10^7$  bacteroids mg<sup>-1</sup> fresh weight nodule in argon/oxygen nodules and  $14.1 \times 10^7$  bacteroids mg<sup>-1</sup> fresh weight in air nodules. The percent of infected area, relative to total nodule cross section area, was also greater in air grown nodules (59 compared to 47 %).

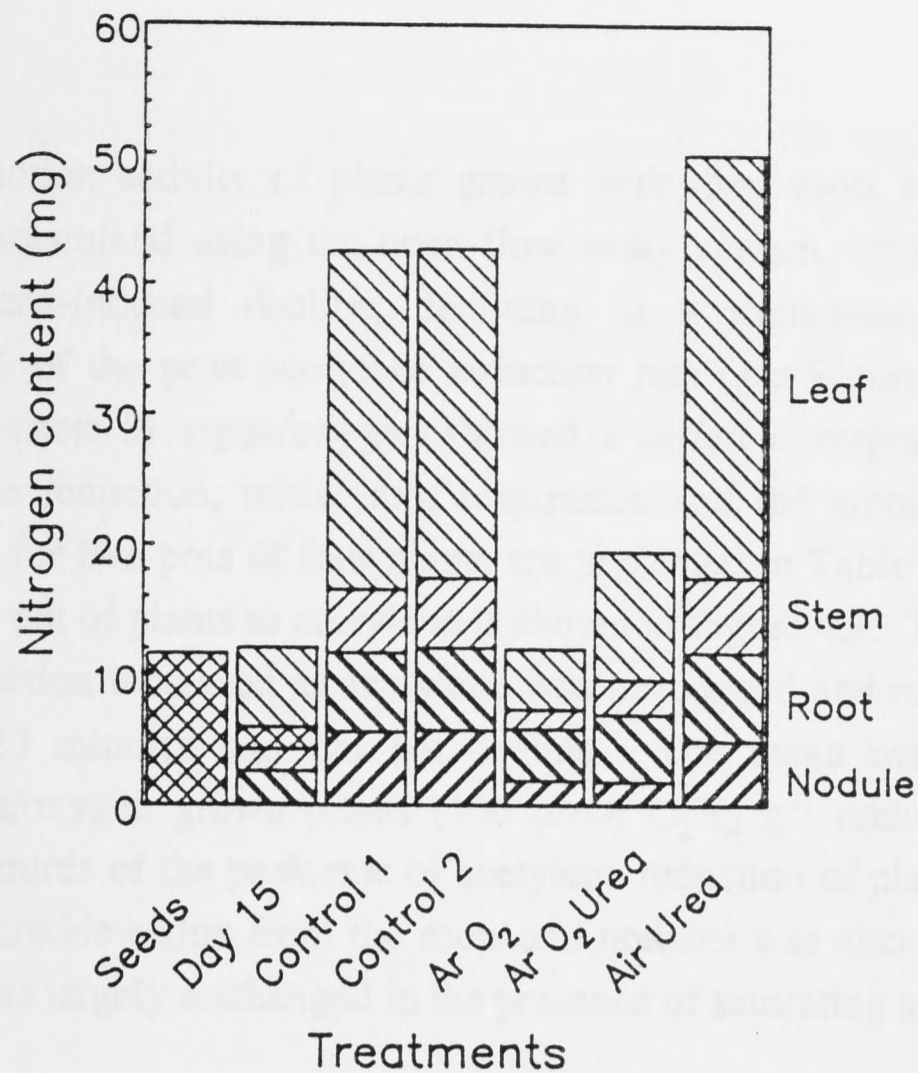


Figure 4.8 : Nitrogen content of plants grown with roots exposed to air or argon/oxygen, with and without foliar fertilization by urea. Details of the treatments are presented in Figure 4.6, page 50.

▨ represents cotyledon, ▨ leaf, ▨ stem, ▨ root and ▨ nodule.

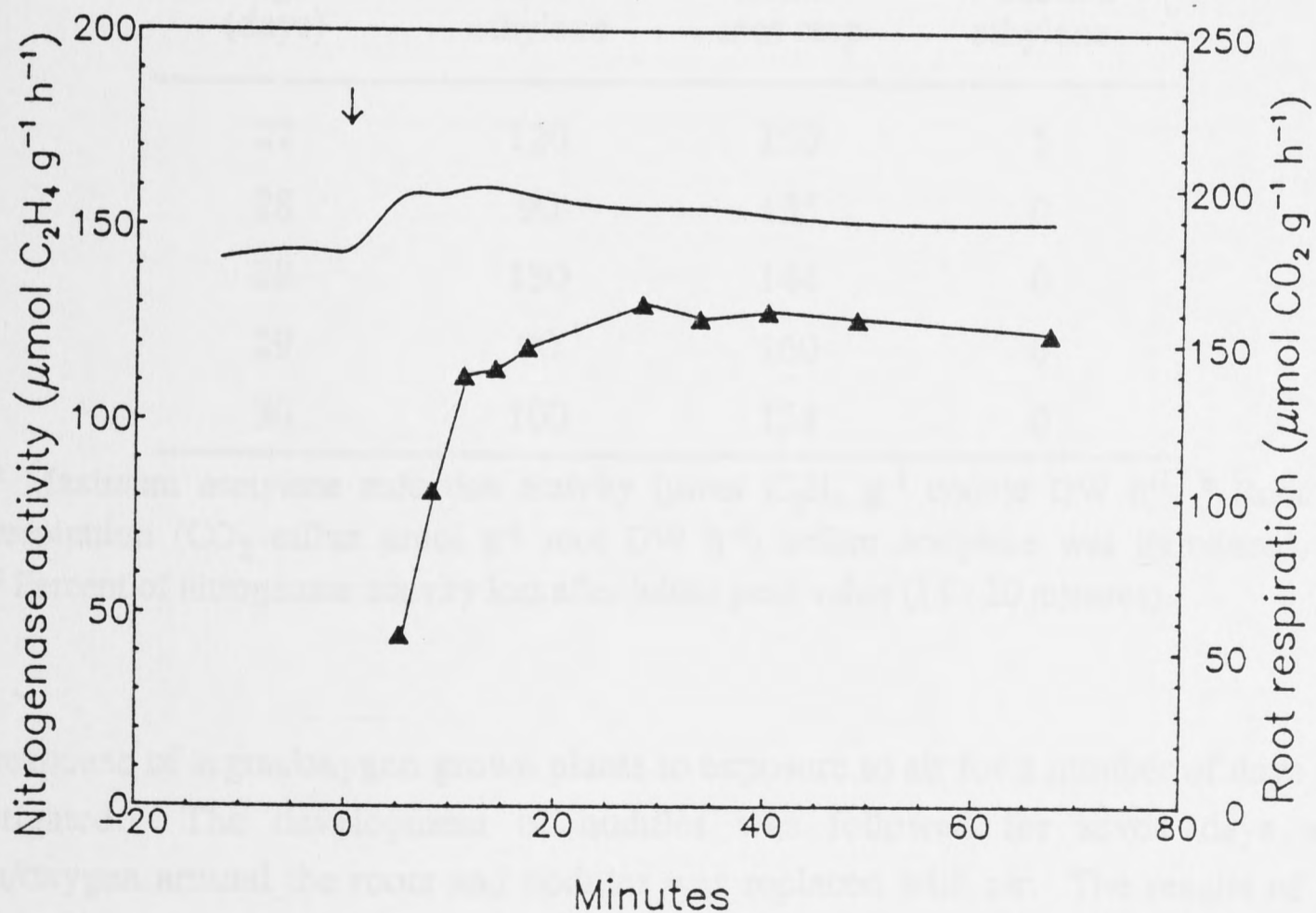


Figure 4.9 : Nitrogenase activity and nodulated root respiration (CO<sub>2</sub> efflux) of plants grown in argon/oxygen assayed on day 27 using an open-flow system. Acetylene (8 kPa) was introduced at time zero (arrow). Nitrogenase activity (—▲—) is μmol C<sub>2</sub>H<sub>4</sub> g<sup>-1</sup> nodule DW h<sup>-1</sup>. Root respiration (—) is μmol CO<sub>2</sub> g<sup>-1</sup> root DW h<sup>-1</sup>.

*Physiology*

The acetylene reduction activity of plants grown with their roots exposed to air or argon/oxygen was examined using the open-flow assay system. Plants grown in air showed an acetylene-induced decline, declining to a minimum mean value of approximately 40 % of the peak acetylene reduction rate (see Figure 4.2, Table 4.2). Plants grown with roots in argon/oxygen showed a different response to acetylene. Maximum acetylene reduction, initial root respiration and the amount of decline in acetylene reduction for five pots of four plants are presented in Table 4.4 and a typical response of a single pot of plants to acetylene is shown in Figure 4.9. This figure shows how ethylene production increased as acetylene was introduced and reached a constant level after 10 to 20 minutes and did not decline. The mean maximum ethylene production in argon/oxygen grown plants ( $106 \mu\text{mol C}_2\text{H}_4 \text{ g}^{-1} \text{ nodule DW h}^{-1}$ ) was approximately two thirds of the peak rate of acetylene reduction of plants grown in air. The initial carbon dioxide efflux from the roots and nodules was also lower than in air grown plants, but was largely unchanged in the presence of saturating acetylene.

**Table 4.4 :** Acetylene reduction activity and nodulated root respiration in plants grown with their roots in argon/oxygen. The results of experiments from five pots each containing four plants are presented.

Age (days)	Peak <sup>a</sup> ethylene	Initial <sup>b</sup> root resp	% decline <sup>c</sup> ethylene
27	120	150	5
28	90	135	0
28	130	144	0
29	90	160	0
30	100	158	0

<sup>a</sup> Maximum acetylene reduction activity ( $\mu\text{mol C}_2\text{H}_4 \text{ g}^{-1} \text{ nodule DW h}^{-1}$ ), <sup>b</sup> Root respiration ( $\text{CO}_2$  efflux  $\mu\text{mol g}^{-1} \text{ root DW h}^{-1}$ ) before acetylene was introduced,

<sup>c</sup> Percent of nitrogenase activity lost after initial peak value (15 - 20 minutes).

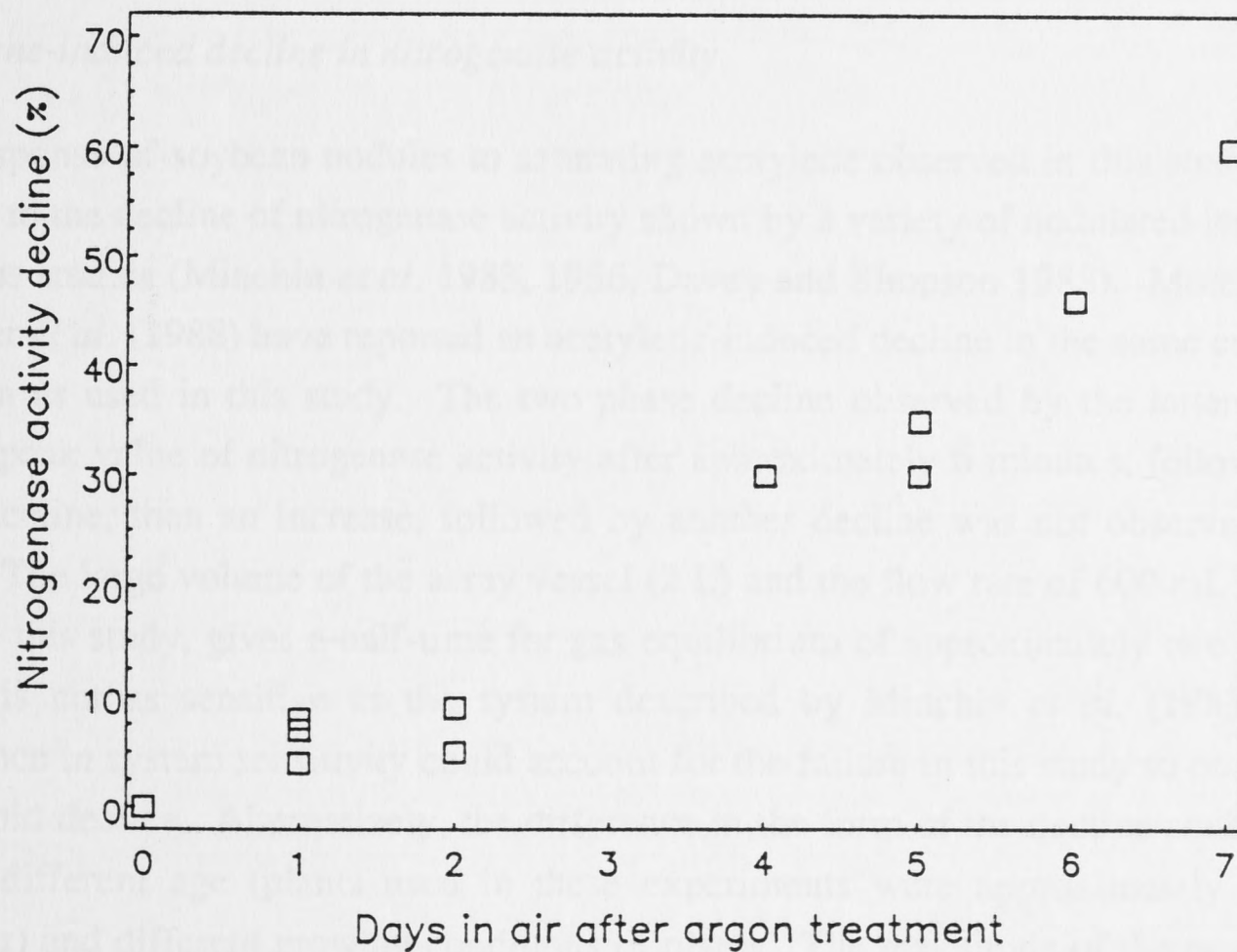
The response of argon/oxygen grown plants to exposure to air for a number of days was investigated. The development of nodules was followed for seven days after argon/oxygen around the roots and nodules was replaced with air. The results of two separate experiments are presented in Table 4.5. The nitrogen content of the nodules gradually increased, as did the soluble haem content. The response of these plants to acetylene in the open-flow system was also examined. Figure 4.10 shows the amount of decline of acetylene reduction, expressed as a percent of the maximum peak value, for

plants grown in air for up to seven days after continuous argon/oxygen treatment. When placed in air these argon/oxygen grown plants gradually developed a greater decline-response to the presentation of acetylene. The specific activity of the nodules from these plants was variable (in the range of 100 to 160  $\mu\text{mol g}^{-1}\text{nodule DW hour}^{-1}$ ), and generally increased with increased time of exposure to air.

**Table 4.5** : Changes in haem and nitrogen content of nodules from plants developed in argon/oxygen and exposed to air for a number of days. Haem content and nitrogen content are the mean of duplicate samples.

Days in air	Haem $\mu\text{mol g}^{-1}$ FW	Nitrogen %
0	0.21	3.85
1	0.16	3.98
2		4.10
4	0.20	
5		4.55
6	0.32	
7		4.83
air <sup>a</sup>	0.44	5.65

<sup>a</sup> plants grown and developed in air only.



**Figure 4.10** : The amount of acetylene-induced decline shown by plants developed in argon/oxygen and placed in air for a number of days.

### 4.3. Discussion

#### *Nodulation*

Levels of ethylene maintained at 1 ppm around the roots led to a decrease in nodulation, but did not totally inhibit nodulation as has been observed in bean (Grobbelaar *et al.* 1971). The decrease in nodule formation at 10 and 100 ppm ethylene was probably due to changes in plant, and especially root, growth. Growing plants in the absence of N<sub>2</sub> did not alter the number of nodules forming on plants. The processes of nodule formation and autoregulation appear unrelated to N<sub>2</sub> fixation *per se*. This confirms work carried out using other techniques, which have shown that nodules can be formed by ineffective strains of rhizobia (Singleton and Stockinger 1983) and that autoregulation occurs before N<sub>2</sub> fixation of nodules begins (Kossak and Bohlool 1984).

#### *Short-term effects of ethylene on nitrogenase activity*

The absence of any effects of ethylene *per se* on nitrogenase activity (Figure 4.1) was an important control experiment which showed that the decline induced by exposure of root nodules to acetylene is not due to a phyto-hormone response caused by acetylene or ethylene. This result is in contrast with the results of Grobbelaar *et al.* (1971) and Goodlass and Smith (1979), mentioned earlier, who, using conventional assays of acetylene reduction and <sup>15</sup>N techniques, observed severe inhibition of ethylene on nitrogenase activity in pea and clover. These results may be reconciled by considering the length of time of treatment application and the different types of plants used.

#### *Acetylene-induced decline in nitrogenase activity*

The response of soybean nodules to saturating acetylene observed in this study is very similar to the decline of nitrogenase activity shown by a variety of nodulated legumes in previous studies (Minchin *et al.* 1983, 1986, Davey and Simpson 1988). More recently Schuller *et al.* (1988) have reported an acetylene-induced decline in the same cultivar of soybean as used in this study. The two phase decline observed by the latter authors, with a peak value of nitrogenase activity after approximately 6 minutes, followed by a rapid decline, then an increase, followed by another decline was not observed in this study. The large volume of the assay vessel (2 L) and the flow rate of 600 mL minute<sup>-1</sup> used in this study, gives a half-time for gas equilibrium of approximately two minutes, which is not as sensitive as the system described by Minchin *et al.* (1983). This difference in system sensitivity could account for the failure in this study to observe the first rapid decline. Alternatively, the difference in the form of the decline could be due to the different age (plants used in these experiments were approximately 10 days younger) and different growing conditions of plants. The magnitude of the peak values of ethylene production and the relative size of the final decline was similar in this and

previous (Minchin *et al.* 1986, Schuller *et al.* 1988) studies. A two phase decline of CO<sub>2</sub> efflux was observed in some pots when argon/oxygen gas mixtures replaced air in the open-flow system (Figure 4.3).

The responses of CO<sub>2</sub> efflux to acetylene in my experiments were similar to those observed by Schuller *et al.* (1988), showing a slight increase in CO<sub>2</sub> efflux which peaked at a time corresponding to peak ethylene production, as shown in Figure 4.2. This peak of CO<sub>2</sub> efflux may or may not be significant. It may be induced by the switching of gas mixtures and consequent disturbance of flow rates. However, in my experiments, care was taken to minimise flow rate fluctuations and CO<sub>2</sub> was monitored for one to two hours before each assay to ensure root activity was stable. The peak of CO<sub>2</sub> efflux occurred consistently in assays with acetylene or argon/oxygen (Figure 4.3). If this peak truly reflects increased CO<sub>2</sub> release, it is probably related to alterations in the metabolism of the nodules. The peak occurs as acetylene saturates nitrogenase and NH<sub>3</sub> production ceases. A burst of CO<sub>2</sub> production may occur as nitrogenase activity becomes briefly uncontrolled while carbon substrates are still available. This in turn, could lead to an increase in ethylene production, to a level over and above the nitrogenase activity occurring before the decline. Ammonium has been shown to inhibit the nitrogenase activity of nodule bries (Salminen 1981). Since NH<sub>3</sub> production stops when acetylene is reduced, the peak of CO<sub>2</sub> efflux may represent a brief period where nitrogenase activity and respiration increase before a decline is induced by other factors.

The absence of an acetylene-induced decline in soybean nodules reported by other workers (Weisz and Sinclair 1987a,b, Drevon *et al.* 1988b, Heckmann *et al.* 1989) may be explained by the observation recorded in this chapter that nodules grown submerged in solution do not show an acetylene-induced decline. Drevon *et al.* (1988b) and Heckmann *et al.* (1989) transferred plants from hydroponic to aeroponic conditions 12 hours before assays and Weisz and Sinclair (1987a,b) transferred their plants one day before the assays. It is unclear whether the nodules on the plants grown by Weisz and Sinclair (1987a,b) developed in solution or in air.

The recovery of nitrogenase activity with the addition of oxygen, observed here with soybeans, has been described previously (Witty *et al.* 1984) and has led to the conclusion that the resistance of the nodule to the diffusion of oxygen is increased upon exposure to acetylene or nitrogen free atmospheres. Oxygen does stimulate nitrogenase activity after acetylene exposure, but the mechanism and the role of this stimulation deserve special attention. This aspect is dealt with in detail in Chapter 6 and Chapter 8.

#### *Development and physiology of nodules in the absence of N<sub>2</sub>*

Nodulated plants grown with their roots exposed to argon/oxygen become very nitrogen limited. Growth of these plants was significantly reduced relative to control plants and



was only partially recovered with foliar application of urea. Of particular interest is the observation that these plants continued to express nitrogenase activity, albeit at a lower specific activity than that of air grown nodules. Pate *et al.* (1984) and Atkins *et al.* (1984) report similar results of continued expression of nitrogenase activity in nodules exposed to argon/oxygen. In these plants, the substrate of nitrogenase is protons, which are reduced and released as H<sub>2</sub>.

The absence of an acetylene-induced decline in plants grown with their root systems in argon/oxygen is a novel result. It provides a useful control to show that the acetylene-induced decline is not due to the effect of acetylene on a process unrelated to nitrogen fixation. The absence of the decline in these nodules lends further support to the suggestion that it is the disappearance of the products of nitrogen fixation which trigger the acetylene-induced decline (Minchin *et al.* 1983). Argon/oxygen developed nodules have not been exposed to the products of nitrogen fixation and ammonia assimilation, and therefore, show no reaction when nitrogenase switches from reducing protons to reducing acetylene. The endogenous activity of nodules grown in argon/oxygen is significantly lower than air grown nodules and this suggests that they may be already "regulated". Indeed, the mean initial root respiration of plants grown in argon/oxygen was the similar to the mean minimum value of root respiration of air plants after they were exposed to acetylene.

The gradual development of a response to acetylene in plants placed in air after argon/oxygen treatment shows that factors important for the expression of the acetylene-induced decline develop over a time period of days and require the nodule to be producing fixed nitrogen. This relatively long period of time is possibly consistent with anatomical development, although the nitrogen deficient state of these nodules is probably a factor limiting their subsequent development in air. Nodules developed first in air, then exposed to argon/oxygen and subsequently to air again (Pate *et al.* 1984, Atkins *et al.* 1984), rapidly recover the ability to fix and assimilate nitrogen, although the extent of the acetylene-induced decline throughout these treatments has not been investigated.

### *Conclusion*

The experiments presented in this chapter support the conclusion of Minchin *et al.* (1986) that the conventional acetylene reduction assay is too inaccurate for use in detailed physiological studies. Acetylene, by virtue of its inhibitory action, does however, provide a tool for investigating the regulation of nitrogenase activity in root nodules. This is dealt with further in Chapter 6. The use of low partial pressures of acetylene for the detection and quantification of nitrogenase activity, without the complication of the acetylene-induced decline, is examined in Chapter 5.

## Chapter 5

### Measurement of Nitrogenase Activity with Subsaturating Acetylene Pressures

#### 5.1. Introduction

##### *Measurement of nitrogen fixation*

Measuring the rate of nitrogen fixation is important in many agronomic, physiological and biochemical investigations. Symbiotic plants receive a portion of their nitrogen from applied and soil sources and a portion from nitrogen fixation. The stable isotope  $^{15}\text{N}$  can be used to detect the relative importance of these sources, but experiments using  $^{15}\text{N}$  are expensive in terms of chemicals, equipment and time. The resolution of  $^{15}\text{N}$  experiments is limited by the requirement of relatively large samples for destructive analysis by mass spectrometer, partly because of the natural background of  $^{15}\text{N}$  (0.365 atom-%) (Bergersen 1980). The proportion of ureides in the xylem sap provides a measure of the relative contribution of symbiotic and soil nitrogen (Herridge *et al.* 1978, McClure and Israel 1979). However, accurate conversion to rates of nitrogen fixation is difficult and it does not offer the high resolution of activity, that is often required in physiological experiments.  $^{13}\text{N}$  is the longest lived radioactive isotope of nitrogen, with a half-life of 10 minutes (Minchin 1986). Its use is limited to experiments of less than one hour which must be carried out at the site of  $^{13}\text{N}$  production.

Concomitant with the reduction of nitrogen by nitrogenase, is the production of hydrogen (Robson and Postgate 1980) and the measurement of the rate of hydrogen production by root nodules is an approach used by some laboratories to estimate nitrogen fixation (Layzell *et al.* 1989). This method also has disadvantages. A sensitive  $\text{H}_2$  detector is required and the biological system assayed must not express an uptake hydrogenase. Conversion of a hydrogen production rate into a nitrogen reduction rate requires knowledge of the electron allocation coefficient for nitrogenase, which may vary considerably with experimental treatments (Rainbird *et al.* 1983).

The reduction of acetylene to ethylene by nitrogenase has been used extensively to measure nitrogenase activity and estimate nitrogen fixation. When acetylene is present at a saturating concentration, almost all the electron flux through nitrogenase reduces

acetylene to ethylene (Meeks *et al.* 1978). However, the recent discovery of the dramatic inhibitory effects of saturating acetylene on nodular nitrogenase activity (Minchin *et al.* 1983), have shown that the conventional acetylene reduction assay is inaccurate and its use even in comparative experiments is seriously questioned (Minchin *et al.* 1986).

An alternative is the use of subsaturating acetylene pressures to measure a small portion of total nitrogenase activity and to extrapolate to higher pressures.

#### *Use of subsaturating acetylene to measure nitrogenase activity*

The complications of using subsaturating acetylene to assay nitrogenase activity include the effects of the product and reactant (as plant growth regulators) on the physiology of the plant, the difficulty of determining the relative importance of enzyme kinetics and diffusion kinetics on the acetylene reduction rate, and, finally, not understanding the effects of experimental treatments on enzyme or diffusion kinetics.

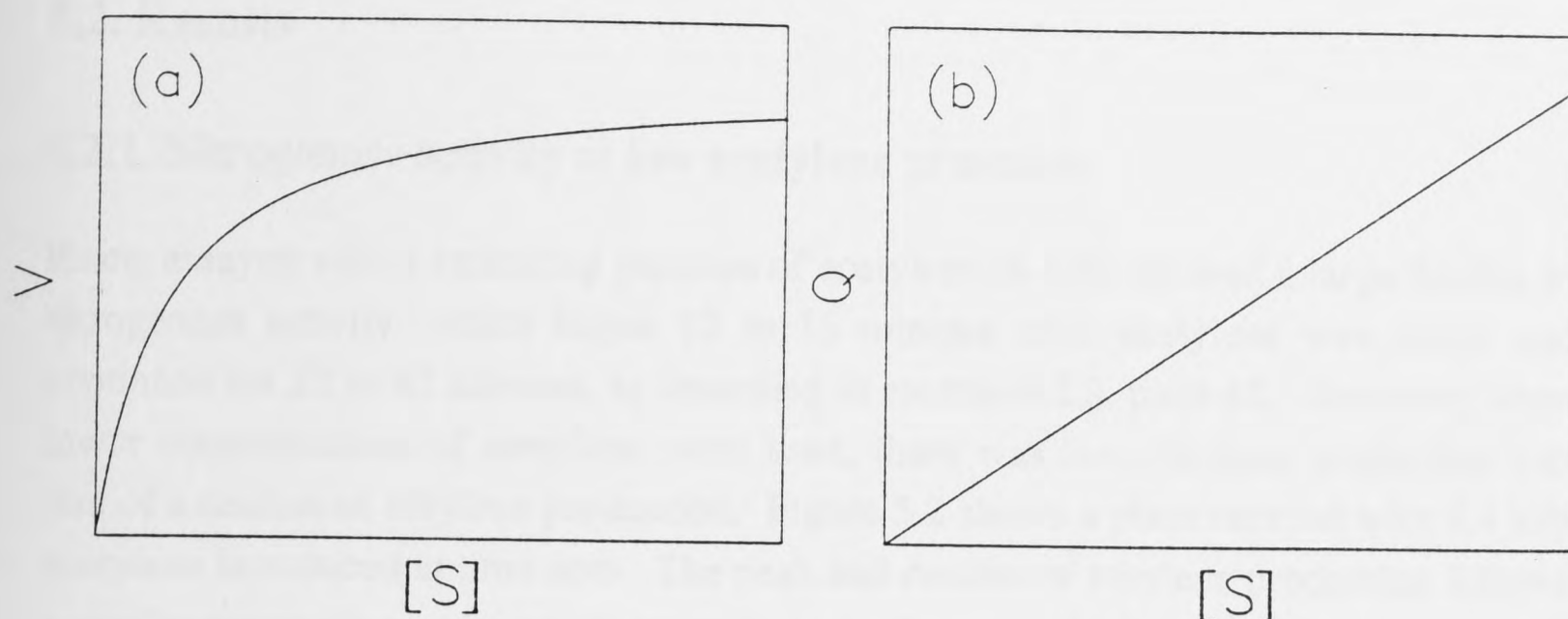
The relative importance of enzyme kinetics and diffusion kinetics on substrate reaction rates depend upon the concentration of the substrate, the resistance to diffusion of the substrate and the enzyme activity rate. The Michaelis-Menten equation which relates enzyme activity to the concentration of the substrate,

$$V = \frac{V_{max} \times [S]}{K_M + [S]}$$

predicts a hyperbolic response of enzyme activity to substrate concentration (Figure 5.1a), while rates of diffusion are linearly related to substrate concentration by Fick's Law,

$$Q = -DA \frac{dc}{dx}$$

where  $\frac{dc}{dx}$  equals the concentration gradient (Figure 5.1b).



**Figure 5.1 :** (a) Relationship between enzyme activity ( $V$ ) and concentration of a substrate ( $[S]$ ) and (b) relationship between diffusion rate ( $Q$ ) and concentration of a substrate ( $[S]$ ).

The interactions of enzyme kinetics and diffusion kinetics in root nodules have been examined in mathematical models (Denison *et al.* 1983b, Jones *et al.* 1987), where the effects of parameters which alter enzyme kinetics and diffusion kinetics can be examined. Davis (1988) criticizes Denison *et al.* (1983b) for separate treatment of diffusion and enzyme kinetics.

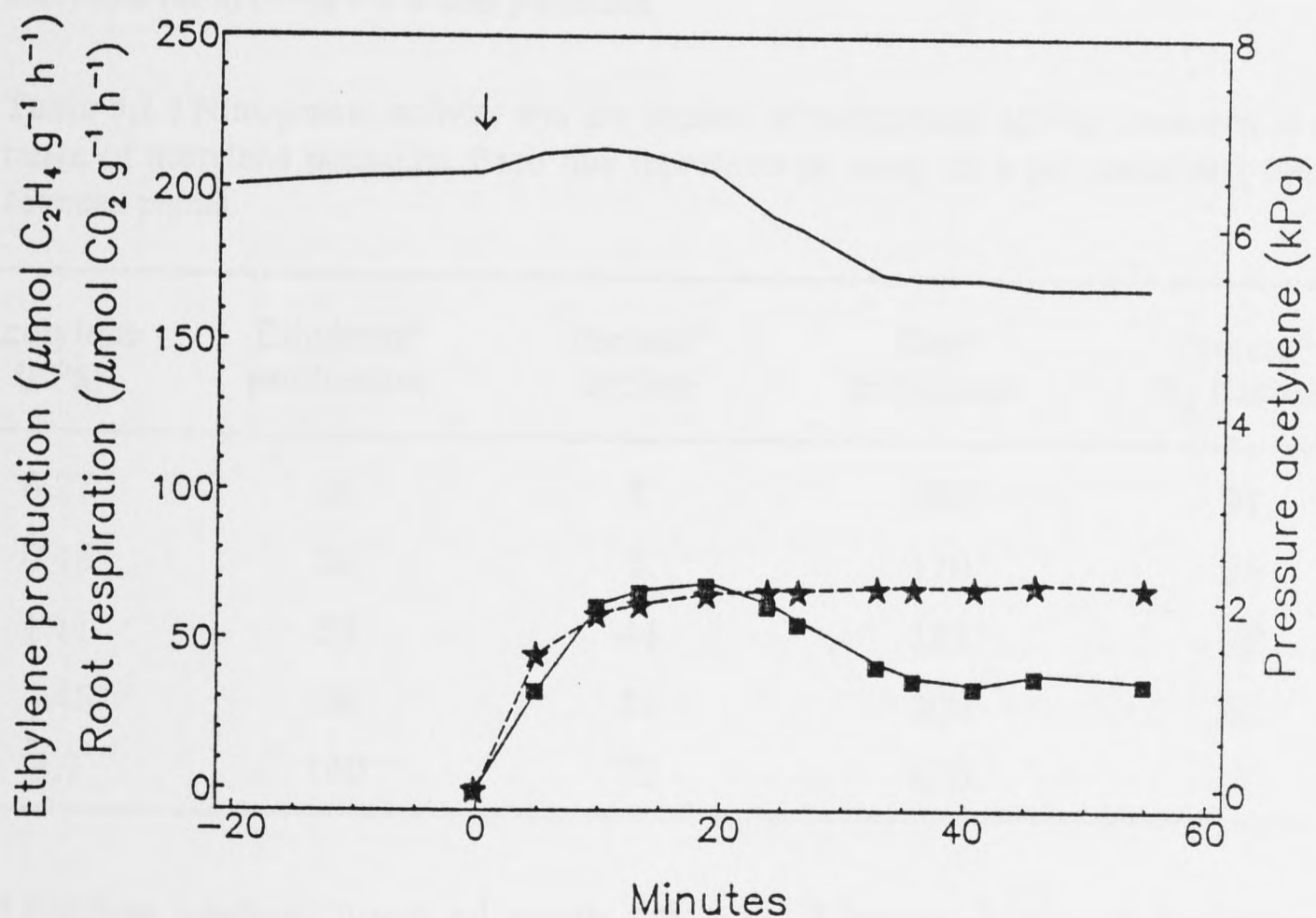
The use of subsaturating acetylene to detect a portion of nitrogenase activity, allows measurement of nitrogenase activity without the inhibitory effects of saturating acetylene. Denison *et al.* (1983a) used an open system with 0.2 kPa acetylene present to measure continuous acetylene reduction in soybeans. They were able to continuously monitor ethylene production over periods of hours or days and reported no adverse effects on the plants, as a result of this exposure. Recently, Davey and Simpson (1988) have examined the effect of subsaturating acetylene on clover nodules using an open flow system and found no inhibition of nitrogenase activity below 0.4 kPa acetylene and partial inhibition above this pressure, with the amount of inhibition increasing with increasing acetylene pressure. In both these reports the difficulty of determining the actual rate of nitrogen fixation from subsaturating acetylene data was acknowledged.

In this chapter, an examination of the effects of subsaturating pressures of acetylene on ethylene production in soybean nodules is carried out using an open-flow assay system. A method for continuously detecting nitrogenase activity without noticeably altering root respiration or nitrogenase activity is described. Some of the theoretical interactions of enzyme and diffusion kinetics at low acetylene pressures are examined in a model that calculates transient acetylene reduction as a function of acetylene pressures.

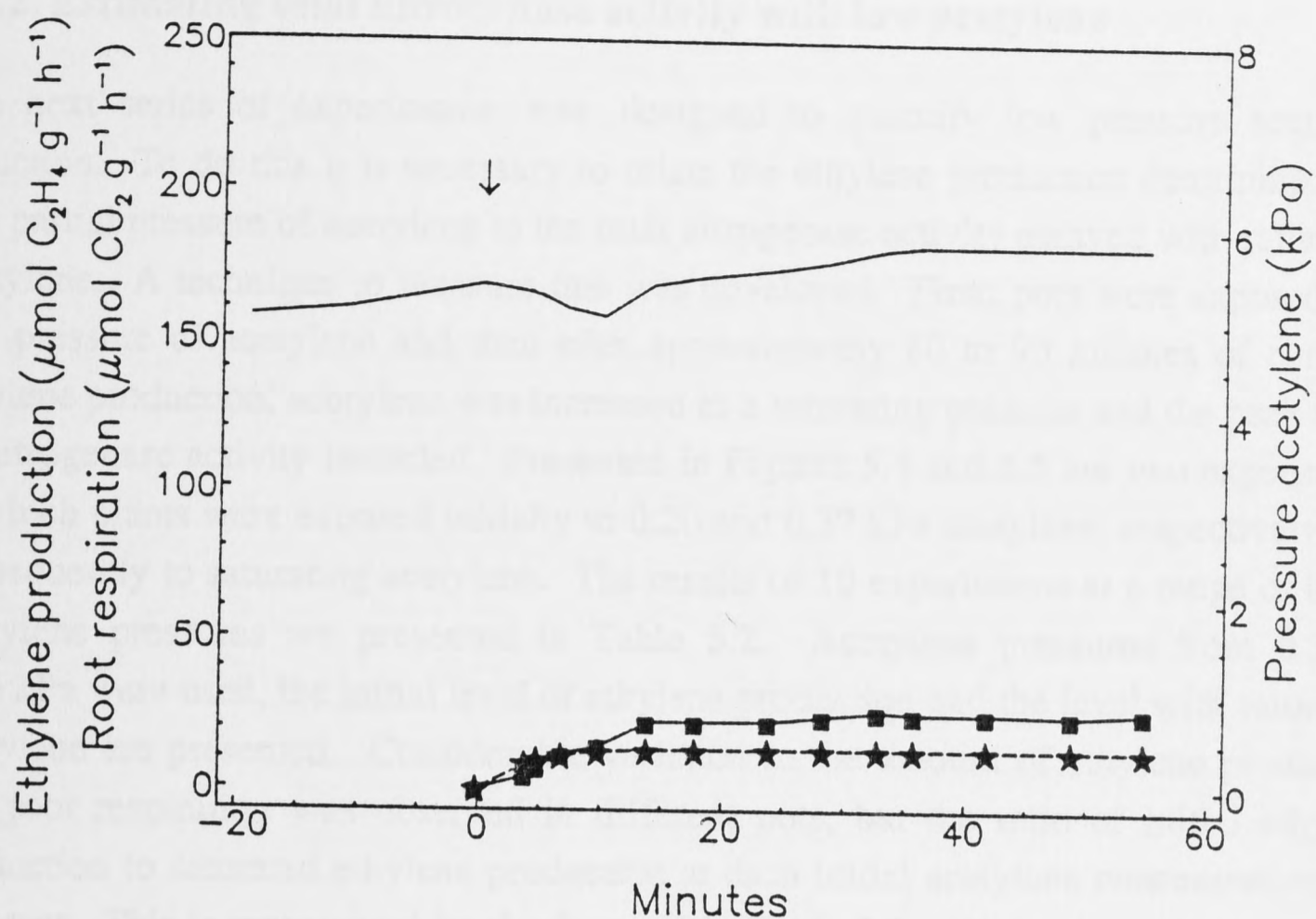
## 5.2. Results

### 5.2.1. Nitrogenase activity at low acetylene pressures

Plants assayed with a saturating pressure of acetylene (8 kPa) showed a large decline in nitrogenase activity, which began 10 to 15 minutes after acetylene was added and continued for 20 to 45 minutes, as described in section 4.2.3, page 45. However, when lower concentrations of acetylene were used, there was less ethylene production and less of a decline in ethylene production. Figure 5.2 shows a plant assayed with 2.4 kPa acetylene introduced at time zero. The peak and decline of ethylene production follows a similar pattern to an assay with saturating acetylene, but both the peak and decline are smaller. If an acetylene pressure less than 1 kPa is used then almost no decline is observed (Figure 5.3). The exposure of nodulated root systems, in the open-flow system, to acetylene concentrations less than 0.5 kPa did not cause a significant decline in nodulated root respiration or nitrogenase activity over periods of up to three to four hours (data not shown). Table 5.1 presents the results of five sets of plants assayed at various pressures of acetylene. As the acetylene pressure used in the assays was reduced, less nitrogenase activity was detected and the decline in root respiration and nitrogenase activity was also reduced.



**Figure 5.2 :** Exposure of nodulated roots to 2.4 kPa acetylene in an open-flow assay. 2.4 kPa acetylene was introduced to the root system of four plants in a single pot at time zero (arrow) and ethylene production (—■— μmol C<sub>2</sub>H<sub>4</sub> g<sup>-1</sup> nodule DW h<sup>-1</sup>) and root respiration (— μmol CO<sub>2</sub> g<sup>-1</sup> root DW h<sup>-1</sup>) monitored. The pressure of acetylene (kPa) (-★-) is also presented.



**Figure 5.3 :** Exposure of nodulated roots to 0.5 kPa acetylene in an open-flow assay. 0.5 kPa acetylene was introduced to the root system of four plants in a single pot at time zero (arrow) and ethylene production ( $\text{---}\blacksquare\text{---}$   $\mu\text{mol C}_2\text{H}_4 \text{ g}^{-1} \text{ nodule DW h}^{-1}$ ) and root respiration ( $\text{---}$   $\mu\text{mol CO}_2 \text{ g}^{-1} \text{ root DW h}^{-1}$ ) monitored. The pressure of acetylene (kPa) ( $\text{---}\star\text{---}$ ) is also presented.

**Table 5.1 :** Nitrogenase activity and the decline of nitrogenase activity observed at a range of acetylene pressures. Each line represents an assay on a pot containing four soybean plants.

Acetylene (kPa)	Ethylene <sup>a</sup> production	Percent <sup>b</sup> decline	Root <sup>c</sup> respiration	Percent <sup>d</sup> N <sub>2</sub> fixation
0.27	16	8	190	91
0.48	26	5	170	86
1.11	53	44	185	70
2.45	68	50	200	62
8.7	140	72	170	0

<sup>a</sup> Ethylene produced ( $\mu\text{mol g}^{-1} \text{ nodule DW h}^{-1}$ ). <sup>b</sup> Percent decline of nitrogenase activity observed after the introduction of acetylene. <sup>c</sup> Initial nodulated root CO<sub>2</sub> efflux ( $\mu\text{mol g}^{-1} \text{ root DW h}^{-1}$ ). <sup>d</sup> Estimated percent of nitrogen fixation remaining, calculated assuming a maximum rate of  $45 \mu\text{mol N}_2 \text{ g}^{-1} \text{ nodule DW h}^{-1}$  and an electron allocation to N<sub>2</sub> of 0.75. At saturating acetylene (8.7 kPa) nitrogen reduction is completely inhibited.

### 5.2.2. Estimating total nitrogenase activity with low acetylene

The next series of experiments was designed to quantify low pressure acetylene reduction. To do this it is necessary to relate the ethylene production determined at a low partial pressure of acetylene to the total nitrogenase activity assayed with saturating acetylene. A technique to measure this was developed. First, pots were exposed to a low pressure of acetylene and then after approximately 80 to 90 minutes of constant ethylene production, acetylene was increased to a saturating pressure and the peak value of nitrogenase activity recorded. Presented in Figures 5.4 and 5.5 are two experiments in which plants were exposed initially to 0.20 and 0.37 kPa acetylene, respectively, and subsequently to saturating acetylene. The results of 10 experiments at a range of initial acetylene pressures are presented in Table 5.2. Acetylene pressures from 0.20 to 0.86 kPa were used, the initial level of ethylene production and the level with saturating acetylene are presented. Considerable variation in the amount of ethylene production and root respiration was observed in different pots, but the ratio of initial ethylene production to saturated ethylene production at each initial acetylene concentration was constant. This is represented by the factor K in Table 5.2, which relates the amount of ethylene detected at a subsaturating pressure of acetylene to the saturating acetylene reduction activity.

$$K = \frac{[C_2H_2] \times ARA_{sat}}{ARA_{sub}}$$

Where  $ARA_{sat}$  and  $ARA_{sub}$  are the ethylene production at saturating (8 kPa) and subsaturating acetylene ( $[C_2H_2]$ ) respectively.

K has a mean of  $2.24 \pm 0.15$  (95 % confidence limit) calculated from the data in Table 5.2. The two experiments carried out at 0.86 kPa acetylene were not used for calculating the mean, as a considerable proportion (40 %) of total activity was detected at this pressure acetylene and this may have caused an inhibition of the maximum rate determined after the initial exposure. It is clearly difficult to determine the proportion of activity detected above 0.5 kPa acetylene, since pressures above this level may begin to cause an acetylene-induced decline, making subsequent analysis difficult.

The factor K can be used to estimate the total nitrogenase activity in plants grown under the standard conditions outlined in Chapter 2 and exposed to subsaturating acetylene pressures of less than 0.5 kPa.

$$\text{Nitrogenase activity} = \frac{\text{ethylene detected}}{\text{acetylene kPa}} \times 2.24 \pm 0.15 \text{ (SE 95\%)}$$

Equation 5.1

Using the mean value of nitrogenase activity determined with saturating acetylene in my experiments, of  $180 \mu\text{mol } C_2H_4 \text{ g}^{-1} \text{ nodule DW h}^{-1}$ , the proportion of electrons

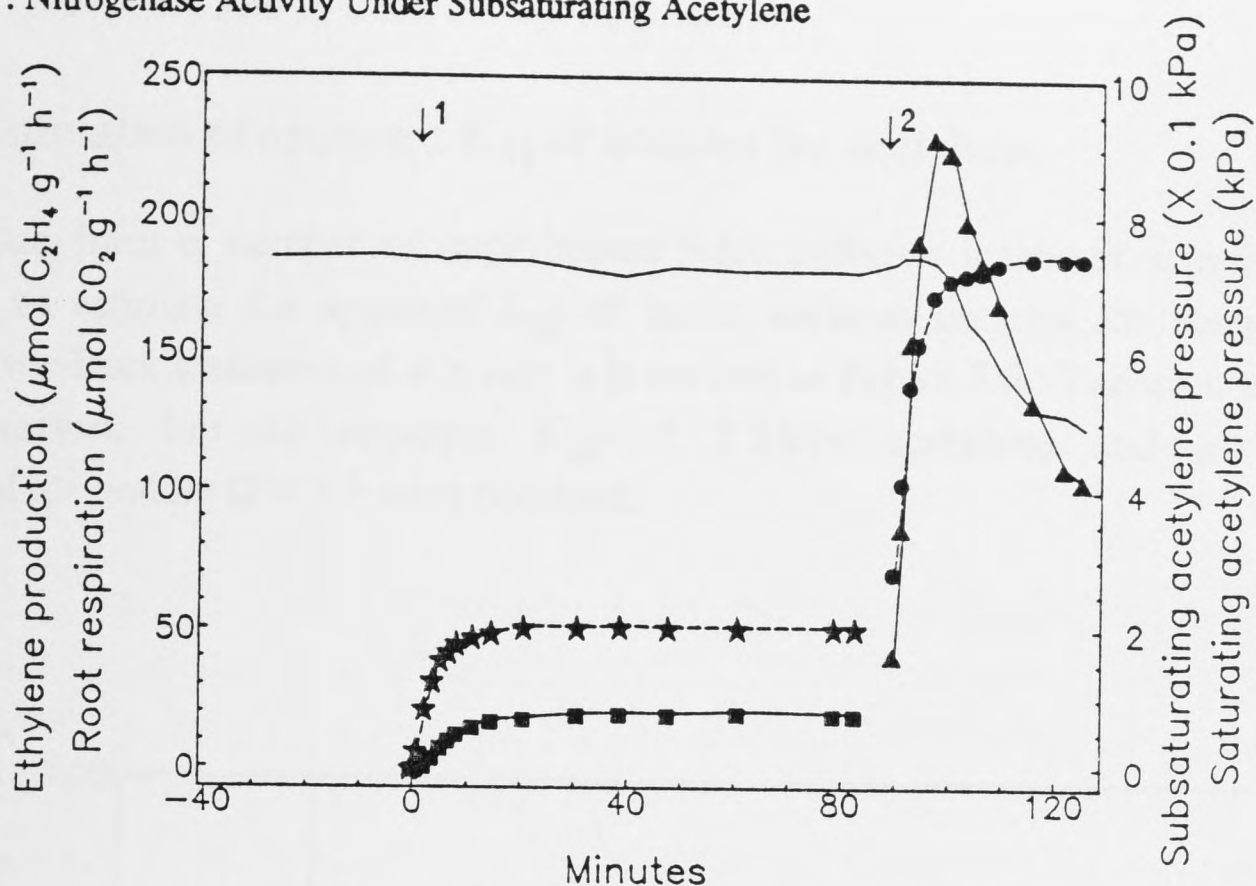
allocated to acetylene at 0.2 kPa acetylene pressure will be less than 10 % of the total nitrogenase electron flux. The remaining 90 % + of activity will continue to fix nitrogen and protons, and as such the metabolism of the nodules will be largely unaltered.

**Table 5.2 :** Ethylene production at subsaturating and saturating pressures of acetylene at a range of low acetylene pressures. Each line represents an individual assay with a pot containing four plants. Pots were exposed initially to the subsaturating acetylene pressure and ethylene production recorded; They were subsequently exposed to saturating acetylene and peak ethylene production was determined.

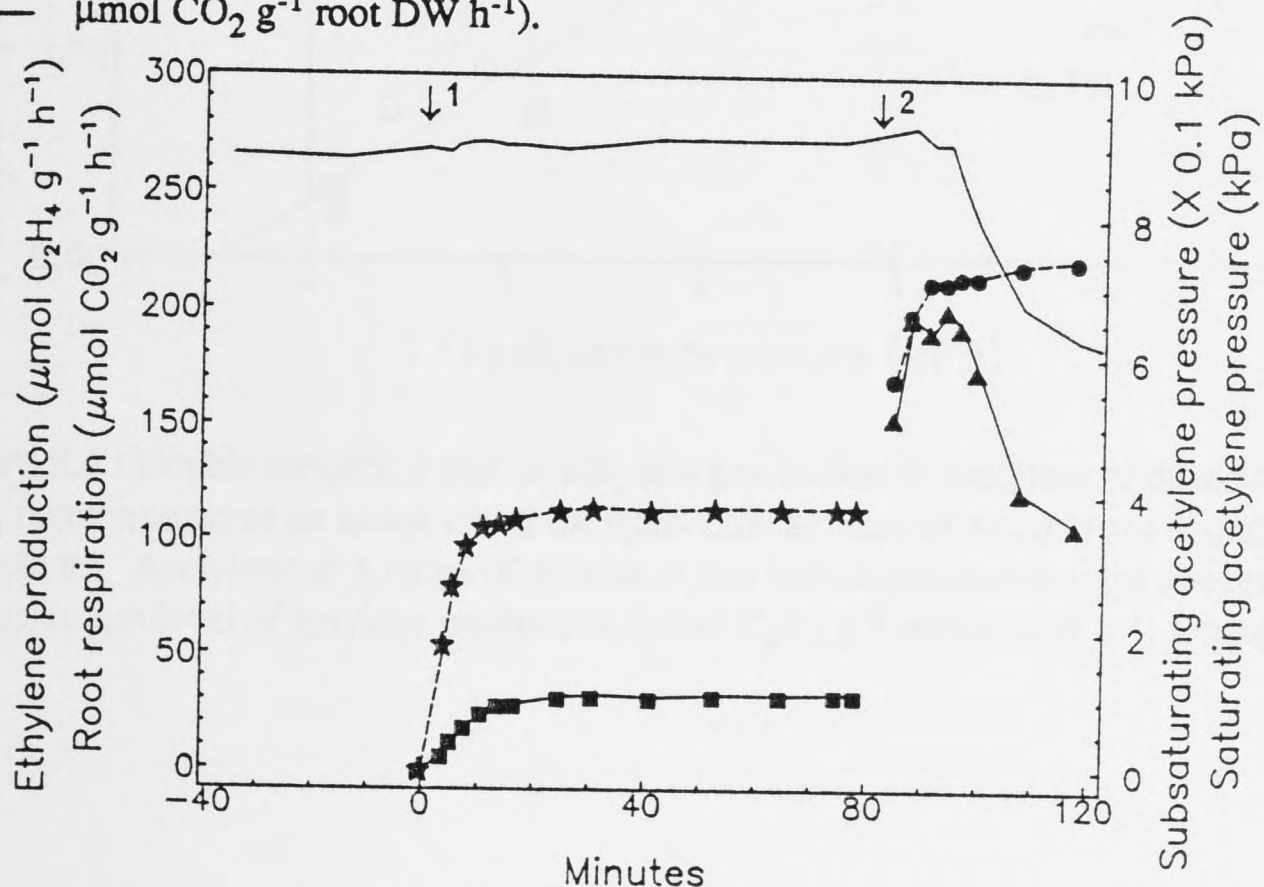
Acetylene <sup>a</sup> (kPa)	Subsat. <sup>b</sup> ethylene	Saturating <sup>c</sup> ethylene	Fraction <sup>d</sup> detected	K <sup>e</sup>	Root <sup>f</sup> respiration
0.20	18	183	0.098	2.03	181
0.20	20	228	0.088	2.28	184
0.20	6.8	65	0.105	1.91	92
0.21	14.0	165	0.084	2.47	263
0.21	15.3	172	0.089	2.36	252
0.21	14.6	162	0.090	2.33	234
0.37	33	203	0.162	2.27	270
0.38	33	201	0.162	2.31	262
0.86	70	170	0.412	2.09	219
0.86	68	174	0.391	2.20	248

<sup>a</sup> Initial acetylene pressure. <sup>b</sup> Ethylene produced at initial low acetylene pressure ( $\mu\text{mol g}^{-1}\text{nodule DW h}^{-1}$ ). <sup>c</sup> Peak ethylene produced at saturating (8 kPa) acetylene pressure ( $\mu\text{mol g}^{-1}\text{nodule DW h}^{-1}$ ). <sup>d</sup> Fraction of the peak of saturating nitrogenase activity that was detected at the initial acetylene pressure. <sup>e</sup> K is a factor calculated by multiplying the subsaturating acetylene pressure by the ethylene production at saturating pressure and dividing by the ethylene production at the subsaturating pressure. As this factor is relatively constant, it is useful in predicting maximum acetylene rates from data obtained with subsaturating acetylene (see text). <sup>f</sup> Initial nodulated root respiration ( $\text{CO}_2$  efflux) as  $\mu\text{mol g}^{-1}\text{root DW h}^{-1}$ .





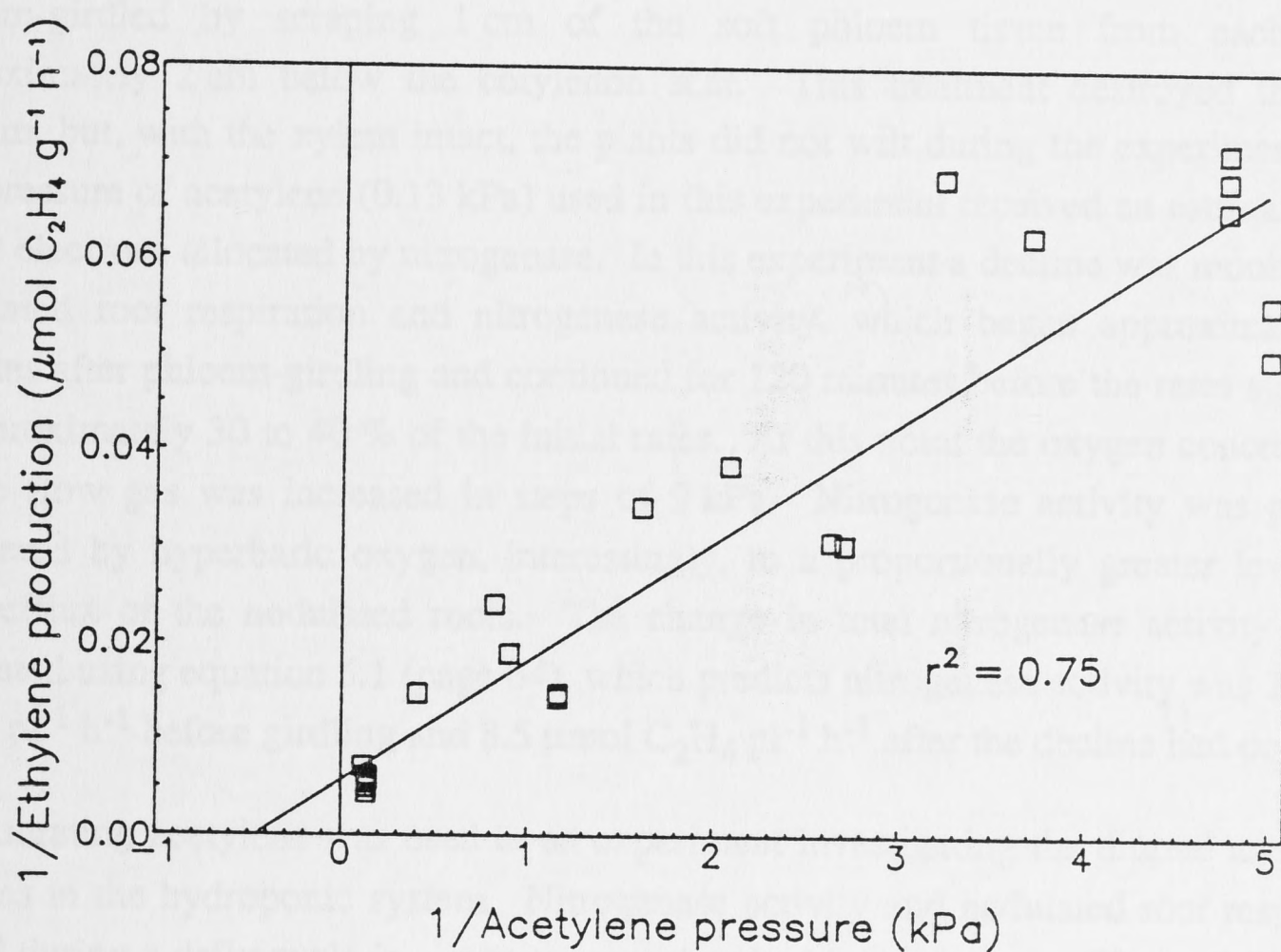
**Figure 5.4 :** Exposure of nodulated roots, initially to a subsaturating pressure of acetylene and subsequently to a saturating pressure of acetylene. The figure represents an assay, using the open-flow system, of a single pot containing four plants. The initial low level of acetylene ( $- \star -$  0.20 kPa) was introduced at time zero (arrow 1) and ethylene production was determined ( $- \blacksquare -$   $\mu\text{mol C}_2\text{H}_4 \text{ g}^{-1}$  nodule DW  $\text{h}^{-1}$ ). Saturating acetylene ( $- \bullet -$ ) was introduced 90 minutes after the low acetylene (arrow 2) and total nitrogenase activity was followed ( $- \blacktriangle -$   $\mu\text{mol C}_2\text{H}_4 \text{ g}^{-1}$  nodule DW  $\text{h}^{-1}$ ). Root respiration was monitored throughout the experiment ( $-$   $\mu\text{mol CO}_2 \text{ g}^{-1}$  root DW  $\text{h}^{-1}$ ).



**Figure 5.5 :** Exposure of nodulated roots, initially to a subsaturating pressure of acetylene and subsequently to a saturating pressure of acetylene. The figure represents an assay, using the open-flow system, of a single pot containing four plants. The initial low level of acetylene ( $- \star -$  0.37 kPa) was introduced at time zero (arrow 1) and ethylene production was determined ( $- \blacksquare -$   $\mu\text{mol C}_2\text{H}_4 \text{ g}^{-1}$  nodule DW  $\text{h}^{-1}$ ). Saturating acetylene ( $- \bullet -$ ) was introduced 82 minutes after the low acetylene (arrow 2) and total nitrogenase activity was followed ( $- \blacktriangle -$   $\mu\text{mol C}_2\text{H}_4 \text{ g}^{-1}$  nodule DW  $\text{h}^{-1}$ ). Root respiration was monitored throughout the experiment ( $-$   $\mu\text{mol CO}_2 \text{ g}^{-1}$  root DW  $\text{h}^{-1}$ ).

### 5.2.3. Estimation of apparent $K_M$ of nodules for acetylene

Using data from a number of experiments with different levels of acetylene, it is possible to estimate the apparent  $K_M$  of intact soybean nodules for acetylene. A Lineweaver-Burk treatment of this data is presented in Figure 5.6. Variation in the data was observed, but an apparent  $K_M$  of 2.2 kPa acetylene and a  $V_{max}$  of  $180 \mu\text{mol g}^{-1}$  nodule DW  $\text{h}^{-1}$  were obtained.



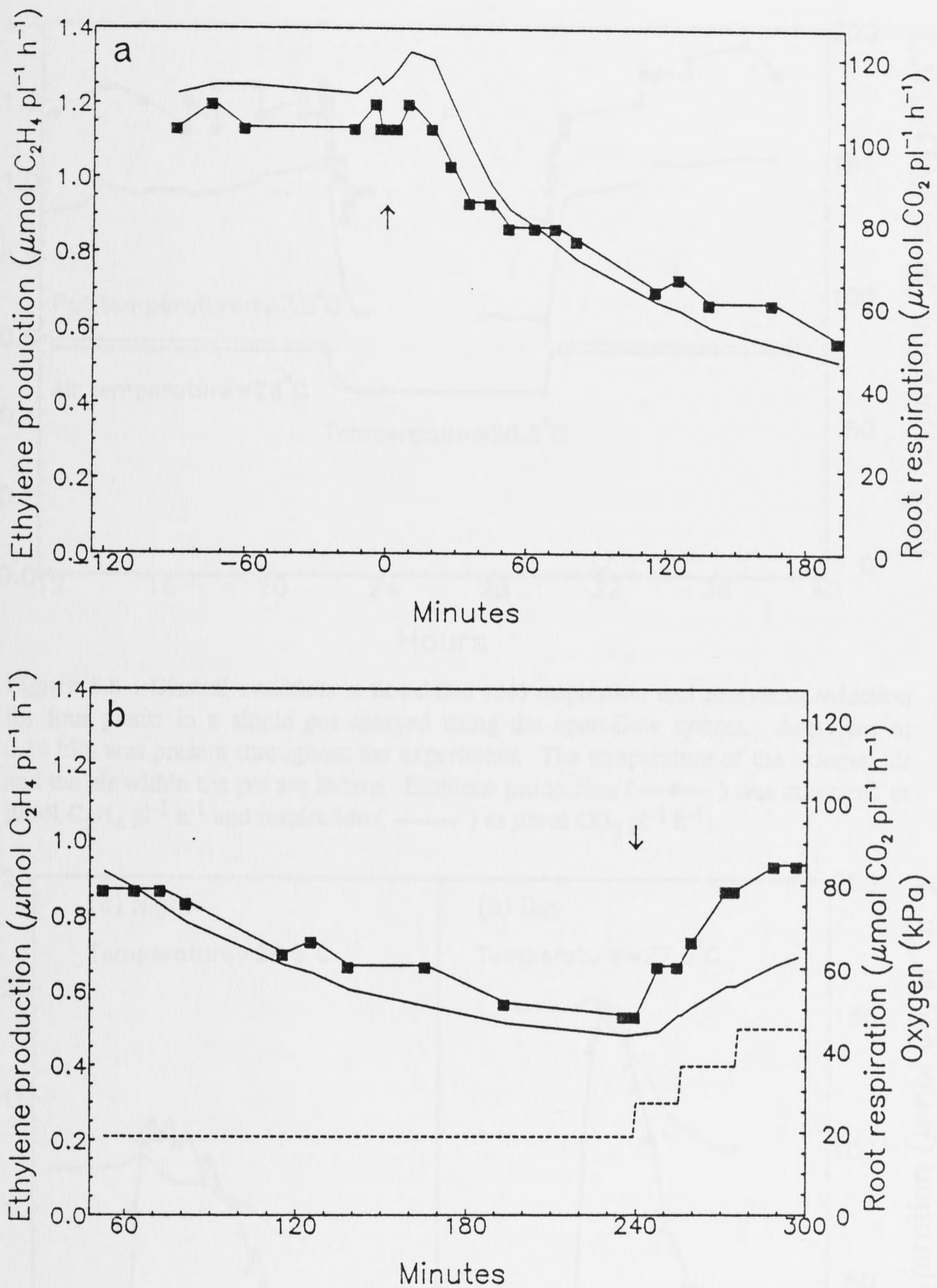
**Figure 5.6 :** Double reciprocal plot of ethylene production v. acetylene concentration. Each point represents an assay, using the open-flow system, of a single pot containing four plants. Acetylene at a range of pressures was introduced into the gas stream and the maximum level of ethylene production ( $\mu\text{mol C}_2\text{H}_4 \text{ g}^{-1}$  nodule DW  $\text{h}^{-1}$ ) recorded.

#### 5.2.4. Use of low pressures of acetylene in physiological studies

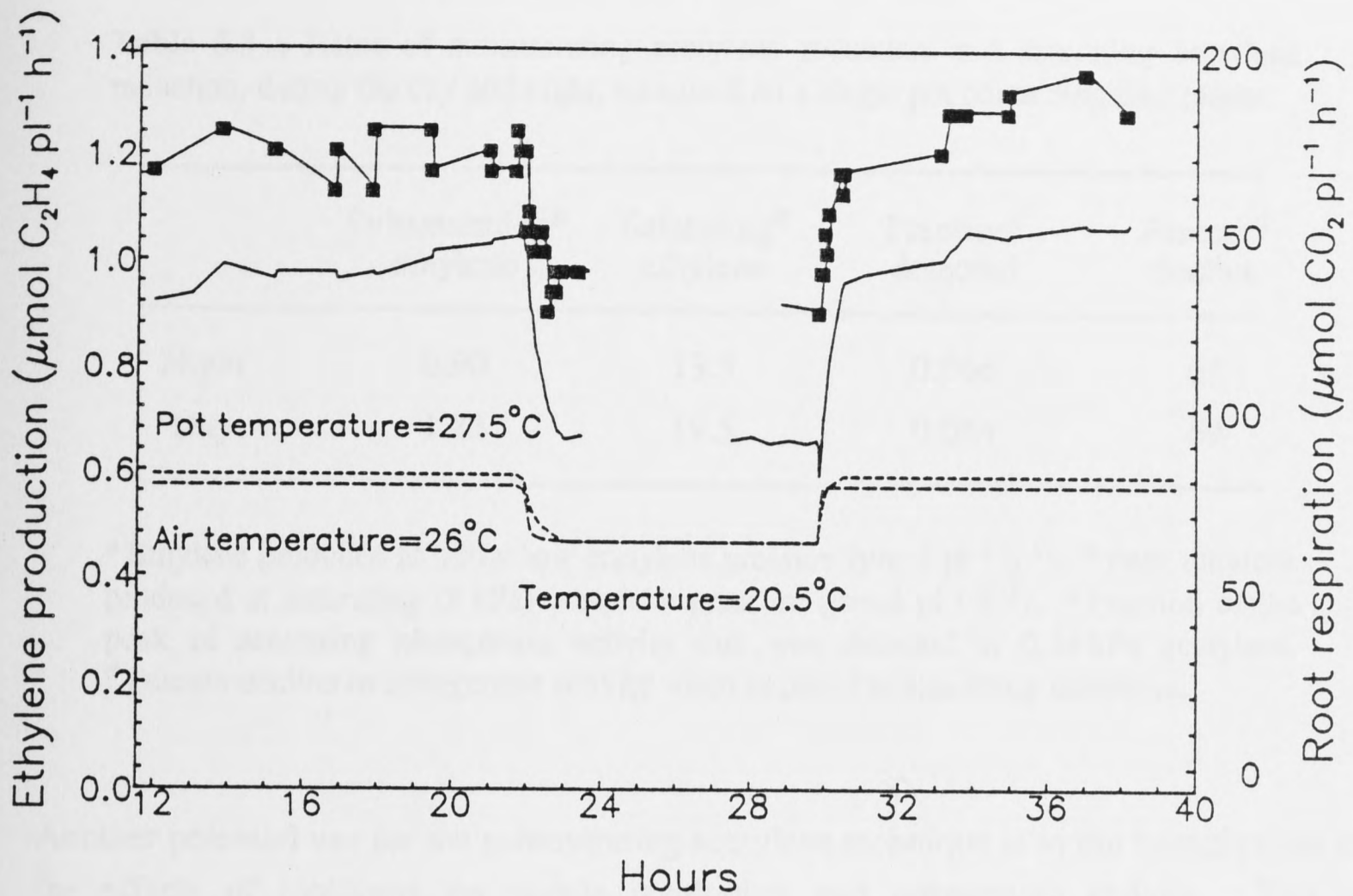
Saturating pressures of acetylene totally inhibit nitrogen fixation with consequences for nodule and plant metabolism in the short and long-term. Acetylene, introduced at a pressure lower than 0.5 kPa, had no apparent effect on plants over a period of hours and was therefore considered to be suitable for examining the effects of various treatments on nitrogenase activity.

The effect of phloem girdling on nitrogenase activity was examined using the open-flow system and subsaturating acetylene (Figure 5.7). Four plants in a single pot were all phloem-girdled by scraping 1 cm of the soft phloem tissue from each stem, approximately 2 cm below the cotyledon scar. This treatment destroyed the stem phloem, but, with the xylem intact, the plants did not wilt during the experiment. The low pressure of acetylene (0.13 kPa) used in this experiment received an estimated 7 % of the electrons allocated by nitrogenase. In this experiment a decline was monitored in nodulated root respiration and nitrogenase activity, which began approximately 10 minutes after phloem-girdling and continued for 120 minutes before the rates stabilized at approximately 30 to 40 % of the initial rates. At this point the oxygen concentration in the flow gas was increased in steps of 9 kPa. Nitrogenase activity was partially recovered by hyperbaric oxygen, interestingly, to a proportionally greater level than  $\text{CO}_2$  efflux of the nodulated roots. The change in total nitrogenase activity can be estimated using equation 5.1 (page 64), which predicts nitrogenase activity was  $20 \mu\text{mol C}_2\text{H}_4 \text{ pl}^{-1} \text{ h}^{-1}$  before girdling and  $8.5 \mu\text{mol C}_2\text{H}_4 \text{ pl}^{-1} \text{ h}^{-1}$  after the decline had occurred.

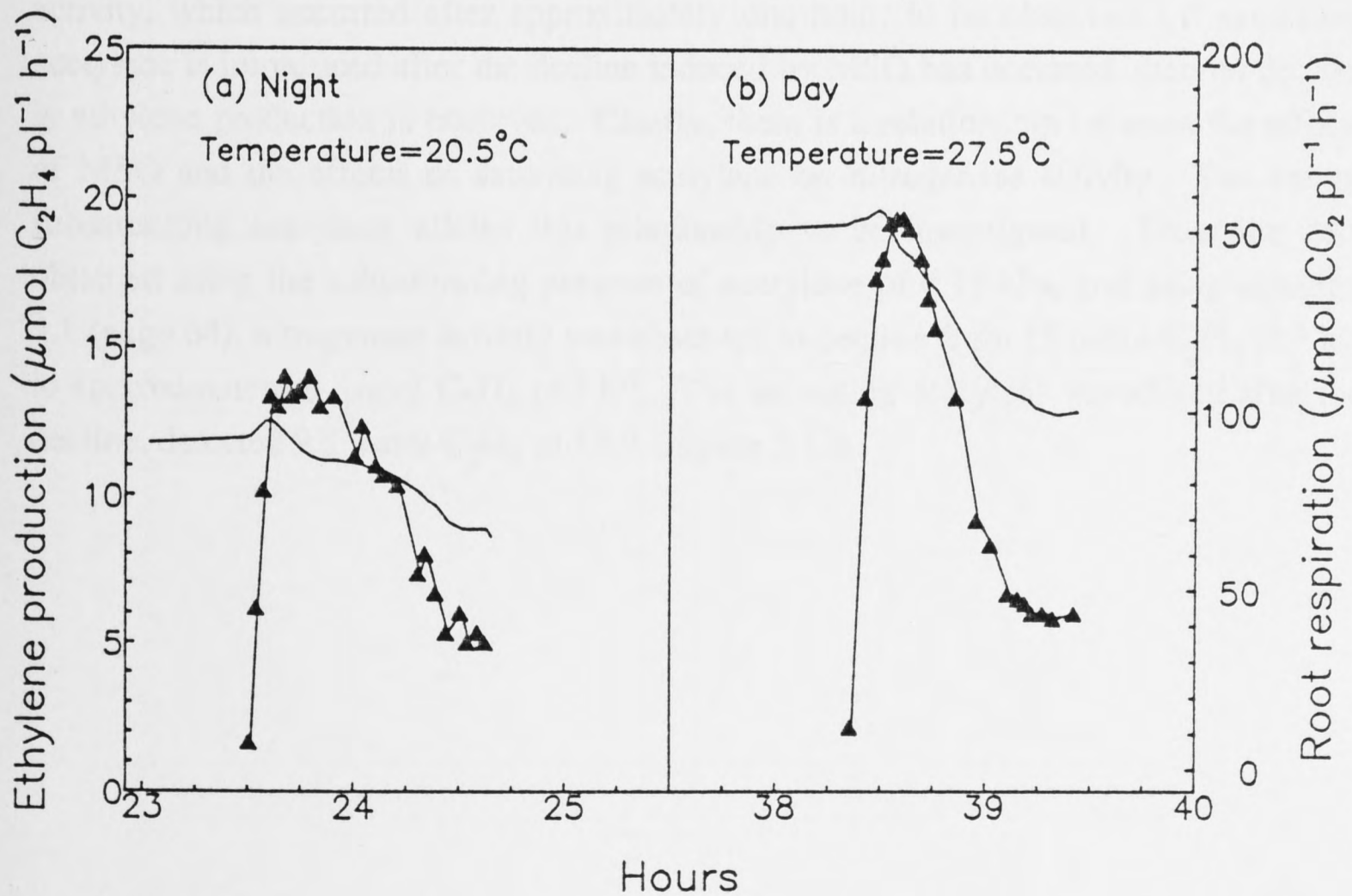
Subsaturating acetylene was used in an experiment investigating the diurnal activity of nodules in the hydroponic system. Nitrogenase activity and nodulated root respiration varied during a daily cycle in a manner associated with temperature (Figure 5.8). Total nitrogenase activity was detected by exposing the plants to saturating acetylene, once at night and once, at completion of the experiment, during the day (Figure 5.9). The ratio of acetylene reduction at subsaturating (0.14 kPa) and saturating acetylene pressures, was approximately constant (6.5 %). A proportionally similar sized decline occurred during the day or night (approximately 65 %) (Table 5.3), although the decline occurred more rapidly during the day (completed in 45 minutes), than at night (completed in 60 minutes).



**Figure 5.7 (a) :** Effect of phloem-girdling on nodulated root respiration and acetylene reduction of four plants in a single pot, assayed with the open-flow system. The plants were phloem-girdled 2 cm below the cotyledon scar at time zero (arrow). Acetylene at 0.13 kPa was present throughout the experiment. **(b) :** Oxygen stimulation of respiration and nodule ethylene production after phloem-girdling. Oxygen was increased in steps of approximately 9 kPa beginning (arrow) 240 minutes after phloem-girdling. Ethylene production was measured as (—■—)  $\mu\text{mol C}_2\text{H}_4 \text{ pl}^{-1} \text{ h}^{-1}$  and respiration as (—)  $\mu\text{mol CO}_2 \text{ pl}^{-1} \text{ h}^{-1}$ .



**Figure 5.8 :** Diurnal variation in nodulated root respiration and acetylene reduction for four plants in a single pot assayed using the open-flow system. Acetylene at 0.14 kPa was present throughout the experiment. The temperature of the external air and the air within the pot are shown. Ethylene production (—■—) was measured as  $\mu\text{mol C}_2\text{H}_4 \text{ pl}^{-1} \text{ h}^{-1}$  and respiration (—) as  $\mu\text{mol CO}_2 \text{ pl}^{-1} \text{ h}^{-1}$ .



**Figure 5.9 :** Assay of the acetylene-induced decline during the night and day. Four plants in a single pot were exposed to saturating acetylene (8 kPa) during the night (a) and again during the following day (b). The temperature of the air within the pot is shown. Ethylene production (—▲—) was measured as  $\mu\text{mol C}_2\text{H}_4 \text{ pl}^{-1} \text{ h}^{-1}$  and nodulated root respiration (—) as  $\mu\text{mol CO}_2 \text{ pl}^{-1} \text{ h}^{-1}$ .

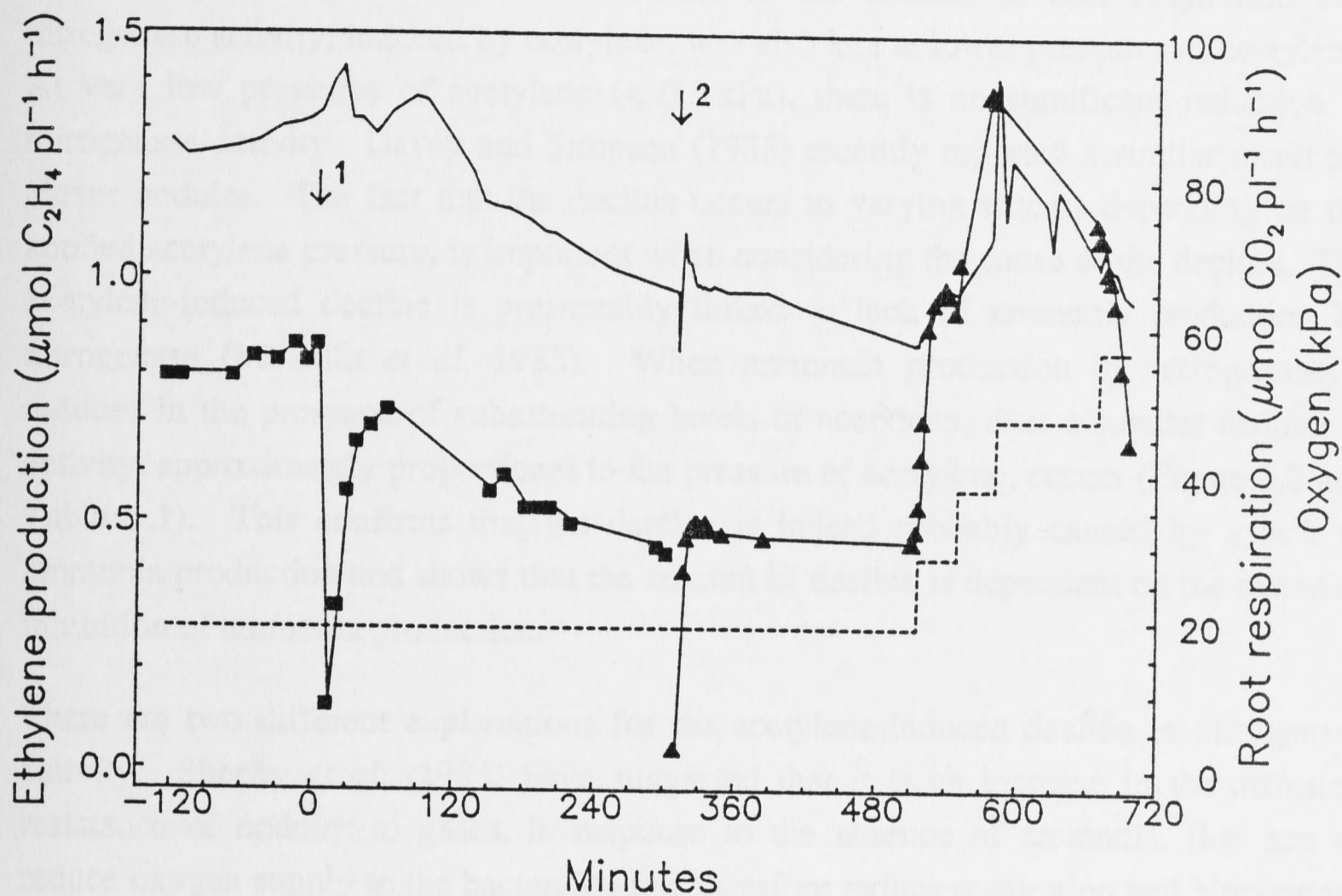
**Table 5.3** : Rates of subsaturating acetylene reduction and saturating acetylene reduction, during the day and night, measured on a single pot containing four plants.

	Subsaturating <sup>a</sup> ethylene	Saturating <sup>b</sup> ethylene	Fraction <sup>c</sup> detected	Percent <sup>d</sup> decline
Night	0.90	13.5	0.066	63
Day	1.25	19.5	0.064	69

<sup>a</sup> Ethylene produced at initial low acetylene pressure ( $\mu\text{mol pl}^{-1} \text{h}^{-1}$ ). <sup>b</sup> Peak ethylene produced at saturating (8 kPa) acetylene pressure ( $\mu\text{mol pl}^{-1} \text{h}^{-1}$ ). <sup>c</sup> Fraction of the peak of saturating nitrogenase activity that was detected at 0.14 kPa acetylene.

<sup>d</sup> Percent decline in nitrogenase activity when exposed to saturating acetylene.

Another potential use for the subsaturating acetylene technique is in the investigation of the effects of inhibitors on nodule respiration and nitrogenase activity. This is examined in detail in the next chapter. In the experiment presented here, a solution containing methionine sulfoximine (MSO), an inhibitor of glutamine synthetase, was sprayed onto the nodulated root system of four plants at time zero (Figure 5.10). The presence of subsaturating acetylene allowed the subsequent decline in nitrogenase activity, which occurred after approximately one hour, to be observed. If saturating acetylene is introduced after the decline induced by MSO has occurred, then no decline in ethylene production is observed. Clearly, there is a relationship between the effects of MSO and the effects of saturating acetylene on nitrogenase activity. The use of subsaturating acetylene allows this relationship to be investigated. From the data obtained using the subsaturating pressure of acetylene of 0.13 kPa, and using equation 5.1 (page 64), nitrogenase activity was observed to decline from  $15 \mu\text{mol C}_2\text{H}_4 \text{pl}^{-1} \text{h}^{-1}$  to approximately  $8 \mu\text{mol C}_2\text{H}_4 \text{pl}^{-1} \text{h}^{-1}$ . The saturating acetylene introduced after the decline, detected  $9.5 \mu\text{mol C}_2\text{H}_4 \text{pl}^{-1} \text{h}^{-1}$  (Figure 5.10).



**Figure 5.10** : Effect of spraying methionine sulfoximine (MSO) on the nodulated root systems of four plants in a single pot, assayed using the open-flow assay system. Acetylene at 0.13 kPa was present until 300 minutes. Five mL of a solution of 50 mM MSO in 5 mM MES buffer was sprayed onto the roots and nodules of the plants at time zero (arrow 1). Saturating acetylene (8 kPa) was introduced at 300 minutes (arrow 2). Oxygen (-----) was increased in steps of 9.5 kPa beginning at 495 minutes. Ethylene production was measured as  $\mu\text{mol C}_2\text{H}_4 \text{ pl}^{-1} \text{ h}^{-1}$  at 0.13 kPa acetylene (—■—) and as  $\mu\text{mol C}_2\text{H}_4 \text{ pl}^{-1} \times 20$  at 8 kPa acetylene (—▲—). Root respiration (—) was measured as  $\mu\text{mol CO}_2 \text{ pl}^{-1} \text{ h}^{-1}$ .

## 5.3. Discussion

### 5.3.1. Nitrogenase activity and the acetylene-induced decline

Ethylene production decreased as the acetylene pressure was lowered. This indicates that the proportion of the total nitrogenase activity reducing acetylene decreased as acetylene pressure decreased. The extent of the decline in root respiration and nitrogenase activity, induced by acetylene, was also less at lower pressures of acetylene. At very low pressures of acetylene (< 0.5 kPa), there is no significant reduction in nitrogenase activity. Davey and Simpson (1988) recently reported a similar result for clover nodules. The fact that the decline occurs to varying extents depending on the applied acetylene pressure, is important when considering the cause of the decline. The acetylene-induced decline is presumably linked to lack of ammonia production by nitrogenase (Minchin *et al.* 1983). When ammonia production by nitrogenase is reduced in the presence of subsaturating levels of acetylene, then a smaller decline in activity, approximately proportional to the pressure of acetylene, occurs (Figure 5.2 and Table 5.1). This confirms that the decline is indeed probably caused by a lack of ammonia production and shows that the amount of decline is dependent on the extent of inhibition of ammonia production.

There are two different explanations for the acetylene-induced decline in nitrogenase activity. Sheehy *et al.* (1983) have suggested that it is an increase in the diffusion resistance of nodules to gases, in response to the absence of ammonia, that acts to reduce oxygen supply to the bacteroids and therefore reduce respiration and nitrogenase activity. This change in diffusion resistance must be triggered by metabolic factors although the exact mechanism of how this occurs has not been determined. Witty *et al.* (1987) have microscopically observed changes in the air-spaces at the boundary of the infected zone and inner cortex and within the infected zone. After exposure to high oxygen, air-spaces within these regions were observed to disappear. With an elegant hypothesis, Walsh *et al.* (1989a) have proposed that disruption of phloem supply of sucrose to the nodule will upset the osmotic balance maintained between the symplast and the apoplast in the cortex and cause water movement into the intercellular spaces, which may restrict gas passage. A similar disruption in ureide production, caused by the absence of N<sub>2</sub> fixation (inhibited by acetylene), may cause an increase in diffusion resistance in an analogous manner. A halt in ureide production, while ureides continue to be exported from the nodule, may alter the osmotic balance of cells in the inner cortex and cause water movements which may restrict gas diffusion.

An alternative theory to explain the acetylene-induced decline is to consider the decline an entirely metabolic response to the absence of ammonia. Carbon and nitrogen metabolism is linked in cells and the absence of ammonia may influence reductant and



energy supply to nitrogenase. This may occur at the bacteroid level, where the presence of ammonia may positively affect the activity of carbon degrading enzymes or at the level of carbon supply by the plant to the bacteroid. Copeland *et al.* (1989a) have reported that the activity of malic enzyme in bacteroids is increased in the presence of ammonia. Kahn *et al.* 1985 have outlined a hypothesis where a nitrogen and carbon containing compound is exchanged for ammonia across the peribacteroid membrane. According to this model, when ammonia is not produced by the bacteroid, carbon supply is restricted. Inconsistent with this theory is the increased respiration and nitrogenase activity of nodules observed when the oxygen concentration surrounding the nodules is increased after exposure to stress (Witty *et al.* 1984), which suggests that nitrogenase activity is more oxygen limited than carbon limited. However, the observed increase in respiration could be the result of a respiratory protection mechanism and altered carbon metabolism in the bacteroids.

I will continue to discuss these two theories as 1/ the diffusion hypothesis and 2/ the metabolic hypothesis, throughout this thesis.

It is possible to explain the partial effect of subsaturating acetylene with the metabolic hypothesis, since partial decrease in ammonia or in compounds produced during ammonia assimilation, could alter the quantity of carbon compounds available within nodules and thus affect nitrogenase activity in a proportional manner. According to the diffusion hypothesis, the partial effects of subsaturating acetylene are explained by a partial change in the resistance of the diffusion barrier to oxygen. This implies a very fine control of the barrier. Control by a diffusion barrier may even be "auto-catalytic". If ammonia production is partially inhibited (by acetylene), the diffusion of oxygen is reduced, therefore ammonia production is further reduced, and so on. This possible response would make fine control of the barrier difficult. These effects of acetylene are discussed further in Chapters 6 and 8.

### 5.3.2. Quantitative determination of nitrogenase activity

Under the growth and assay conditions used in this study it was possible to estimate total nitrogenase activity from activities obtained under subsaturating conditions. The relationship (Table 5.2) found was:

$$\text{Nitrogenase activity} = \frac{\text{ethylene detected}}{\text{acetylene (kPa)}} \times 2.24$$

Nitrogen fixation rates predicted by this method are close to expected rates from growth analysis studies. At 27 to 30 days, individual plant nitrogenase rates determined using low acetylene and equation 5.1 were generally between 18 and 25  $\mu\text{mol C}_2\text{H}_4 \text{ h}^{-1}$ ; assuming an electron allocation coefficient to  $\text{N}_2$  of 0.75, this represents 3 to 4.2 mg N  $\text{day}^{-1}$ . Growth analysis and modelling of growth during this period (see section 3.3, page 35), predicts nitrogen fixation rates of 4 to 5 mg  $\text{pl}^{-1} \text{ day}^{-1}$ .

The relationship observed between trace ethylene production, acetylene pressure and maximum nitrogenase activity (equation 5.1) may only hold with the cultivar and conditions used in this study, or it may be more universal. This has not been investigated. It will depend on the relative affinity of nitrogenase for acetylene and the diffusion of acetylene into the nodule in different symbioses. The nitrogenase enzyme is very similar across different types of bacteria and its relative affinity for  $N_2$  and  $C_2H_2$  is probably similar. If all nodules have the same resistance to the diffusion of oxygen (they are generally all adapted to air), then they may have the same resistance to diffusion of acetylene. However, differences may arise where pathways for diffusion are different. Acetylene and oxygen have similar diffusion coefficients in air and water, but in water acetylene is 33 times more soluble than oxygen and 70 times more soluble than nitrogen. Any changes in the relative diffusion pathways between air and water in different nodule types would affect the relative diffusion of acetylene and oxygen. Experimental analysis of the response of different types of nodules is required before the method could be utilized more widely. However, this technique is useful for soybean (cv. Bragg) and is used further in Chapter 6. To understand how different factors may influence ethylene production at low acetylene pressures, it is possible to model ethylene production from acetylene and examine how various changes in parameters may affect maximum and detected rates of ethylene production.

### 5.3.3. Model of ethylene production at low pressures of acetylene

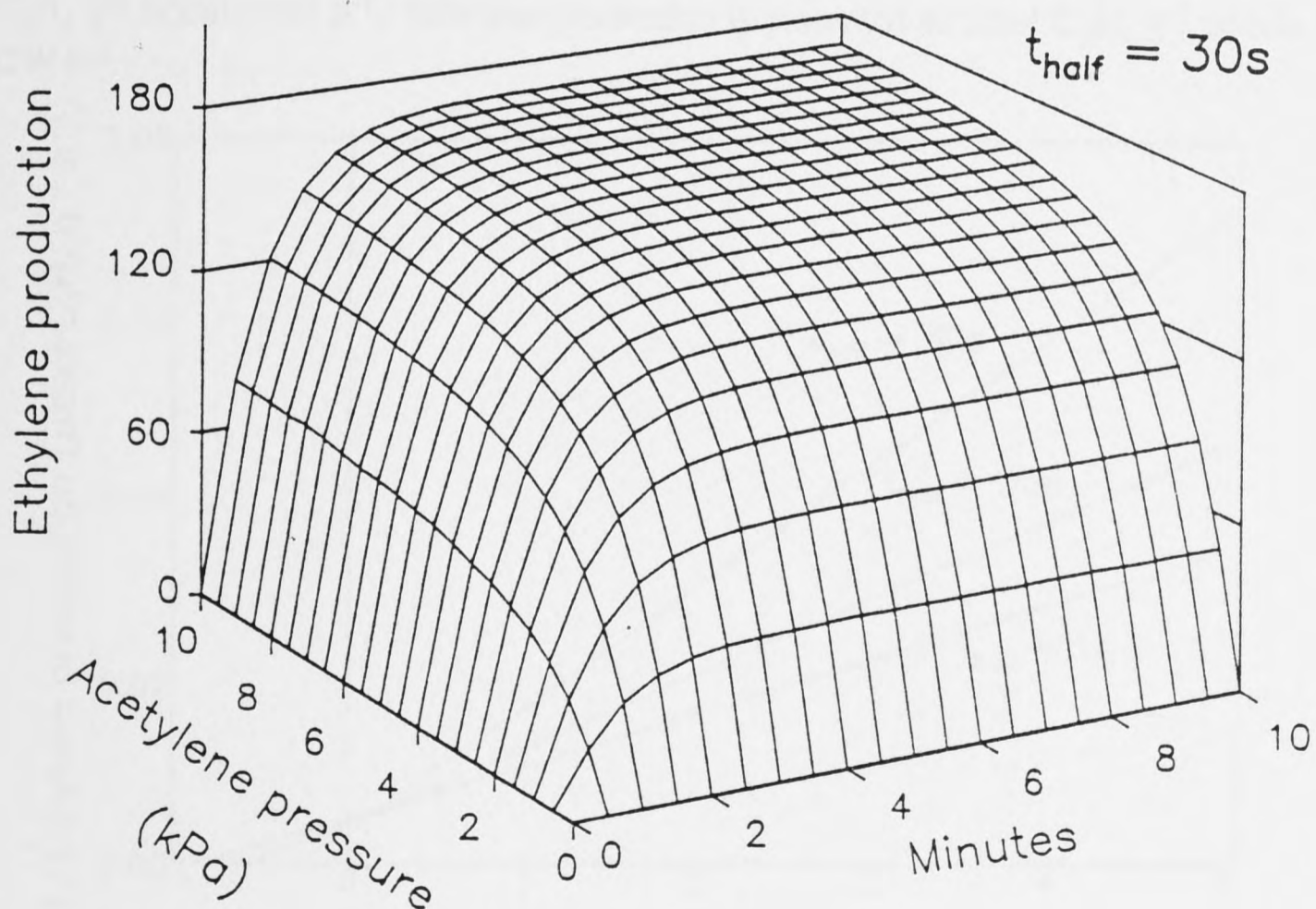
A program which calculates internal acetylene concentrations and ethylene production rates at various times after the introduction of various pressures of acetylene was written in BASIC. A copy of the program is in Appendix II. The amount of acetylene inside nodules is calculated (line 430) as the previous amount of acetylene inside the nodule, minus the ethylene produced, plus the amount of acetylene diffusing in (a function of the difference between the external acetylene concentration and the internal acetylene concentration and the time fraction of the nominated half-time for diffusion (line 420)). The amount of ethylene produced is calculated (lines 450 and 460) from the internal acetylene concentration using the Michaelis-Menten equation,

$$V = \frac{V_{max} \times [S]}{K_M + [S]}$$

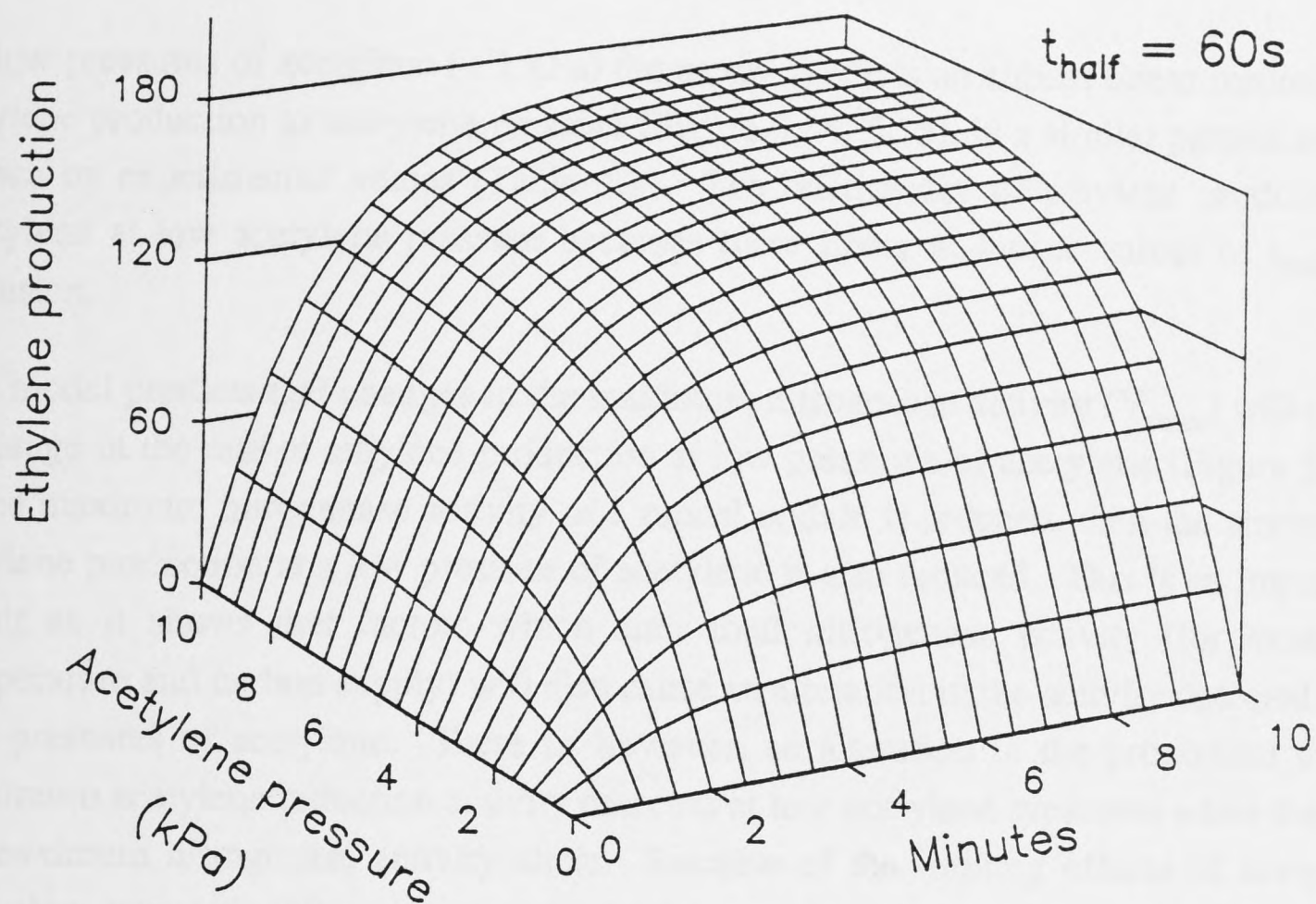
assuming a nitrogenase  $K_M$  of 264  $\mu M$  for acetylene (Hardy *et al.* 1968) and a maximum reaction rate of 180  $\mu mol C_2H_4 g^{-1} nodule DW h^{-1}$  (this study). The program calculates internal acetylene concentration and ethylene production rates at each time step. Ethylene release from nodules is governed by the same  $t_{half}$  for diffusion as acetylene.

The model seems to predict closely the results of experimental studies. The model

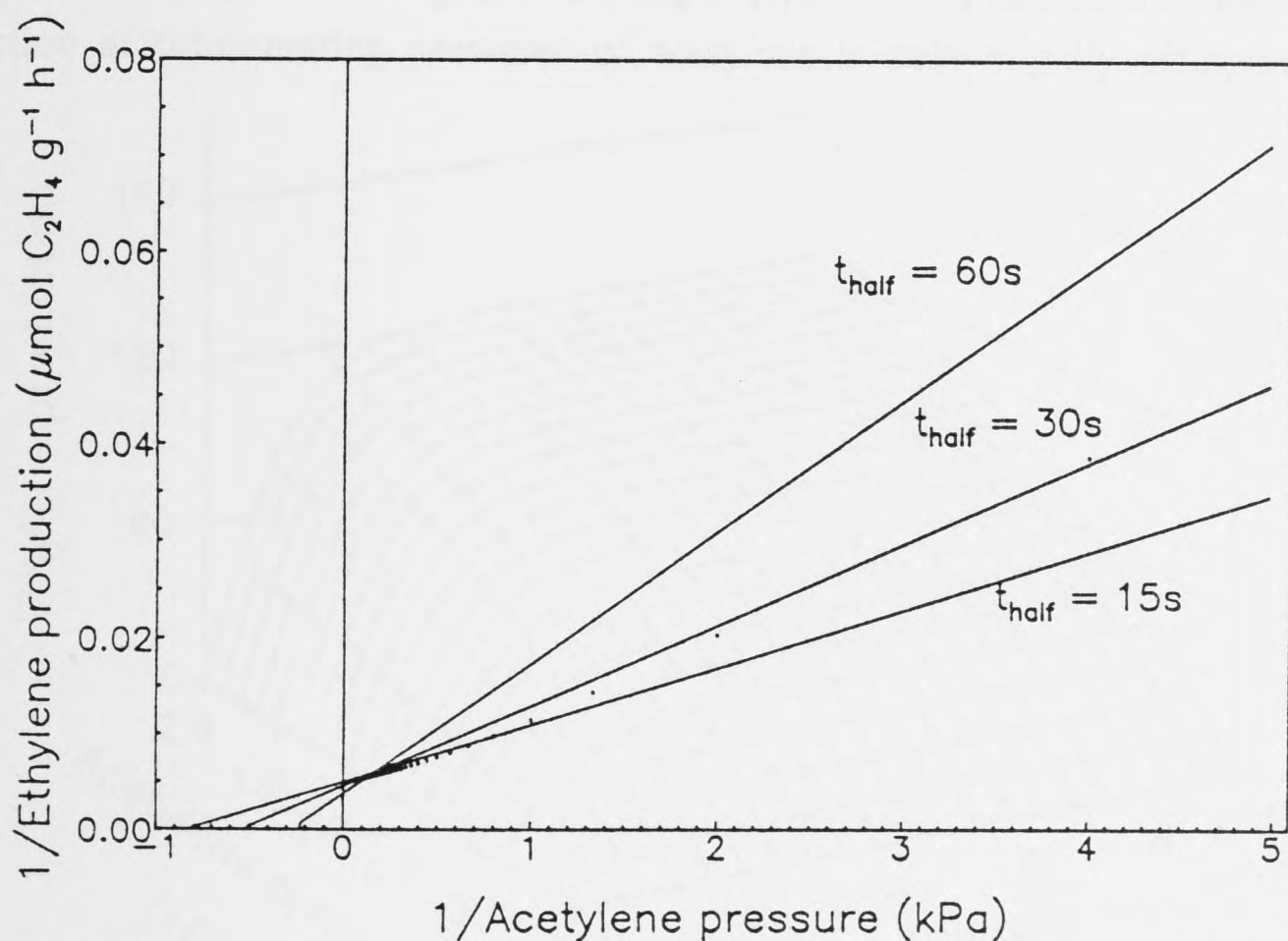
prediction of ethylene production, assuming a  $t_{\text{half}}$  for diffusion of acetylene and ethylene into or out of nodules of 30 s, shows that three to four minutes are required before equilibrium is reached (Figure 5.11). Saturation type kinetics occur at equilibrium. The time to reach equilibrium is prolonged, and saturation occurs at a higher acetylene concentration, if a  $t_{\text{half}}$  of 60 s is modelled (Figure 5.12), although the maximum rate of ethylene production at saturating pressures of acetylene remains the same. The effect of different values of  $t_{\text{half}}$  can be visualized if a Lineweaver Burk plot of the data obtained at equilibrium (40 minutes) is plotted (Figure 5.13). Increasing the half-time for acetylene diffusion increases the apparent  $K_M$ . With a  $t_{\text{half}}$  of 15 s the model predicts an apparent  $K_M$  of 1.1 kPa acetylene, at 30 s an apparent  $K_M$  of 1.8 kPa, and at 60 s an apparent  $K_M$  of 4 kPa. Comparing experimental (Figure 5.6) estimates of apparent  $K_M$  of 2.0 - 2.5 kPa acetylene, with the model (Figure 5.13), gives a prediction of  $t_{\text{half}}$  times for nodules of between 30 and 40 s, which is the  $t_{\text{half}}$  for acetylene that Davis (1984) measured in soybean nodules, using a method examining rates of influx and efflux from nodules.



**Figure 5.11** : Ethylene production at acetylene pressures from 0 to 10 kPa for 10 minutes after the introduction of acetylene, predicted by a model of nodule acetylene reduction. This simulation assumes a  $t_{\text{half}}$  for acetylene and ethylene diffusion of 30 s, a  $K_M$  of nitrogenase for acetylene of 264  $\mu\text{M}$  and a maximum velocity of 180  $\mu\text{mol C}_2\text{H}_4 \text{ g}^{-1} \text{ nodule DW h}^{-1}$ . Ethylene production is presented as  $\mu\text{mol C}_2\text{H}_4 \text{ g}^{-1} \text{ nodule DW h}^{-1}$ .



**Figure 5.12 :** Ethylene production at acetylene pressures from 0 to 10 kPa for 10 minutes after the introduction of acetylene, predicted by a model of nodule acetylene reduction. This simulation assumes a  $t_{\text{half}}$  for acetylene and ethylene diffusion of 60 s, a  $K_M$  of nitrogenase for acetylene of  $264 \mu\text{M}$  and a maximum velocity of  $180 \mu\text{mol C}_2\text{H}_4 \text{ g}^{-1} \text{ nodule DW h}^{-1}$ . Ethylene production is presented as  $\mu\text{mol C}_2\text{H}_4 \text{ g}^{-1} \text{ nodule DW h}^{-1}$ .

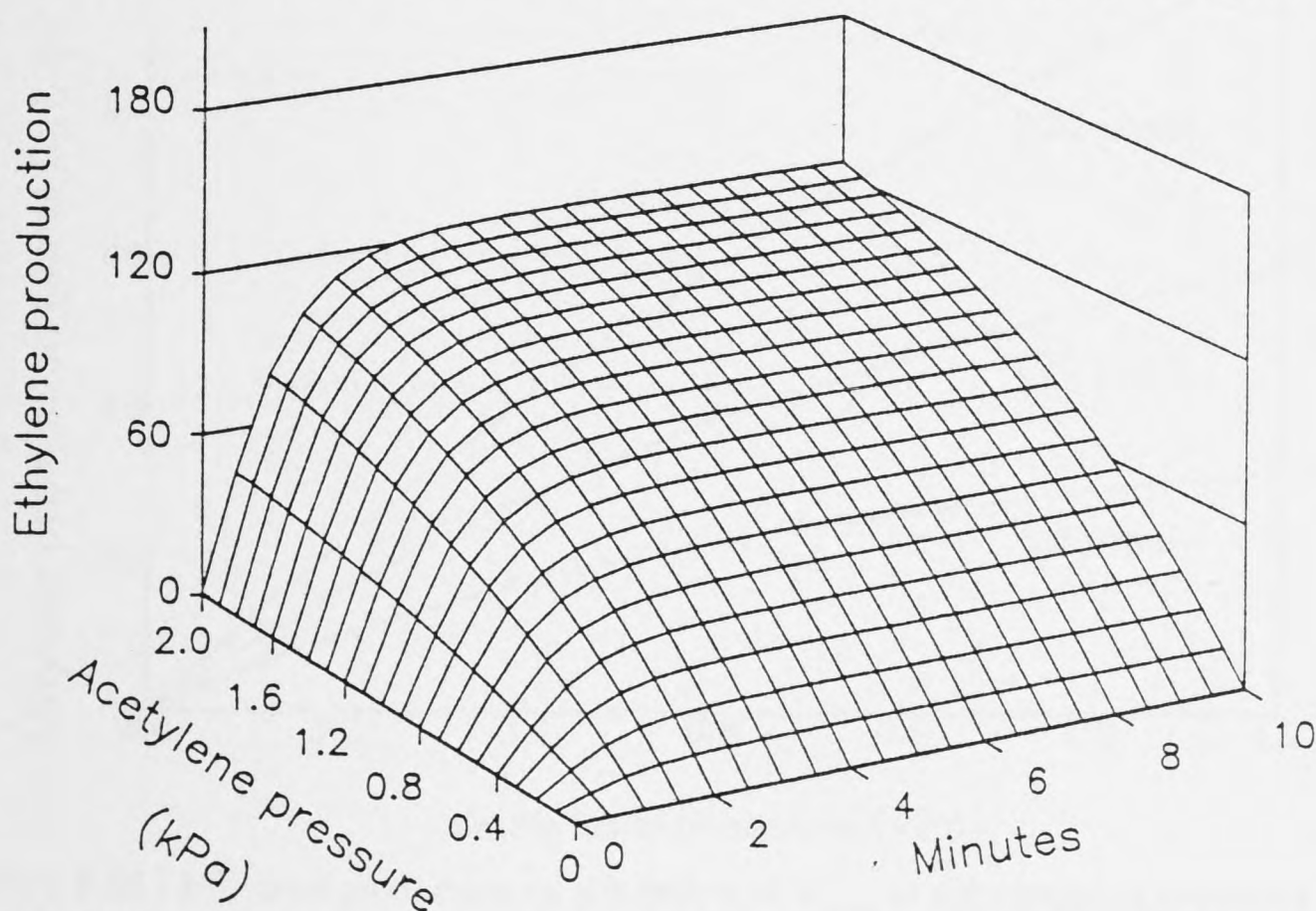


**Figure 5.13 :** A Lineweaver Burk treatment of ethylene production and acetylene pressure at  $t_{\text{half}}$  values for acetylene diffusion of 15, 30 and 60 s, as predicted by a model of nodule acetylene reduction. Data points for  $t_{\text{half}} = 30 \text{ s}$  are presented on the figure. Data was obtained at equilibrium (40 minutes) and the simulation assumes a  $K_M$  of nitrogenase for acetylene of  $264 \mu\text{M}$  and a maximum velocity of  $180 \mu\text{mol C}_2\text{H}_4 \text{ g}^{-1} \text{ nodule DW h}^{-1}$ .

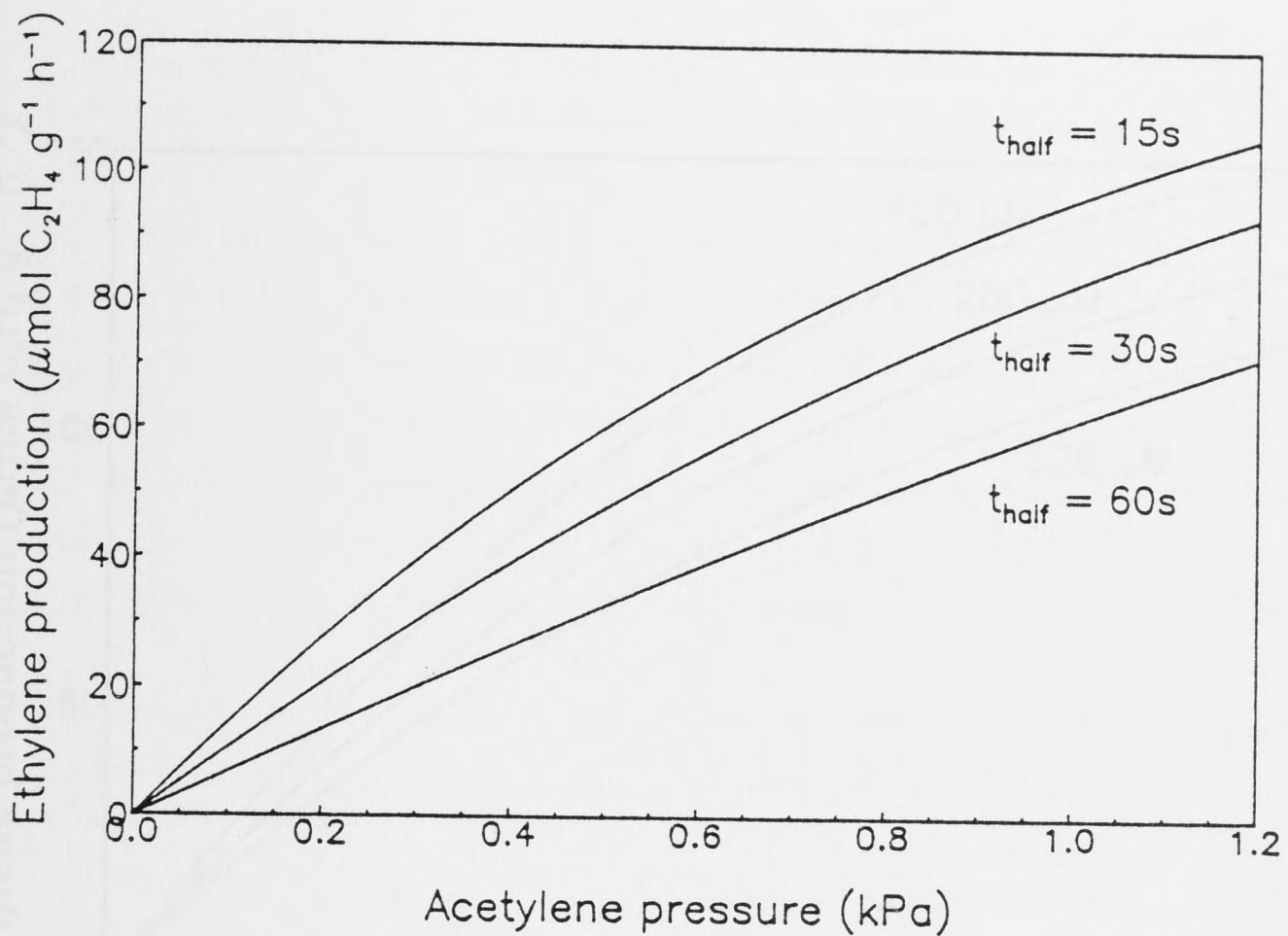
At low pressures of acetylene ( $< 1$  kPa) the model predicts an almost linear response of ethylene production to acetylene pressure (Figure 5.14, 5.15), in a similar pattern to that shown by experimental values (Table 5.2). The relationship of ethylene produced to acetylene at low acetylene pressure becomes more linear at longer values of  $t_{\text{half}}$  for diffusion.

The model predicts that changes in the maximum nitrogenase activity ( $V_{\text{max}}$ ) will cause a change in the rate of ethylene production at low pressures of acetylene (Figure 5.16). If the maximum nitrogenase activity of a model nodule is reduced, then the amount of ethylene production at a low pressure of acetylene is also reduced. This is an important result as it shows that factors which alter total nitrogenase activity (for example, temperature and carbon supply) will also cause an alteration in the activity detected with low pressures of acetylene. There is, however, an alteration in the proportion of the maximum acetylene reduction activity detected at low acetylene pressures when the rate of maximum nitrogenase activity alters. Because of the limiting effects of acetylene diffusion, proportionally more activity is detected by lower acetylene concentrations when the maximum nitrogenase activity declines.

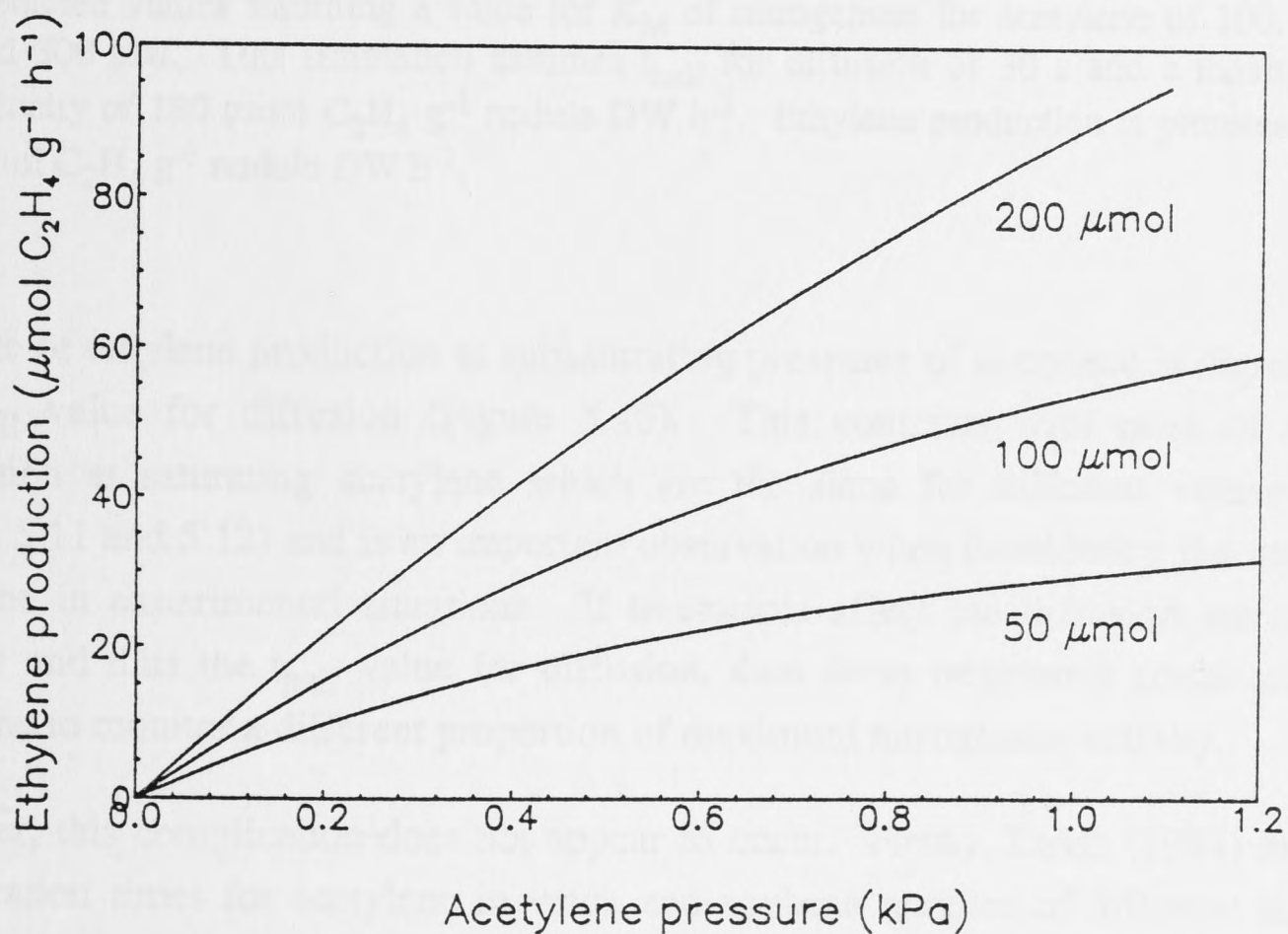
Different theoretical affinities of nitrogenase for acetylene can be modelled. If a  $K_M$  of between 100 and 300  $\mu\text{M}$  for acetylene is assumed, then there is no significant difference in maximum activity at saturating acetylene (data not shown), and ethylene production at subsaturating pressures of acetylene is only slightly different (Figure 5.17).



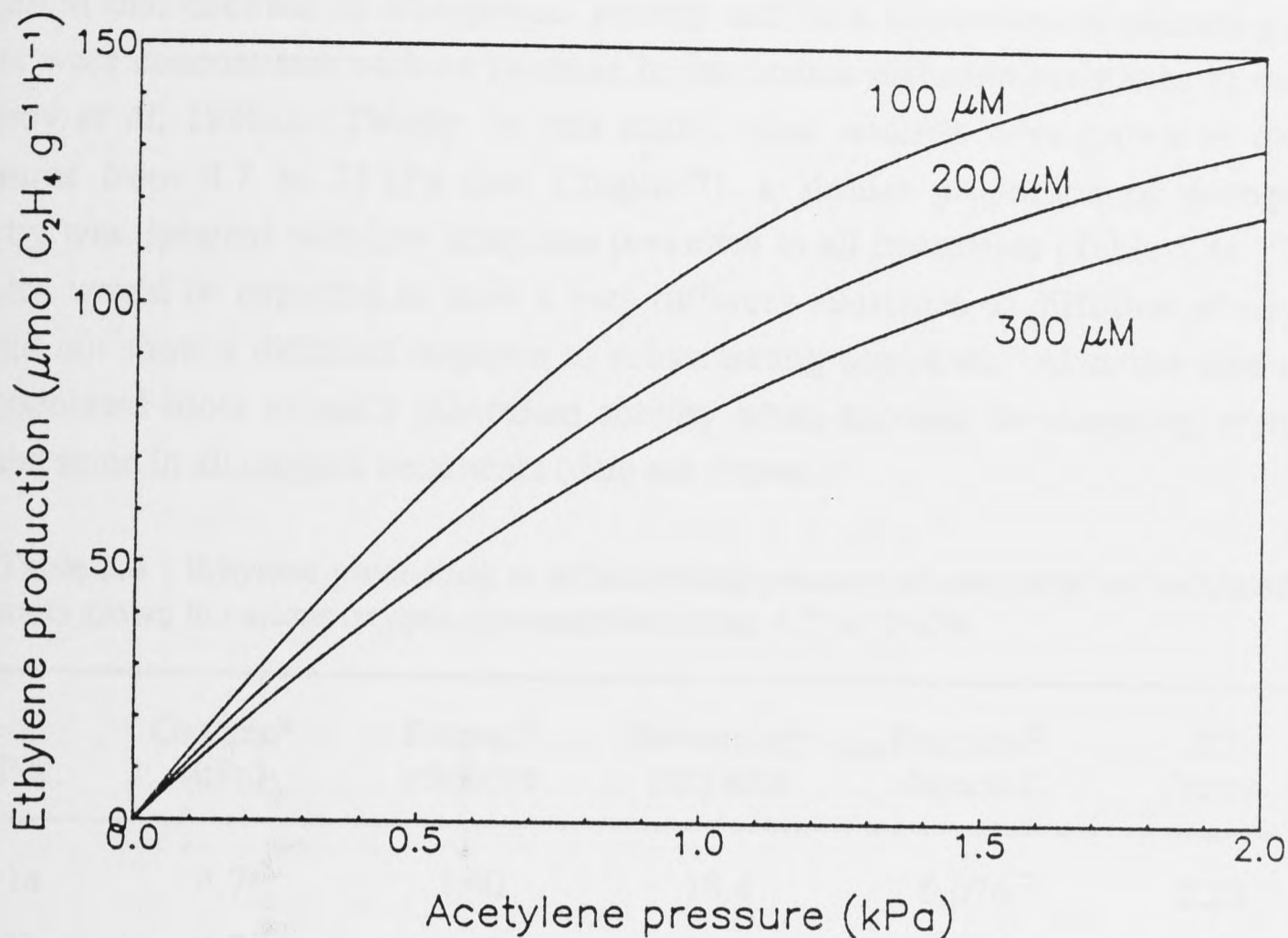
**Figure 5.14** : Ethylene production at acetylene pressures from 0 to 2 kPa for 10 minutes after the introduction of acetylene, predicted by a model of nodule acetylene reduction. Assuming a  $t_{\text{half}}$  for acetylene and ethylene diffusion of 30 s, a  $K_M$  of nitrogenase for acetylene of 264  $\mu\text{M}$  and a maximum velocity of 180  $\mu\text{mol C}_2\text{H}_4 \text{ g}^{-1}$  nodule DW  $\text{h}^{-1}$ . Ethylene production is presented as  $\mu\text{mol C}_2\text{H}_4 \text{ g}^{-1}$  nodule DW  $\text{h}^{-1}$ .



**Figure 5.15 :** Ethylene production as a function of acetylene pressure at subsaturating pressures of acetylene, predicted by a model of nodule acetylene reduction. Curves show predicted values at  $t_{\text{half}}$  times for diffusion of acetylene of 15, 30 and 60 s. This simulation assumes a  $K_M$  of nitrogenase for acetylene of  $264 \mu\text{M}$  and a maximum velocity of  $180 \mu\text{mol C}_2\text{H}_4 \text{ g}^{-1} \text{ nodule DW h}^{-1}$ . Ethylene production is presented as  $\mu\text{mol C}_2\text{H}_4 \text{ g}^{-1} \text{ nodule DW h}^{-1}$ .



**Figure 5.16 :** Ethylene production as a function of  $V_{\text{max}}$  at subsaturating pressures of acetylene, predicted by a model of nodule acetylene reduction. Curves show predicted values assuming maximum rates of 50, 100 and  $200 \mu\text{mol C}_2\text{H}_4 \text{ g}^{-1} \text{ nodule DW h}^{-1}$  acetylene. This simulation assumes  $t_{\text{half}}$  for diffusion of 30 s and a  $K_M$  of nitrogenase for acetylene of  $264 \mu\text{M}$ . Ethylene production is presented as  $\mu\text{mol C}_2\text{H}_4 \text{ g}^{-1} \text{ nodule DW h}^{-1}$ .



**Figure 5.17 :** Ethylene production as a function of  $K_M$  at subsaturating pressures of acetylene, predicted by a model of nodule acetylene reduction. Curves show predicted values assuming a value for  $K_M$  of nitrogenase for acetylene of 100, 200 and 300  $\mu\text{M}$ . This simulation assumes  $t_{\text{half}}$  for diffusion of 30 s and a maximum velocity of  $180 \mu\text{mol C}_2\text{H}_4 \text{ g}^{-1} \text{ nodule DW h}^{-1}$ . Ethylene production is presented as  $\mu\text{mol C}_2\text{H}_4 \text{ g}^{-1} \text{ nodule DW h}^{-1}$ .

The rate of ethylene production at subsaturating pressures of acetylene is dependent on the  $t_{\text{half}}$  value for diffusion (Figure 5.15). This contrasts with rates of ethylene production at saturating acetylene which are the same for different values of  $t_{\text{half}}$  (Figure 5.11 and 5.12) and is an important observation when considering the use of low acetylene in experimental situations. If treatments affect the diffusion resistance of nodules and thus the  $t_{\text{half}}$  value for diffusion, then these treatments could cause low acetylene to monitor a different proportion of maximum nitrogenase activity.

However, this complication does not appear to occur. Firstly, Davis (1984) measured equilibration times for acetylene in vetch and soybean nodules of different sizes and recorded  $t_{\text{half}}$  values for acetylene of approximately 35 s. In nodules subject to various degrees of water stress, with resulting different rates of nitrogenase activity, Davis and Imsande (1988) found no evidence for a large change in diffusion resistance of nodules to acetylene, when they examined lag times for acetylene reduction. Secondly, in the example of the effect of phloem-girdling (Figure 5.7), a decline in low acetylene activity similar to that reported for phloem-girdling experiments using  $\text{H}_2$  production as

an indication of nitrogenase activity (Walsh *et al.* 1987), was observed. These authors suggested that declines in nitrogenase activity and root respiration in phloem-girdled plants were concomitant with an increase in the nodule diffusion resistance to oxygen (Vessey *et al.* 1988a). Thirdly, in this study, when nodules were grown in oxygen pressures from 4.7 to 75 kPa (see Chapter 7), a similar proportion of nitrogenase activity was detected with low acetylene pressures in all treatments (Table 5.4). These nodules would be expected to have a very different resistance to diffusion of oxygen, but did not show a different response to subsaturating acetylene. Also, the time taken for nodulated roots to reach maximum activity when exposed to saturating acetylene was the same in all oxygen treatments (data not shown).

**Table 5.4 :** Ethylene production at subsaturating pressure of acetylene by nodulated roots grown in various oxygen concentrations from 4.7 to 75 kPa.

Pot	Oxygen <sup>a</sup> (kPa)	Subsat. <sup>b</sup> ethylene	Saturating <sup>c</sup> ethylene	Fraction <sup>d</sup> detected	K <sup>e</sup> factor
1a	4.7	1.40	18.4	0.076	2.23
1b	4.7	1.55	21.7	0.071	2.37
2a	19	1.34	17.0	0.079	2.15
2b	19	1.20	15.7	0.077	2.22
3a	47	1.80	22.0	0.082	2.08
3b	47	1.83	22.0	0.083	2.05
4a	75	0.60	9.01	0.067	2.54
4b	75	0.60	8.01	0.075	2.26

<sup>a</sup> Oxygen pressure which roots and nodules were exposed to from 15 days old to assay (29 days). Subsaturating and saturating acetylene reduction assays were carried out at this pressure oxygen. <sup>b</sup> Ethylene produced at 0.14 kPa acetylene ( $\mu\text{mol pl}^{-1} \text{h}^{-1}$ ).

<sup>c</sup> Peak ethylene produced at saturating (8 kPa) acetylene pressure ( $\mu\text{mol pl}^{-1} \text{h}^{-1}$ ).

<sup>d</sup> Fraction of the peak of saturating nitrogenase activity that was detected at 0.14 kPa acetylene. <sup>e</sup> Factor calculated as described in Table 5.2.

Taken together these results suggest that changes in oxygen diffusion resistance of nodules do not cause similar changes in the resistance to acetylene diffusion (or  $t_{\text{half}}$  for acetylene diffusion). This result can probably be explained by differences in the relative pathways for diffusion of oxygen and acetylene. Oxygen diffusion is restricted in the nodule cortex, but oxygen transport in the infected zone is facilitated by leghaemoglobin. Acetylene diffusion will be Fickian throughout the entire nodule and since acetylene is 33 times more soluble in water than oxygen, water-filled pathways will permit a higher comparative flux of acetylene than oxygen.



At subsaturating pressures of acetylene, where acetylene reduction by nitrogenase removes a significant amount of the acetylene diffusing into a nodule, significant gradients of acetylene concentration will probably occur across the infected zone and within infected cells. This effect has not been calculated in this model.

#### 5.3.4. Conclusion

The model described above shows how the quantitative interpretation of data from experiments using low acetylene can be complicated. However, when examined together with the results of the experiments on phloem-girdling, diurnal activity and MSO inhibitor effects, it is concluded that the use of trace acetylene can be valuable for the continuous observation of nitrogenase activity and determination of approximate nitrogenase activity rates under various physiological conditions.

In model predictions, when nitrogenase activity decreases, the activity detected with trace acetylene also decreases (Figure 5.16). The experimental treatments of phloem-girdling and MSO inhibitor application caused a large decrease in nodulated root respiration and ethylene production under trace acetylene, which probably reflects a decrease in nodule nitrogenase activity. Both the diurnal experiment (Figure 5.8, 5.9, Table 5.3), where a similar proportion of nitrogenase activity was detected with trace acetylene during the day and night, and in the oxygen experiment (Table 5.4), where a similar proportion of nitrogenase activity was detected across treatments, show that ethylene production from subsaturating acetylene was a consistent predictor of maximum nitrogenase activity.

Determining the true rate of nitrogenase activity in nodules by any method remains difficult. However, low pressures of acetylene can be used to detect activity and can also be used to predict nitrogenase activity under carefully defined conditions. Low pressures of acetylene can be used to provide a qualitative indication of nitrogenase activity during long term experiments. The next chapter uses this technique of trace acetylene reduction to examine the effects of some inhibitors of nitrogen metabolism on nodule function.

## Chapter 6

### Effects of Inhibitors of Nitrogen Assimilation on Nodulated Root Respiration and Nitrogenase Activity

#### 6.1. Introduction

##### *Regulation of nitrogenase activity*

As detailed in the previous two chapters, exposure of soybean nodules to saturating pressures of acetylene causes a large decline in nodule respiration and nitrogenase activity which can be recovered by increasing external  $pO_2$ , but the mechanism and physiological cause of this decline have not been determined. In their original paper, Minchin *et al.* (1983) proposed that the acetylene-induced decline was probably caused by a lack of ammonia production. More recently they have shown that inhibition of ammonia production within nodules causes an increase in the apparent oxygen diffusion resistance of nodules (Witty *et al.* 1984, 1987) and proposed that the decline is due to the restriction of oxygen availability within nodules.

Many other treatments, such as application of nitrate, decapitation and phloem girdling also induce declines in nodule activity and show characteristic increases in diffusion resistance (Minchin *et al.* 1986, Vessey *et al.* 1988a). Davis and Imsande (1988) questioned this approach and proposed that increases in diffusion resistance are not necessary to maintain low oxygen concentrations inside nodules when external oxygen pressures are increased. They suggested that the acetylene reduction and respiration rate of control nodules was also oxygen limited, although their references (Tjepkema and Yocum 1973, Pankhurst and Sprent 1975a, Ralston and Imsande 1982, Witty *et al.* 1984) refer entirely to studies involving saturating acetylene and/or detached nodules. In better controlled experiments, which used plants which had been carefully treated and assayed by continuous flow techniques (Vessey *et al.* 1988a, Davey and Simpson 1989), no large increase in activity of untreated plants was observed when external oxygen was increased.

##### *Other investigations with inhibitors*

Many aspects of metabolism within soybean nodules have been characterized, especially the major pathways of ammonia assimilation and carbon metabolism. Inhibitors of various reactions of nitrogen metabolism can be used to examine the

acetylene-induced decline in more detail. After the experimental work for this chapter was completed, Atkins *et al.* (1988) reported a similar study examining the effects of the inhibitor allopurinol on cowpea nodules. They found that allopurinol caused severe inhibition of intact or sliced nodule nitrogenase activity, although it did not affect the activity of nodule breis. Increasing the oxygen concentration to 40 % around allopurinol inhibited nodules, increased nitrogenase activity to control plant levels, which were not stimulated by oxygen. Both control and allopurinol inhibited nodules, showed the same, low level of activity at 50 % oxygen.

#### *Inhibitors used in this study*

Four inhibitors of nitrogen metabolism were used to examine how inhibiting different reactions of nodule nitrogen metabolism may affect the nitrogenase activity and respiration of nodules. The inhibitors were; acetylene, methionine sulfoximine (MSO), cycloserine and allopurinol.

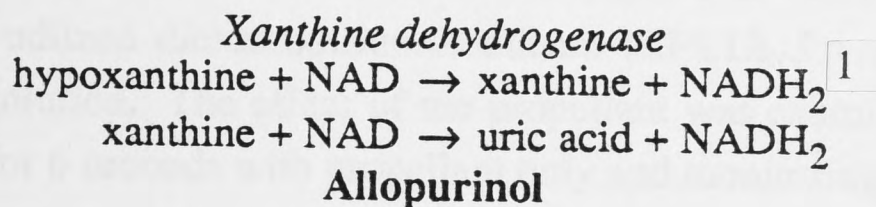
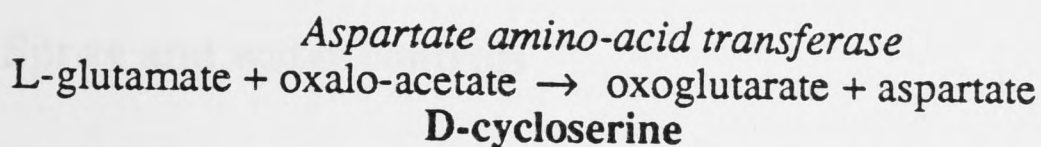
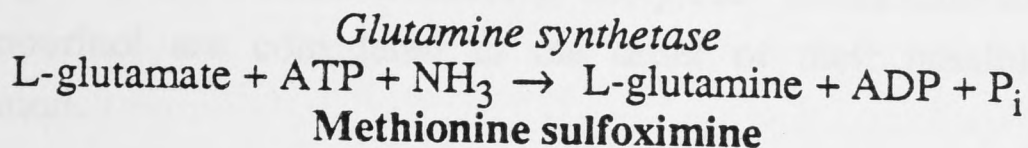
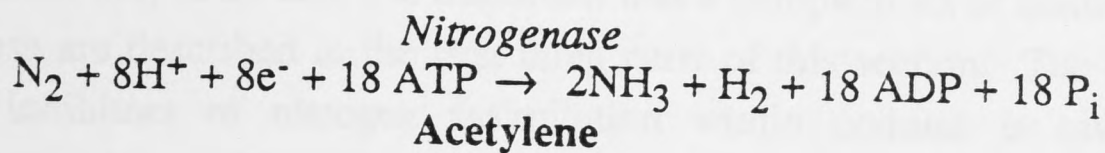
Acetylene acts as a competitive inhibitor of nitrogenase, with respect to  $N_2$ . It is reduced to ethylene and in saturating concentrations completely blocks  $NH_3$  production by nitrogenase. This reaction occurs within the bacteroid.

Methionine sulfoximine (DL-S-[3-Amino-3-carboxypropyl]-S-methyl-sulfoximine, MW = 180.2) inhibits the first step of ammonia assimilation by plant cells within nodules. It is an irreversible inhibitor of glutamine synthetase (Meister 1974), the enzyme which catalyses the production of glutamine from glutamate and ammonia, and which is located in the cytoplasm (Schubert 1986). Inhibition is competitive with glutamate, indicating that MSO binds to the glutamate site of the enzyme. Subsequent phosphorylation of bound MSO causes irreversible inhibition of the enzyme (Meister 1974).

Aspartate amino-transferase, an enzyme which is proposed to catalyse the production of aspartate for ureide synthesis in soybean nodules (Reynolds *et al.* 1982, Schubert 1986), is inhibited by D-cycloserine (D-4-Amino-3-isoxazolidinone, MW = 102.1) (Braunstein 1973). Cycloserine binds at the active site as a quasi-substrate and covalently binds to the active site, thus irreversibly inactivating the enzyme (Braunstein 1973). Aspartate amino-transferase occurs in the plastid (Schubert 1986).

Allopurinol (4-Hydroxypyrazolo[3,4-d]-pyrimidine, MW = 136.1) is an inhibitor of xanthine dehydrogenase (Bray 1975) and was used to determine probable pathways of ureide metabolism within nodules (Reynolds *et al.* 1982). Allopurinol is both a substrate and inhibitor of xanthine dehydrogenase. As an inhibitor its potency is high, and it has been reported to show an apparent dissociation constant for the enzyme-inhibitor complex of  $6 \times 10^{-10}$  M (Bray 1975). In soybean nodules xanthine dehydrogenase catalyses the production of xanthine from hypoxanthine and uric acid

from xanthine, the latter reaction is a key step in purine oxidation and the production of ureides (Reynolds *et al.* 1982). This enzyme is located in the cytoplasm of infected (Triplett 1985) and/or uninfected cells (Nguyen *et al.* 1986). The inhibitors and the reactions they inhibit are summarized below.



#### *Method of application of inhibitors*

Acetylene, as a gas, was added via the assay gas stream at 8 kPa with an equal reduction in the pressure of N<sub>2</sub>. Other inhibitors were dissolved in water solution containing 5 mM MES buffer (pH 6.5). Solutions of 50 mM MSO, 50 mM D-cycloserine and 25 mM allopurinol were prepared. These solutions were applied to the nodulated roots of plants with an aerosol spray pack, which used a siphon/venturi nozzle and CFC12 propellant to produce a fine spray mist. Spray was applied by lifting the lid of pots containing four plants and directing the spray onto and around the nodules formed in the upper regions of the root systems. Five mL was sprayed by the device in approximately 6 seconds. The lid was replaced on the pot and the open-flow assay continued.

<sup>1</sup> this reaction may not be important in nodules (Schubert 1986).

## 6.2. Results

The application of inhibitors to whole nodules *in situ* is a novel method of investigating some aspects of the physiology of nodules. As with any inhibitor studies, problems of interpretation may arise and it is important that a complete set of control experiments is run. These are described in the first three parts of this section. The effect of the four putative inhibitors of nitrogen assimilation within nodules is investigated in the remaining sections. These inhibitors; acetylene, methionine-sulfoximine, cycloserine and allopurinol are considered in the order of their possible effects on nitrogen assimilation.

### 6.2.1. Spray and water controls

Inhibitors were sprayed on to the roots and nodules in water solutions, using a spray-pack, which utilized dichlorodifluoromethane (CFC12, Freon 12) as a propellant, to atomize the solution. The effect of the propellant was examined by spraying the roots and nodules for 6 seconds with propellant only and monitoring root respiration and trace nitrogenase activity using the open-flow assay system with a low pressure of acetylene in the flow gas (Figure 6.1). Spraying with propellant had no effect on nodulated root respiration or nitrogenase activity of plants. This result was expected as CFC12 is a very stable compound and the only likely effect would be via dilution of other gases present. This dilution was not large enough to have any significant effect.

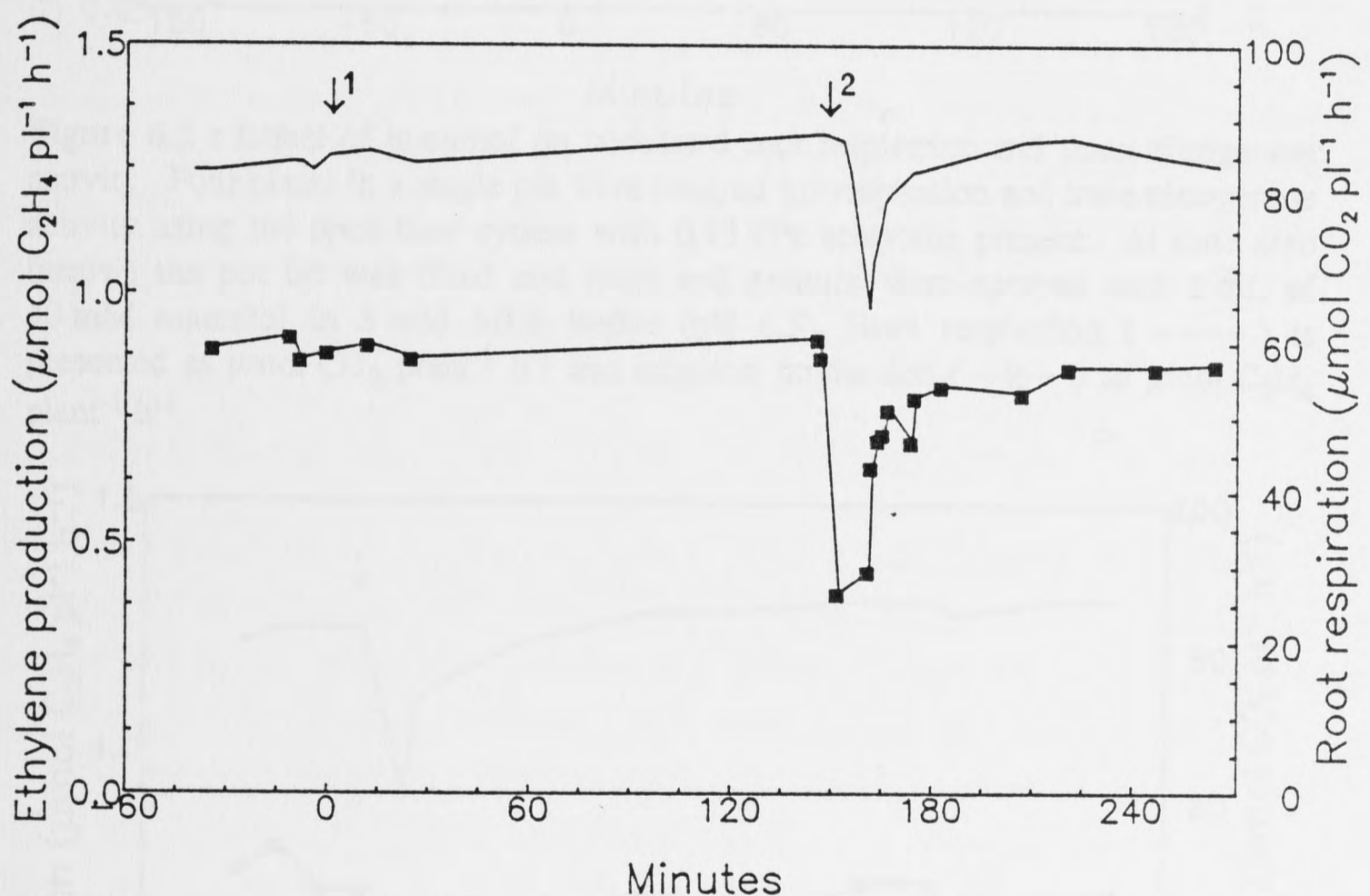
The effect of spraying 5 mL of water onto the roots and nodules of four plants is also presented in Figure 6.1. A rapid decline in nodulated root respiration and trace nitrogenase activity was observed, both of which recovered, after approximately 15 minutes, to rates approximately equal to the rates before spraying. This decline was probably caused by reduced oxygen supply to the nodules, which recovers as the nodules dry. Fifteen minutes after spraying, nodules were observed to be almost dry. This rapid recoverable decline which occurs when water is sprayed on the roots and nodules was repeatedly observed when water solutions containing other compounds were sprayed onto the roots and nodules.

### 6.2.2. Osmotic and ionic controls

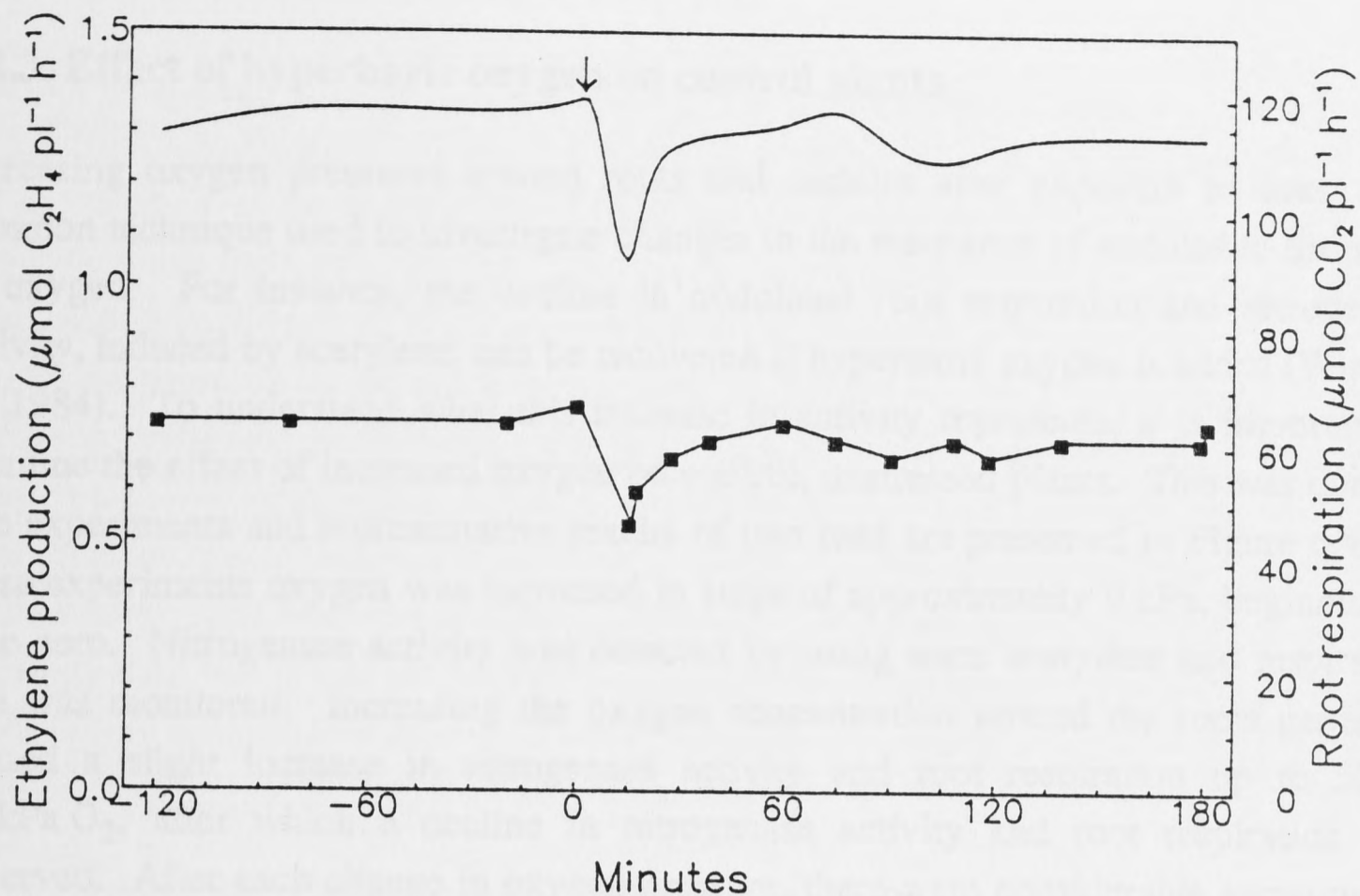
Control experiments spraying a solution of an osmotically active compound (mannitol) and salt (KCl) were carried out to ensure that the effect of inhibitors was not due to osmotic or ionic effects. Figure 6.2 shows an experiment where 5 mL of 50 mM mannitol in 5 mM MES was sprayed onto the roots and nodules of four plants and respiration and trace nitrogenase activity monitored using the open-flow system. An immediate decline in nodulated root respiration and nitrogenase activity occurred which recovered in a pattern similar to control water spray experiments. In four separate

experiments where 50 mM mannitol was sprayed onto roots and nodules, after this initial decline and recovery, no other significant changes in root respiration or nitrogenase activity were observed over the next three to four hours. Spraying 5 mL of a 50 mM osmoticum had no apparent effect on nodules.

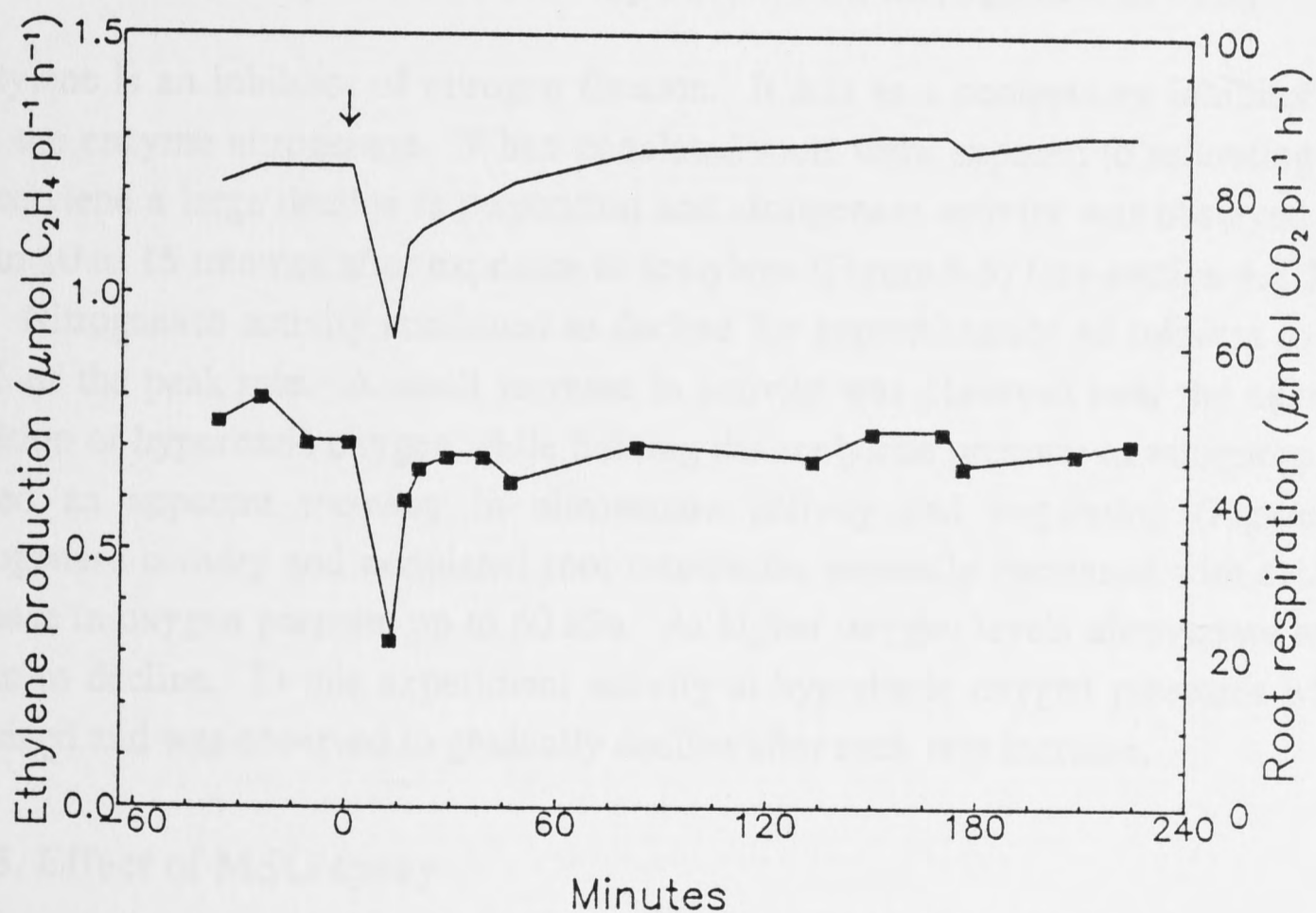
Spraying 50 mM KCl in 5 mM MES had a similar effect on respiration and nitrogenase activity as spraying water or mannitol solution. Nodulated roots showed a rapid decline in respiration and trace nitrogenase activity which recovered after approximately 15 to 20 minutes and remained constant for another four hours (Figure 6.3). Adding KCl at the same concentration as inhibitors shows that any effects of inhibitors are probably not caused by ionic effects.



**Figure 6.1** : Effect of gas propellant spray and water spray on nodulated root respiration and trace nitrogenase activity. Four plants in a single pot were assayed for respiration and trace nitrogenase activity using the open-flow system with 0.13 kPa acetylene present. At time zero (arrow 1) the pot lid was lifted and roots and nodules were sprayed with CFC12 for 6 seconds. At 150 minutes (arrow 2) 5 mL of water was sprayed onto the roots and nodules using CFC12 as a propellant. Root respiration (—) is presented as  $\mu\text{mol CO}_2 \text{ plant}^{-1} \text{ h}^{-1}$  and ethylene production (—■—) as  $\mu\text{mol C}_2\text{H}_4 \text{ plant}^{-1} \text{ h}^{-1}$ .



**Figure 6.2 :** Effect of mannitol on nodulated root respiration and trace nitrogenase activity. Four plants in a single pot were assayed for respiration and trace nitrogenase activity using the open-flow system with 0.13 kPa acetylene present. At time zero (arrow) the pot lid was lifted and roots and nodules were sprayed with 5 mL of 50 mM mannitol in 5 mM MES buffer (pH 6.5). Root respiration ( — ) is presented as  $\mu\text{mol CO}_2 \text{ plant}^{-1} \text{ h}^{-1}$  and ethylene production ( —■— ) as  $\mu\text{mol C}_2\text{H}_4 \text{ plant}^{-1} \text{ h}^{-1}$ .



**Figure 6.3 :** Effect of KCl on nodulated root respiration and trace nitrogenase activity. Four plants in a single pot were assayed for respiration and trace nitrogenase activity using the open-flow system with 0.13 kPa acetylene present. At time zero (arrow) the pot lid was lifted and roots and nodules were sprayed with 5 mL of 50 mM KCl in 5 mM MES buffer (pH 6.5). Root respiration ( — ) is presented as  $\mu\text{mol CO}_2 \text{ plant}^{-1} \text{ h}^{-1}$  and ethylene production ( —■— ) as  $\mu\text{mol C}_2\text{H}_4 \text{ plant}^{-1} \text{ h}^{-1}$ .

### 6.2.3. Effect of hyperbaric oxygen on control plants

Increasing oxygen pressures around roots and nodules after exposure to stress is a common technique used to investigate changes in the resistance of nodules to diffusion of oxygen. For instance, the decline in nodulated root respiration and nitrogenase activity, induced by acetylene, can be recovered if hyperbaric oxygen is added (Witty *et al.* 1984). To understand what this increase in activity represents, it is important to examine the effect of increased oxygen on control, unstressed plants. This was done in five experiments and representative results of two runs are presented in Figure 6.4. In these experiments oxygen was increased in steps of approximately 9 kPa, beginning at time zero. Nitrogenase activity was detected by using trace acetylene and respiration rate was monitored. Increasing the oxygen concentration around the roots generally caused a slight increase in nitrogenase activity and root respiration up to 50 to 60 kPa O<sub>2</sub>, after which a decline in nitrogenase activity and root respiration was observed. After each change in oxygen pressure, there were considerable variations in nitrogenase activity and root respiration. In the five experiments, doubling the oxygen pressure from 19 to 38 kPa (in two steps of 9 kPa) caused a mean increase in trace nitrogenase activity of 14 % ( $\pm 8$ , 95 % confidence limit) and a mean increase in nodulated root respiration (CO<sub>2</sub> efflux) of 5 % ( $\pm 7$ )

### 6.2.4. Effect of acetylene on root respiration and nitrogenase activity

Acetylene is an inhibitor of nitrogen fixation. It acts as a competitive inhibitor of N<sub>2</sub> with the enzyme nitrogenase. When nodulated roots were exposed to saturating levels of acetylene a large decline in respiration and nitrogenase activity was observed which began 10 to 15 minutes after exposure to acetylene (Figure 6.5) (see section 4.2.3, page 45). Nitrogenase activity continued to decline for approximately 40 minutes to a rate 44 % of the peak rate. A small increase in activity was observed over the next hour. Addition of hyperbaric oxygen while holding the acetylene pressure at saturating levels caused an apparent recovery in nitrogenase activity and respiration (Figure 6.5). Nitrogenase activity and nodulated root respiration generally increased with each step increase in oxygen pressure up to 60 kPa. At higher oxygen levels nitrogenase activity began to decline. In this experiment activity at hyperbaric oxygen pressures was not sustained and was observed to gradually decline after each step increase.

### 6.2.5. Effect of MSO spray

Methionine sulfoximine inhibits glutamine synthetase, the first enzyme of the pathway of ammonia assimilation in nodules. In an initial experiment 310  $\mu$ M MSO was added to the nutrient solution of a pot containing four plants and nodulated root CO<sub>2</sub> efflux was continuously monitored. Root respiration continued at a constant level for 5 hours



after MSO was added and then began a slow and gradual decline over the next 15 hours to a level approximately 60 % of the initial respiration rate. This experiment was important as it demonstrated that MSO had a significant effect on nodulated root respiration. A method of spraying the roots and nodules with 5 mL of solution was developed to enable more rapid responses to be observed (see section 6.1, page 85). Figure 6.6 presents an experiment in which a solution of MSO was sprayed onto the roots and nodules at time zero. There was an immediate decline in activity which recovered to pre-spray levels, before a second, longer-term decline was observed. Four to five hours after spraying with MSO, trace nitrogenase activity was reduced to approximately one-half of the original rate and nodulated root respiration reduced to approximately two-thirds of the initial rate. In seven experiments, exposing plants to MSO, caused a mean decline of 40 % in trace nitrogenase activity and 30 % in nodulated root respiration (Table 6.1).

If nodulated roots showing an MSO-induced decline were exposed to hyperbaric oxygen, then an apparent recovery in trace nitrogenase activity and nodulated root respiration was observed (Figure 6.6). Increasing oxygen pressure increased trace nitrogenase activity to levels equal to or slightly greater than pre-decline rates and increased nodulated root respiration to rates approximately equal to the initial rate. A doubling of the oxygen pressure from 19 to 38 kPa in the flow gas caused a mean increase of 60 % ( $\pm 36$ , 95 % confidence level) in trace nitrogenase activity and 22 % ( $\pm 12$ ) in nodulated root respiration.

A second interesting observation was recorded when MSO treated plants were exposed to saturating acetylene (see Figure 5.10, page 72). In control plants, exposure to saturating acetylene caused a rapid decline in root respiration and nitrogenase activity (see Figure 6.5), but plants which had been sprayed with MSO and subsequently declined in activity, showed no further decline in response to acetylene. Acetylene reduction in those plants was constant for at least 60 to 90 minutes after the introduction of saturating acetylene. Subsequent exposure of nodulated roots to hyperbaric oxygen increased respiration and nitrogenase activity (Figure 5.10), although activities were not sustained at high oxygen pressures.

#### 6.2.6. Effect of cycloserine spray

Cycloserine is an inhibitor of aspartate amino-transferase (Braunstein 1973), an enzyme that catalyses the production of aspartate for ureide synthesis in nodules (Reynolds *et al.* 1982). In two experiments using the open-flow system, a solution containing cycloserine was sprayed on the roots and nodules of plants (Table 6.1). A brief decline in nodulated root respiration and trace nitrogenase activity was observed (Figure 6.7), similar to control water sprayed plants. For two to three hours following the spraying no significant decline in activity was observed in either experiment, although a small

decrease in trace nitrogenase activity was observed in the experiment shown in Figure 6.7. Spraying a solution of cycloserine on the roots and nodules did not appear to cause the dramatic declines observed after exposure of nodulated roots to acetylene or MSO.

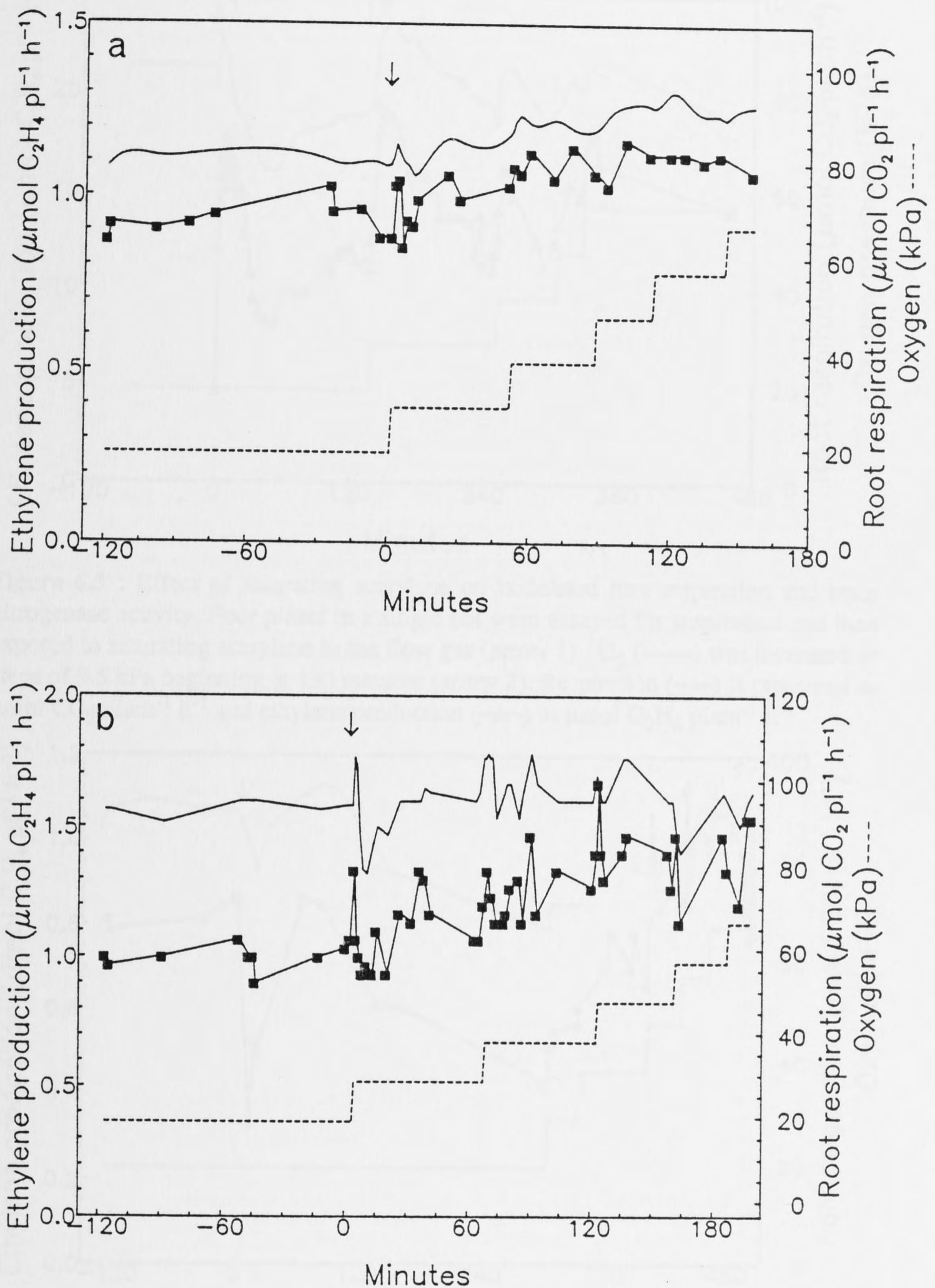
### 6.2.7. Effect of allopurinol spray

Allopurinol inhibits xanthine dehydrogenase, a key enzyme in ureide synthesis in soybean nodules (Reynolds *et al.* 1982). The effect of spraying nodulated roots with a solution containing allopurinol was examined in five experiments using the open-flow system, summarized in Table 6.1. A typical response of spraying with allopurinol solution is shown in Figure 6.8. Immediately after spraying, trace nitrogenase activity and nodulated root respiration declined and then rapidly recovered, in a pattern similar to control plants. After 45 to 60 minutes a significant decline in respiration and trace nitrogenase activity occurred. The mean decline in nodulated root respiration and nitrogenase activity, from five experiments, after spraying with allopurinol, was 18 % and 22 % respectively. When allopurinol treated plants were exposed to hyperbaric pressures of oxygen, trace nitrogenase activity and respiration (CO<sub>2</sub> efflux) increased with increasing oxygen to a rate approximately equal to the initial rate occurring at 38 kPa oxygen (Figure 6.8). Generally the magnitude of declines and recoveries in allopurinol treated nodulated roots was not as large as in nodulated roots exposed to acetylene or MSO.

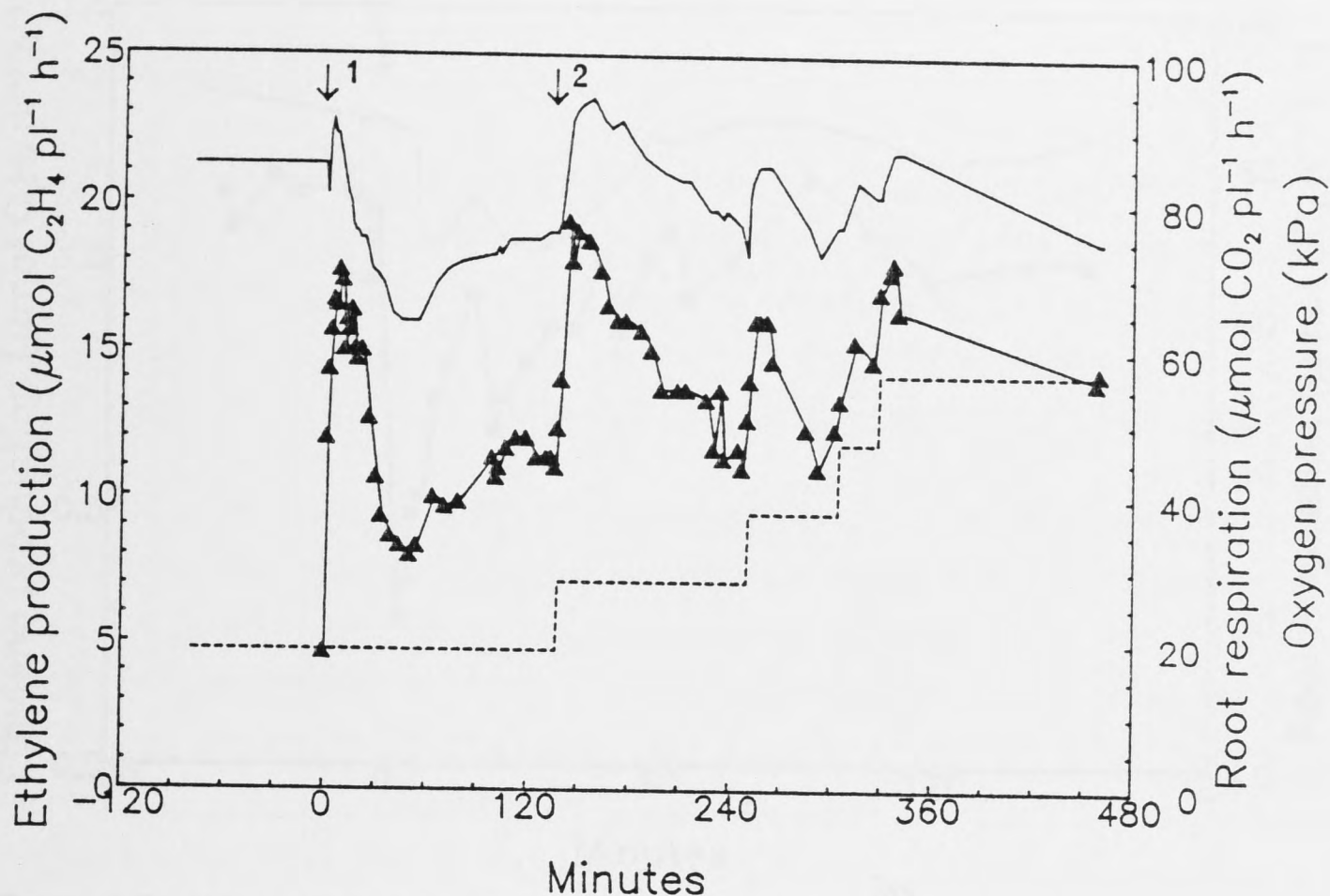
**Table 6.1** : Summary of the effect of four inhibitors of nitrogen metabolism on the respiration and nitrogenase activity of nodulated roots of soybean.

Inhibitor <sup>a</sup>	Percent decline <sup>b</sup> root respiration	Percent decline <sup>c</sup> nitrogenase activity	Increase with <sup>d</sup> extra oxygen
Acetylene	35	50	-
	33	43	-
	25	55	yes
	34	65	yes
	mean (acetylene)	31.7	53.2
MSO	65	-	-
	27	20	-
	22	44	yes
	22	40	yes
	15	30	yes
	35	60	yes
	30	40	yes
mean (MSO)	30.8	39	
Cycloserine	0	5	-
	0	0	-
Allopurinol	33	-	-
	21	22	-
	6.5	25	yes
	11	10	-
	17	30	yes
mean (allopurinol)	17.7	21.8	

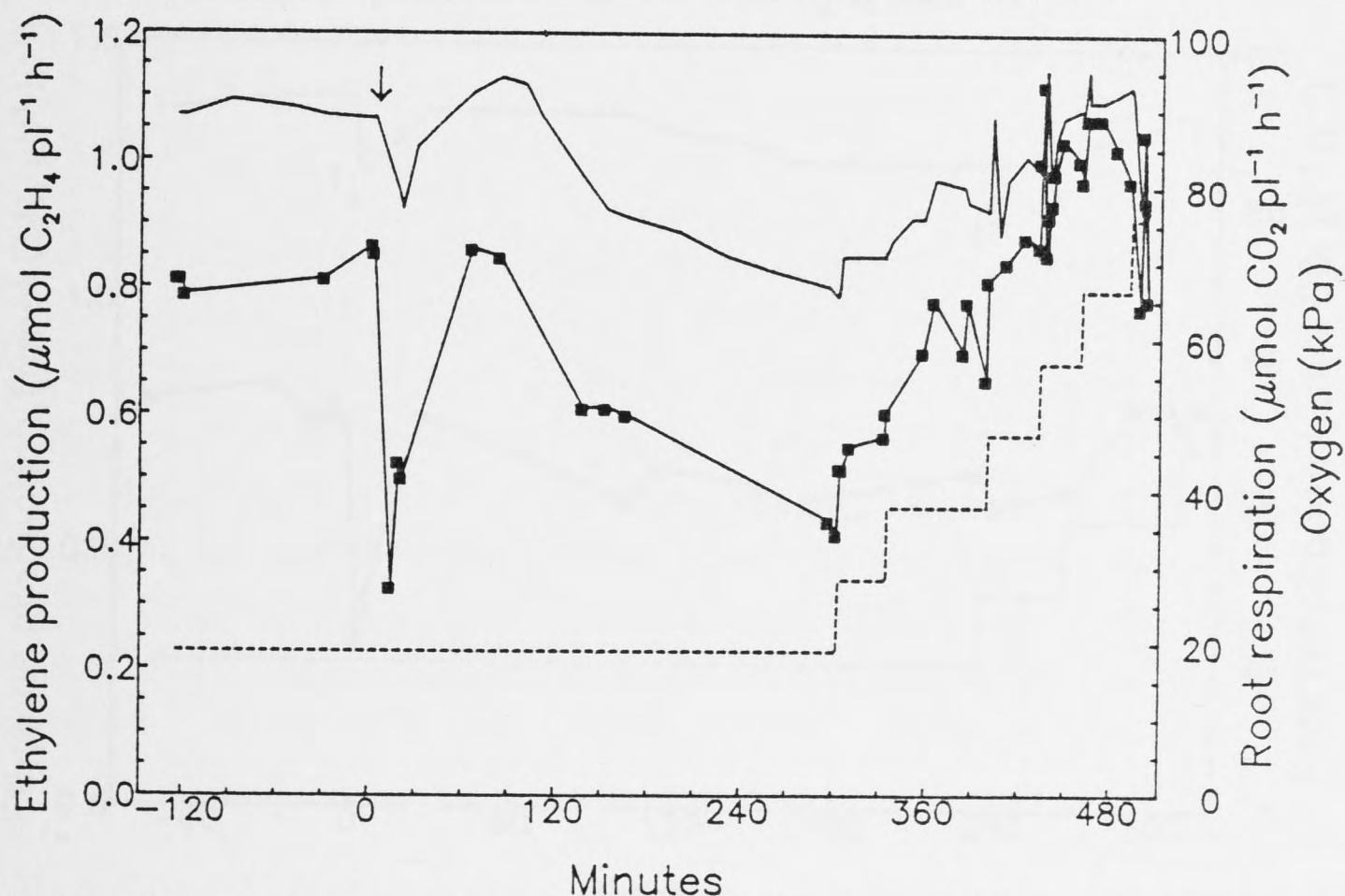
<sup>a</sup> Inhibitors were applied to the nodulated root systems of four soybean plants per pot as follows; acetylene as gas at 8 kPa, methionine sulfoximine (MSO) and cycloserine as 5 mL of 50 mM spray and allopurinol as 5 mL of 25 mM spray. <sup>b</sup> Decline observed in nodulated root respiration rate after inhibitor was applied. <sup>c</sup> Decline observed in saturating acetylene reduction (acetylene as inhibitor) or in subsaturating (0.13 kPa) acetylene reduction (MSO, cycloserine and allopurinol). <sup>d</sup> Significant increase in activity at hyperbaric oxygen. (- = not examined)



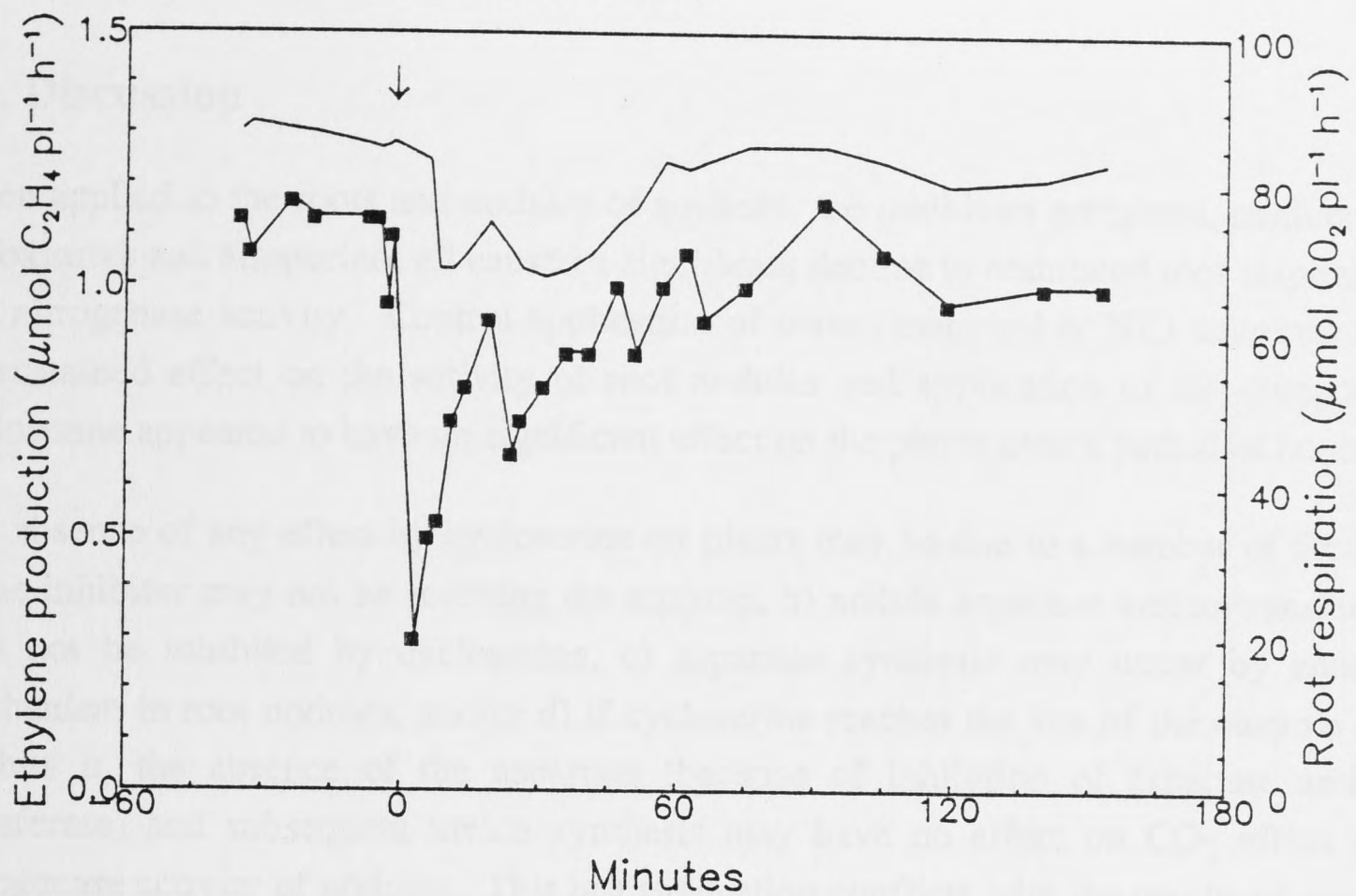
**Figure 6.4 (a)** : Effect of increased oxygen on nodulated root respiration and trace nitrogenase activity. Four plants in a single pot were assayed for respiration and trace nitrogenase activity using the open-flow system with 0.13 kPa acetylene present. Oxygen was increased from time zero (arrow) in steps of 9.5 kPa. Root respiration (—) is presented as  $\mu\text{mol CO}_2 \text{ plant}^{-1} \text{ h}^{-1}$  and ethylene production (—■—) as  $\mu\text{mol C}_2\text{H}_4 \text{ plant}^{-1} \text{ h}^{-1}$ .  
**(b)** : Replicate experiment as above.



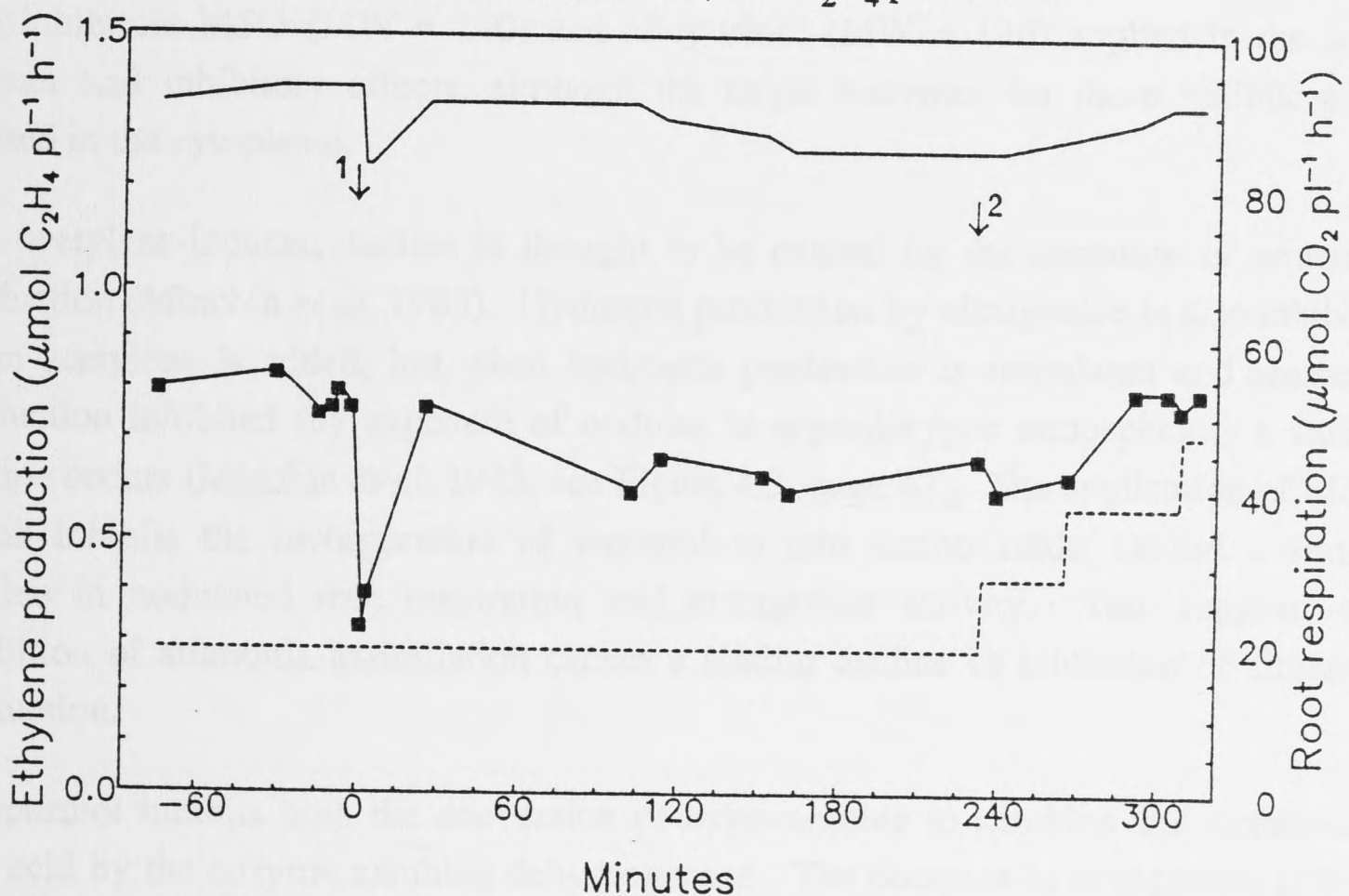
**Figure 6.5 :** Effect of saturating acetylene on nodulated root respiration and trace nitrogenase activity. Four plants in a single pot were assayed for respiration and then exposed to saturating acetylene in the flow gas (arrow 1).  $\text{O}_2$  (-----) was increased in steps of 9.5 kPa beginning at 130 minutes (arrow 2). Respiration (—) is presented as  $\mu\text{mol CO}_2 \text{ plant}^{-1} \text{ h}^{-1}$  and ethylene production ( $\blacktriangle$ ) as  $\mu\text{mol C}_2\text{H}_4 \text{ plant}^{-1} \text{ h}^{-1}$ .



**Figure 6.6 :** Effect of methionine sulfoximine (MSO) on nodulated root respiration and trace nitrogenase activity. Four plants in a single pot were assayed for respiration and trace nitrogenase activity using the open-flow system with 0.13 kPa acetylene present. At time zero (arrow) the pot lid was lifted and roots and nodules sprayed with 5 mL of 50 mM MSO in 5 mM MES (pH 6.5). Oxygen (-----) was increased in steps of 9.5 kPa beginning at 300 minutes. Respiration (—) is presented as  $\mu\text{mol CO}_2 \text{ plant}^{-1} \text{ h}^{-1}$  and ethylene production ( $\blacksquare$ ) as  $\mu\text{mol C}_2\text{H}_4 \text{ plant}^{-1} \text{ h}^{-1}$ .



**Figure 6.7 :** Effect of cycloserine on nodulated root respiration and trace nitrogenase activity. Four plants in a single pot were assayed for respiration and trace nitrogenase activity using the open-flow system with 0.13 kPa acetylene present. At time zero (arrow) the pot lid was lifted and roots and nodules sprayed with 5 mL of 50 mM D-cycloserine in 5 mM MES (pH 6.5). Respiration (—) is presented as  $\mu\text{mol CO}_2 \text{ plant}^{-1} \text{ h}^{-1}$  and ethylene production (—■—) as  $\mu\text{mol C}_2\text{H}_4 \text{ plant}^{-1} \text{ h}^{-1}$ .



**Figure 6.8 :** Effect of allopurinol on nodulated root respiration and trace nitrogenase activity. Four plants in a single pot were assayed for respiration and trace nitrogenase activity using the open-flow system with 0.13 kPa acetylene present. At time zero (arrow 1) the pot lid was lifted and roots and nodules sprayed with 5 mL of 25 mM allopurinol in 5 mM MES buffer (pH 6.5).  $\text{O}_2$  (-----) was increased in steps of 9.5 kPa beginning at 230 minutes (arrow 2). Respiration (—) is presented as  $\mu\text{mol CO}_2 \text{ plant}^{-1} \text{ h}^{-1}$  and ethylene production (—■—) as  $\mu\text{mol C}_2\text{H}_4 \text{ plant}^{-1} \text{ h}^{-1}$ .

### 6.3. Discussion

When applied to the roots and nodules of soybean, the inhibitors acetylene, methionine sulfoximine and allopurinol all caused a significant decline in nodulated root respiration and nitrogenase activity. Control application of water, mannitol or KCl solutions had no sustained effect on the activity of root nodules and application of the compound cycloserine appeared to have no significant effect on the plants over a period of hours.

The absence of any effect by cycloserine on plants may be due to a number of factors; a) the inhibitor may not be reaching the enzyme, b) nodule aspartate amino-transferase may not be inhibited by cycloserine, c) aspartate synthesis may occur by another mechanism in root nodules, and/or d) if cycloserine reaches the site of the enzyme and inhibits it, the absence of the aspartate (because of inhibition of aspartate amino-transferase) and subsequent ureide synthesis may have no effect on CO<sub>2</sub> efflux and nitrogenase activity of nodules. This last suggestion conflicts with the results of studies with allopurinol, an inhibitor which affects CO<sub>2</sub> efflux and nitrogenase activity, and has a site of action after aspartate incorporation into the ureide biosynthetic pathway.

Cycloserine may not reach the enzyme. Cycloserine is a compound of molecular weight 102.1 and it may not get into the plastid, the site of aspartate amino-transferase. The inhibitors MSO (MW = 180) and allopurinol (MW = 136) applied in the same manner had inhibitory effects, although the target enzymes for these inhibitors are located in the cytoplasm.

The acetylene-induced decline is thought to be caused by the cessation of ammonia production (Minchin *et al.* 1983). Hydrogen production by nitrogenase is also inhibited when acetylene is added, but when hydrogen production is stimulated and ammonia production inhibited (by exposure of nodules to argon/oxygen atmospheres) a similar decline occurs (Minchin *et al.* 1983, see Figure 4.3, page 47). The application of MSO, which inhibits the incorporation of ammonium into amino acids, caused a similar decline in nodulated root respiration and nitrogenase activity. This suggests that inhibition of ammonia assimilation causes a similar decline as inhibition of ammonia production.

Allopurinol inhibits both the conversion of hypoxanthine to xanthine and xanthine to uric acid by the enzyme xanthine dehydrogenase. The decrease in nitrogenase activity and nodulated root respiration which occurred after application of allopurinol implies that inhibition of ureide production at a late stage of biosynthesis, can cause a similar decline as inhibition of ammonia production and glutamate formation at early stages of ureide biosynthesis.

When saturating acetylene was added to nodulated roots which had been previously

sprayed with MSO, no further decline in respiration or nitrogenase activity was observed. This is evidence that the consequences of  $C_2H_2$  and MSO inhibition were similar. Furthermore, exposure of nodulated roots that had been exposed to either acetylene, MSO or allopurinol, to hyperbaric oxygen, caused a restoration of nitrogenase activity and respiration. This suggests that the resistance to diffusion of oxygen was increased in these nodules. Exposure of control plants to hyperbaric oxygen generally caused only a slight increase in nitrogenase activity and nodulated root respiration.

Stopping the formation of ammonium, glutamate or uric acid results in inhibition of the pathways of ureide synthesis in nodules. The absence of ammonium or glutamate will feed-forward to further inhibit reactions of ureide biosynthesis, because of a shortage of substrates. An increase in the xanthine (or hypoxanthine) concentration within nodules will probably feed-back to inhibit purine biosynthesis. Thus it appears that each of the active inhibitors used here would cause a decrease in amino acid and ureide synthesis. Just how these changes in metabolism lead to an increase in the apparent diffusion resistance of nodules to oxygen is unknown.

#### *Changes in the diffusion resistance of nodules to oxygen*

Reduced rates of nitrogenase activity which involve an apparent increase in the diffusion resistance of nodules have been observed for treatments involving exposure to acetylene (Witty *et al.* 1984), nodule detachment (Hunt *et al.* 1987), moisture stress (Pankhurst and Sprent 1975a, Durand *et al.* 1987, Davey and Simpson 1988), nitrate (Hartwig *et al.* 1987; Vessey *et al.* 1988a) and phloem girdling (Vessey *et al.* 1988a). Exposure to the ammonia assimilation inhibitors, MSO and allopurinol, can now be added to this list, as increased oxygen was observed to recover the nitrogenase activity of MSO (Table 6.1) and allopurinol treated nodules (Table 6.1, Atkins *et al.* 1988).

Changes in diffusion resistance of nodules may be due to changes in a water-filled zone occurring in the inner cortex, which has been proposed to act as a barrier to oxygen diffusion in soybean nodules (Witty *et al.* 1986). Walsh *et al.* (1989a) suggested that a significant portion of nodule water arrives by mass flow with sucrose via the phloem. They suggested that when phloem import of sucrose ceases, a decrease in the turgor pressure of cortical cells will occur and water may leave the cortical cells, enter the intercellular spaces and restrict gas passage. Inhibiting ureide synthesis within nodules may have similar effects on the osmolarity of cortical cells, if ureide transport is assumed to occur primarily through these cells. A decrease in the amount of ureides produced, while ureides continue to be exported, will reduce the osmotic pressure of these cells, allowing water to move out, which in turn may block adjacent air-spaces. When the air-spaces are blocked, the distance of water-filled diffusion across the nodule cortex is increased and oxygen diffusion is restricted. Rates of ureide production in nodules and the possible role of cell osmolarity changes in the regulation of nitrogenase activity are further examined in Chapter 8.



## Chapter 7

# Nodule Adaptation to Altered Oxygen Pressure

### 7.1. Introduction

The results of work referenced or presented in previous chapters suggests that the regulation of oxygen supply to the infected zone of nodules may be involved in the response of nodules to stress. This chapter examines the barriers to oxygen diffusion within soybean nodules.

It is proposed that layers of cells within the inner cortex provide a barrier to oxygen diffusion in soybean nodules (Tjepkema 1979), and despite many physiological (Tjepkema and Yocum 1973, 1974, Witty *et al.* 1987) and modelling (Sinclair and Goudriaan 1981, Sheehy *et al.* 1985, 1987, Hunt *et al.* 1988) experiments demonstrating the importance of this barrier, there has been relatively limited anatomical investigation of the inner cortex.

The technique of exposing nitrogen fixing systems to a range of oxygen pressures has been useful for determining mechanisms which restrict oxygen diffusion in these systems. By exposing cultured *Frankia* to a range of growth oxygen pressures, Parsons *et al.* (1987) demonstrated that the thickness of the *Frankia* vesicle wall increased with increasing  $pO_2$  and was probably the major site of resistance to oxygen movement. Similar experiments with *Alnus* and *Myrica* nodules have aided in determining the location of the resistance to oxygen movement in these symbioses (Silvester *et al.* 1988a,b). In this chapter an investigation of soybean nodule adaptation to oxygen pressures is presented, and in particular, changes in the structure of the nodule cortex are examined.

Short-term restriction of oxygen diffusion has been used as an explanation for decreases in nodule activity observed after exposure of nodules to stress (see previous chapters). In this chapter the response of nodules grown at different oxygen pressures to acetylene is examined. This allowed investigation of possible short-term changes in oxygen diffusion resistance in plants showing a long term adaptation to various oxygen pressures.

## 7.2. Results

Plants were grown with roots in pots which contained oxygen pressures of 4.7, 19, 47 and 75 kPa, from day 15, when nodules first appeared, until harvest at day 30, when nitrogenase activity and root respiration were measured, nodule samples collected for examination and plant dry weight determined.

### 7.2.1. Plant Growth

Plant dry weight at 30 days was affected by oxygen pressure around the roots and nodules (Figure 7.1). Plants grown with roots and nodules exposed to oxygen pressures of 4.7, 19 and 47 kPa did not differ significantly in overall dry weight and the relative size of each plant part was similar. However, with a  $pO_2$  of 75 kPa around the roots, plants were significantly smaller at 30 days and appeared to have suffered prolonged nitrogen starvation. There was a trend towards higher nodule dry weights at lower oxygen concentrations.

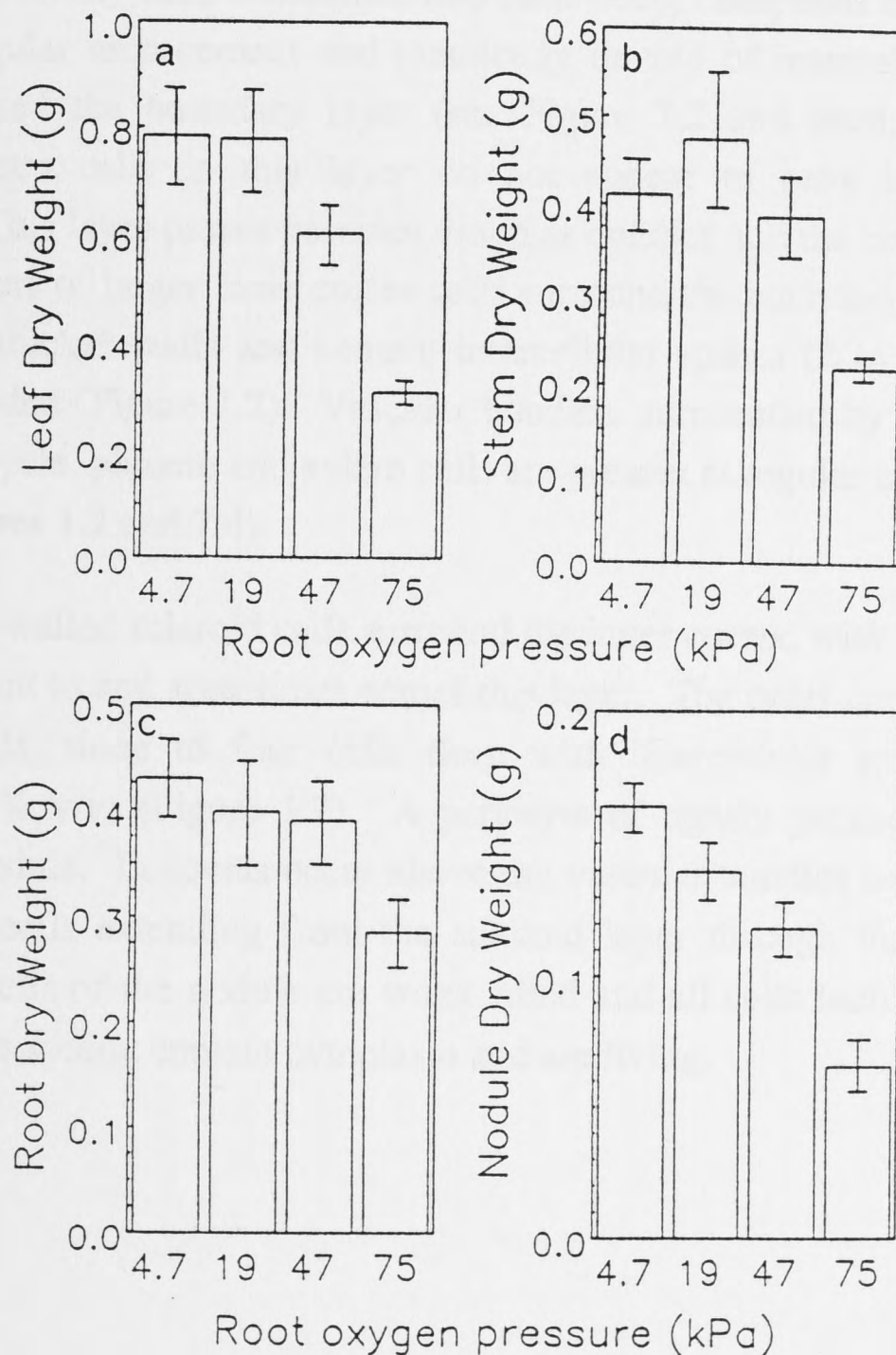


Figure 7.1 : Dry weight of plant parts at 30 days after plants were transferred to pots with roots and nodules sealed in different oxygen concentrations at day 15. (a) leaf, (b) stem, (c) root and (d) nodule. Error bars are 95 % confidence intervals.

## 7.2.2. Nodule structure

### *Typical nodule structure*

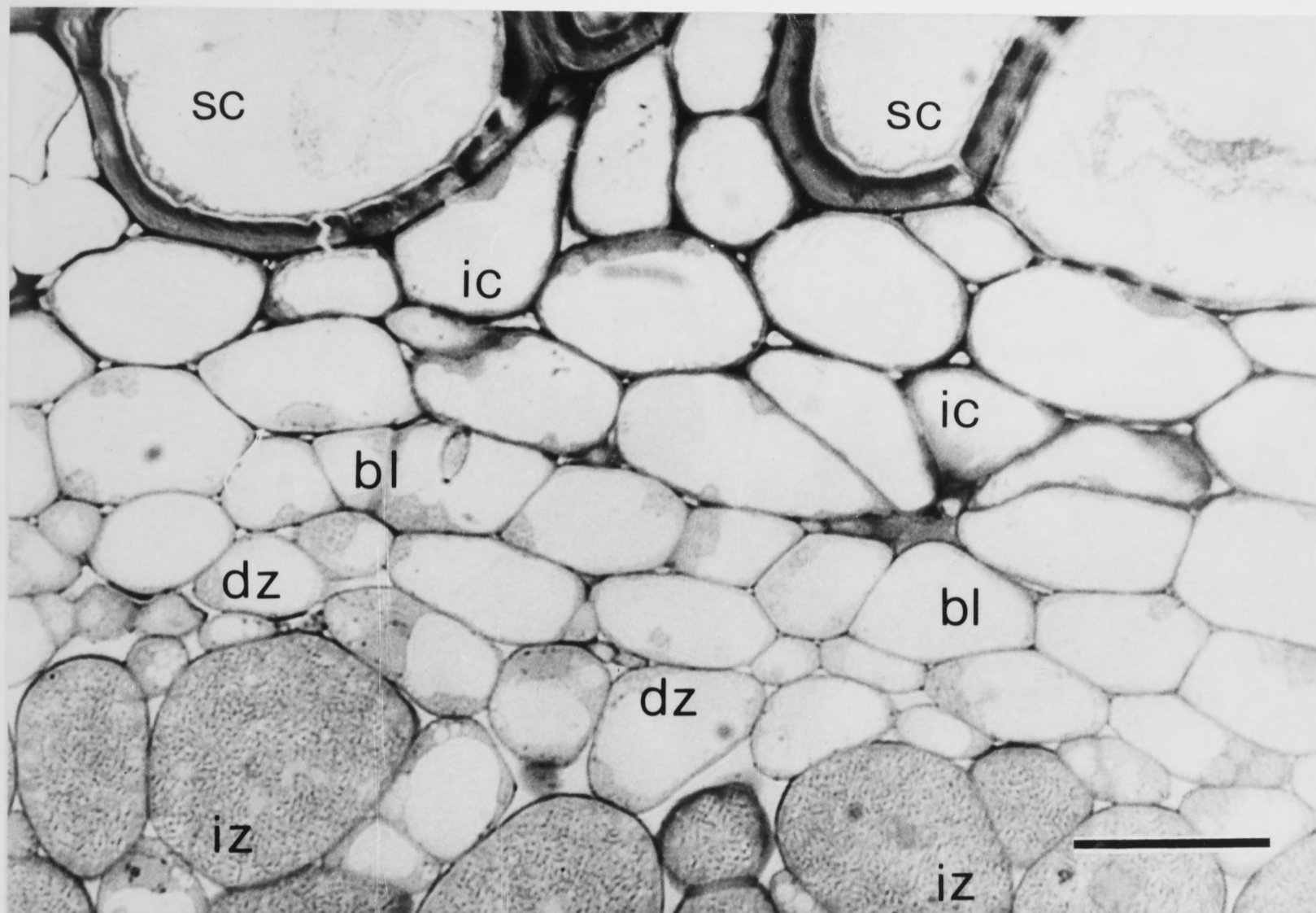
The cellular anatomy of a nodule grown in ambient (19 kPa) oxygen and examined in transverse section can be summarized as follows;

The central infected zone is composed of large infected cells and smaller uninfected cells, in a ratio of approximately 1:1, with infected cells being concentrated towards the outside of this zone. Some uninfected cells form rays two to three cells wide which form planes through the infected region. Intercellular spaces occur at every three cell junction, making up 3 to 4 % of the volume.

Surrounding the entire infected zone are one or two layers of uninfected cells with a large volume of intercellular spaces between them (ca. 5 %). This zone is shown in Figure 7.2 and was called the distributing zone. Encircling this zone is a layer of smaller cells, generally one, sometimes two cells deep, composed of thin-walled cells, packed in a regular arrangement and practically devoid of intercellular spaces. This zone was labelled the boundary layer (see Figure 7.2 and section 8.5, page 125). Junctions between cells in this layer do not appear to have intercellular spaces (Figure 7.10). This layer passes between vascular bundles and the central infected zone. Two to four layers of larger inner cortex cells surround the boundary layer. These cells generally have thicker walls and contain intercellular spaces (2 to 3 % v/v), some of which are occluded (Figure 7.2). Vascular bundles, surrounded by an endodermis and containing pericycle, phloem and xylem cells are present at regular intervals in the inner cortex (see Figures 1.2 and 7.4).

A layer of thick-walled scleroid cells surround the inner cortex, with intercellular spaces occurring adjacent to and sometimes across this layer. The outer cortex is composed of parenchyma cells, three to four cells deep with intercellular spaces at some cell junctions (ca. 5 % v/v) (Figure 1.2). A periderm of tightly packed, convoluted cells surrounds the nodule. Lenticels occur above the vascular bundles and are composed of loosely packed cells extending from the scleroid layer through the outer cortex and periderm. All cells of the nodule are water filled and all cells including the scleroids, but excluding the xylem, contain cytoplasm and are living.

## 7.2



**Figure 7.2 :** Light micrograph of a transverse section of the inner cortex region of a nodule grown at ambient oxygen (19 kPa). Bacteroid containing cells of the infected zone (iz) are present in the bottom of the figure. Above the infected zone is a layer of uninfected cells containing many intercellular spaces, labelled the distributing zone (dz). Above the distributing zone is a layer composed of cells with thin, radially orientated walls and very few intercellular spaces, labelled the boundary layer (bl). A layer composed of larger cells with intercellular spaces (ic) extends across the remainder of the inner cortex from the boundary layer to the scleroid cells (sc). The nodule was from a plant aged 30 days, inoculated at day 5. Bar represents 50  $\mu\text{m}$ .

*Effect of long-term  $pO_2$  on nodule structure*

Nodule external morphology was different across the oxygen treatments. Nodules which developed in low oxygen pressures were white and the entire surface was covered with loosely packed cells. Nodules grown at near ambient oxygen pressures had characteristic banded lenticels, composed of loosely packed parenchyma cells, while nodules from high oxygen pressures had a largely unbroken periderm with very little external lenticel development (Figure 7.3).

Transverse sections (1  $\mu\text{m}$ , cut through the centre, perpendicular to the nodule axis) of resin embedded nodules were examined for possible differences in nodule structure. On a gross scale, nodule anatomy was similar across all treatments, with the previously described (see Figure 1.2, Sprent 1972, Bergersen 1982) outer cortex, scleroid layer, inner cortex and infected zones present.

Bacteroid numbers in the infected cells were estimated by counts using light microscope sections. There was a similar density of approximately 23 bacteroids per 100  $\mu\text{m}^2$  ( $\pm 2$ , 95 % confidence limit) in most infected cells of nodules examined which had developed in 4.7, 19 or 47 kPa oxygen, although in the infected cells of two out of seven nodules examined grown at 4.7 kPa oxygen, a lower density of approximately 15 bacteroids per 100  $\mu\text{m}^2$  was observed. The other five nodules examined, grown at 4.7 kPa oxygen, had a mean infected cell bacteroid density of 22 ( $\pm 2$ ) per 100  $\mu\text{m}^2$ . The bacteroid density was consistently lower in nodules developed in 75 kPa oxygen, which had a mean density of 15 ( $\pm 1.5$ ) bacteroids per 100  $\mu\text{m}^2$ . Within the infected zone, infected to uninfected cell ratios were constant in all treatments (approximately 1:1). However, in nodules grown at 75 kPa oxygen, infected cells were smaller and uninfected cells comparatively larger than in other treatments. This produced a greater volume of uninfected tissue (see Figures 7.4, 7.5).

The distribution of intercellular spaces was examined in these sections. Numbers of intercellular spaces were determined by light microscopy and the mean distribution was calculated in the following zones; a) central infected zone, b) distributing zone, c) inner cortex, d) outer cortex. The central infected zone is composed of infected and uninfected cells. The distributing zone is defined as the layer of cells on the inside of the inner cortex which form an interconnecting network of air-spaces surrounding the infected cells. This zone was seen in *Pisum* and *Phaseolus* (Witty *et al.* 1987) and was clearly observed by phase contrast microscopy in fresh sections of soybean nodules (this study). The inner cortex is the layer of cells from the outside of the distributing layer to the scleroid layer and the outer cortex is taken from the scleroid layer outwards. The scleroid layer is not included in this analysis, although intercellular spaces were observed, occurring adjacent to, and sometimes across this layer (Figures 7.4, 7.5). Numbers of intercellular spaces in these zones are presented in Table 7.1 as the

percentage of three cell junctions which had an unoccluded intercellular space. It was not possible to tell from light microscopy whether a three cell junction had no intercellular space or if the space had been occluded. Both these types of junctions were scored as not containing an intercellular space (see transmission electron microscopy below).

**Table 7.1 :** Mean percentage of three cell junctions which had an unoccluded intercellular space, in various zones of nodules grown at different oxygen pressures. Four nodules from each oxygen treatment were sectioned and four or five fields of each zone from each nodule were counted. Approximately 25 cell junctions were examined per microscope field. ( $\pm 95\%$  confidence limits).

Tissue	4.7 kPa	19 kPa	47 kPa	75 kPa
Outer cortex	73 $\pm$ 12	55 $\pm$ 9	48 $\pm$ 13	27 $\pm$ 7
Inner cortex	70 $\pm$ 8	58 $\pm$ 9	44 $\pm$ 8	33 $\pm$ 9
Distributing layer	97 $\pm$ 3	100 $\pm$ 1	97 $\pm$ 3	97 $\pm$ 3
Infected zone	99 $\pm$ 1	100 $\pm$ 1	100 $\pm$ 1	100 $\pm$ 1

The approximate area represented by these intercellular spaces was estimated from light micrographs using a digitizer palette and micro-computer (Table 7.2). The data presented provide an indication of the area of intercellular spaces, although the reservations expressed by Bergersen and Goodchild (1973a) and Silvester *et al.* (1988b) on the difficulties of measuring air-spaces in nodules are probably warranted. Embedding, sectioning and staining may change the apparent size of these spaces. Furthermore, variation is also introduced because of the occurrence of structures such as lenticels, vascular bundles and uninfected cell rays (see Figures 7.4, 7.5). The best approach would be to examine serial sections throughout an entire nodule, but this was beyond the scope of the present study.

**Table 7.2 :** Approximate area of intercellular spaces present in four different zones of nodules grown at various oxygen tensions. Intercellular space area in the outer cortex, inner cortex and distributing layer are the mean of measurements from four micrographs for each oxygen treatment. Infected zone data is the mean of measurements from two micrographs for each oxygen treatment.

Tissue	4.7 kPa	19 kPa	47 kPa	75 kPa
	Percent of total area.			
Outer cortex	11	5.3	2.0	0.65
Inner cortex	1.5	1.7	0.93	0.50
Distributing layer	6.4	3.9	4.6	4.2
Infected zone	3.2	3.5	3.6	3.2

Intercellular spaces had a similar distribution in the infected zone and in the distributing layer in all treatments. Virtually every junction between cells in these zones contained an intercellular space, regardless of oxygen treatment. The distribution of spaces in the inner and outer cortex was very different across the treatments, with intercellular space number and size decreasing in both zones in nodules grown in higher oxygen pressures. This is shown clearly in Figures 7.4 and 7.5. Both figures are included, firstly to provide representative examples and secondly because they show different parts of the nodule cortex. Figure 7.4 shows sections with vascular bundles and a zone of loosely packed cells in the outer cortex (a lenticel) which occurs in each section above the bundles. A section of cortical cells in between vascular bundles from each treatment is presented in Figure 7.5. Lenticels, the region of loosely packed cells in the outer cortex, were observed in sections of nodules from all treatments, although the surface of nodules formed at 47 and 75 kPa oxygen, were generally smooth (Figure 7.3) and the periderm was more densely packed (Figures 7.4, 7.5).

Transmission electron micrographs confirmed the variation in cell structure and intercellular space distribution in the cortex. Sections extending across the cortex and into the infected zone, from at least three different nodules grown at each oxygen pressure, were examined. Micrographs from nodules grown at 4.7 and 47 kPa are presented to compare structure within the distributing layer (Figure 7.6), inner cortex (Figure 7.7) and outer cortex (Figure 7.8). Structure of cells within the infected zone and the distributing layer were similar across all treatments (Figure 7.6 and see also Figures 8.2, 8.3).

Intercellular spaces within the inner cortex showed a different distribution. At higher oxygen pressures cells were more closely packed and a larger number of intercellular spaces were occluded with an electron dense material (Figures 7.7, 8.2, 8.3), although occluded and unoccluded intercellular spaces were observed in all treatments. Examples of intercellular spaces and occluded spaces are shown in Figure 7.9.

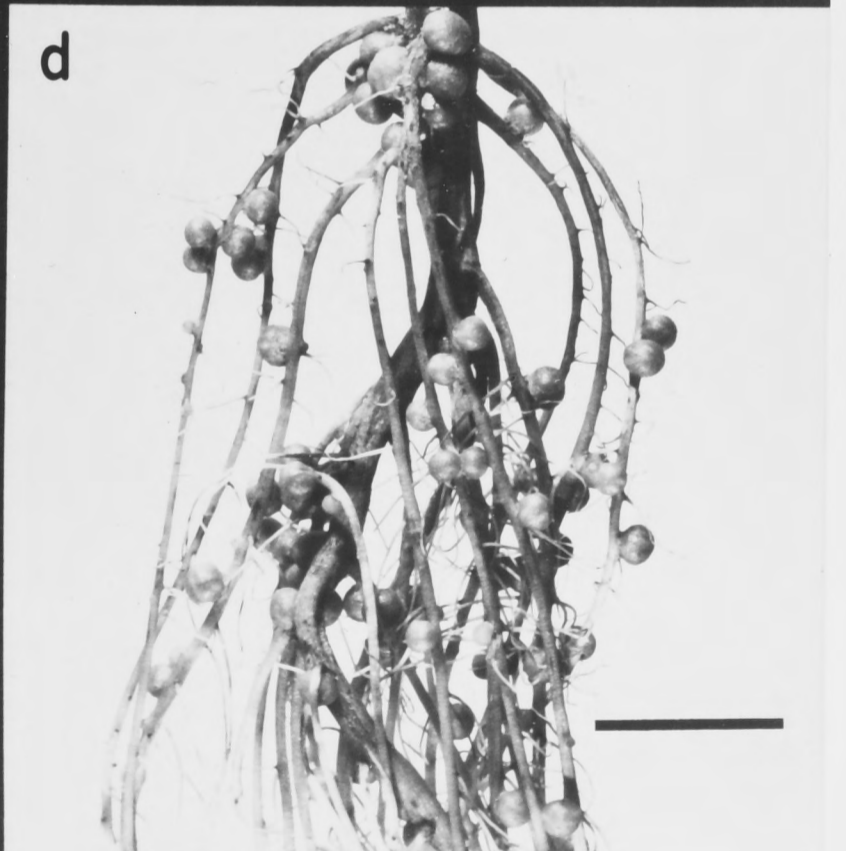
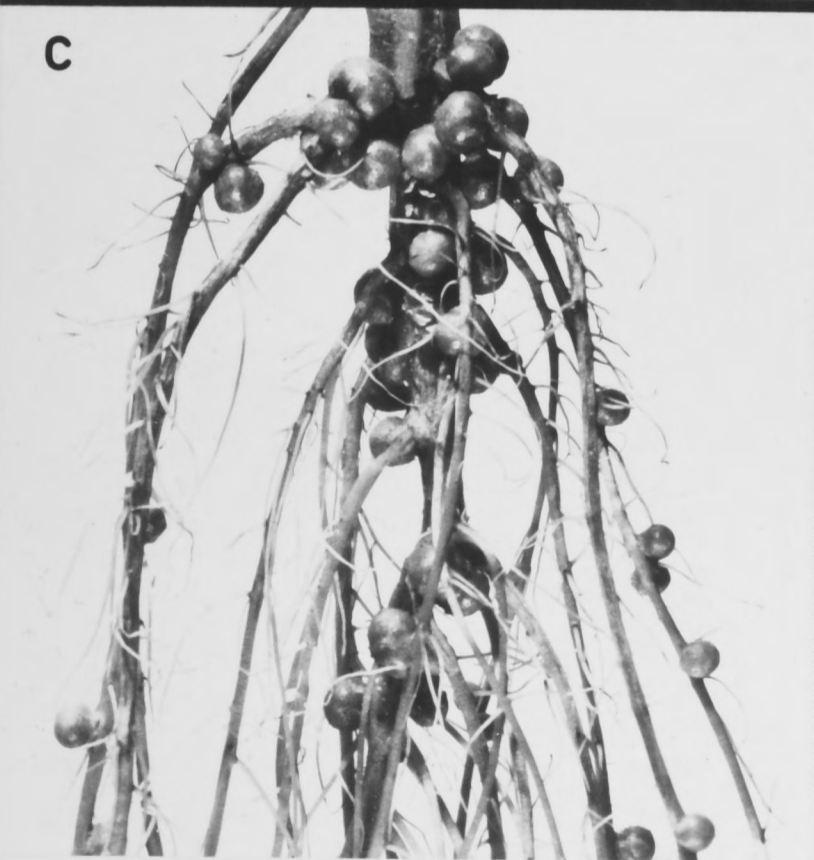
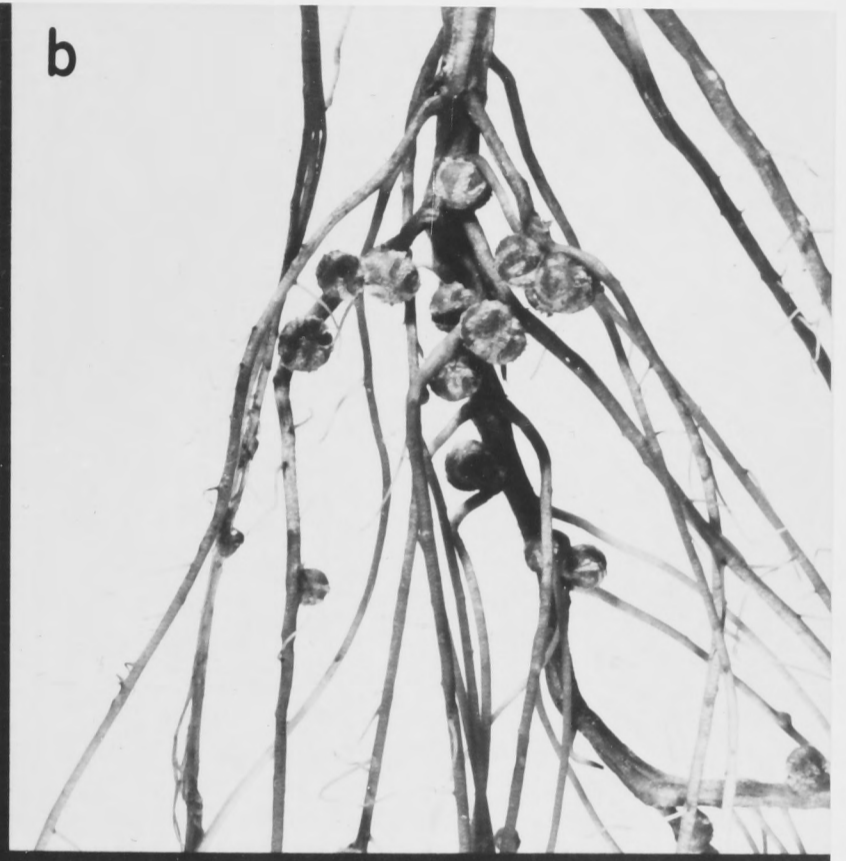
The loosely packed cells of the outer cortex from nodules grown at low oxygen pressures contained many large unoccluded intercellular spaces. These spaces were smaller and less frequent in the outer cortex of nodules grown at higher oxygen pressures. In these nodules, cells in the periderm often appeared compressed with convoluted walls separated by a densely staining material (Figure 7.8).

A layer of cells occurring at the inside of the inner cortex, with thin walls and very few intercellular spaces (the boundary layer, see page 100) was observed in all nodule sections regardless of growth  $pO_2$ . This layer was further examined by preparing tangential sections through the cortex of a nodule grown at 19 kPa oxygen (Figure 7.10). No radially orientated intercellular spaces appear to occur in this layer as all three cell junctions were tightly packed in all sections examined.

**Figure 7.3 :** Nodulated roots of plants aged 30 days (inoculated at day 5) grown at oxygen pressures of 4.7 kPa (a), 19 kPa (b), 47 kPa (c) and 75 kPa (d). Bar represents 10 mm.



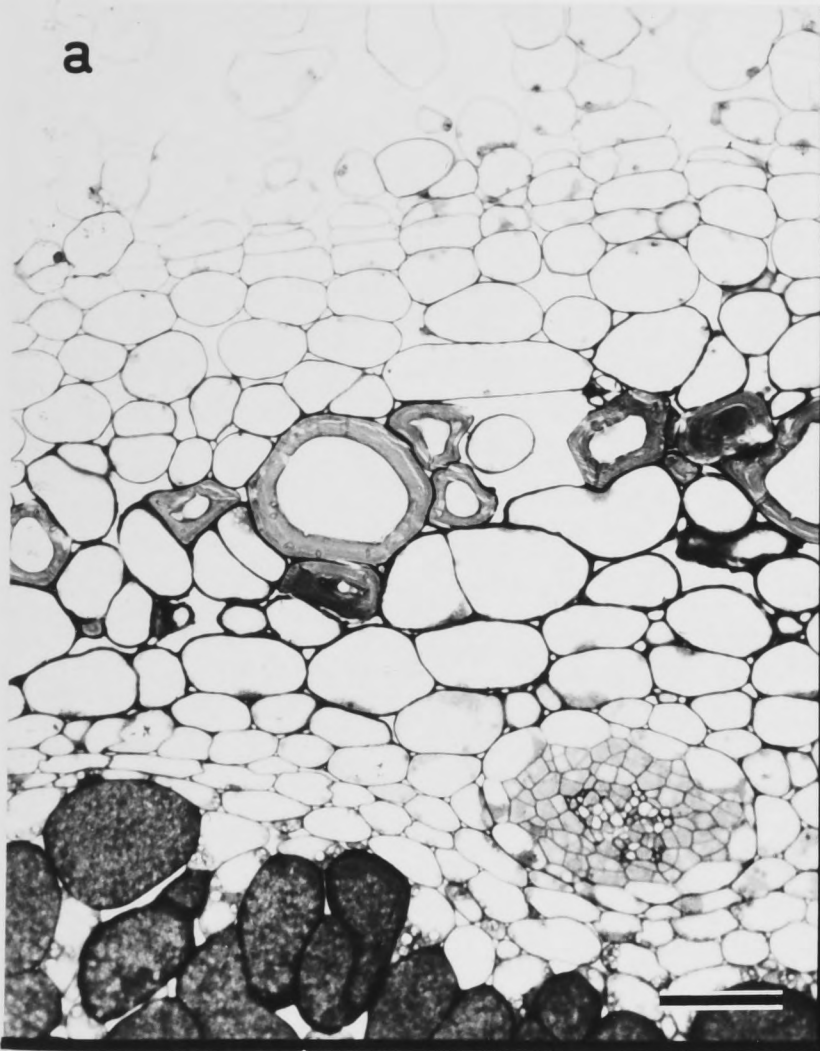
7.3



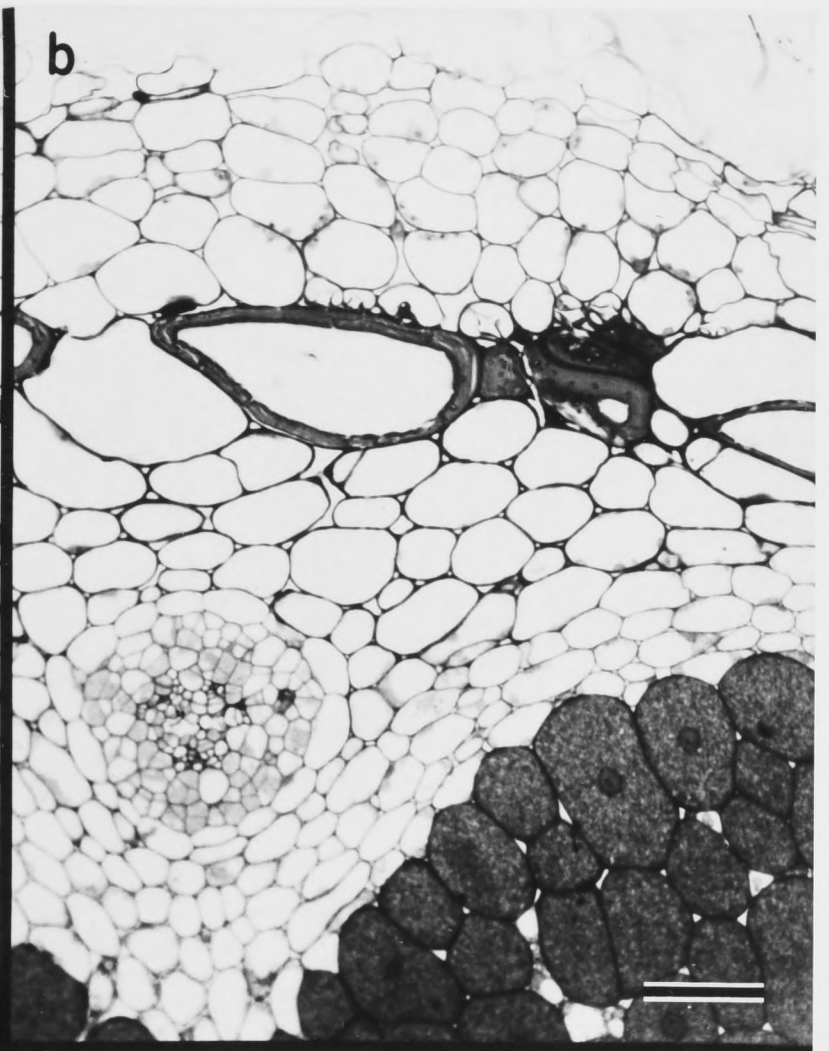
**Figure 7.4 :** Light micrographs of transverse sections of the cortex region of nodules grown at oxygen pressures of 4.7 kPa (a), 19 kPa (b), 47 kPa (c) and 75 kPa (d). Each section has a vascular bundle in the inner cortex and a region of cells with larger intercellular spaces (lenticels) present in the outer cortex, above the vascular bundle. Plants were aged 30 days, inoculated at day 5. Bars represent 50  $\mu\text{m}$ .

7.4

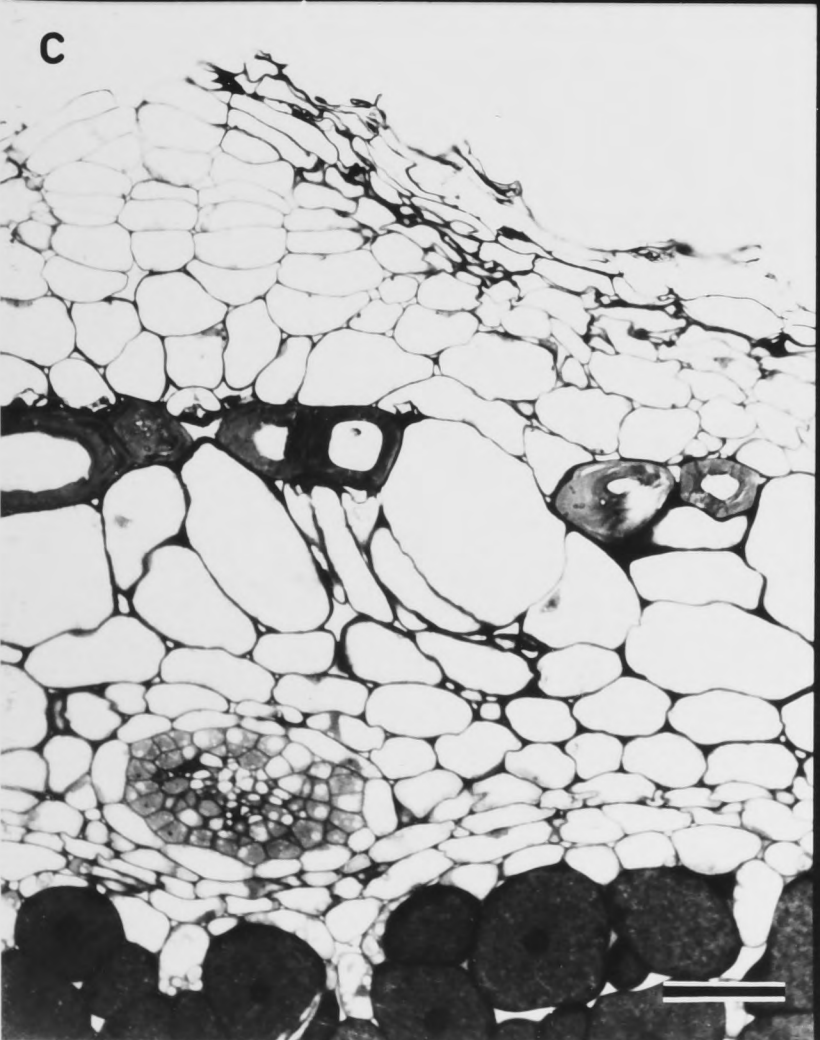
a



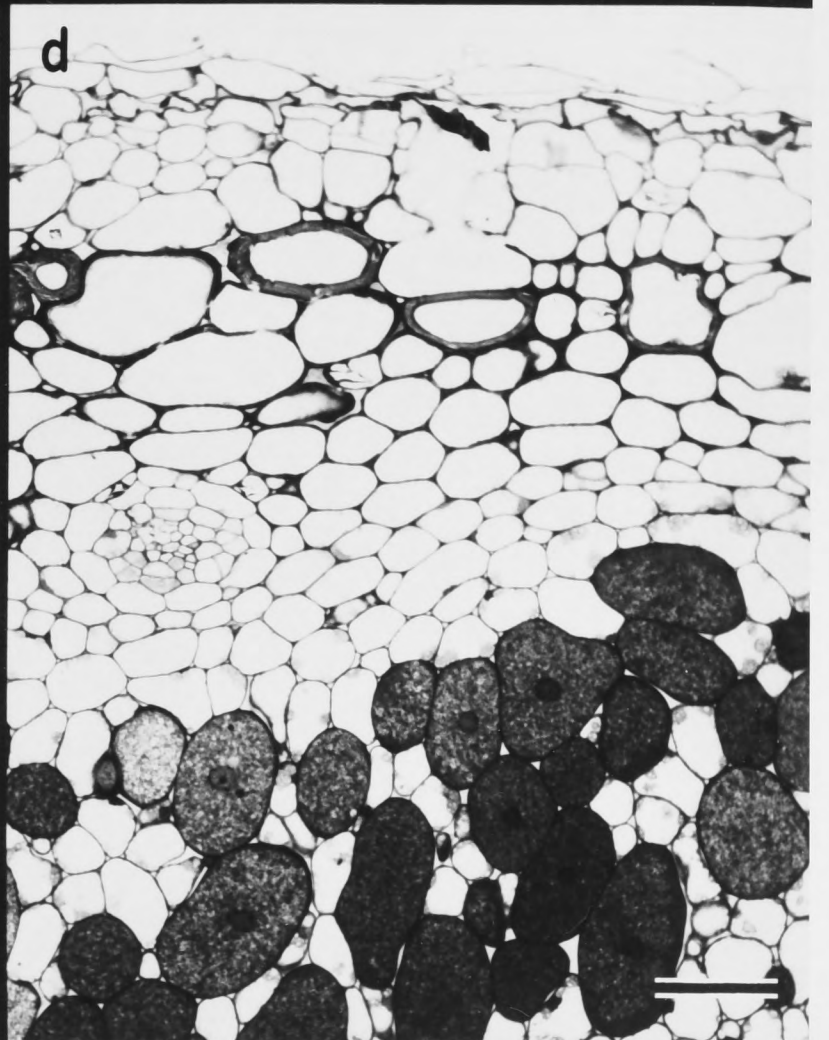
b



c

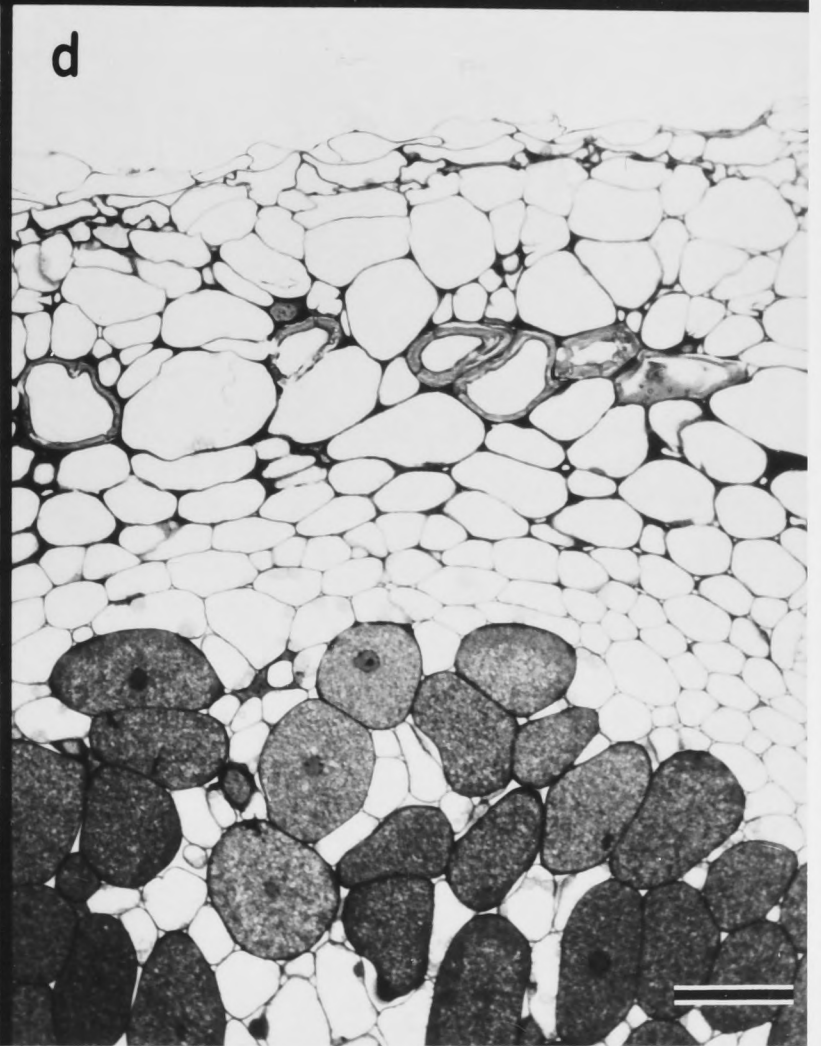
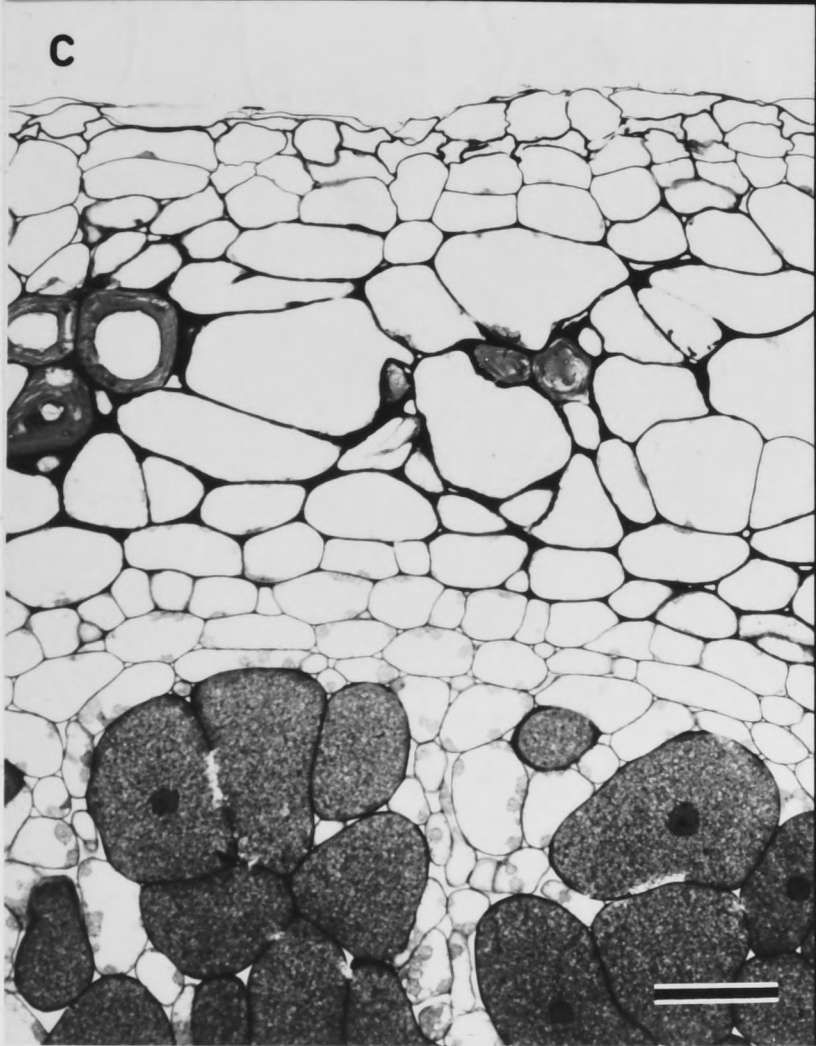
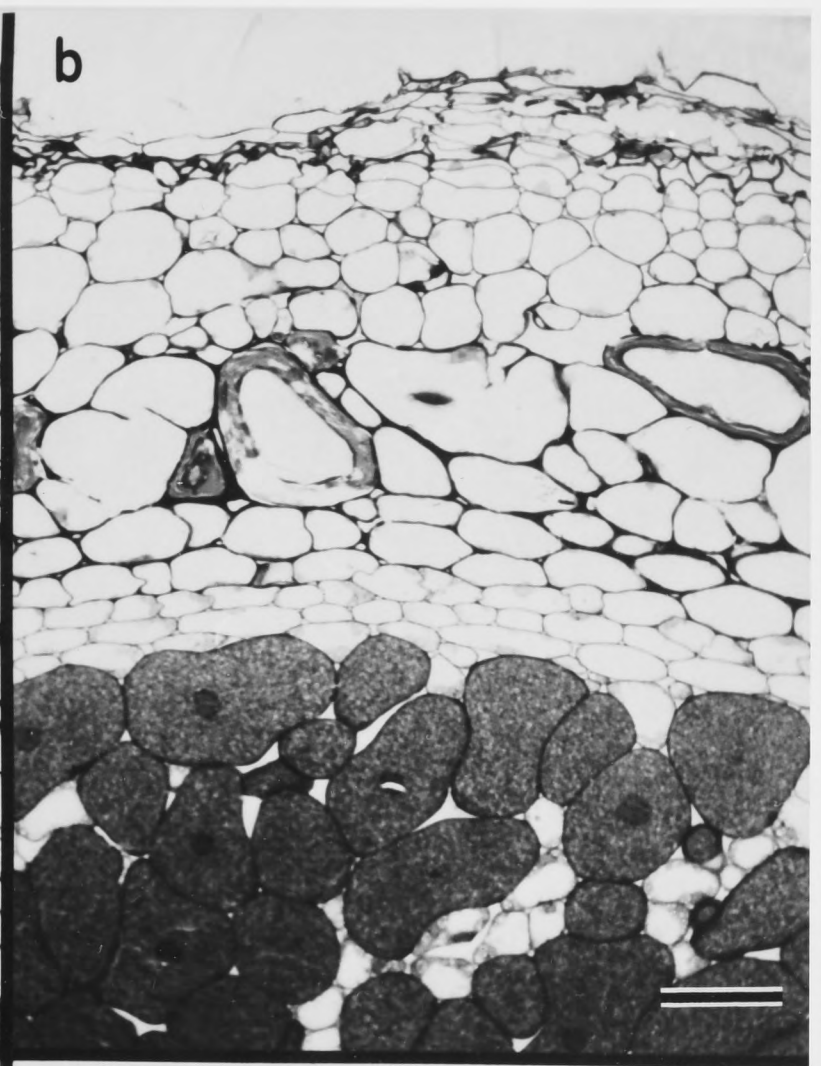
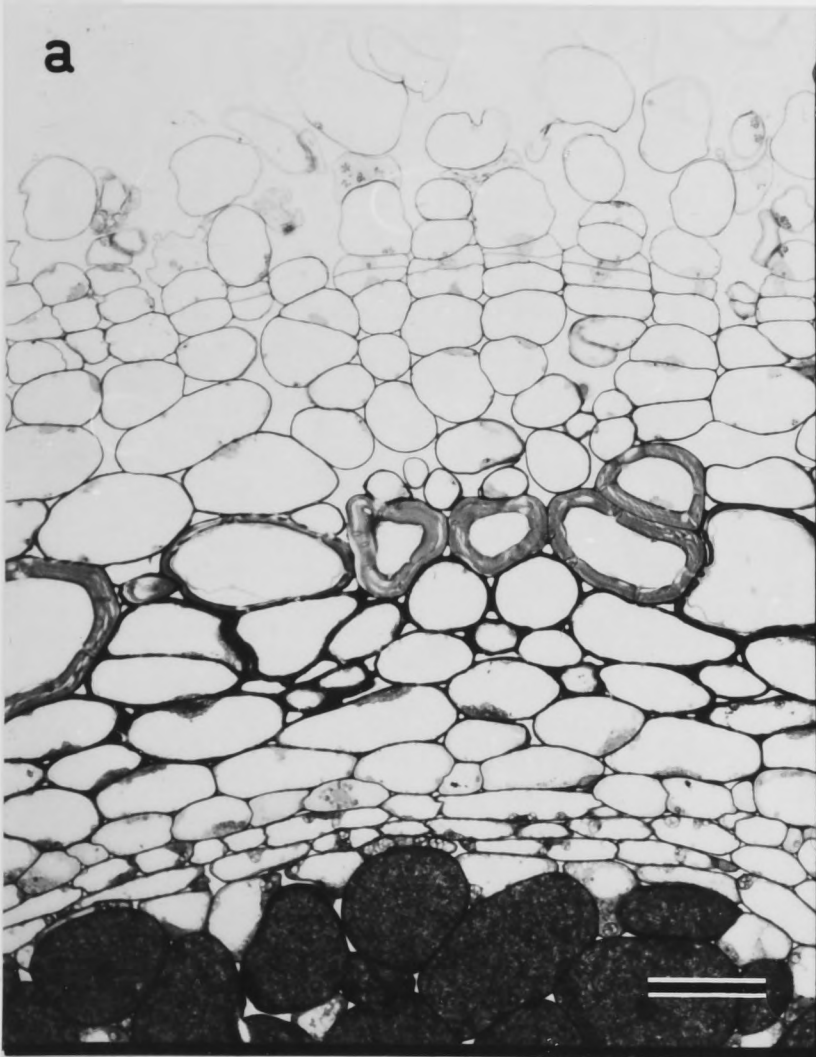


d



**Figure 7.5 :** Light micrographs of transverse sections of the cortex region of nodules grown at oxygen pressures 4.7 kPa (a), 19 kPa (b), 47 kPa (c) and 75 kPa (d). Micrographs were taken in the cortex region between vascular bundles. Plants were aged 30 days, inoculated at day 5. Bars represent 50  $\mu\text{m}$ .

7.5



**Figure 7.6 :** Transmission electron micrographs of the distributing zone of cells and intercellular spaces present on the outside of the infected region. Plants were aged 30 days, inoculated at day 5. Bars represent 5  $\mu\text{m}$ .

(a) Nodule grown at 4.7 kPa  $\text{O}_2$ . Infected zone is to the upper left and inner cortex to the lower right.

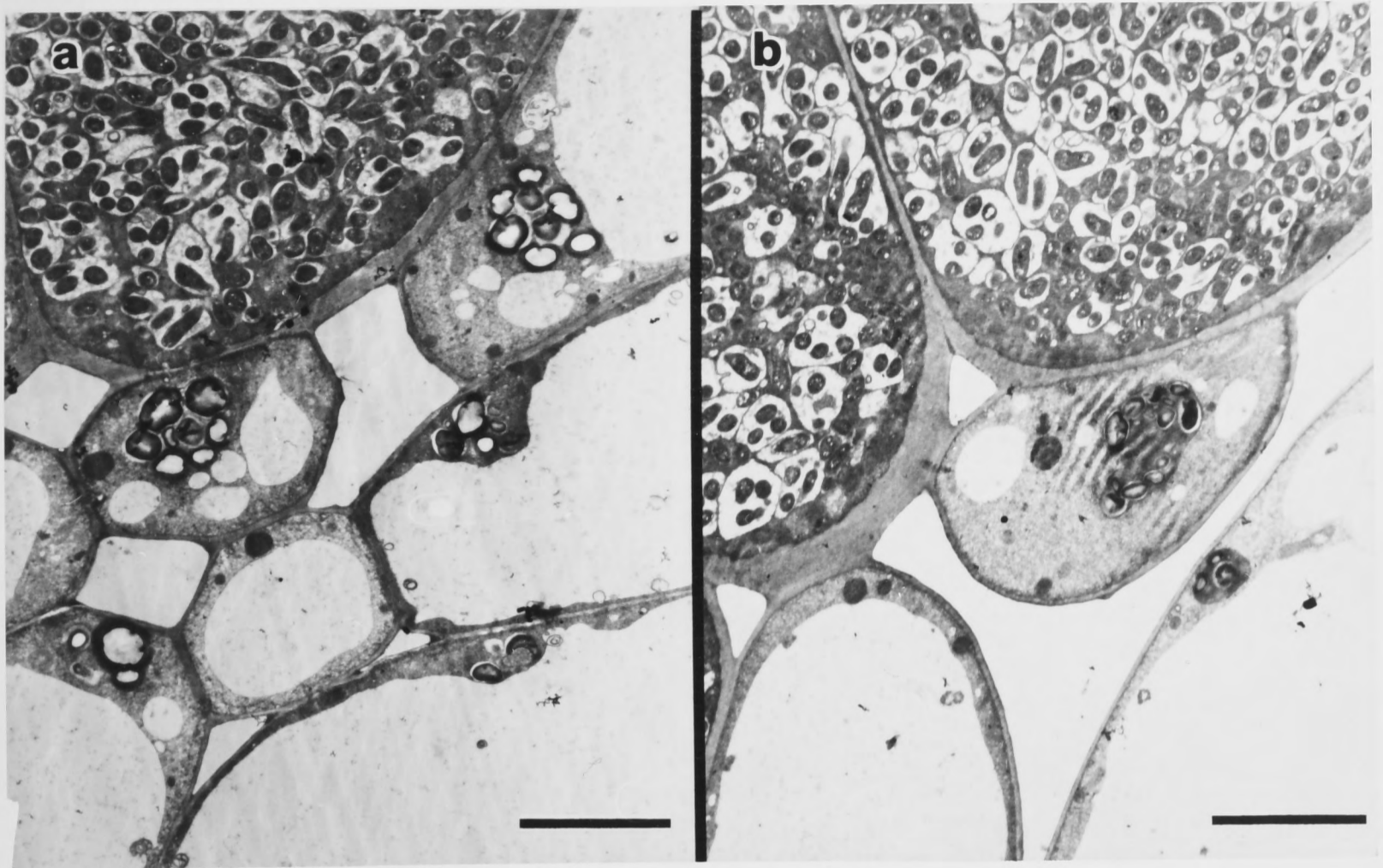
(b) Nodule grown at 47 kPa  $\text{O}_2$ . Infected zone is to the upper left and inner cortex to the lower right.

**Figure 7.7 :** Transmission electron micrographs of cells and intercellular spaces present in the inner cortex. Plants were aged 30 days, inoculated at day 5. Bars represent 5  $\mu\text{m}$ .

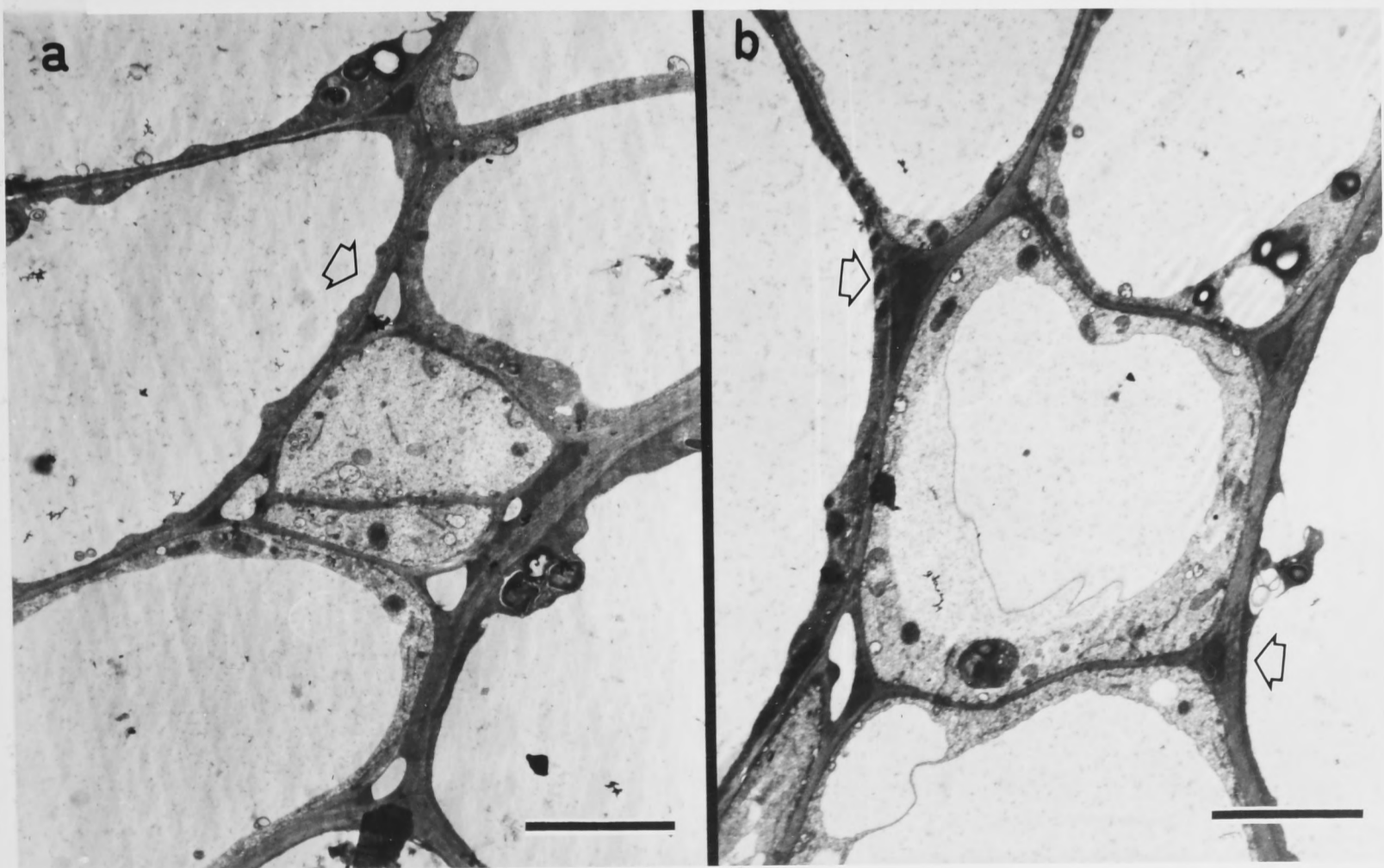
(a) Nodule grown at 4.7 kPa  $\text{O}_2$ . Infected zone is to the upper left (not visible) and scleroid cells to the lower right (not visible). The high frequency of unoccluded intercellular spaces is demonstrated (arrow).

(b) Nodule grown at 47 kPa  $\text{O}_2$ . Infected zone is to the left (not visible) and scleroid cells to the right (not visible). A greater proportion of intercellular spaces were occluded in nodules grown at this oxygen pressure (arrows).

7.6



7.7



**Figure 7.8 :** Transmission electron micrographs of cells of the outer cortex. Plants were aged 30 days, inoculated at day 5. Bars represent 5  $\mu\text{m}$ .

(a) Nodule grown at 4.7 kPa  $\text{O}_2$ . Micrograph showing intercellular space and regular packing of cells in the periderm.

(b) Nodule grown at 47 kPa  $\text{O}_2$ . Micrograph showing convoluted cells with occluded intercellular spaces in the periderm.

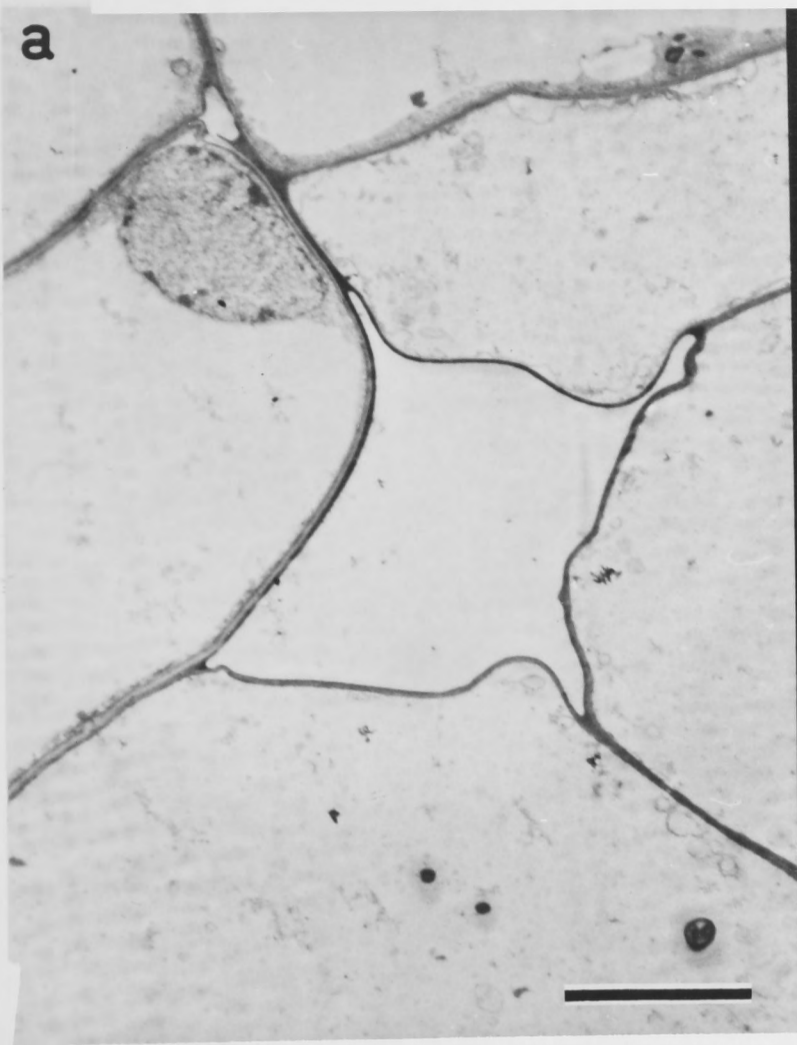
**Figure 7.9 :** Transmission electron micrographs of intercellular spaces present in the inner cortex. Plants were aged 30 days, inoculated at day 5.

(a) Intercellular spaces present between cells showing partial occlusion. Bar represents 5  $\mu\text{m}$ .

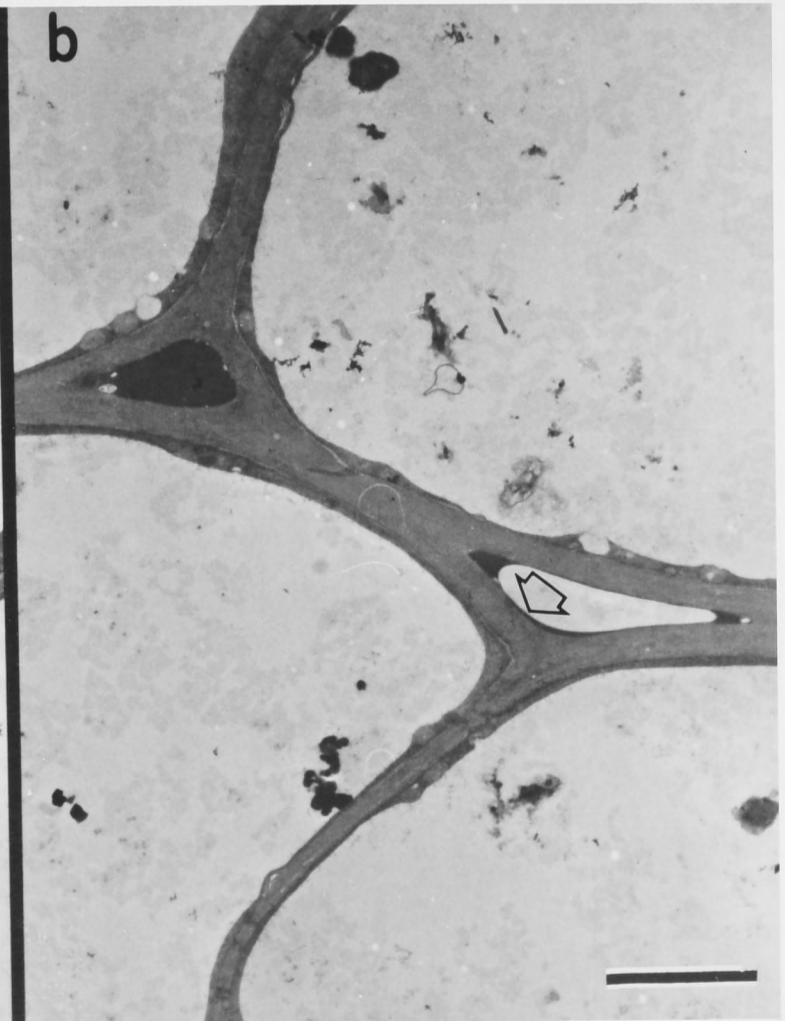
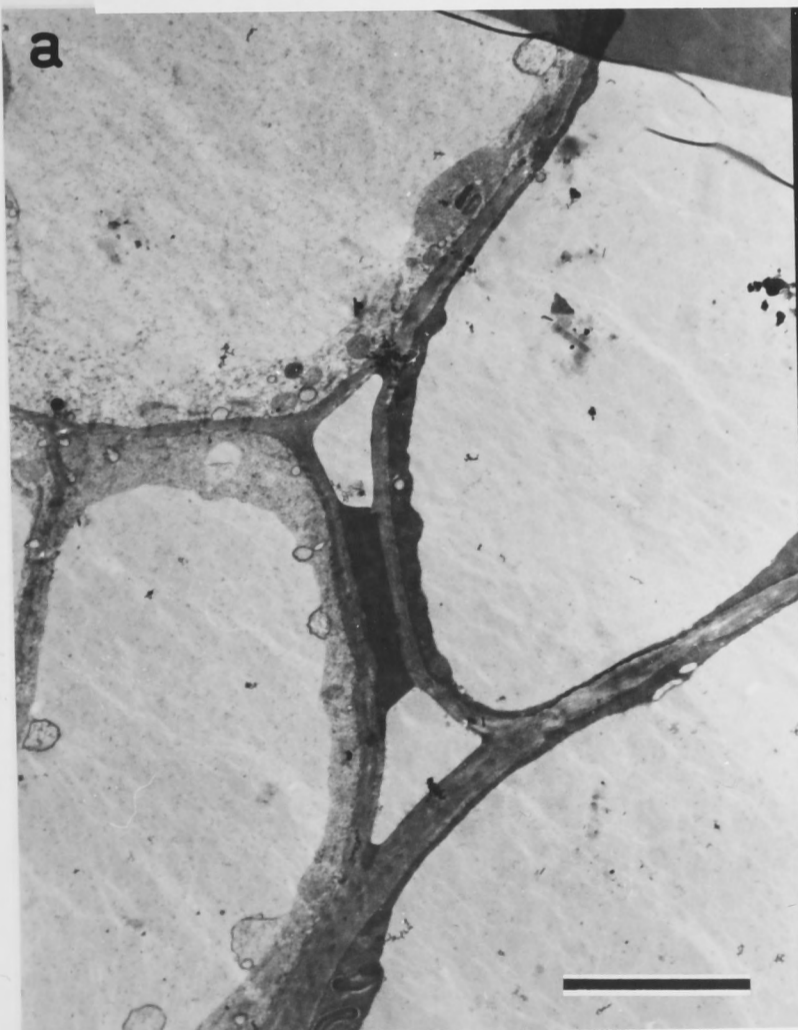
(b) Micrograph shows an occluded and unoccluded intercellular space. A thin, electron dense layer can be seen coating the wall surrounding the unoccluded intercellular space (arrow). Bar represents 2  $\mu\text{m}$ .



7.8



7.9

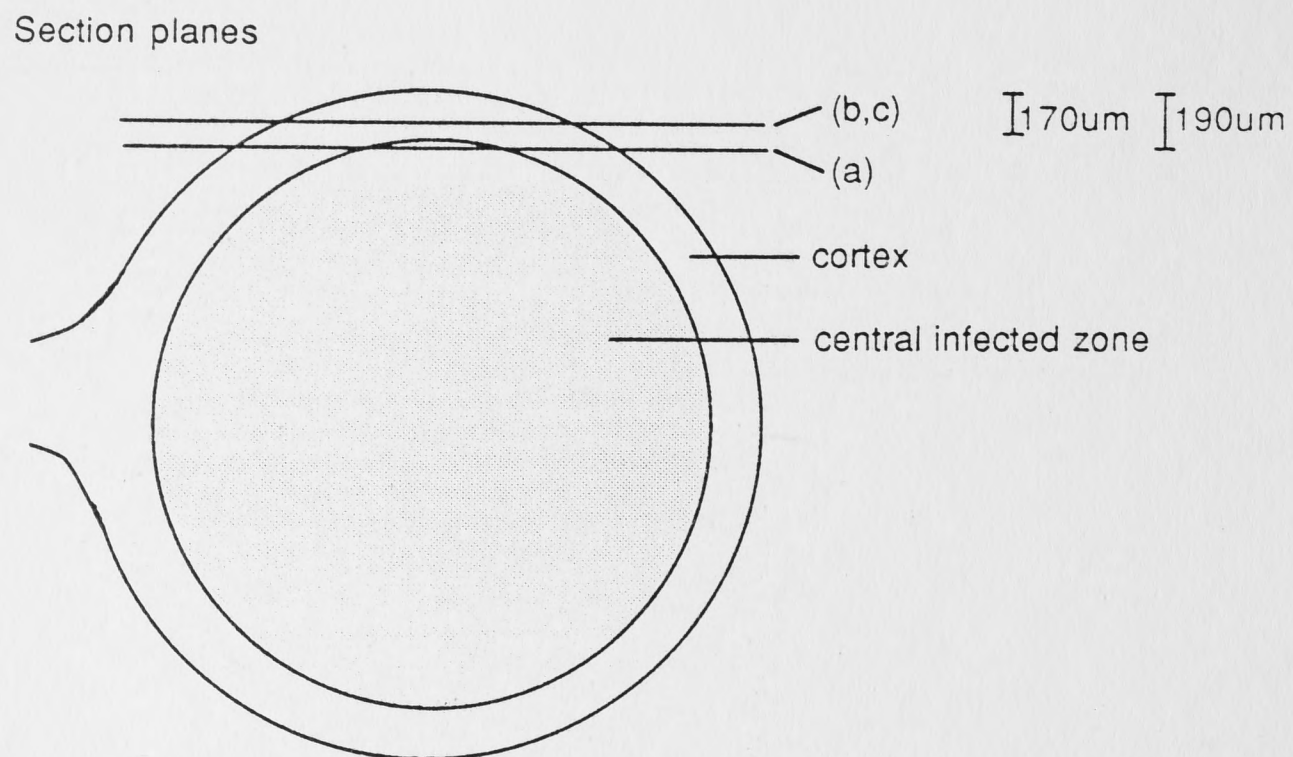


**Figure 7.10 :** Light micrographs of tangential sections of the inner cortex of a nodule grown at 19 kPa oxygen. For orientation, see the diagram below.

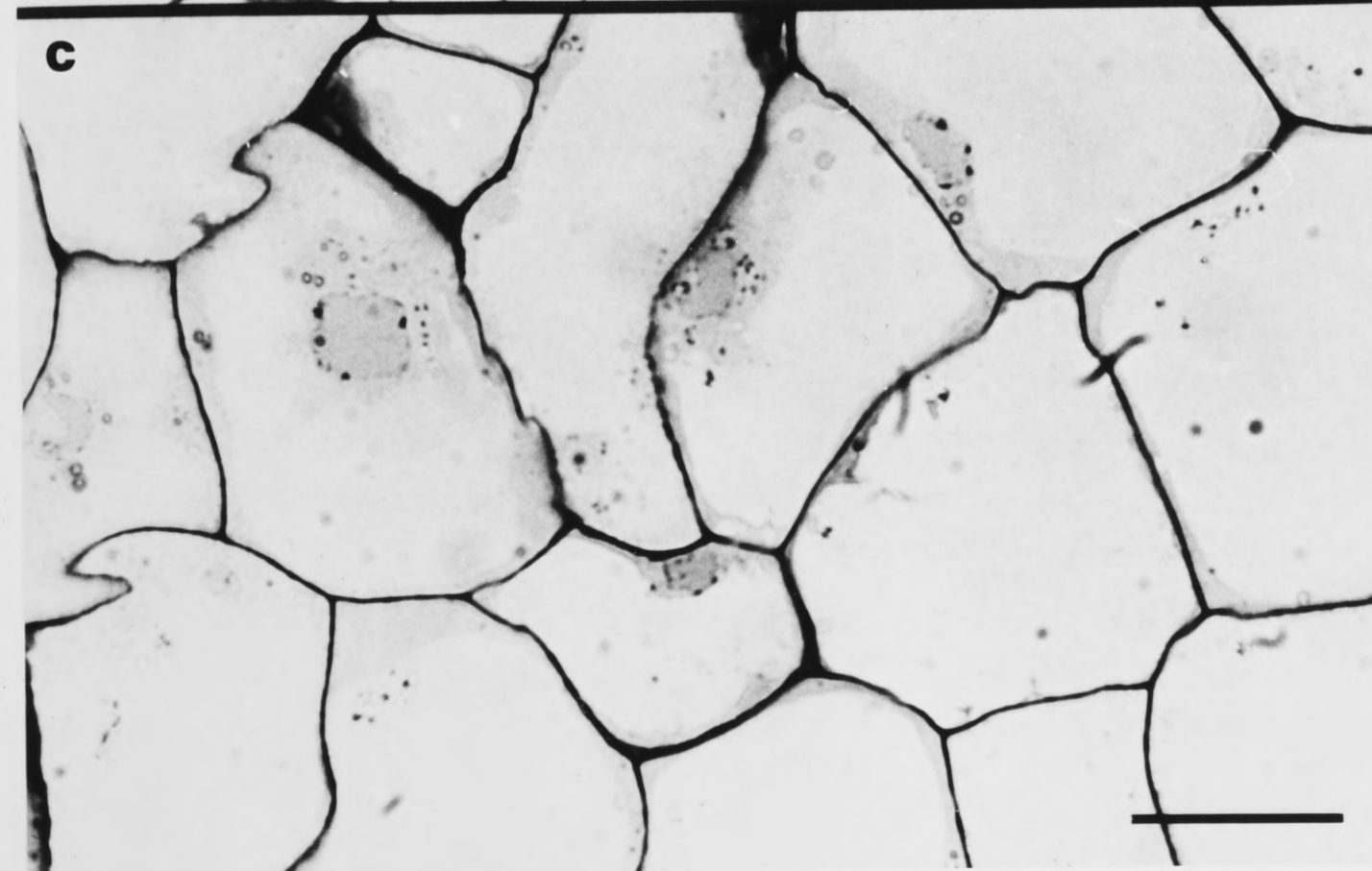
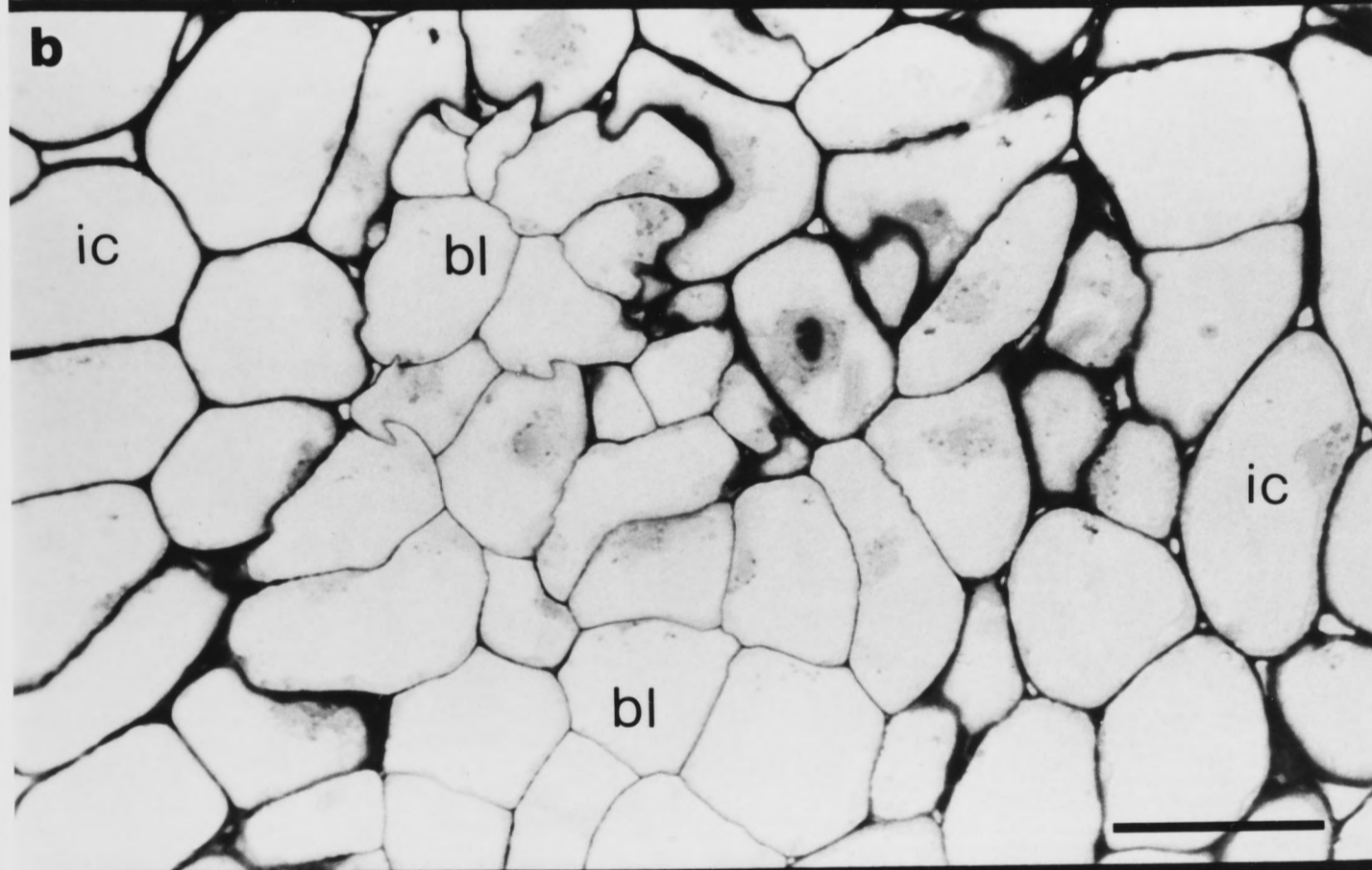
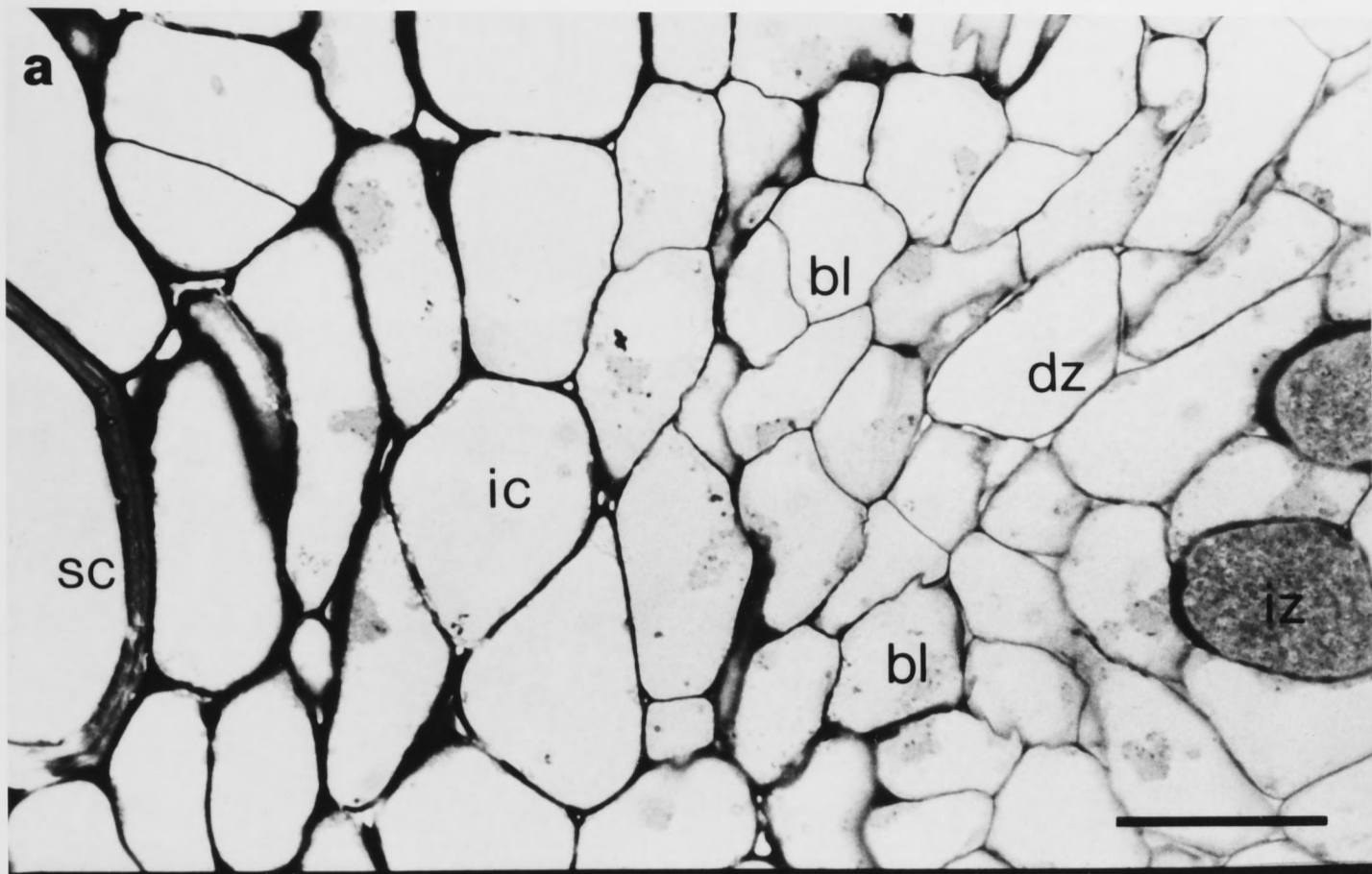
(a) Section passing tangentially through central infected zone (iz) and obliquely through distributing zone (dz), boundary layer (bl), inner cortex (ic) and scleroid cells (sc). Maximum section depth is approximately 190  $\mu\text{m}$  from the nodule surface. Bar represents 50  $\mu\text{m}$ .

(b) Section passing tangentially through inner cortex (ic) and boundary layer cells (bl). Intercellular spaces are present between cells in the inner cortex, but do not occur between cells in the boundary layer. Maximum section depth is approximately 170  $\mu\text{m}$  from the nodule surface. Bar represents 50  $\mu\text{m}$ .

(c) High power micrograph of a tangential section through boundary layer cells. Intercellular spaces do not occur. Section depth is approximately 170  $\mu\text{m}$  from the nodule surface. Bar represents 20  $\mu\text{m}$ .



7.10



### 7.2.3. Nodule physiology

Root respiration and nitrogenase activity were investigated in the sealed pots using the open gas flow system. Respiration was measured as CO<sub>2</sub> efflux, firstly at the oxygen pressure at which plants were grown and subsequently after 8 kPa acetylene was introduced (N<sub>2</sub> pressure was reduced simultaneously by 8 kPa). Under these conditions, maximum nitrogenase activity and the extent of the acetylene-induced decline could be determined. Typical results are shown in Figure 7.11, which presents rates of CO<sub>2</sub> efflux and ethylene production of single pots containing four plants, following addition of saturating acetylene at time zero. Mean values for three measurements of maximum specific nitrogenase activity and the extent of acetylene-induced decline are presented in Table 7.3. Plants grown at 4.7, 19 and 47 kPa O<sub>2</sub> all showed similar maximum specific activities and extent of decline, but plants grown at 75 kPa O<sub>2</sub> had considerably lower initial acetylene reduction activity and did not show a decline.

The soluble haem content of nodules grown at 4.7, 19 and 47 kPa O<sub>2</sub> was similar, but haem content of nodules grown at 75 kPa O<sub>2</sub> was considerably lower (Table 7.3).

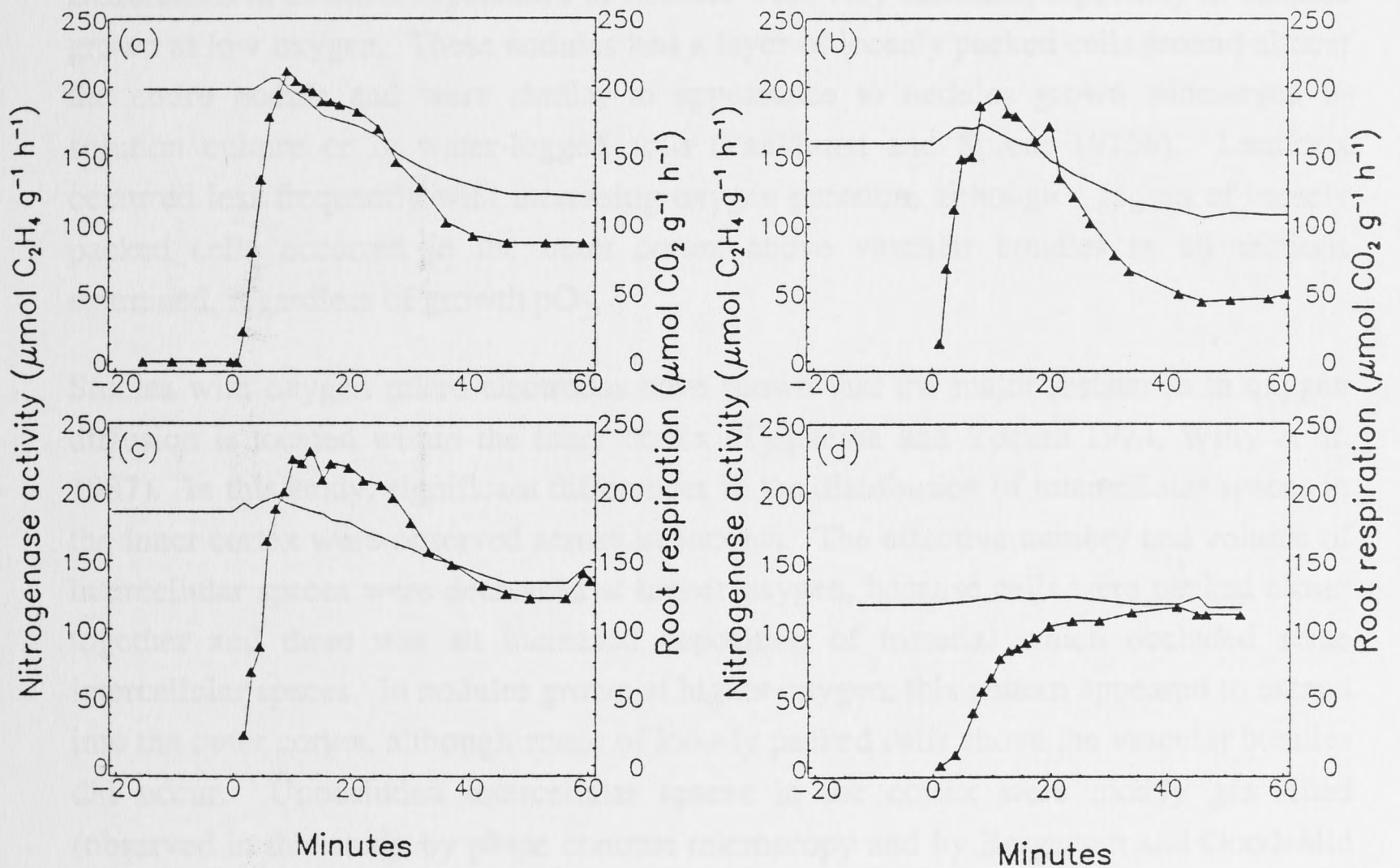
**Table 7.3 :** Mean values of maximum acetylene reduction activity, extent of acetylene-induced decline and haem content from nodules grown at four different oxygen levels. Acetylene reduction activities (ARA) were measured using an open flow system using pots containing four plants and are expressed as the mean of three assays per treatment. Haem content is the mean of duplicate samples.

Oxygen (kPa)	Maximum ARA $\mu\text{mol C}_2\text{H}_4 \text{ g}^{-1}\text{DW h}^{-1}$	Mean decline (%)	Haem content $\mu\text{mol g}^{-1} \text{FW}$
4.7	199	45	0.271
19	178	54	0.295
47	191	45	0.279
75	133	3	0.160

Nodules grown at 4.7, 19 and 47 kPa oxygen showed a similar response to acetylene (Figure 7.11 a,b,c). These plants had a peak in acetylene reduction activity of approximately 200  $\mu\text{mol C}_2\text{H}_4 \text{ g}^{-1}\text{DW hr}^{-1}$  between 6 and 15 minutes after exposure to acetylene began. Acetylene reduction activity and CO<sub>2</sub> efflux then declined for a further 30 to 40 minutes, after which a more or less steady state occurred.

Nodules grown at 75 kPa oxygen consistently showed a different response to saturating levels of acetylene (Figure 7.11 d). These plants showed no peak immediately after exposure began and maintained a steady rate of acetylene reduction activity and

nodulated root respiration following introduction of acetylene. They were capable of fixing nitrogen, but not at the high specific activity of the other plants grown at lower oxygen levels. The specific activity of these plants corresponded approximately to the post-decline rate of the other treatments.



**Figure 7.11 :** Nitrogenase activity and nodulated root respiration, measured by continuous flow, of plants grown at 4.7 kPa  $\text{O}_2$  (a), 19 kPa  $\text{O}_2$  (b), 47 kPa  $\text{O}_2$  (c) and 75 kPa  $\text{O}_2$  (d). Data are the results from one representative pot of four plants assayed at the oxygen concentration at which they were grown and are expressed on a dry weight basis. Nitrogenase activity ( $\text{---}\blacktriangle\text{---}$ ) is expressed as  $\mu\text{mol C}_2\text{H}_4 \text{ g}^{-1} \text{ nodule DW h}^{-1}$  and root respiration ( $\text{---}$ ) as  $\mu\text{mol CO}_2 \text{ g}^{-1} \text{ root DW h}^{-1}$ .

### 7.3. Discussion

#### *Adaptation to oxygen pressure*

Plants grown at 4.7, 19 and 47 kPa O<sub>2</sub> had similar growth characteristics, and their nodules similar respiration rates, maximum acetylene reduction rates and soluble haem content. This suggests that the oxygen concentration within the infected zone was maintained throughout these treatments, at similar low levels. It also implies a change in the resistance to oxygen diffusion between the exterior and the infected zones of the nodule as external oxygen pressure was varied.

Differences in external appearance of nodules were very dramatic, especially in nodules grown at low oxygen. These nodules had a layer of loosely packed cells around almost the entire nodule and were similar in appearance to nodules grown submerged in solution culture or in water-logged soils (Pankhurst and Sprent 1975b). Lenticels occurred less frequently with increasing oxygen pressure, although a region of loosely packed cells occurred in the outer cortex above vascular bundles in all sections examined, regardless of growth pO<sub>2</sub>.

Studies with oxygen micro-electrodes have shown that the major resistance to oxygen diffusion is located within the inner cortex (Tjepkema and Yocum 1974, Witty *et al.* 1987). In this study, significant differences in the distribution of intercellular spaces in the inner cortex were observed across treatments. The effective number and volume of intercellular spaces were decreased at higher oxygen, because cells were packed closer together and there was an increased deposition of material which occluded some intercellular spaces. In nodules grown at higher oxygen, this pattern appeared to extend into the outer cortex, although zones of loosely packed cells above the vascular bundles did occur. Unoccluded intercellular spaces in the cortex were mostly gas filled (observed in this study by phase contrast microscopy and by Bergersen and Goodchild 1973a) and so changes in the size and numbers of these air-spaces would affect gaseous diffusion within nodules. With the approximate 10<sup>4</sup> difference in the gaseous and aqueous diffusion coefficients of oxygen, the effect of this difference in anatomy on oxygen diffusion would be great. Changes in the number, length or size of these intercellular spaces would effectively change the depth of the water-filled zone and allow oxygen concentration in the critical infected cells to be maintained at levels suitable for efficient nitrogenase activity (Table 7.3).

#### *Gas pressure within nodules*

If there is a water-filled barrier present in the cortex around the entire infected zone, then there will be differences in total gas pressure in the infected zone, in nodules of different oxygen treatments. Oxygen gas pressures within the intercellular spaces in the

infected zone were probably very close to zero under all treatments and yet oxygen pressures around the roots were maintained between 4.7 and 75 kPa, with nitrogen making up the balance to atmospheric pressure (ca. 94 kPa in Canberra). Consideration of different gas diffusion rates (mainly rapid CO<sub>2</sub> diffusion out of the infected region) leads to the conclusion that a greater pressure differential would occur in nodules grown at higher oxygen pressures and a smaller pressure differential in nodules grown at lower oxygen pressure. This prediction of difference in total gas pressure occurs in mathematical models of nodule gas exchange (Sheehy *et al.* 1987; Hunt *et al.* 1988) when it is assumed a water-filled diffusion barrier exists around the infected zone. In tangential sections through the inner cortex (Figure 7.10), it is clear that the boundary layer of cells forms such a water-filled zone. Whether gas connections occur through this zone in some regions (such as under vascular bundles, or at the nodule-root attachment zone) has not been determined. Measurement of total gas pressure within the infected zone would show whether air pathways are continuous between the infected zone and the exterior air or if there is an entire water-filled barrier around the nodule.

#### *Short-term changes in nodule activity*

The changes in distribution of cortical air-spaces observed here demonstrate the long-term adaptation of soybean nodules to different oxygen pressures, but they may also be useful in the investigation of the short-term responses of nodules to gases such as oxygen and acetylene and other treatments presented in Chapters 4 and 6.

The results presented in this chapter clearly show that the morphology of the nodule cortex changes when roots were exposed to increasing external oxygen pressures, yet between 4.7 and 47 kPa pO<sub>2</sub> nodule nitrogenase activity remained sensitive to applied acetylene (Figure 7.11). There are at least three possible explanations for these observations.

(1) The long-term changes in oxygen diffusion pathways, which occur upon adaptation to growth at different external pO<sub>2</sub>, involve a different part of the nodule structure than that which is involved in the short-term changes which occur rapidly upon sudden exposure to acetylene and oxygen. Witty *et al.* (1987) observed changes in the air-spaces on the inside of the inner cortex and infected zone of *Pisum* and *Phaseolus* nodules during short-term adjustment to external pO<sub>2</sub> and concluded that this zone was inside the major resistance to oxygen movement. The region they described as changing, is equivalent to the distributing layer described here. This zone, containing a large volume of intercellular spaces, maintained a similar appearance in all treatments. Similarly, the boundary layer, composed of cells packed together in a regular arrangement forming a water-filled zone encircling the infected zone, was present in nodules from all treatments. Either or both of these layers of cells may be involved in short-term changes of oxygen diffusion, and possible mechanisms of action are examined in Chapter 8.

(2) Both short and long-term changes in gas diffusion may involve the same part of the nodule, but flexibility of the diffusion barrier is maintained despite significant changes in cell morphology and air-space volume during adaptation to  $pO_2$ . If this is the case, then the absence of an acetylene-induced decline in nitrogenase activity in nodules grown at excessively high (75 kPa)  $pO_2$  (Figure 7.11d), is presumably due to the virtual elimination of intercellular spaces in the inner cortex; that is, the diffusion pathways in nodules grown at 75 kPa oxygen were already shut down (thus limiting nitrogenase activity) to such an extent that further restriction was not possible when acetylene was applied.

(3) A third explanation for the results presented here is that the acetylene-induced decline in nitrogenase activity does not directly involve changes in gas diffusion pathways; for example, metabolic changes such as a change in the nature of carbon substrate supplied to the bacteroid, upon exposure to acetylene, could lead to a decrease in nitrogenase activity and change the oxygen requirements of infected cell metabolism. Such changes have been observed with isolated bacteroids metabolizing different substrates (Bergersen and Turner 1989). These discoveries may have implications for the understanding of whole nodule physiology, which at present, are not recognised.

### *Conclusion*

The results presented here support the hypothesis that oxygen diffusion into soybean nodules is restricted by a water-filled zone occurring in the inner cortex and surrounding the infected zone, although the infrequent occurrence of gas connections across this zone cannot be entirely ruled out. Soybean nodules showed the ability to adapt to oxygen pressures above and below ambient levels and this adaptation involved a decrease in cortical intercellular air-spaces with increasing oxygen pressure. This decrease in number and size of intercellular spaces was the result of a change in cell structure and the deposition of an electron dense material within intercellular spaces. Nodules developed in oxygen pressures from 4.7 to 47 kPa showed a similar inhibition by saturating acetylene, suggesting that putative acetylene-induced changes in oxygen diffusion resistance occur by a different mechanism than that involved in long-term adaptation to oxygen.



## Chapter 8

### General Discussion

Approximately 21,000 Pa oxygen is present in air and this is reduced to a solution equivalent pressure of 1 Pa (10 nM) within soybean nodules by active respiration of tissue and the presence of a barrier to gas diffusion. A balance between oxygen diffusion and oxygen use is maintained and the oxygen sensitive enzyme, nitrogenase, functions efficiently within nodules. This balance must be flexible; nitrogenase activity is regulated as nodules grow and environmental conditions change. Adaptation is required. Plants show many responses which are short-term or long-term adaptations to environmental conditions. Some of these adaptations are involved in the regulation of nitrogen fixation.

#### 8.1. The Acetylene-Induced Decline and Nodule Adaptation to Oxygen

Many nitrogen fixing organisms and symbioses show the ability to adapt to different oxygen pressures. Free living *Frankia* produce vesicles which are almost certainly the site of nitrogen fixation (Murry *et al.* 1984). The wall thickness of these vesicles is observed to increase dramatically when *Frankia* is grown at high oxygen pressures (Parsons *et al.* 1987), and it is proposed that the thick wall produced provides an increased diffusion resistance to oxygen (Parsons *et al.* 1987). A similar adaptation is observed in the *Frankia* within *Alnus* root nodules when they are exposed to different oxygen pressures (Silvester *et al.* 1988a). In addition to increases in the apparent thickness of the *Frankia* vesicle wall in response to increased oxygen, a decrease in the size and distribution of air-spaces within the nodule was observed (Silvester *et al.* 1988a). Adaptation of *Myrica* nodules to different oxygen pressures seems to involve an alteration of the nodule-root surface area and the distribution of air-spaces within the nodule (Silvester *et al.* 1988b). These changes in the distribution of air-spaces in the infected zone observed in *Alnus* and *Myrica*, contrast with the results presented here (Chapter 7). In soybean nodules the distribution of air-spaces in the infected zone did not change significantly with oxygen pressure. Rather, adaptation of soybean to different oxygen pressures appears to involve changes in the air-spaces within the cortex. This observation supports the conclusion that the major resistance to oxygen diffusion in soybean nodules occurs in the cortex (Tjepkema and Yocum 1974, Witty *et al.* 1987). These differences in morphological adaptation are of interest when considering the occurrence of the acetylene-induced decline.

Declines in response to acetylene have been reported for *Alnus*, *Casuarina*, *Ceanothus*, *Datisca* and *Myrica* (Tjepkema *et al.* 1988, Silvester *et al.* 1988a,b), although these declines occur rapidly and there is generally a recovery in nitrogenase activity within 20 minutes, to levels generally only slightly lower than pre-decline rates (Tjepkema *et al.* 1988). The cause of these declines in activity is not considered to involve an increase in the diffusion resistance of nodules to oxygen (Tjepkema *et al.* 1988). The initial rapid decline in actinorhizal plants is not accompanied by a large change in respiration (Tjepkema *et al.* 1988), and resistance of the *Frankia* vesicle, which probably forms the major diffusion resistance to oxygen in *Alnus* nodules (Silvester *et al.* 1988a), is unlikely to alter rapidly in response to acetylene.

Actinorhizal plants have the ability to adapt to long-term changes in oxygen, but they show little short-term adaptation to oxygen. Exposure of *Alnus* and *Myrica* nodules to oxygen pressures significantly above or below growth pressures caused declines in activity (Silvester *et al.* 1988a,b). In comparison, soybean nodules in this study were able to adapt rapidly to changes in external oxygen concentration. Both this apparent short-term adaptation to oxygen and the declines in activity observed after exposure to acetylene or phloem girdling, seem to involve a mechanism that is present in legumes, but not in actinorhizal plants.

## 8.2. Oxygen Diffusion Within the Nodule

An understanding of soybean nodule gas exchange can be obtained by relating aspects of nodule structure and physiology to the physical laws of gas diffusion. Of particular interest is the diffusion of oxygen into nodules and this can be modelled in a relatively simple manner.

A single nodule with a radius of 1.5 mm will be considered. External gas pressures of 101.3 kPa and solubility values and diffusion coefficients at 27°C are used. It is assumed that the central infected zone (radius 1.265 mm) contains 60 % of the nodule volume (Bergersen 1982) and the inner cortex and outer cortex together contain 40 % of the total volume (radius 0.235 mm). The central zone is assumed to contain 4 % (v/v) air-spaces which are interconnecting (this study Chapter 7, Bergersen and Goodchild 1973a). The outer zone is assumed to contain 5 % interconnecting air-spaces. In both these regions the air-spaces are accepted as being predominantly radially orientated. Thus the mean area for diffusion in a radial direction (towards the centre of the nodule) is taken as 3 % of the spherical surface area (2 % orientated tangentially).

### *Oxygen uptake within the nodule*

Measured values of respiration rates of nodule tissue can be obtained from the literature (converted to SI units and g<sup>-1</sup> nodule DW and assuming an RQ of 1);  $1.24 \times 10^{-7}$  mol O<sub>2</sub>

$\text{g}^{-1}$  nodule DW  $\text{s}^{-1}$  (Weisz and Sinclair 1987a),  $2.2 \times 10^{-7}$  (Vessey *et al.* 1988b),  $0.98 \times 10^{-7}$  (Sinclair and Goudriaan 1981) and  $1.67 \times 10^{-7}$  (Davis *et al.* 1987).

Assuming a value of  $1.6 \times 10^{-7}$  mol  $\text{O}_2$   $\text{g}^{-1}$  nodule DW  $\text{s}^{-1}$ , this corresponds to a whole nodule respiration rate of  $0.032$  mol  $\text{m}^{-3}$   $\text{s}^{-1}$ , given a FW:DW ratio of 5:1 and a nodule density of 1.0. Further, it is assumed for this analysis that 90 % of the respiration of a nodule occurs in the central zone (site of nitrogen fixation and ammonia assimilation) which occupies 60 % of the nodule volume; thus the oxygen consumption of this zone would be  $0.048$  mol  $\text{m}^{-3}$   $\text{s}^{-1}$ .

#### *Oxygen diffusion within the infected zone*

The free solution oxygen concentration in the infected cells of the central infected zone is of the order of 10 nM (Bergersen 1982). This is a concentration of  $1.0 \times 10^{-5}$  mol  $\text{m}^{-3}$ , which in equilibrium represents a gas phase concentration of  $3.7 \times 10^{-4}$  mol  $\text{m}^{-3}$  (1 Pa). The actual gas phase concentration of this region must be above this value to provide a gradient for diffusion into the rapidly respiring infected cells. Sheehy and Bergersen (1986) have described a model of gas diffusion within the infected cell which demonstrates the importance of leghaemoglobin to facilitate diffusion within the cell. Furthermore, they predicted that a gradient of free dissolved oxygen will be present across the infected cell, with the concentration at the inside layer of peribacteroid units being approximately 75 to 80 % of the concentration at the outside layer.

This analysis can be continued for the infected region as a whole. It is assumed the centre of a nodule of 1.5 mm diameter has an oxygen gas phase concentration of 1 Pa, oxygen consumption throughout the infected zone (1.265 mm radius) is constant ( $0.048$  mol  $\text{m}^{-3}$ ), and the infected zone contains 3 % air-space area in a radial direction, through which all diffusion occurs. The equation of Crank (1975) can be used to determine the concentration gradient required to maintain a pressure of 1 Pa  $\text{O}_2$  in the centre of the nodule.

$$Q = 4 \pi D t \frac{a b}{b-a} (C_2 - C_1) \quad \text{or} \quad (C_2 - C_1) = \frac{Q (b-a)}{4 \pi D t a b}$$

Where  $C_2 - C_1$  is the concentration gradient required for diffusion of flux ( $Q/t$ ), with a diffusion coefficient  $D$ , across a spherical shell with external radius  $b$  and internal radius  $a$ .

This equation assumes no consumption in the layer  $b-a$ . To circumvent this, an iterative program was written to sequentially calculate the concentration gradient required to drive diffusion across  $0.1 \mu\text{m}$  steps with a sequential adjustment of total respiration (Appendix IIIa). The gradient required across the entire infected zone is the sum of the gradients at each step.

According to this model, a gradient of 59 Pa across the infected zone would be required to maintain rapid enough diffusion. While this gradient is small when compared to the gradient of 59 Pa to 21000 Pa in the atmosphere, it represents a significant gradient across the infected zone. Sinclair and Goudriaan (1981) predicted that respiration and air-space resistance within the infected zone would cause a concentration difference of approximately 40 Pa, while other models of diffusion within nodules have ignored this gradient (Sheehy *et al.* 1985, 1987, Hunt *et al.* 1988). However, the assumption of uniform respiration, used in the analysis above, is not necessarily warranted. In soybean a concentration of infected cells towards the outside of nodules is observed (Chapter 7, Bergersen and Goodchild 1973a, Bergersen 1982) and this will cause a decrease in the gradient of oxygen required. Nevertheless, infected cells at the centre of a nodule will be exposed to a lower concentration of oxygen than those cells on the periphery of the infected zone. In the context of gradients of oxygen occurring throughout the infected zone as calculated here, and across the infected cell (Sheehy and Bergersen 1986), it is interesting to observe that the rates and efficiency of nitrogen fixation and respiration of isolated bacteroids is different at different oxygen concentrations (Bergersen and Turner 1989).

#### *Oxygen diffusion within the cortex*

Nodule respiration and the resistances to oxygen diffusion within the infected cells and the infected zone, discussed above, are insufficient to protect nitrogenase from the oxygen concentration present in air. Modelling studies (Sinclair and Goudriaan 1981, Sheehy *et al.* 1985, 1987, Hunt *et al.* 1988) predict that a resistance to oxygen diffusion must reside in the cortex and this is supported by experimental investigations (Tjepkema and Yocum 1974, Tjepkema 1979, Witty *et al.* 1987). To maintain a concentration gradient of the order of 21000 Pa, this resistance must be large and probably occurs as an entirely water-filled zone surrounding the infected zone (Chapter 7, Witty *et al.* 1986, Hunt *et al.* 1988).

The mean depth of water required in the cortex to restrict diffusion to calculated fluxes across a gradient of 21000 to 60 Pa, can be estimated by a similar procedure to that outlined above, except that in this case it is assumed there is no consumption in the zone *b-a* (Appendix IIIb). A diffusion coefficient of  $2.5 \times 10^{-9} \text{ m}^2 \text{ s}^{-1}$  for oxygen in nodule solution (Davis *et al.* 1987) was assumed and a model nodule size of 1.5 mm radius with an infected volume of 60 %, radius 1.265 mm was used. The concentration difference required for diffusion of oxygen through the air-spaces of the outer cortex (3 % in the radial direction) was calculated to be less than 20 Pa. The mean depth of the water-filled zone required to maintain a gradient of 20920 Pa must therefore be 29.4  $\mu\text{m}$ , according to this model.

This approach can be used to predict the mean depth of the water-filled zone required

by nodules grown in different oxygen tensions, such as in the experiments presented in Chapter 7. For nodules of 1.5 mm radius (the approximate size of nodules at 30 days, see Figure 7.3) this model calculates that a water-filled depth of 7  $\mu\text{m}$  is required at 4.7 kPa external  $\text{O}_2$ , 28  $\mu\text{m}$  at 19 kPa, 74  $\mu\text{m}$  at 47 kPa and 122  $\mu\text{m}$  at 75 kPa external  $\text{O}_2$ . This analysis only predicts the mean water-filled depth and it is clear from Figures 7.4 and 7.5 that the cortex is heterogeneous. Intercellular spaces are observed at cell junctions almost throughout the nodule cortex. However, the differences in frequency of intercellular spaces observed in the cortex of sections from nodules grown at different oxygen pressures (see Table 7.1, page 103, Figures 7.4, 7.5), provide support for the model.

Because an increased resistance is required at higher oxygen pressures, the minimum functional size for nodules will be larger. Indeed, the slower growth and development of plants grown at 75 kPa oxygen can be partially explained by the requirement of a larger water-filled space at high oxygen pressures. Using the method of Sheehy and Thornley (1988), a minimum nodule radius for a nodule developing in 75 kPa of 1.04 mm can be calculated from their data, or 0.97 mm using the data of the model above. This compares with the predicted minimum functional size of a nodule developed in air of 0.55 mm (their data) or 0.52 mm (data above). The predicted minimum nodule volume at 75 kPa is approximately seven times larger than that for nodules developed in air. Because of this effect, the initiation of nitrogen fixation within nodules on plants grown at higher oxygen concentrations is probably retarded by several days, extending the nitrogen starvation phase and slowing growth (Chapter 3).

Assuming that oxygen diffusion underlies short-term responses of nodule respiration to various treatments, the model analysis can be used to predict the increase in resistance that is required to cause a decrease in respiration and nitrogenase activity similar to that observed after acetylene or other inhibitors are introduced (Chapter 6). For the respiration rate to decrease by one-half within the central zone, the model predicts that the effective water-filled distance must have increased from 29.4 to 60  $\mu\text{m}$ . Further, to cause acetylene-induced declines, these changes in water depth must occur within minutes (Figure 4.2) and therefore probably involve changes in cell turgor. In this context a discussion of the relative rates of metabolism of critical processes within nodules may be useful.

### 8.3. Rates of Metabolism in Nodules

#### *Oxygen consumption*

A mean oxygen consumption of  $0.032 \text{ mol O}_2 \text{ m}^{-3} \text{ s}^{-1}$  was estimated earlier (see page 117) for the whole nodule, or  $0.048 \text{ mol O}_2 \text{ m}^{-3} \text{ s}^{-1}$  for the infected zone, assuming an infected zone volume of 60 %.

Leghaemoglobin occurs at a concentration of approximately 4 mM (Bergersen 1982), in the cytosol of the infected cells. The cytosol makes up approximately 14 % of the infected cell volume (Bergersen 1982), and the infected cells themselves are 77 % of the volume of the central infected zone (Bergersen 1982). This represents an "average" concentration of 425  $\mu\text{M}$  or  $0.425 \text{ mol m}^{-3}$  in the infected zone. (Compared with whole nodule values of 280  $\mu\text{M}$  soluble haem determined in Chapter 7, Table 7.3.) At 30 % oxygenation (Appleby (1969) estimates 20 %, while King *et al.* (1988) estimate 36 %), this gives an equivalent oxygen solution concentration of  $0.127 \text{ mol O}_2 \text{ m}^{-3}$ . An average free soluble oxygen in the infected and uninfected cells of 20 nM is estimated (Bergersen (1982) estimates 10 nM in infected cells). Therefore the water occupying 96 % of the volume of the infected zone contains a free  $\text{O}_2$  concentration of  $1.9 \times 10^{-5} \text{ mol O}_2 \text{ m}^{-3}$ . The 4 % air-spaces of the infected zone, at  $2.4 \times 10^{-2} \text{ mol O}_2 \text{ m}^{-3}$  (60 Pa maximum), contain a total of  $9.7 \times 10^{-4} \text{ mol O}_2 \text{ m}^{-3}$ . The total concentration of oxygen in the inner cortex is therefore  $0.128 \text{ mol O}_2 \text{ m}^{-3}$ .

In the outer cortex, 5 % air-spaces saturated with air contain approximately  $0.425 \text{ mol O}_2 \text{ m}^{-3}$  and the soluble oxygen fraction equilibrated with this pressure contains  $0.220 \text{ mol O}_2 \text{ m}^{-3}$ . The oxygen concentration in the outer cortex is  $0.64 \text{ mol O}_2 \text{ m}^{-3}$ , and that in the whole nodule is  $0.33 \text{ mol O}_2 \text{ m}^{-3}$ .

At the respiration rates used in the model above, the total amount of oxygen contained within the infected zone would be respired in 2.7 seconds and the oxygen contained within a whole nodule in 10.5 seconds.

#### *Ureide metabolism*

Ureides and a small portion of amides are exported from nodules at a rate approximately equal to the rate of nitrogen fixation. Nitrogenase activity in this study approximated  $200 \mu\text{mol C}_2\text{H}_4 \text{ g}^{-1} \text{ nodule DW h}^{-1}$ , which converts, to  $47 \mu\text{mol N}_2 \text{ g}^{-1} \text{ nodule DW h}^{-1}$  or  $5.2 \times 10^{-3} \text{ mol N m}^{-3} \text{ s}^{-1}$ , assuming an electron allocation coefficient of 0.7, a dry weight to fresh weight ratio of 5:1 and a nodule density of  $1 \text{ g cm}^{-3}$ . This is equivalent to  $1.3 \times 10^{-3} \text{ mol ureides m}^{-3} \text{ s}^{-1}$ .

Nodules contain approximately 6 to 12  $\mu\text{mol ureides g}^{-1} \text{ FW}$ , (Walsh *et al.* 1989a) or 6 to 12  $\text{mol ureides m}^{-3}$ . This is equivalent to the amount of  $\text{N}_2$  fixed in 77 to 154 minutes.

#### *Sucrose metabolism*

Sucrose is the carbon compound supplied to nodules (Kouchi *et al.* 1985), and is also the soluble carbohydrate at the highest concentration in nodules (Streeter 1980), being present at approximately  $3 \text{ mg g}^{-1} \text{ nodule FW}$ . This concentration of sucrose ( $3 \text{ kg m}^{-3}$ ) contains  $105 \text{ mol C m}^{-3}$ . At the respiration and ureide production rates calculated

above, and assuming an RQ of 1 for respiration, this represents 47 minutes<sup>1</sup> of potential carbon use within the nodule. At the rates of respiration and ureide production used in these calculations, nodules would respire a quantity of carbon equivalent to their total carbon content (40 % of the dry weight) in 50 hours. Nodules must therefore import sucrose at approximately  $3.1 \times 10^{-3}$  mol sucrose  $m^{-3} s^{-1}$ , a rate approximately twice the rate of ureide export (see above).

If these estimates of oxygen turnover and flux into nodules are correct, and similar rates to these occur in *Pisum* and *Phaseolus* nodules, then explanations for observed changes in internal oxygen concentrations when external oxygen is increased (Witty *et al.* 1987) need to be re-evaluated. After an increase in external oxygen, internal oxygen concentration would be expected to increase in seconds; it does not (Witty *et al.* 1987), implying that the increased oxygen flux is utilized by nodule metabolism. The observed increase in internal oxygen that occurs after one to two minutes probably represents a subsequent inability of nodule metabolism to use all the increased oxygen flux. Following this, it appears a change in nodule resistance occurs.

The data used in these calculations have been obtained from a number of sources and therefore the results are only approximate. However, this analysis does show that the metabolism of nodules is rapid and provides some indication of the relative flux of metabolites within nodules. The rate of oxygen turnover on a whole nodule scale is approximately 270 times faster than sucrose turnover and 600 times faster than ureide turnover. Any alteration in the resistance of nodules to oxygen diffusion will therefore have an almost instantaneous effect on nodule physiology. Inhibition of sucrose supply or ureide production will begin to have a significant effect on nodule physiology within minutes.

#### 8.4. Possible Metabolic Control of Nodule Activity

Many treatments cause a decrease in the activity of legume root nodules in a manner that is best explained by an increase in the diffusion resistance of the nodule cortex to oxygen. The experimental results presented in this thesis provide more evidence that nitrogenase activity may be regulated by oxygen supply. Nodule physiology appears to be very finely balanced, so that any changes in carbon supply, nitrogen fixation rate, or external gas concentrations can cause an increase in the apparent diffusion resistance of the cortex to oxygen and therefore cause a decrease in nitrogen fixation. Any significant reduction of oxygen consumption within the infected zone also requires an increase in the resistance of the nodule to oxygen, in order to protect nitrogenase from oxygen damage.

---

<sup>1</sup> $105 / (1.3 \times 10^{-3} \times 4 + 0.032) = 2820 \text{ s} = 47 \text{ minutes}$

Nonetheless, it is possible to explain the observed declines in nitrogenase activity without invoking an increase in the resistance of nodules to oxygen. After exposure to stress, consumption of oxygen within nodules may remain the same, even though nitrogenase activity and CO<sub>2</sub> efflux may decline.

In the absence of ammonia production (for example, when acetylene is present) or after phloem girdling treatments, carbon supply to the bacteroids may be reduced. Isolated bacteroids, maintained in a continuous flow system at low oxygen concentration, show a dramatic decrease in RQ when malate supply is reduced (Bergersen and Turner 1989). As malate is diluted from the medium, bacteroids continue to respire oxygen at the same rate, but produce only one-half as much carbon dioxide. Most whole plant investigations (including those described in this thesis) measure CO<sub>2</sub> efflux only and may therefore observe a decline in CO<sub>2</sub> production by nodules when in fact there may have been little change in oxygen consumption. In this case, reducing power in the bacteroids may be directed more towards oxygen and away from nitrogen (or acetylene). Likewise, different carbon substrates in bacteroids may support very different N<sub>2</sub> fixation/O<sub>2</sub> consumption ratios (Bergersen and Turner 1989).

However, "declined" nodules show a recovery of respiratory and nitrogenase activities in response to hyperbaric oxygen, a response which is generally not observed in control plants. This "recovery" in stressed nodules could also be due to a change in their carbon metabolism and the presence of extra oxygen inducing respiratory protection pathways in the bacteroids (Bergersen and Turner 1975). Why control plants do not show an increase in activity under high oxygen is, however, unexplained under this hypothesis. Further, in intact clover nodules assayed in a sealed container, no change in nodule RQ was observed when oxygen concentration was increased (Davey and Simpson 1989). These experiments should be repeated with soybean and with plants before and after exposure to stress (such as acetylene).

Conversely, if there is a mechanism in root nodules whereby the diffusion barrier within the nodule cortex changes in response to the central infected zone oxygen concentration, then the metabolism within the infected zone may regulate nodule activity. Increased respiration could lower internal oxygen causing a decrease in the resistance of the nodule cortex to oxygen, while decreased respiration could cause an increase in the oxygen concentration and a subsequent increase in the diffusion resistance of the nodule cortex. In this way bacteroid respiration could regulate nodule activity. Since respiration and nitrogen fixation rates of isolated bacteroids have been shown recently to change in response to external carbon supply (Bergersen and Turner 1989), changes in the rate of sucrose import to the nodule and consequently carbon supply to the bacteroids (such as occur upon phloem girdling), may induce changes in cortical oxygen diffusion. The observed decline in nodule activity (Figure 5.8) begins 20 to 30 minutes after girdling and is consistent with the time scale of sucrose utilization calculated above.



Carbon supplied to bacteroids may also be restricted when nitrogen fixation is inhibited. Under the mechanism proposed by Kahn *et al.* (1985), viewed in its widest sense, carbon is made available to the bacteroids by the plant only in exchange for fixed nitrogen. With this type of mechanism, inhibition of nitrogen fixation and assimilation, by acetylene, argon/oxygen or MSO, may lead to a reduction in carbon supply to bacteroids. Again, the time scale of the observed acetylene-induced declines are consistent with inhibition by such a mechanism. In my experiments, inhibition of acetylene reduction began approximately 10 minutes after exposure to saturating acetylene. This lag may represent the time required for depletion of nodule ammonium pools by ureide metabolism, and depletion of carbon pools by bacteroid metabolism.

Even if nodule metabolism is regulated by changes in bacteroid respiration rates, it is still essential that a variable diffusion barrier, which alters in response to oxygen concentration, is present in the cortex, in order to protect nitrogenase from excess oxygen.

### 8.5. Alteration of the Diffusion Resistance of Nodules

Whether the resistance to the diffusion of oxygen through the cortex alters in response to changes in oxygen concentration, or is regulated by other factors, a mechanism allowing alteration of this resistance is required. This change in diffusion resistance is considered to be caused by changes in the number or distribution of air-spaces in the inner cortex (Witty *et al.* 1986, 1987), although exactly how this may occur is unknown.

Intercellular spaces within the inner cortex of soybean nodules appear to be surrounded by relatively thick walls, and some are occluded with a densely staining material (Figure 7.9). The expansion or contraction of cells in the inner cortex, in response to osmotic changes, is probably not sufficient to cause the complete collapse of these spaces. In the sections examined in this study, by light and transmission electron microscopy, numerous intercellular spaces were examined and only two spaces were observed which were completely collapsed. However, deformation of whole cells in the inner cortex was seen in many sections (see *Boundary layer* below). The deposition of the densely staining material, which blocks many of these spaces (Figures 7.7, 7.9), is unlikely to occur at rates which could account for observed declines.

Water movement between the symplast and the apoplast may fill these inner cortex air-spaces. Changes in the osmotic potential of cells in the inner cortex will occur when carbon supply is limited or nitrogen fixation is decreased. Sucrose, supplied via the phloem in the cortex is probably largely broken down within the cortex (Kouchi *et al.* 1988, Copeland *et al.* 1989b) and is probably utilized as triose phosphates or organic acids within the infected zone. Thus, concentrations of sucrose and glycolytic intermediates will be highest in the cortex. Ureides, on the other hand, are produced in

the infected zone and transported in the xylem. Ureide concentration will therefore be higher in the infected zone. Stopping either sucrose supply or ureide production may upset the osmotic balance between the cortical cells and the cells of the infected zone. From the rates of sucrose utilization and ureide production calculated above, significant changes in the concentration of these compounds within cells would be expected within 5 to 10 minutes of the restriction of supply. It is unlikely that the very rapid changes in the resistance to oxygen diffusion (in the order of two minutes), observed in response to some treatments (Witty *et al.* 1986, 1987, King *et al.* 1988) could be accounted for by this mechanism.

### *Boundary layer*

In soybean nodules examined in this study, a distinct layer of cells was observed on the inside of the inner cortex (Figure 8.1). These cells could be involved in changes of the resistance to oxygen diffusion in nodules, since they form a layer which surrounds the entire infected zone. These cells form a regular layer, generally one, sometimes two cells thick, just external to the distributing zone in the inner cortex. It is composed of flattened cells, packed with a brick-like structure and for the purpose of this discussion will be referred to as the boundary layer (see Figures 7.2, 7.4, 7.5). This layer has been observed in lupin and pea (Dixon *et al.* 1981) and cowpea (Sen *et al.* 1986). It is clearly visible in the montage of a soybean nodule section presented by Newcomb *et al.* (1979).

Walls between cells in this layer are radially orientated and relatively thin (Figures 8.1c, 8.2, 8.3). Intercellular spaces occur on either side, but no space has been observed traversing this layer. Radial cell junctions in this layer are tightly packed and when examined in tangential sections, intercellular spaces between cells are not observed (Figure 7.10). This layer of cells is visible in both transverse and longitudinal sections of nodules, indicating it surrounds the entire nodule. This layer passes between the vascular bundles and the infected zone and is visible in the micrographs of nodule sections presented in Figures 1.2, 7.4 and 7.5. The radial walls in this boundary layer are generally 10 to 20  $\mu\text{m}$  long and appear to be easily distorted. In some resin-mounted sections these walls are often convoluted, effectively shortening the height of these cells and decreasing their volume (Figures 8.1b, 8.3). In other sections, these walls are relatively straight and cells of this layer have a large volume (Figures 8.1a, 8.2). This distortion may be an artifact of embedding. However, other thin-walled cells present in the sections, such as bacteroid containing cells and lenticel cells, are not distorted. Resin-embedded sections were prepared from nodule slices less than 1 mm thick, fixed in 2.5 % glutaraldehyde, and dehydrated through an ethanol series. This boundary layer of cells has also been observed in fresh hand cut sections from soybean nodules grown in sand and distortion of radial walls was observed in some of these sections (results not shown).

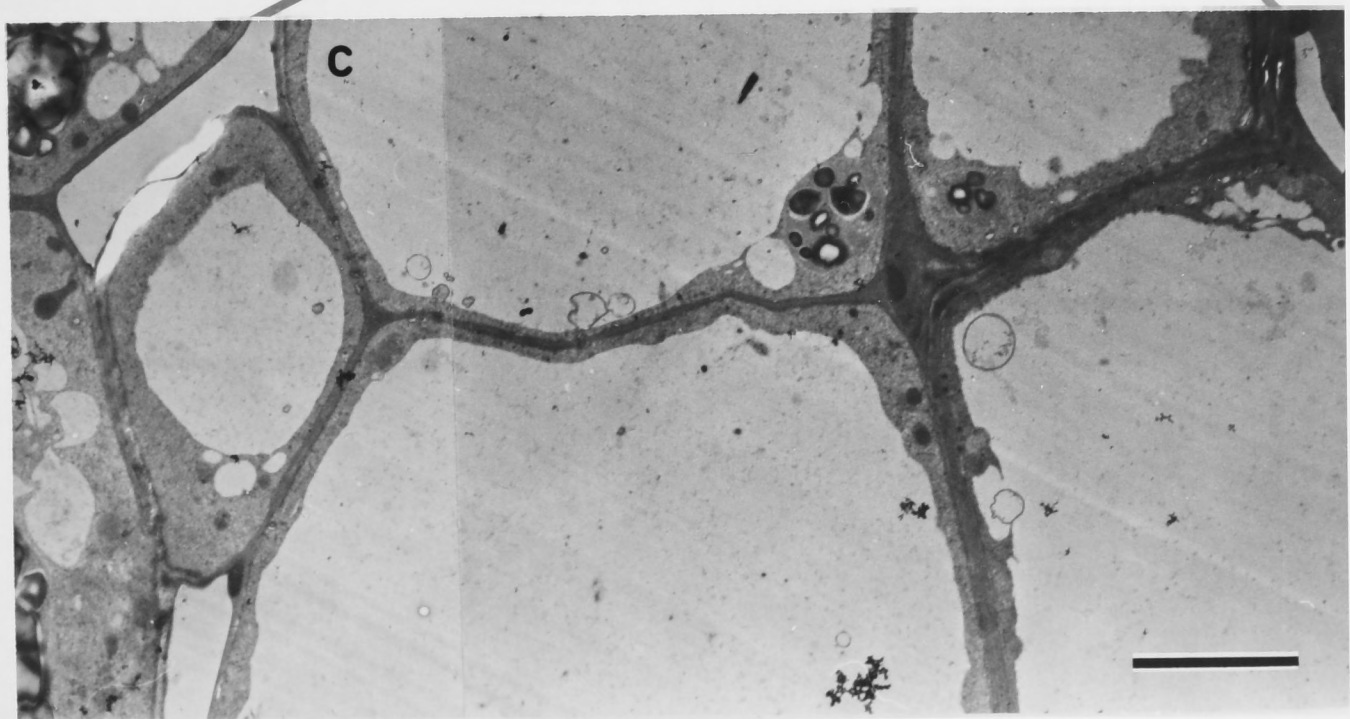
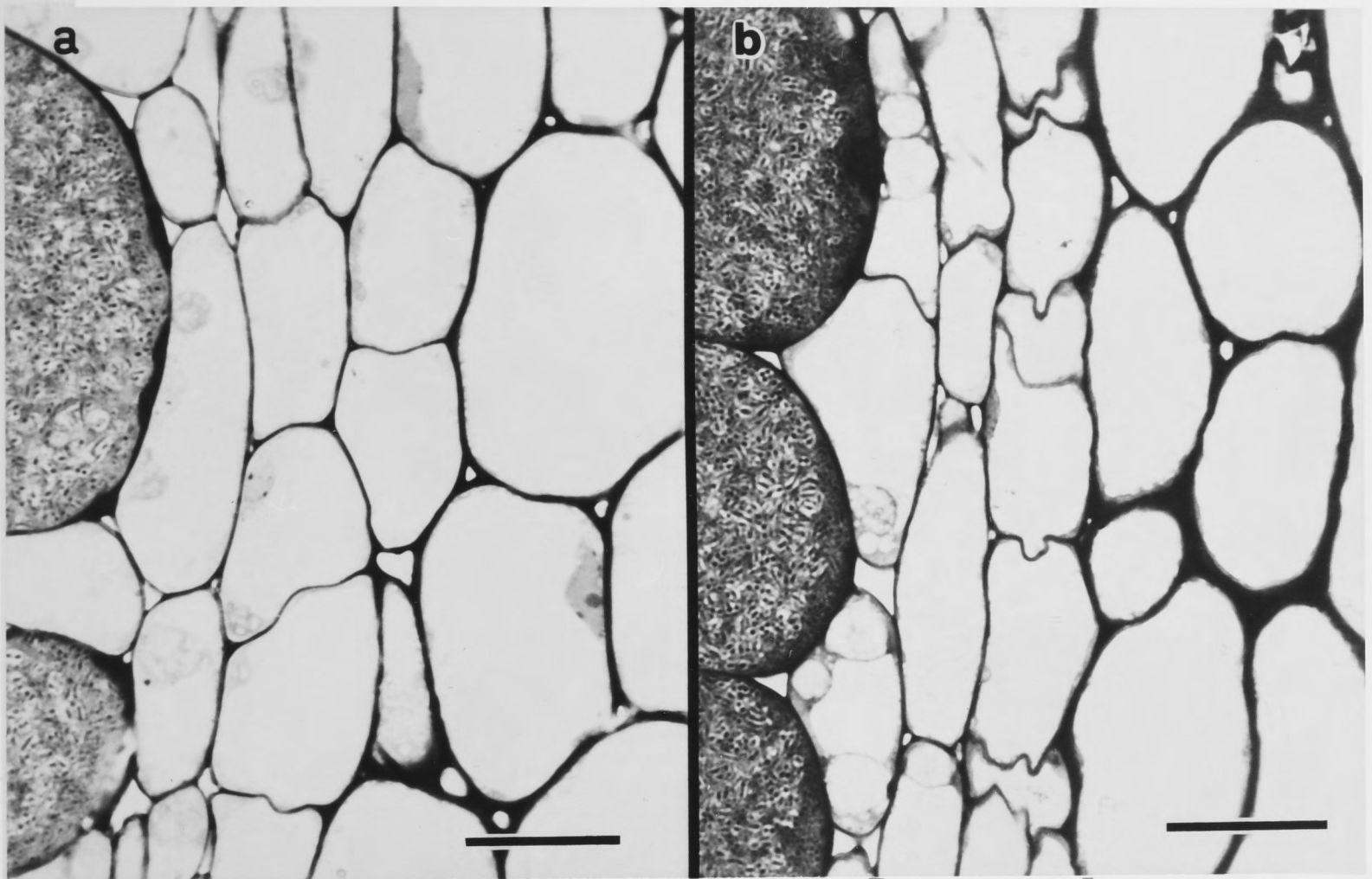
**Figure 8.1** : Boundary cell layer on the inside of the inner cortex.

(a) Section showing turgid boundary layer cells from a nodule grown at 47 kPa oxygen pressure from a plant aged 30 days, inoculated at day 5. Bar represents 20  $\mu\text{m}$ .

(b) Section showing collapsed boundary layer cells from a nodule grown at 47 kPa oxygen pressure from a plant aged 30 days, inoculated at day 5. Bar represents 20  $\mu\text{m}$ .

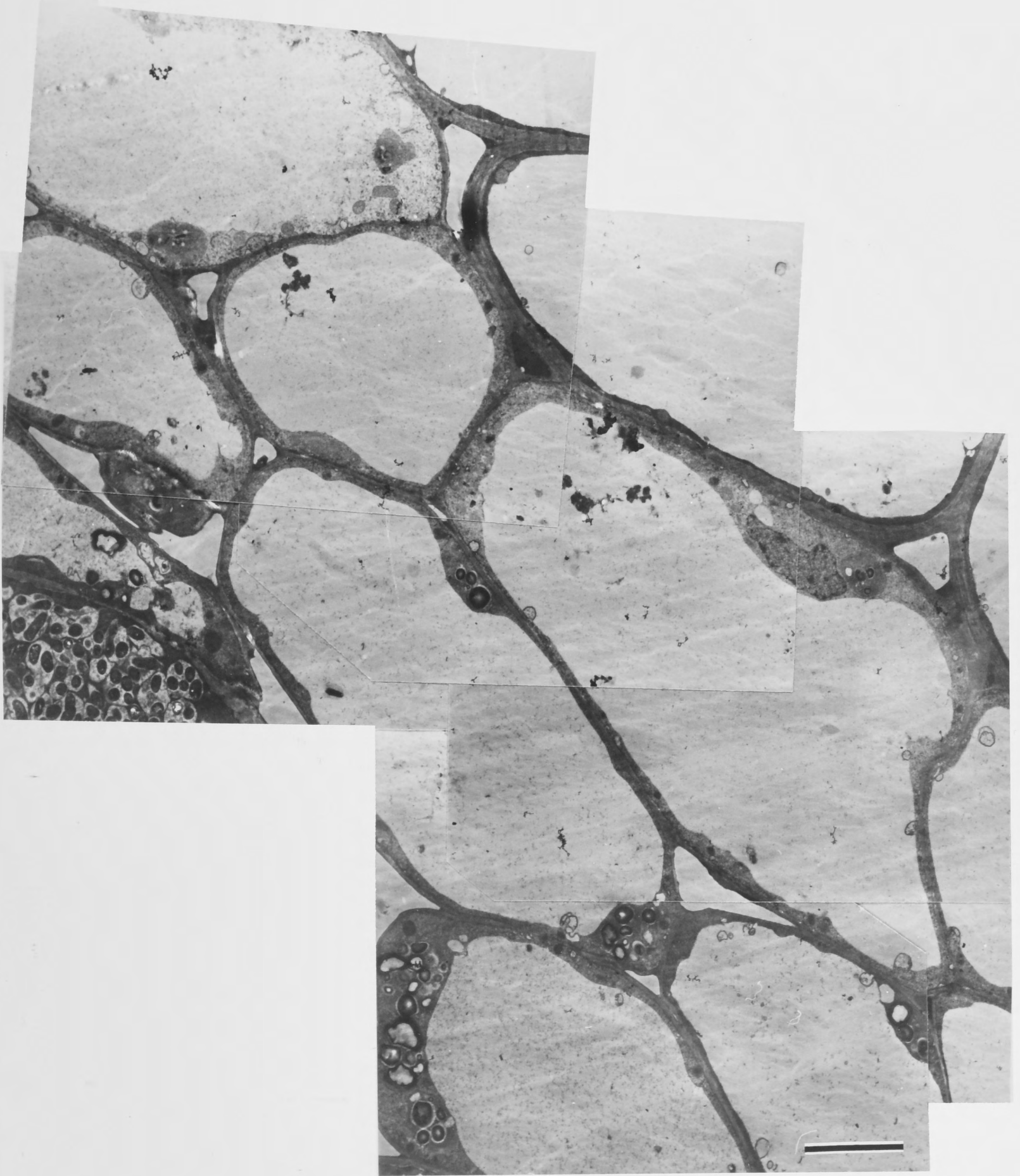
(c) Transmission electron micrograph of thin cell wall present between cells in the boundary layer, of a nodule developed in 19 kPa oxygen. The plant was aged 30 days, inoculated at day 5. Infected zone (not visible) is to the left and the scleroid layer is to the right (not visible). Bar represents 5  $\mu\text{m}$ .

8.1



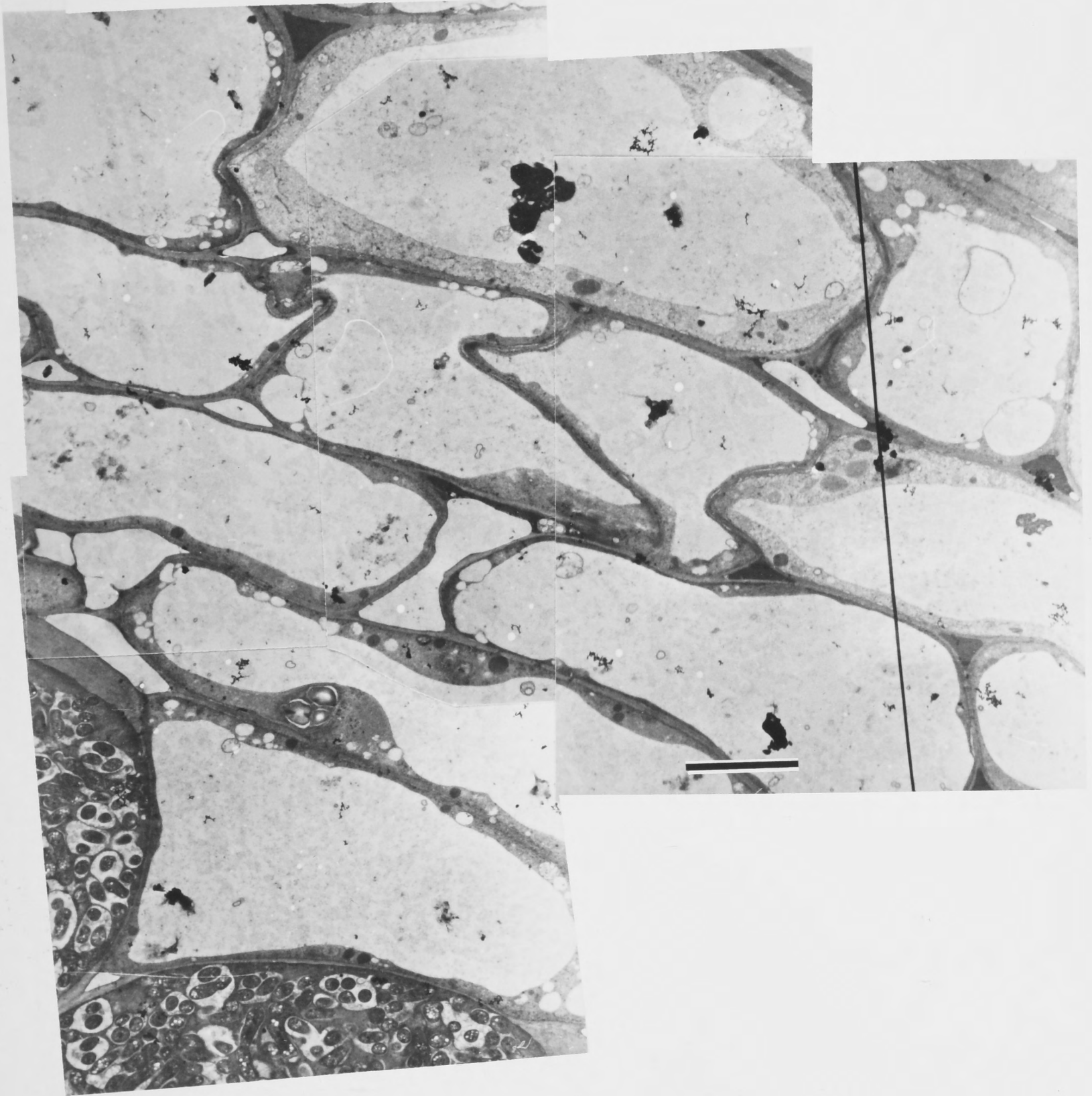
**Figure 8.2 :** Montage of transmission electron micrographs of the inner zone of the inner cortex. The section shows turgid boundary layer cells of a nodule developed in 19 kPa oxygen, The plant was aged 30 days, inoculated at day 5. Infected zone is to the lower left and scleroid layer (not visible) is to the upper right. Bar represents 5  $\mu\text{m}$ .

8.2



**Figure 8.3 :** Montage of transmission electron micrographs of the inner zone of the inner cortex. The section shows collapsed boundary layer cells of a nodule developed in 4.7 kPa oxygen, from a plant aged 30 days, inoculated at day 5. Infected zone is to the lower left and scleroid layer (not visible) is to the upper right. Bar represents 5  $\mu\text{m}$ .

8.3





The thin radial walls in this layer of cells which appears to form a continuous water-filled zone around the nodule may be an important feature. If this layer formed a significant part of the fixed resistance of the nodule cortex to oxygen diffusion, then an advantage in having thick-walled, inflexible cells, such as those observed in the outer part of the inner cortex and the scleroid layer would be expected. Thin walls suggest that either the shape of these cells is maintained permanently by hydrostatic pressure, or that these cells are extensible.

Changes in the shape of these cells may alter diffusion in two ways.

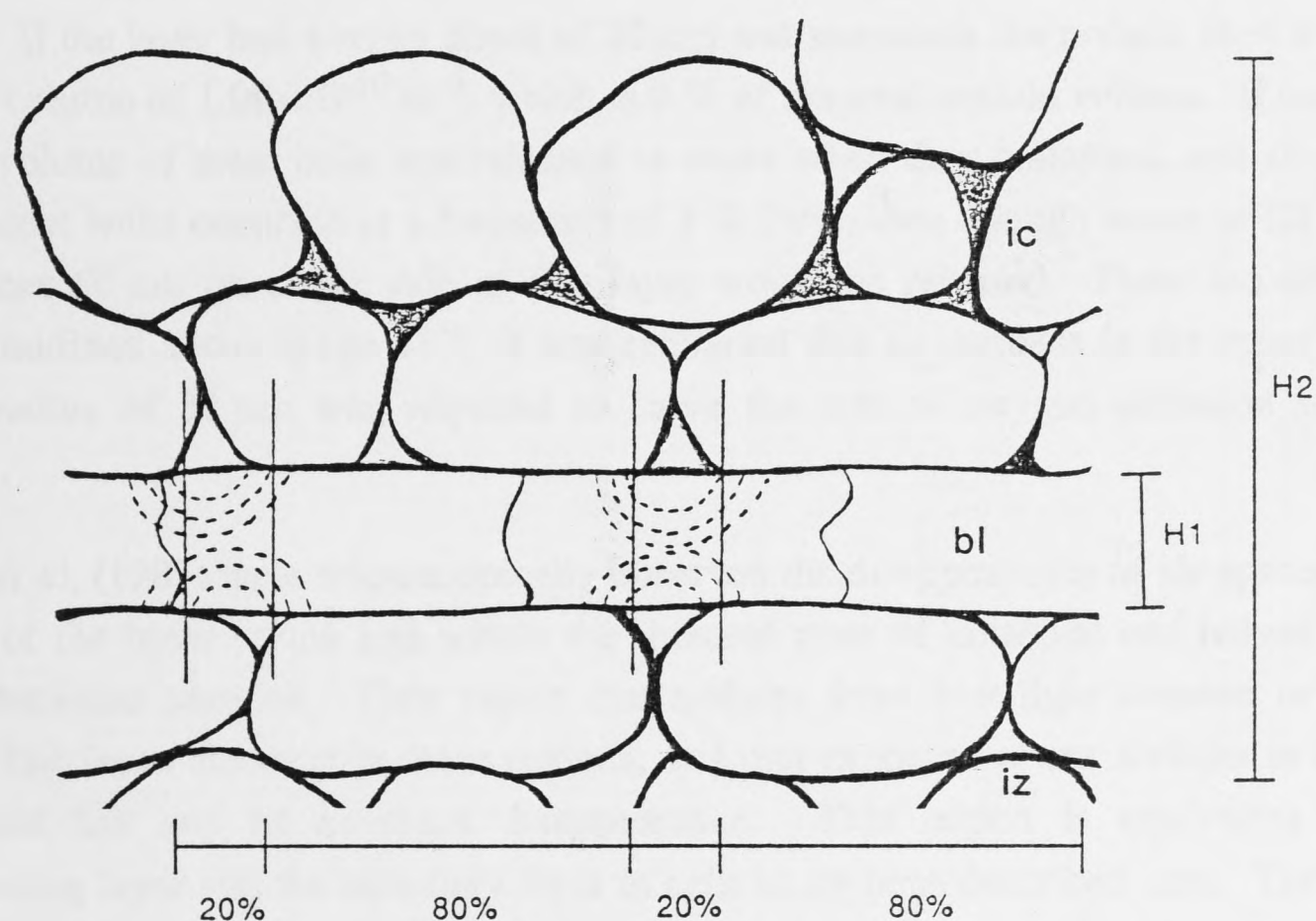
1. If it is assumed that air-spaces which occur on the inside of this layer connect to the network of cells permeating the infected zone (this is almost certainly correct), and that air-spaces on the outside of this layer connect to the outer cortex and the outside air, then a decrease in the distance between those air-spaces, caused by changes in the depth of the boundary layer, would lead to a decrease in the mean water-filled radius. This in turn would decrease the resistance of the cortex to the diffusion of oxygen. Conversely, increasing the diffusion resistance of the cortex would involve an expansion of the volume of these cells.

This mechanism would only operate if the water released upon collapse of cells did not enter the intercellular spaces and if the intercellular spaces themselves did not collapse as the boundary layer cells collapsed. Woolley (1983) has proposed that air-spaces are maintained in roots (against a capillary potential) by the presence of a hydrophobic layer on the cell wall surface. Menisci can be seen bulging into air-spaces in potato tuber, indicating that such an anti-wetting layer is present (Woolley 1983). Air-spaces in nodules may be maintained in a similar manner; Bergersen and Goodchild (1973a) observed an electron dense layer surrounding the lumen of intercellular spaces, which may represent an anti-wetting layer. This electron dense layer was also observed in this study, in intercellular spaces in the cortex and the infected zone (see Figure 7.9b), but a detailed survey of the distribution and form of this layer in intercellular spaces of the cortex was not carried out. The apoplastic water, released when the boundary layer cells are collapsed, may be able to flow freely out from the nodule via the xylem.

The effect of changing the distance between air-spaces on either side of the boundary layer can be estimated. For active nodules, a mean water-filled barrier of approximately 30  $\mu\text{m}$  was calculated above (page 119), which represents a resistance of 12000  $\text{sm}^{-1}$  ( $R = \frac{H}{D_w}$ ).

Where  $R$  = resistance in  $\text{sm}^{-1}$ ,  $H$  = the mean depth of the water-filled zone and  $D_w$  = diffusion coefficient for oxygen within the cortex (Davis *et al.* 1987).

If the effective area for diffusion between air-spaces across the boundary layer is taken as 20 % of the boundary layer area (depth  $H_1$  and resistance  $R_1$ ) and 80 % remains for diffusion across a longer distance (depth  $H_2$  and resistance  $R_2$ ) (see Figure 8.4), then the total resistance of these two parallel paths can be calculated.  $R_{Total} = \frac{R_1 \times R_2}{(R_1 + R_2)}$  (resistors in parallel law). When the boundary layer is collapsed (Figure 8.3), letting  $H_1 = 9 \mu\text{m}$  and  $H_2 = 74 \mu\text{m}$ , and taking into account respective areas of 20 % and 80 %, then  $R_1 = 18000 \text{ sm}^{-1}$  and  $R_2 = 37000 \text{ sm}^{-1}$ ; therefore  $R_{Total} = 12100 \text{ sm}^{-1}$ . If the boundary layer is expanded (Figure 8.2), and the distance between air-spaces increased to  $25 \mu\text{m}$  ( $H_1$ ) and  $90 \mu\text{m}$  ( $H_2$ ) then  $R_1$  would =  $50000 \text{ sm}^{-1}$ ,  $R_2 = 45000 \text{ sm}^{-1}$ , and  $R_{Total} = 23700 \text{ sm}^{-1}$ .



**Figure 8.4 :** Diagram illustrating parallel diffusion across a variable water-filled distance. Central infected zone (iz), boundary layer (bl) and inner cortex (ic) are labelled.

These assumptions and calculations predict that a change in the distance across the boundary layer from  $9 \mu\text{m}$  to  $25 \mu\text{m}$  may alter the effective resistance from  $12100$  to  $23700 \text{ sm}^{-1}$ . This is equivalent to a change in depth of the water-filled zone from  $30 \mu\text{m}$  to  $59 \mu\text{m}$  and would reduce oxygen flux into the infected zone of the nodule by one-half. It is interesting to note that in sections of nodules grown at  $75 \text{ kPa}$  oxygen, the boundary layer was largely expanded (Figure 7.4, 7.5). In sections of nodules grown at  $4.7 \text{ kPa}$  oxygen a high proportion of the boundary layer cells were collapsed (Figure 7.4, 7.5). While this effect could be an artifact of fixation and embedding, it may also indicate that the diffusion barrier was maintained at its maximum in the highest oxygen treatment.

2. Alternatively, if water contained within the boundary cells moved into the air-spaces on either side of the layer as the cells collapse, then this would effectively decrease the pore size and increase the diffusion resistance of the cortex. If the collapsed and turgid cells observed in prepared sections of nodules are representative of physiological changes, then a considerable volume of water, equivalent to one third or even one-half the volume of this layer of cells, would be released (Figures 8.2, 8.3). In this case the presence of collapsed cells in sections from the low oxygen treatment may represent the collapse of the barrier in response to exposure to oxygen pressures of air before they were fixed for sectioning.

The volume of water released upon collapse of the boundary layer can be estimated. In a nodule of radius 1.5 mm, this layer will occur at approximately 1.3 mm from the centre. If the layer had a mean depth of 20  $\mu\text{m}$  and surrounds the nodule, then it would have a volume of  $1.08 \times 10^{-10} \text{ m}^3$ , which is 3 % of the total nodule volume. If one third of the volume of these cells was released as water when they collapsed, and air-spaces in adjacent walls occurred at a frequency of 5 % (v/v), then enough water to fill all the air-spaces 60  $\mu\text{m}$  on either side of this layer would be released. From the diffusion model outlined above (page 117), it was estimated that an increase in the mean water-filled radius of 31  $\mu\text{m}$  was required to halve the rate of oxygen diffusion into the nodule.

Witty *et al.* (1987) have microscopically observed the disappearance of air-spaces at the inside of the inner cortex and within the infected zone of detached and halved *Pisum* and *Phaseolus* nodules. They report that nodules from low light stressed or wilted plants had fewer airspaces in these regions, and that exposure of cut nodules to oxygen increased the rate of air-space disappearance. This region is equivalent to the distributing layer and the boundary layer of cells in soybean described here. The reason why water should suddenly be able to fill these air-spaces requires further investigation. Woolley (1983) predicts that air-spaces with a wettable surface and a diameter of 2  $\mu\text{m}$  (nodule air-spaces have similar diameters, see Figures 7.9, 8.2, 8.3, and Bergersen and Goodchild 1973a), should theoretically be filled with water. He proposes that air-spaces exist because a non-wettable surface surrounds them. After the death of root cells, air-spaces between the cells rapidly fill with water, implying cells may have an active role in maintaining the non-wettable surface (Woolley 1983). Whether changes in the air-spaces of *Pisum* and *Phaseolus* nodules involve changes in the wettability of air-space walls or changes in the apoplastic water pressure remains to be determined.

## 8.6. How Could the Cortex Cells Respond to Oxygen ?

A change in the size of cells in the boundary layer may occur in response to oxygen. These cells are just external to the infected zone, where oxygen concentrations are extremely low (Bergersen 1982). If the oxygen concentration within the infected zone were to increase, the inner surface of these boundary cells would be exposed to a higher oxygen level and this may induce the active movement of ions causing a change in the osmotic potential and consequently the volume of the cell.

In legumes, leaf movement is caused by changes in the volume of pulvinus cells and involves the transport of osmotica (principally  $K^+$ ) between cells (Freudling *et al.* 1988). Stomatal movement in plants in response to various stimuli is correlated with changes in  $K^+$  ion concentrations between guard cells and subsidiary cells (Zeiger 1983). Of particular interest to this discussion is the report that stomata will sometimes open in response to low oxygen (Salisbury and Ross 1978), suggesting that at least some plant cells show an osmotic response to changes in oxygen concentrations. Similar movement of ions and water may occur in legume root nodules. Exposure of the cells in the boundary layer to oxygen may cause them to either pump ions out, making them lose water and collapse, or it may cause them to accumulate ions, take up water and expand. In this way, either case outlined above can be explained and could cause an increase in the diffusion resistance of nodules.

A simple mechanism to explain the first case outlined above can be invoked. If cells of the boundary layer have an electrogenic, ATP-requiring proton extrusion mechanism on the plasmalemma (similar to that of guard cells (Zeiger 1983)), located adjacent to the infected zone, then exposure to increased oxygen could stimulate oxidative phosphorylation, cause extrusion of protons, uptake of  $K^+$  ions and, subsequently, water, thus causing a swelling of the cells. This would increase the distance between air-spaces across the boundary layer, and thus increase the resistance to diffusion and decrease oxygen supply to the inner surface of these cells. When oxygen concentration is low on the inner surface of these cells, the gradient of  $K^+$  would not be maintained, the cells would lose  $K^+$  and water, and collapse.

The second case outlined above can be explained if it is assumed that the boundary layer can be compressed by the expansion of adjacent cells. In response to increased oxygen, cells of the infected zone may take up  $K^+$  ions, expand slightly and cause compression of the boundary layer with concomitant release of water and blockage of air-spaces.

## 8.7. Future Work

The previous discussion of the regulation of oxygen supply is simply conjecture; more experiments examining this boundary layer, and other cortical cells are required before firm conclusions on the nature of cortical diffusion resistance and mode of action of possible changes in this resistance can be reached. The comments of Woolley (1983), who recognised the importance of maintenance of air-spaces in leaves, fruits, tubers and roots, while acknowledging that we do not understand how these air-spaces are maintained, also apply to root nodules. Some new and imaginative experiments examining cells and intercellular air-spaces within the nodule cortex are required. This requires both structural and physiological studies.

Changes in the structure of the cortex could be examined in nodules before and after exposure to treatments such as acetylene and oxygen. The structure of nodules grown in argon/oxygen, which do not show an acetylene-induced decline, could be examined. The experiments of Witty *et al.* (1987), examining air-space distribution in response to stress and oxygen, should be repeated with soybean nodules. Nodule width may change in response to treatments and could be examined with a LVDT (linearly variable differential transformer) transducer, allowing measurements in the order of a few  $\mu\text{m}$ . Fresh hand cut sections of nodules and quick freezing techniques may allow observation of changes in the air-spaces and shape of cortex cells. Application of fusicoccin to nodules may be interesting (fusicoccin promotes extrusion of protons in a variety of tissues and thus causes stomatal opening in leaves (Zeiger 1983)). Can nodules show an acetylene-induced decline and recover from the decline in the presence of fusicoccin? Histochemical localization of  $\text{K}^+$  in cells and cell walls of cortical cells, and attempts to measure apoplastic and symplastic concentrations of  $\text{K}^+$ , may be fruitful. It may also be possible to study the osmotic relations of isolated cortical cells. The possibilities are almost endless and the prospect of discovering a changing diffusion barrier exciting.

## 8.8. Conclusion

In the last 10 years advances in our understanding of the physiology of legume root nodules have been considerable. In 1979 the nitrogen transport compounds in soybean had just been determined and in the following years the nitrogen assimilation metabolism of nodules was rapidly investigated. The possible role of the diffusion resistance of the cortex in regulating activity of nodules has been investigated with earnest in the 1980s, suggesting an active role for the cortex in the physiology of nodules. The importance of cortical cells in the long-term regulation of oxygen supply and the possible role of these cells in short-term regulation has been demonstrated in this thesis. Also, in the last few years the arrangement of vascular bundles in the cortex has been detailed and the role of this transport system in the removal of nitrogen compounds and the supply of sucrose investigated. Research has shown that cortical cells may be the major sites of sucrose catabolism, possibly supplying the infected cells with triose phosphates and organic acids. A transporter on the peribacteroid membrane appears to supply organic acids to the bacteroids and bacteroid metabolism has been found to show considerable plasticity in response to carbon and oxygen supply.

In the next 10 years an integration of this research together with past and future results will lead to a more detailed understanding of the physiology and the regulation of this physiology within legume root nodules.

## References

- Abeles, F.B. (1973). *Ethylene in Plant Biology*. Academic Press, New York, London.
- Afza, R., Hardarson, G., Zapata, F. and Danso, S.K.A. (1987). Effects of delayed soil and foliar N fertilization on yield and N<sub>2</sub> fixation of soybean. *Plant and Soil*, **97**, 361-368.
- Appleby, C.A. (1969). Properties of leghaemoglobin *in vivo*, and its isolation as ferrous oxyleghaemoglobin. *Biochimica et Biophysica Acta*, **188**, 222-229.
- Appleby, C.A. (1984). Leghemoglobin and *Rhizobium* respiration. *Annual Review of Plant Physiology*, **35**, 443-478.
- Appleby, C.A. and Bergersen, F.J. (1980). Preparation and experimental use of leghaemoglobin. In; *Methods for Evaluating Biological Nitrogen Fixation*. Ed: F.J. Bergersen. John Wiley and Sons Ltd, Chichester.
- Arnon, D.I. (1949). Copper enzymes in isolated chloroplasts. Polyphenoloxidase in *Beta vulgaris*. *Plant Physiology*, **24**, 1-15.
- Atkins, C.A., Pate, J.S. and Shelp, B.J. (1984). Effects of short term N<sub>2</sub> deficiency on N metabolism in legume nodules. *Plant Physiology*, **76**, 705-710.
- Atkins, C.A., Sanford, P.J., Storer, P.J. and Pate, J.S. (1988). Inhibition of nodule functioning in cowpea by a xanthine oxidoreductase inhibitor, allopurinol. *Plant Physiology*, **88**, 1229-1234.
- Bell, C.J. (1981). The testing and validation of models. In; *Mathematics and Plant Physiology*. Eds; D.A. Rose and D.A. Charles-Edwards. Academic Press, London.
- Bergersen, F.J. (1962). The effects of partial pressure of oxygen upon respiration and nitrogen fixation by soybean root nodules. *Journal of General Microbiology*, **29**, 113-125.
- Bergersen, F.J. (1965). Ammonia - an early stable product of nitrogen fixation by soybean root nodules. *Australian Journal of Biological Sciences*, **18**, 1-9.
- Bergersen, F.J. (1970). The quantitative relationship between nitrogen fixation and the acetylene-reduction assay. *Australian Journal of Biological Sciences*, **23**, 1015-1025.
- Bergersen, F.J. (1980). Measurement of nitrogen fixation by direct means. In; *Methods for Evaluating Biological Nitrogen Fixation*. Ed; F.J. Bergersen. John Wiley and Sons Ltd, Chichester.

- Bergersen, F.J. (1982). *Root nodules of legumes : Structure and functions*. Research Studies Press. John Wiley and Sons Ltd, Chichester.
- Bergersen, F.J. and Goodchild, D.J. (1973a). Aeration pathways in soybean root nodules. *Australian Journal of Biological Sciences*, **26**, 729-740.
- Bergersen, F.J. and Goodchild, D.J. (1973b). Cellular location and concentration of leghaemoglobin in soybean root nodules. *Australian Journal of Biological Sciences*, **26**, 741-756.
- Bergersen, F.J. and Turner, G.L. (1967). Nitrogen fixation by the bacteroid fraction of breis of soybean root nodules. *Biochimica et Biophysica Acta*, **141**, 507-515.
- Bergersen, F.J. and Turner, G.L. (1975). Leghaemoglobin and the supply of O<sub>2</sub> to nitrogen-fixing root nodule bacteroids: Presence of two oxidase systems and ATP production at low free O<sub>2</sub> concentration. *Journal of General Microbiology*, **91**, 345-354.
- Bergersen, F.J. and Turner, G.L. (1989). Bacteroids from soybean root nodules: Respiration and N<sub>2</sub>-fixation in flow chamber reactions with oxyleghaemoglobin. *Philosophical Transactions of the Royal Society, London* (in press).
- Bisseling, T., Van Straten, J. and Houwaard, F. (1980). Turnover of nitrogenase and leghaemoglobin in root nodules of *Pisum sativum*. *Biochimica et Biophysica Acta*, **610**, 360-370.
- Boon-Long, P., Egli, D.B. and Leggett, J.E. (1983). Leaf N and photosynthesis during reproductive growth in soybeans. *Crop Science*, **23**, 617-620.
- Braunstein, A.E. (1973). Amino group transfer. In; *The Enzymes, Volume IX, Third Edition*. Ed; P.D. Boyer. Academic Press, New York, London.
- Bray R.C. (1975). Molybdenum iron-sulfur flavin hydroxylases and related enzymes. In; *The Enzymes, Volume XII, Third Edition*. Ed; P.D. Boyer. Academic Press, New York, London.
- Carroll, B.J., Hansen, A.P., McNeil, D.L. and Gresshoff, P.M. (1987). Effect of oxygen supply on nitrogenase activity of nitrate- and dark-stressed soybean (*Glycine max* (L.) Merr.) plants. *Australian Journal of Plant Physiology*, **14**, 679-687.
- Clauss, H., Mortimer, D.C. and Gorham, P.R. (1964). Time-course study of translocation of products of photosynthesis in soybean plants. *Plant Physiology*, **39**, 269-273.



- Clever, H.L. and Battino, R. (1975). The solubility of gases in liquids. In; *Techniques in Chemistry, Volume VIII, Part 1, Solutions and Solubilities*. Ed; M.R.J. Dack. John Wiley and Sons, New York.
- Copeland, L., Quinnell, R.G. and Day, D.A. (1989a). Malic enzyme activity in bacteroids from soybean nodules. *Journal of General Microbiology* **135**, 2005-2011.
- Copeland, L., Vella, J. and Hong, Z. (1989b). Enzymes of carbohydrate metabolism in soybean nodules. *Phytochemistry*, **28**, 57-61.
- Crank, J. (1975). *The Mathematics of Diffusion*. Oxford University Press, London.
- Criswell, J.G., Havelka, U.D., Quebedeaux, B. and Hardy, R.W.F. (1976). Adaptation of nitrogen fixation by intact soybean nodules to altered rhizosphere  $pO_2$ . *Plant Physiology*, **58**, 622-625.
- Dart, P.J. and Wildon, D.C. (1970). Nodulation and nitrogen fixation by *Vigna sinensis* and *Vicia atropurpurea*: The influence of concentration, form, and site of application of combined nitrogen. *Australian Journal of Agricultural Research*, **21**, 45-56.
- Davey, A.G. and Simpson, R.J. (1988). Nitrogenase activity by subterranean clover and other temperate pasture legumes. *Australian Journal of Plant Physiology*, **15**, 657-667.
- Davey, A.G. and Simpson, R.J. (1989). Changes in nitrogenase activity and nodule diffusion resistance of subterranean clover in response to  $pO_2$ . *Journal of Experimental Botany*, **40**, 149-158.
- Davis, L.C. (1984). Diffusion of gases through plant tissues. *Plant Physiology*, **76**, 854-857.
- Davis, L.C. (1988). Limitations on the analysis of acetylene reduction by soybean at low levels of acetylene. *Annals of Botany*, **61**, 179-183.
- Davis, L.C. and Imsande, J. (1988). Direct test for altered gas exchange rates in water-stressed soybean nodules. *Annals of Botany*, **61**, 169-177.
- Davis, L.C., Erickson, L.E. and Jones, G.T. (1987). Diffusion and reaction in root nodules. *CRC Critical Reviews in Biotechnology*, **7**, 43-95.
- Day, D.A. and Mannix, M. (1988). Malate oxidation by soybean nodule mitochondria and the possible consequences for nitrogen fixation. *Plant Physiology and Biochemistry*, **26**, 567-573.
- Day, D.A., Lambers, H., Bateman, J., Carroll, B.J. and Gresshoff, P.M. (1986). Growth comparisons of a supernodulating soybean (*Glycine max*) mutant and its wild type parent. *Physiologia Plantarum*, **68**, 375-382.

- Day, D.A., Price, G.D. and Udvardi, M.K. (1989). Membrane interface of the *Bradyrhizobium japonicum* - *Glycine max* symbiosis: peribacteroid units from soybean nodules. *Australian Journal of Plant Physiology*, **16**, 69-84.
- Dean, J.A. (1973). *Lange's Handbook of Chemistry. Eleventh Edition*. McGraw-Hill Book Company, New York.
- Denison, R.F., Sinclair, T.R., Zobel, R.W., Johnson, M.N. and Drake, G.M. (1983a). A non-destructive field assay for soybean nitrogen fixation by acetylene reduction. *Plant and Soil*, **70**, 173-182.
- Denison, R.F., Weisz, P.R. and Sinclair, T.R., (1983b). Analysis of acetylene reduction rates of soybean nodules at low acetylene concentrations. *Plant Physiology*, **73**, 648-651.
- Dilworth, M. (1966). acetylene reduction by nitrogen-fixing preparations from *Clostridium pasteurianum*. *Biochimica et Biophysica Acta*, **127**, 285-294.
- Dilworth, M. and Glenn, A. (1984). How does a legume nodule work? *Trends in Biochemical Sciences*, **9**, 519-523.
- Dixon, R.O.D., Blunden, E.A.G. and Searl, J.W. (1981). Intercellular space and hydrogen diffusion in pea and lupin root nodules. *Plant Science Letters*, **23**, 109-116.
- Downie, J.A. and Johnston, A.W.B. (1988). Nodulation of legumes by *Rhizobium*. *Plant, Cell and Environment*, **11**, 403-412.
- Drennan, D.S.H. and Norton, C. (1972). The effect of ethrel on nodulation in *Pisum sativum* L. . *Plant and Soil*, **36**, 53-57.
- Drevon, J.J., Heckmann, M.O., Soussana, J.F. and Salsac, L. (1988a). Inhibition of nitrogen fixation by nitrate assimilation in legume-*Rhizobium* symbiosis. *Plant Physiology and Biochemistry*, **26**, 197-203.
- Drevon, J.J., Kalia, V.C., Heckmann, M.O. and Pedelahore, P. (1988b). *In situ* open-flow assay of acetylene reduction activity by soybean root nodules: influence of acetylene and oxygen. *Plant Physiology and Biochemistry*, **26**, 73-78.
- Duke, S.H., Schrader, L.E., Henson, C.A., Servaites, J.C., Vogelzang, R.D. and Pendleton, J.W. (1979). Low root temperature effects on soybean nitrogen metabolism and photosynthesis. *Plant Physiology*, **63**, 956-962.
- Durand, J., Sheehy, J.E. and Minchin, F.R. (1987). Nitrogenase activity, photosynthesis and nodule water potential in soybean plants experiencing water deprivation. *Journal of Experimental Botany*, **38**, 311-321.

- Emerich, D.W., Anthon, G.E., Hayes, R.R., Karr, D.B., Liang, R., Preston, G.G., Smith, M.T. and Waters, J.K. (1988). Metabolism of *Rhizobium*-leguminous plant nodules with an emphasis on bacteroid carbon metabolism. In; *Nitrogen Fixation: Hundred Years After*. Eds; H. Bothe, F.J. de Bruijn and W.E. Newton. Gustav Fischer, Stuttgart, New York.
- FAO Production Yearbook (1986). Volume 40. *FAO Statistics Series No. 76*. Food and Agricultural Organisation of the United Nations, Rome.
- Fishbeck, K., Evans, H.J. and Boersma, L.L. (1973). Measurement of nitrogenase activity of intact legume symbionts *in situ* using the acetylene reduction assay. *Agronomy Journal*, **65**, 429-433.
- Freudling, C., Starrach, N., Flach, D., Gradmann, D. and Mayer, W.E. (1988). Cell walls as reservoirs of potassium ions for reversible volume changes of pulvinar motor cells during rhythmic leaf movements. *Planta*, **175**, 193-203.
- Glinski, J. and Stepniewski, W. (1985). *Soil Aeration and its Role for Plants*. CRC Press Inc., Boca Raton, Florida.
- Goodlass, G. and Smith, K.A. (1979). Effects of ethylene on root extension and nodulation of pea (*Pisum sativum* L.) and white clover (*Trifolium repens* L.). *Plant and Soil*, **51**, 387-395.
- Grobbelaar, N., Clarke, B. and Hough, M.C. (1971). The nodulation and nitrogen fixation of isolated roots of *Phaseolus vulgaris* L.. III The effect of carbon dioxide and ethylene. *Plant and Soil*, Special Volume, 215-223.
- Hardy, R.W.F., Burns, R.C. and Holsten, R.D. (1973). Applications of the acetylene-ethylene assay for measurement of nitrogen fixation. *Soil Biology and Biochemistry*, **5**, 47-81.
- Hardy, R.W.F., Holsten, R.D., Jackson, E.K. and Burns, R.C. (1968). The acetylene-ethylene assay for N<sub>2</sub> fixation: Laboratory and field evaluation. *Plant Physiology*, **43**, 1185-1207.
- Harris, M., Mackender, R.O. and Smith, D.L. (1986). Photosynthesis of cotyledons of soybean seedlings. *New Phytologist*, **104**, 319-329.
- Hartwig, U., Boller, B. and Nösberger, J. (1987). Oxygen supply limits nitrogenase activity of clover nodules after defoliation. *Annals of Botany*, **59**, 285-291.
- Heckmann, M.O., Drevon, J.J., Saglio, P. and Salsac, L. (1989). Effect of oxygen and malate on NO<sub>3</sub><sup>-</sup> inhibition of nitrogenase in soybean nodules. *Plant Physiology*, **90**, 224-229.

- Herridge, D.F., Atkins, C.A., Pate, J.S. and Rainbird, R.M. (1978). Allantoin and allantoic acid in the nitrogen economy of the cowpea (*Vigna unguiculata* [L.] Walp.). *Plant Physiology*, **62**, 495-498.
- Howitt, S.M. and Gresshoff, P.M. (1985). Ammonia regulation of glutamine synthetase in *Rhizobium* sp. ANU289. *Journal of General Microbiology*, **131**, 1433-1440.
- Huang, C., Boyer, J.S. and Vanderhoef, L.N. (1975). Acetylene reduction (nitrogen fixation) and metabolic activities of soybean having various leaf and nodules water potentials. *Plant Physiology*, **56**, 222-227.
- Hunt, R. (1982). *Plant growth curves. The functional approach to plant growth analysis*. Edward Arnold Ltd. London.
- Hunt, S., Gaito, S.T. and Layzell, D.B. (1988). Model of gas exchange and diffusion in legume nodules. II. Characterisation of the diffusion barrier and estimation of the concentrations of CO<sub>2</sub>, H<sub>2</sub> and N<sub>2</sub> in the infected cells. *Planta*, **173**, 128-141.
- Hunt, S., King, B.J., Canvin, D.T. and Layzell, D.B. (1987). Steady and nonsteady state gas exchange characteristics of soybean nodules in relation to the oxygen diffusion barrier. *Plant Physiology*, **84**, 164-172.
- Jacobs, M.H. (1967). *Diffusion Processes*. Springer-Verlag, Berlin Heidelberg New York.
- Jones, G.T., Davis, L.C., Ghosh Hajra, A.K. and Erickson, L.E. (1987). Modeling and analysis of diffusion and reaction in legume nodules. *Biotechnology and Bioengineering*, **29**, 279-288.
- Jost, W. (1960). Diffusion in solids, liquids and gases. In; *Physical Chemistry*. 1. Ed; E.M. Loebl. Academic Press, New York.
- Kahn, M.L., Kraus, J. and Somerville, J.E. (1985). A model of nutrient exchange in the *Rhizobium*-legume symbiosis. In; *Nitrogen Fixation Research Progress*. Eds; H.J. Evans, P.J. Bottomley and W.E. Newton. Martinus Nijhoff Publishers, Dordrecht, Boston, Lancaster.
- Kennedy, I.R. (1966). Primary products of symbiotic nitrogen fixation I. Short-term exposures of Serradella nodules to <sup>15</sup>N<sub>2</sub>. *Biochimica et Biophysica Acta*, **130**, 285-294.
- Kerr, P.S., Rufty, T.W. and Huber, S.C. (1985). Changes in nonstructural carbohydrates in different parts of soybean (*Glycine max* [L.] Merr.) plants during a light/dark cycle and in extended darkness. *Plant Physiology*, **78**, 576-581.

- King, B.J., Hunt, S. Weagle, G.E., Walsh, K.B., Pottier, R.H., Canvin, D.T. and Layzell, D.B. (1988). Regulation of O<sub>2</sub> concentration in soybean nodules observed by *in situ* spectroscopic measurement of leghemoglobin oxygenation. *Plant Physiology*, **87**, 296-299.
- Kossak, R.M. and Bohlool, B.B. (1984). Suppression of nodule development of one side of a split-root system of soybeans caused by prior inoculation of the other side. *Plant Physiology*, **75**, 125-130.
- Kouchi, H. and Nakaji, K. (1985). Utilization and metabolism of photoassimilated <sup>13</sup>C in soybean roots and nodules. *Soil Science and Plant Nutrition*, **31**, 323-334.
- Kouchi, H. and Yoneyama, T. (1984). Dynamics of carbon photosynthetically assimilated in nodulated soya bean plants under steady-state conditions. 2. The incorporation of <sup>13</sup>C into carbohydrates, organic acids, amino acids and some storage compounds. *Annals of Botany*, **53**, 883-896.
- Kouchi, H., Fukai, K., Katagiri, H., Minamisawa, K. and Tajima, S. (1988). Isolation and enzymological characterization of infected and uninfected cell protoplasts from root nodules of *Glycine max*. *Physiologia Plantarum*, **73**, 327-334.
- Kouchi, H., Nakaji, K., Yoneyama, T. and Ishizuka, J. (1985). Dynamics of carbon photosynthetically assimilated in nodulated soya bean plants under steady state conditions. 3. Time-course study of <sup>13</sup>C incorporation into soluble metabolites and respiratory evolution of <sup>13</sup>CO<sub>2</sub> from roots and nodules. *Annals of Botany*, **56**, 333-346.
- Lawn, R.J. and Brun, W.A. (1974). Symbiotic nitrogen fixation in soybeans. I. Effect of photosynthetic source-sink manipulations. *Crop Science*, **14**, 11-16.
- Layzell, D.B., Gaito, S.T. and Hunt, S. (1988). Model of gas exchange and diffusion in legume nodules. I. Calculation of gas exchange rates and the energy cost of N<sub>2</sub> fixation. *Planta*, **173**, 117-127.
- Layzell, D.B., Hunt, S., King, B.J., Walsh, K.B. and Weagle, G.E. (1989). A multichannel system for steady state and continuous measurements of gas exchanges from legume roots and nodules. In; *Applications of Continuous and Steady State Methods in Root Biology*. Eds; J.G. Torrey and L. Winship. Kluwer Publishers, The Netherlands.
- Layzell, D.B., Rochman, P. and Canvin, D.T. (1984). Low root temperatures and nitrogenase activity in soybean. *Canadian Journal of Botany*, **62**, 965-971.
- Mahon, J.D. and Child, J.J. (1979). Growth response of inoculated peas (*Pisum sativum*) to combined nitrogen. *Canadian Journal of Botany*, **57**, 1687-1693.

- McClure, P.R. and Israel, D.W. (1979). Transport of nitrogen in the xylem of soybean plants. *Plant Physiology*, **64**, 411-416.
- Mederski, H.J. and Streeter, J.G. (1977). Continuous, automated acetylene reduction assays using intact plants. *Plant Physiology*, **59**, 1076-1081.
- Meeks, J.C., Wolk, C.P., Schilling, N., Shaffer, P.W., Avissar, Y. and Chien, W. (1978). Initial organic products of fixation of [ $^{13}\text{N}$ ] dinitrogen by root nodules of soybean (*Glycine max*). *Plant Physiology*, **61**, 980-983.
- Meister, A. (1974). Glutamine synthetase of mammals. In; *The Enzymes, Volume X, Third Edition*. Ed; P.D. Boyer. Academic Press, New York, London.
- Michal, G. (1982). *Biochemical Pathways*. Boehringer Mannheim GmbH. Mannheim, West Germany.
- Minchin, F.R., Sheehy, J.E., Minguéz, M.I. and Witty, J.F. (1985). Characterization of the resistance to oxygen diffusion in legume nodules. *Annals of Botany*, **55**, 53-60.
- Minchin, F.R., Sheehy, J.E. and Witty, J.F. (1986). Further errors in the acetylene reduction assay : Effects of plant disturbance. *Journal of Experimental Botany*, **37**, 1581-1591.
- Minchin, F.R., Summerfield, R.J., Hadley, P., Roberts, E.H. and Rawsthorne, S. (1981). Carbon and nitrogen nutrition of nodulated roots of grain legumes. *Plant, Cell and Environment*, **4**, 5-26.
- Minchin, F.R., Witty, J.F., Sheehy, J.E. and Müller, M. (1983). A major error in the acetylene reduction assay: Decreases in nodular nitrogenase activity under assay conditions. *Journal of Experimental Botany*, **34**, 641-649.
- Minchin, P.E.H. (1986). Why use short lived isotopes ? In; *Short Lived Isotopes in Biology*. Ed; P.E.H. Minchin. Department of Scientific and Industrial Research, DSIR Bulletin 238, Wellington, New Zealand.
- Morell, M. and Copeland, L. (1984). Enzymes of sucrose breakdown in soybean nodules. Alkaline invertase. *Plant Physiology*, **74**, 1030-1034.
- Murry, M.A., Fontaine, M.S. and Tjepkema, J.D. (1984). Oxygen protection of nitrogenase in *Frankia* sp. HFP Ar13. *Archives of Microbiology*, **139**, 162-166.
- Newcomb, W., Sippell, D. and Peterson, R.L. (1979). The early morphogenesis of *Glycine max* and *Pisum sativum* root nodules. *Canadian Journal of Botany*, **57**, 2603-2616.

- Nguyen, J., Machal, L., Vidal, J., Perrot-Rechenmann, C. and Gadal, P. (1986). Immunochemical studies on xanthine dehydrogenase of soybean root nodules. *Planta*, **167**, 190-195.
- Nutman, P.S. (1956). The influence of the legume in root-nodule symbiosis. A comparative study of host determinants and functions. *Biological Reviews*, **31**, 109-151.
- Pankhurst, C.E. and Sprent, J.I. (1975a). Effects of water stress on the respiratory and nitrogen-fixing activity of soybean root nodules. *Journal of Experimental Botany*, **26**, 287-304.
- Pankhurst, C.E. and Sprent, J.I. (1975b). Surface features of soybean root nodules. *Protoplasma*, **85**, 85-98.
- Parker, M.B. and Boswell, F.C. (1980). Foliage injury, nutrient uptake, and yield of soybeans as influenced by foliar fertilization. *Agronomy Journal*, **72**, 110-113.
- Parsons, R., Silvester, W.B., Harris, S., Gruijters, W.T.M. and Bullivant, S. (1987). *Frankia* vesicles provide inducible and absolute oxygen protection for nitrogenase. *Plant Physiology*, **83**, 728-731.
- Pate, J.S. (1975). Transport in symbiotic systems fixing nitrogen. In; *Encyclopaedia of Plant Physiology, Transport in Plants II, Part B Tissues and Organs*. Eds; U. Lüttge and M.G. Pitman. Springer-Verlag, Berlin Heidelberg New York.
- Pate, J.S. and Dart, P.J. (1961). Nodulation studies in legumes IV. The influence of inoculum strain and time of application of ammonium nitrate on symbiotic response. *Plant and Soil*, **15**, 329-346.
- Pate, J.S., Atkins, C.A., Layzell, D.B. and Shelp, B.J. (1984). Effects of N<sub>2</sub> deficiency on transport and partitioning of C and N in a nodulated legume. *Plant Physiology*, **76**, 59-64.
- Price, G.D., Day, D.A. and Gresshoff, P.M. (1987). Rapid isolation of intact peribacteroid envelopes from soybean nodules and demonstration of selective permeability to metabolites. *Journal of Plant Physiology*, **130**, 157-164.
- Rainbird, R.M., Atkins, C.A. and Pate, J.S. (1983). Diurnal variation in the functioning of cowpea nodules. *Plant Physiology*, **72**, 308-312.
- Rainbird, R.M., Hitz, W.D. and Hardy, R.W.F. (1984). Experimental determination of the respiration associated with soybean/*Rhizobium* nitrogenase function, nodule maintenance, and total nodule nitrogen fixation. *Plant Physiology*, **75**, 49-53.

- Ralston, E.J. and Imsande, J. (1982). Entry of oxygen and nitrogen into intact soybean nodules. *Journal of Experimental Botany*, **33**, 208-214.
- Reynolds, P.H.S., Boland, M.J., Blevins, D.G., Randall, D.D. and Schubert, K.R. (1982). Ureide biogenesis in leguminous plants. *Trends in Biochemical Sciences*, **7**, 366-368.
- Robson, R.L. and Postgate, J.R. (1980). Oxygen and hydrogen in biological nitrogen fixation. *Annual Reviews of Microbiology*, **34**, 183-207.
- Ryle, G.J.A., Arnott, R.A., Powell, C.E. and Gordon, A.J. (1983). Comparisons of the respiratory effluxes of nodules and roots in six temperate legumes. *Annals of Botany*, **52**, 469-477.
- Ryle, G.J.A., Powell, C.E. and Gordon, A.J. (1978). Effect of source of nitrogen on the growth of fiskeby soya bean : the carbon economy of whole plants. *Annals of Botany*, **42**, 637-648.
- Ryle, G.J.A., Powell, C.E. and Gordon, A.J. (1985a). Defoliation in white clover: Regrowth, photosynthesis and N<sub>2</sub> fixation. *Annals of Botany*, **56**, 9-18.
- Ryle, G.J.A., Powell, C.E. and Gordon, A.J. (1985b). Short-term changes in CO<sub>2</sub> evolution associated with nitrogenase activity in white clover in response to defoliation and photosynthesis. *Journal of Experimental Botany*, **36**, 634-643.
- Salisbury, F.B. and Ross, C.W. (1978). *Plant Physiology Second Edition*. Wadsworth Publishing Company, Inc. Belmont, California.
- Salminen, S.O. (1981). Effect of NH<sub>4</sub><sup>+</sup> on nitrogenase activity in nodule breis and bacteroids from *Pisum sativum* L.. *Biochimica et Biophysica Acta*, **658**, 1-9.
- Schollhorn, R. and Burris, R.H. (1966). Study of intermediates in nitrogen fixation. *Federation Proceedings*, **25**, 710.
- Schubert, K.R. (1986). Products of biological nitrogen fixation in higher plants : Synthesis, transport and metabolism. *Annual Review of Plant Physiology*, **37**, 539-574.
- Schuller, K.A., Minchin, F.R. and Gresshoff, P.M. (1988). Nitrogenase activity and oxygen diffusion in nodules of soyabean cv. Bragg and a supernodulating mutant: Effects of nitrate. *Journal of Experimental Botany*, **39**, 865-877.
- Schweitzer, L.E. and Harper, J.E. (1980). Effect of light, dark and temperature on root nodule activity (acetylene reduction) of soybeans. *Plant Physiology*, **65**, 51-56.



- Sen, D. and Weaver, R.W. (1985). Role of nodule size on the nitrogenase activity in cowpea. In; *Nitrogen Fixation Research Progress*. Eds; H.J. Evans, P.J. Bottomley and W.E. Newton. Martinus Nijhoff Publishers, Dordrecht, Boston, Lancaster.
- Sen, D., Weaver, R.W. and Bal, A.K. (1986). Structure and organization of effective peanut and cowpea root nodules induced by rhizobial strain 32H1. *Journal of Experimental Botany*, **37**, 356-363.
- Sheehy, J.E. and Bergersen, F.J. (1986). A simulation study of the functional requirements and distribution of leghaemoglobin in relation to biological nitrogen fixation in legume root nodules. *Annals of Botany*, **58**, 121-136.
- Sheehy, J.E. and Thornley, J.H.M. (1988). Oxygen, the *NifA* gene, nodule structure and the initiation of nitrogen fixation. *Annals of Botany*, **61**, 605-609.
- Sheehy, J.E., Bergersen, F.J., Minchin, F.R., and Witty, J. (1987). A simulation study of gaseous diffusion resistance, nodule pressure gradients and biological nitrogen fixation in soyabean nodules. *Annals of Botany*, **60**, 345-351.
- Sheehy, J.E., Minchin, F.R., and Witty, J.F. (1983). Biological control of the resistance to oxygen flux in nodules. *Annals of Botany*, **52**, 565-571.
- Sheehy, J.E., Minchin, F.R., and Witty, J.F. (1985). Control of nitrogen fixation in a legume nodule: an analysis of the role of oxygen diffusion in relation to nodule structure. *Annals of Botany*, **55**, 549-562.
- Silisbury, J.H. (1977). Energy requirement for symbiotic nitrogen fixation. *Nature*, **267**, 149-150.
- Silvester, W.B., Silvester, J.K. and Torrey, J.G. (1988a). Adaptation of nitrogenase to varying oxygen tension and the role of the vesicle in root nodules of *Alnus incana* ssp. *rugosa*. *Canadian Journal of Botany*, **66**, 1772-1779.
- Silvester, W.B., Whitbeck, J., Silvester, J.K. and Torrey, J.G. (1988b). Growth, nodule morphology, and nitrogenase activity of *Myrica gale* with roots grown at various oxygen levels. *Canadian Journal of Botany*, **66**, 1762-1771.
- Sinclair, T.R. and Goudriaan, J. (1981). Physical and morphological constraints on transport in nodules. *Plant Physiology*, **67**, 143-145.
- Singleton, P.W. and Stockinger, K.R. (1983). Compensation against ineffective nodulation in soybean. *Crop Science*, **23**, 69-72.

- Singleton, P.W. and van Kessel, C. (1987). Effect of localized nitrogen availability to soybean half-root systems on photosynthate partitioning to root and nodules. *Plant Physiology*, **83**, 552-556.
- Sprent, J.I. (1972). The effects of water stress on nitrogen-fixing root nodules. II. Effects on the fine structure of detached soybean nodules. *New Phytologist*, **71**, 443-450.
- Sprent, J.I. (1979). *The Biology of Nitrogen-Fixing Organisms*. McGraw-Hill Book Company (UK) Ltd, London.
- Sprent, J.I. (1989). Which steps are essential for the formation of functional legume nodules? *New Phytologist*, **111**, 129-153.
- Streeter, J.G. (1980). Carbohydrates in soybean nodules II. Distribution of compounds in seedlings during the onset of nitrogen fixation. *Plant Physiology*, **66**, 471-476.
- Streeter, J.G. (1988). Inhibition of legume nodule formation and N<sub>2</sub> fixation by nitrate. *CRC Critical Reviews in Plant Sciences*, **7**, 1-23.
- Sutton, W.D. (1983). Nodule development and senescence. In; *Nitrogen Fixation, Volume 3 Legumes*. Ed; W.J. Broughton. Clarendon Press, Oxford.
- Tjepkema, J.D. (1979). Oxygen relations in leguminous and actinorhizal nodules. In; *Symbiotic nitrogen fixation in the management of temperate forests*. Eds; J.C. Gordon, C.T. Wheeler and D.A. Perry. Forest Research Laboratory, Oregon State University, Corvallis, Oregon 97331.
- Tjepkema, J.D. and Yocum, C.S. (1973). Respiration and oxygen transport in soybean nodules. *Planta*, **115**, 59-72.
- Tjepkema, J.D. and Yocum, C.S. (1974). Measurement of oxygen partial pressure within soybean nodules by oxygen microelectrodes. *Planta*, **119**, 351-360.
- Tjepkema, J.D., Schwintzer, C.R. and Monz, C.A. (1988). Time course of acetylene reduction in nodules of five actinorhizal genera. *Plant Physiology*, **86**, 581-583.
- Tolley-Henry, L. and Raper, C.D. (1986). Expansion and photosynthetic rate of leaves of soybean plants during onset of and recovery from nitrogen stress. *Botanical Gazette*, **147**, 400-406.
- Triplett, E.W. (1985). Intercellular nodule localization and nodule specificity of xanthine dehydrogenase in soybean. *Plant Physiology*, **77**, 1004-1009.

- Turner, G.L. and Gibson, A.H. (1980). Measurement of nitrogen fixation by indirect means. In; *Methods for Evaluating Biological Nitrogen Fixation*. Ed; F.J. Bergersen. John Wiley and Sons Ltd, Chichester.
- Upmeyer, D.J. and Koller, H.R. (1973). Diurnal trends in net photosynthetic rate and carbohydrate levels of soybean leaves. *Plant Physiology*, **51**, 871-874.
- Vance, C.P., Egli, M.A., Griffith, S.M. and Miller, S.S. (1988). Plant regulated aspects of nodulation and N<sub>2</sub> fixation. *Plant, Cell and Environment*, **11**, 413-427.
- Vessey, J.K., Walsh, K.B. and Layzell, D.B. (1988a). Oxygen limitation of N<sub>2</sub> fixation in stem-girdled and nitrate-treated soybean. *Physiologia Plantarum*, **73**, 113-121.
- Vessey, J.K., Walsh, K.B. and Layzell, D.B. (1988b). Can a limitation in phloem supply to nodules account for the inhibitory effect of nitrate on nitrogenase activity in soybean? *Physiologia Plantarum*, **74**, 137-146.
- Walsh, K.B., Canny, M.J. and Layzell, D.B. (1989a). Vascular transport and soybean nodule function: II. A role for the phloem supply in product export. *Plant, Cell and Environment* (in press).
- Walsh, K.B., McCully, M.E. and Canny, M.J. (1989b). Vascular transport and soybean nodule function: nodule xylem is a blind alley, not a throughway. *Plant, Cell and Environment*, **12**, 395-405.
- Walsh, K.B., Vessey, J.K. and Layzell, D.B. (1987). Carbohydrate supply and N<sub>2</sub> fixation in soybean. *Plant Physiology*, **85**, 137-144.
- Weisz, P.R. and Sinclair, T.R. (1987a). Regulation of soybean nitrogen fixation in response to rhizosphere oxygen. 1. Role of nodule respiration. *Plant Physiology*, **84**, 900-905.
- Weisz, P.R. and Sinclair, T.R. (1987b). Regulation of soybean nitrogen fixation in response to rhizosphere oxygen. 2. Quantification of nodule gas permeability. *Plant Physiology*, **84**, 906-910.
- Witty, J.F., Minchin, F.R., Sheehy, J.E. and Miguez, M.I. (1984). Acetylene-induced changes in the oxygen diffusion resistance and nitrogenase activity of legume root nodules. *Annals of Botany*, **53**, 13-20.
- Witty, J.F., Minchin, F.R., Skøt, L. and Sheehy, J.E. (1986). Nitrogen fixation and oxygen in legume root nodules. *Oxford Surveys of Plant Molecular and Cell Biology*, **3** 275-314.

Witty, J.F., Skøt, L. and Revsbech, N.P. (1987). Direct evidence for changes in the resistance of legume root nodules to O<sub>2</sub> diffusion. *Journal of Experimental Botany*, **38**, 1129-1140.

Woolley, J.T. (1983). Maintenance of air in intercellular spaces of plants. *Plant Physiology*, **72**, 989-991.

Yokota, A. and Kitaoka, S. (1985). Correct pK values for dissociation constant of carbonic acid lower the reported Km values of ribulose biphosphate carboxylase to half. Presentation of a nomograph and an equation for determining the pK values. *Biochemical and Biophysical Research Communications*, **131**, 1075-1079.

Zeiger, E. (1983). The biology of stomatal guard cells. *Annual Review of Plant Physiology*, **34**, 441-475.

## Appendix I

```

05      !                               SOYFIX
07      !
10      !           BASIC FILE TO CALCULATE SOYBEAN GROWTH RATES
15      !
18      !                               Richard Parsons 1989
20      !
25      open "sim1.dat" for output as file #1
27      open "sim2.dat" for output as file #2
28      let appN=0
30      let nodno=23
37      let daylength=16
39      let night=24-daylength
40      let day = 0
41      let cotyori=195
43      let appn=0
44      let xleafarea = 0
45      let cotyarea = 0
46      let rootdw = 0
47      let stemdw = 0
48      let xleafdw = 0
49      let noddw = 0
50      let cotydw=cotyori
52      let availnit=0
53      let nodnitavail=0
54      let cotypsyn= .2
56      let xleafpsyn= .7
60      let cotyorinit = 6
62      let xleafpsex=0
64      let xleafin=0
66      let stemin=0
68      let rootin=0
70      let maxnitposs=0
72      let photosyn=0
74      let rootgroresp=0
76      let stemgroresp=0
78      let xleafgroresp=0
80      let nodgroresp=0
82      let rootin=0
84      let stemin=0
86      let xleafin=0
88      let nodin=0
90      let rootin2=0
92      let photosyn=0
94      let plantdw=cotyori
120     let initialnit = cotydw * cotyorinit/100
122     let cotynittot = initialnit
300
400     ! Printing of data by day and plant part to file 1
403
406     print #1,day;'coty';cotydw;cotypsex;cotyresp;cotyori
408     print #1,day;'stem';stemdw;stemmainresp;stemresp;stemin
410     print #1,day;'xleaf';xleafdw;photosyn*2.38;xleafresp;xleafin
412     print #1,day;'root';rootdw;rootmainresp;rootresp;rootin2
414     print #1,day;'nod';noddw;nodmainresp;nodresp;nodin
416     print #1,
430
432     ! Printing of data by day and nitrogen content to file 2
436
440     print day;plantdw;xleafnit;availnit;cotynitavail;
445     print nodnitavail;nodindresp;nodmainresp

```

```

450 print #2 ,day;'coty';cotynittot ;cotydw
460 print #2 ,day;'stem';stemnittot ;stemdw
470 print #2 ,day;'xleaf';xleafnittot ;xleafdw
480 print #2 ,day;'root';rootnittot ;rootdw
490 print #2 ,day;'nod';nodnittot ;noddw
500 print #2,
504
510 if day > 17 then let cotydw = 0 ! (cotyledon fall)
520
530 if day < 3 then goto 600 ! (for day < 3)
550 if day > 29 then goto 10000 ! (finish)
560 goto 700 ! (for day > 3)
570
600 ! Calculation of root and stem increase < 3 days
604 ! Export of carbon only from cotyledon
610
620 cotyexport =(cotyori/30*.52) !because coty has high C content
630 let rootdw = rootdw + cotyexport*.4 * 2.50 *.5
635 ! rootDW = previous DW + cotyexport * partition * oxidation
638 ! * proportion respired
640 let stemdw = stemdw + cotyexport*.3 * 2.38 *.5
650 let xleafdw = xleafdw + cotyexport*.3 *2.38 *.5
680
690 goto 900 ! (Calculation of respiration)
692 ! For day < 3 no photosynthesis input
694
700 ! Cotyledon export
710
720 cotyexport = cotyori/30 * .52
725 if day >17 then cotyexport = 0 !(cotyledon fall)
730 if day > 17 then cotydw= 0 !(cotyledon fall)
732 let rootin = cotyexport*.6 * 2.50
740 let stemin = cotyexport*.3 * 2.38
750 let xleafin = cotyexport*.1 * 2.38
760
770 ! Cotyledon Photosynthesis
774
780 if day < 6 then let cotyarea = 4 else let cotyarea = 6
782 ! (cotyledon area in cm2)
785 if day > 17 then cotyarea = 0
790 let cotypsex = cotyarea * cotypsyn /44*12*60*60*daylength /10000
792 ! cotypsex = cotyarea * cotypsyn / (umol)*sec*min*hours /cm2
794 ! (cotyledon photosynthesis export as mg C day-1)
804
810 ! Leaf Photosynthesis
820 !
830 if day < 16 then let xleafarea =xleafdw * 10 /25
834 if day >=16 then let xleafarea = xleafdw * 10 / (25+(day-16)*1.0)
836 ! (Density of leaf gets greater with time)
840 let xleafpsex=xleafarea*xleafpsyn*nitfactor/44*12*60*60*daylength/10000
845 !xleafpsex=xleafarea*xleafpsyn*nitfactor/(mmol)*sec*min*hours/cm2
850
855 let photosyn=cotypsex+xleafpsex !(total photosynthate in g carbon)
858
860 ! Allocation of photosynthate
863
864 let xleafin =xleafin + photosyn*.35*2.38 !*partition* carbon/ %carb
866 let stemin = stemin + photosyn *.17*2.38 !*partition* carbon/ %carb
867 if leafdw > 900 then xleafin=xleafin+photosyn*.32
869 if leafdw > 900 then xstemin=xstemin+photosyn*.20
870 let rootin = rootin + photosyn *.48*2.50 !*partition* carbon/ %carb
872 if day < 13 then let rootin2 = rootin

```

```

880   if day>=13 then let rootin2 = rootin *.5      ! (allocation of
884   if day>=13 then let nodin = rootin *.5      ! carbon to roots
886   if day>=20 then let nodin = rootin *.50     ! and nodules at
888   if day>=20 then let rootin2 = rootin *.50   ! different ages
890
900   !           Calculation of maintenance respiration loss
904
906   ! (calculations based as a fraction of dry weight
908   if day > 17 then cotydw = 0
910   if day < 3 then let cotyresp=cotydw*.0015 * 24
           else let cotyresp=cotydw * .002 * night
920   let rootmainresp=rootdw*.003*24*.682
930   let nodmainresp=noddw*.024*24*.682
940   let stemmainresp=stemdw*.003*night
950   let xleafmainresp=xleafdw*.008*night
           ! (DW * resp rate * hours * factor for CO2 to CH2O)
951
952   !           Calculation of growth respiration

953   ! (growth respiration calculated at 0.5 of CHO import)
954   let rootgroresp = rootin2 * .5
955   let stemgroresp = stemin * .5 * night/24
956   let xleafgroresp = xleafin * .5 * night/24
958   let nodgroresp = nodin * .5

959   !           Calculation of total respiration

960   let rootresp = rootmainresp + rootgroresp
962   let stemresp = stemmainresp + stemgroresp
964   let xleafresp = xleafmainresp + xleafgroresp
966   let nodresp = nodmainresp + nodgroresp
986   let resp = cotyresp + rootresp + nodresp + stemresp + xleafresp
987
988   !           Final calculation of daily dry weight
989
996   let cotydw = cotydw - (cotyori/30 + cotyresp) ! (cotyledon
997   ! dry weight reduced by export and respiration)
998   if day > 17 then cotydw=0
1000  let xleafdw= xleafdw + xleafin - xleafresp
1010  let stemdw = stemdw + stemin - stemresp
1015  let noddw= noddw + nodin - nodresp
1020  let rootdw= rootdw + rootin2 - rootresp
1025  let plantdw =cotydw + rootdw + stemdw + xleafdw + noddw
1027
1030  !           Calculation of individual nodule respiration
1033
1035  nodindresp = nodmainresp / nodno
1038
1043  !           Calculation of nitrogen content
1044
1046  Cotynittot = cotynittot - initialnit / 19
1048  If day > 17 then cotynittot = 0
1050  If day <= 17 then cotynitavail = initialnit/19
1051  If day > 17 then cotynitavail = 0
1052  If nodindresp > 0.5 then let nodnitavail = nodmainresp / 8
           else let nodnitavail = 0
1054  let appNavail = rootmainresp * .1 * appN
1056  let availnit =availnit+cotynitavail+nodnitavail+appNavail
1060

```

```

1062      !           Partitioning of nitrogen
1064
1067      let nodnittot=noddw*.060
          !(preferential allocation of nitrogen to nodules)
1068      let availnit2 = availnit - nodnittot
1069      ! Partitioning of N to other parts
1070      let xleafnitposs = xleafdw*.048
1080      let stemnitposs = stemdw*.026
1090      let rootnitposs = rootdw*.036
1100      let maxnitposs = xleafnitposs + stemnitposs + rootnitposs
1110      let nitratio = availnit2 / maxnitposs
1120      let xleafnittot= xleafnitposs*nitratio
1122      let stemnittot= stemnitposs*nitratio
1124      let rootnittot= rootnitposs*nitratio
1150      let xleafnit = xleafnittot/xleafdw*100
1154
1260      !           Effect of leaf N level on photosynthesis
1270
1280      if xleafnit > 4 then nitfactor = 1
1290      if xleafnit < 4 then nitfactor = xleafnit/4
1300
1500      day = day + 1 ! (increment of the day)
1600      goto 400
10000      END

```



## Key to variables for program Soyfix

Variable	Parameter represented (units)
appN	Applied nitrogen (relative only)
appnavail	Applied nitrogen available to plant (mg)
availnit	Total available nitrogen (mg)
availnit2	Available nitrogen minus nodule nitrogen (mg)
cotyarea	Cotyledon surface area (cm <sup>2</sup> )
cotyexport	Cotyledon export of carbon (mg)
cotynitavail	Cotyledon nitrogen available to plant (mg)
cotynittot	Cotyledon nitrogen total (mg)
cotyori	Cotyledon initial dry weight (mg)
cotyorinit	Cotyledon initial nitrogen total (mg)
cotypsex	Cotyledon photosynthesis carbon export (mg)
cotypsyn	Cotyledon photosynthesis rate (mg CO <sub>2</sub> m <sup>-2</sup> s <sup>-1</sup> )
cotyresp	Cotyledon respiration of carbohydrate (mg)
day	Individual day
daylength	Hours of sunshine
initialnit	Initial nitrogen content (mg)
maxnitposs	Maximum nitrogen possible factor
night	Hours of darkness
nitfactor	Relative limitation photosynthesis by leaf nitrogen
nitratio	Ratio of available nitrogen to usable nitrogen
noddw	Nodule dry weight
nodgroresp	Nodule growth respiration (mg carbohydrate)
nodin	Nodule import carbohydrate (mg)
nodindresp	Nodule individual respiration (mg carbohydrate)
nodmainresp	Nodule maintenance respiration (mg carbohydrate)
nodnitavail	Nitrogen available from fixation (mg)
nodnittot	Nodule nitrogen total (mg)
nodno	Nodule number per plant
nodresp	Total nodule respiration (mg)
photosyn	Total cotyledon and leaf photosynthesis (mg carbon)
plantdw	Total plant dry weight (mg)
rootdw	Root dry weight
rootgroresp	Root growth respiration (mg carbohydrate)
rootin	Root import carbohydrate <13 days (mg)
rootin2	Root import carbohydrate >13 days (mg)
rootmainresp	Root maintenance respiration (mg carbohydrate)
rootnitposs	Maximum possible root nitrogen (mg)
rootresp	Total root respiration (mg)
stemdw	Stem dry weight
stemgroresp	Stem growth respiration (mg carbohydrate)
stemin	Stem import carbohydrate (mg)
stemmainresp	Stem maintenance respiration (mg carbohydrate)
stemnitposs	Maximum possible stem nitrogen (mg)
stemresp	Total stem respiration (mg)
xleafarea	Leaf area (cm <sup>2</sup> )
xleafdw	Leaf dry weight (mg)
xleafgroresp	Leaf growth respiration (mg carbohydrate)
xleafin	Leaf import carbohydrate (mg)
xleafmainresp	Leaf maintenance respiration (mg carbohydrate)
xleafnit	Leaf nitrogen percent
xleafnitposs	Maximum possible leaf nitrogen (mg)
xleafpsex	Leaf photosynthesis export (mg carbon)
xleafpsyn	Leaf photosynthesis rate (mg CO <sub>2</sub> m <sup>-2</sup> s <sup>-1</sup> )
xleafresp	Total leaf respiration (mg)

## Appendix II

```
100      !           BASIC FILE TO CALCULATE LOW ACT RATES
150      !
180      !           Richard Parsons 23/6/1989
200      !
210      let halftime = 60
220      let X= .2
230      let nodrad = .2
240      let nodvol = 4/3 * 3.14 * nodrad**3
250      open "LOW3.dat" for output as file #1
270      open "LOW4.dat" for output as file #2
300      for actex = .0000001 to 10 step .2
310          let actsol =actex/101.3*1.03/22.4/1000*1000000
320          let ethy = 0
330          let ethyin = 0
340          let ethytot = 0
350          let ethyouttot = 0
360          let actin = 0
410          for minutes = 0 to 10.0 step X
420          let Y = (1-1/(2**(X*60/halftime)))
430          let actin = actin-ethy+(actsol*nodvol-actin)*Y
440          if minutes = 0 then let actin = 0
450          let velocity =(actin/nodvol*1000)/(264+actin/nodvol*1000)
460          let ethy = 180 / 60 / 5 * velocity * nodvol * X
470          let ethyin = ethyin + ethy
480          let ethyout = ethyin * Y
490          let ethyin = ethyin - ethyout
500          let ethytot = ethy + ethytot
510          let ethyouttot = ethyouttot + ethyout
520          let actrat=actin/(actsol*nodvol)
530          if minutes=0 then let rate=0 else let rate=ethyout/X/nodvol*60*5
700      !print, ;minutes;ethytot;ethyouttot;rate;ethyin;actex;velocity
800      print #1, halftime;minutes;ethy;actrat;rate;
820      print #1;actex;ethytot;actsol;actin;Y;velocity
900      !print #2, minutes;actex;actin;actsol*nodvol
1000     next minutes
2000     next actex
11000    END
```

**Key to variables for model of low pressure acetylene reduction**

<b>Variable</b>	<b>Parameter represented (units)</b>
actex	External acetylene pressure (kPa)
actin	Amount of acetylene inside the nodule ( $\mu\text{mol}$ )
actrat	Ratio of internal acetylene to external acetylene
actsol	Acetylene concentration at equilibrium with external acetylene ( $\mu\text{mol cm}^{-3}$ )
ethy	Amount of ethylene produced within nodule ( $\mu\text{mol}$ )
ethyin	Total ethylene within the nodule ( $\mu\text{mol}$ )
ethyout	Amount of ethylene diffusing out of nodule ( $\mu\text{mol}$ )
ethyouttot	Total ethylene diffused out of nodule ( $\mu\text{mol}$ )
halftime	Half-time for acetylene (ethylene) diffusion (s)
nodrad	Nodule radius (cm)
nodvol	Nodule volume ( $\text{cm}^3$ )
X	Calculation step in time (minutes)
Y	Fraction for diffusion rate calculation (minutes)

## Appendix III

(a)

```

100      !      Model to calculate spherical diffusion
200      !              through central zone
210      !
220      open "mod3.dat" for output as file #1
300      let Q = 0.048
400      let Da = 1.8e-5
500      let H = 1e-7
1000     for a = 1e-7 to 1.265e-3 step H
1100     let b = a + H
1120     let Vcz = 4/3*3.14 * a**3
1180     let Qcz = Vcz * Q
1200     let conc = Qcz*(b-a) / (4*3.14* a*b *0.03 *Da)
1300     let concTot = concTot + conc
1900     next a
2010     print, a;conc;concTot/4.04e-4;qcz;voltot
2020     ! prints concentration in pascals
10000    end

```

(b)

```

100      !      Model to calculate spherical diffusion
200      !              through inner cortex
210      !
220      open "mod.dat" for output as file #1
300      let Q = 0.048
400      let Dw = 2.5e-9
500      let H = 1e-7
1000     for a = 1.265e-3 to 1.5e-3 step H
1100     let b = a + H
1120     let Vcz = 4/3*3.14 * 1.256e-3**3
1180     let Qcz = Vcz * Q
1200     let conc = Qcz * (b-a) / (4 * 3.14 * a*b * Dw)
1300     let concTot = concTot + conc
1810     print, a;conc;concTot*1000;qcz
1820     ! prints concentration total in uM.
1900     next a
10000    end

```